THE ROLE AND REGULATION OF THE UROKINASE RECEPTOR IN ASTHMA AND COPD

By

MICHAEL ANTHONY PORTELLI, B.Pharm. (Hons.) (*Melit.*)

Thesis submitted to the University of Nottingham for the degree of Doctor of Philosophy

June 2013

To Nanna Paola, Nanna Esther, Nannu Joseph & Aunty Mary Anne

for your belief and faith in me

To Mum and Dad, for everything

ABSTRACT

The urokinase plasminogen activator receptor (PLAUR) is a membrane anchored receptor that has been associated with a number of disease states. In these diseases, elevated receptor levels were associated with increased disease aggressiveness and higher mortality rates. Through genetic studies *PLAUR* has been identified as an asthma susceptibility gene. In these studies, coding and untranslated region single nucleotide polymorphisms showed association with asthma diagnosis and decline in lung function. In addition, association with baseline lung function in smokers and PLAUR SNPs was identified. This suggests that PLAUR plays a role in respiratory disease.

Work presented in this thesis aimed to i) identify whether serum levels of PLAUR are associated with obstructive lung disease and lung function parameters, ii) identify novel regulatory mechanisms determining PLAUR levels, both at the genetic level in primary bronchial epithelial cells and at the protein level for serum PLAUR, iii) explore a role for the different isoforms in asthma and COPD and iv) determine novel variation in the PLAUR gene and 5` and 3` distal regions through next generation sequencing.

Levels of the soluble cleaved form of PLAUR in serum were determined to be significantly elevated in COPD and asthma subjects compared to a control population. This identified an association between the soluble cleaved receptor and disease *per se*. However, PLAUR levels in serum could not be related to lung function parameters.

With regards to receptor regulation, a genome-wide association study identified a novel post-translational PLAUR regulatory mechanism. This involved key SNPs in the human plasma kallikrein gene promoter that directed human plasma kallikrein enzymatic activity to cleave PLAUR in a post-translational mechanism. *PLAUR* gene regulation was also investigated via molecular biology, identifying that in primary

bronchial epithelial cells, *PLAUR* regulation involves the gene's 5 prime and 3 prime untranslated regions. Investigation of regulation under multiple stimulations pertinent to respiratory disease identified that cigarette smoke extract selectively elevated the soluble spliced variant of the receptor through a three prime untranslated region mechanism. This suggests that bronchial epithelial damage driven by cigarette smoke may be at least partially mediated by the soluble spliced form of PLAUR.

Overexpression of PLAUR identified that the receptor has an important role in regulating primary bronchial epithelial cell function, including migration and rate of mitochondrial activity. Interestingly, results identified isoform specific roles for the different forms of the receptor suggesting that variant-specific over-expression of PLAUR could have diverse effects on cell function. Importantly this study was also the first to define a role for the soluble spliced form of PLAUR.

Investigation into variation in the PLAUR gene and surrounding regions through next generation sequencing in asthma (n=200) and control (n=200) populations identified a number of novel variants including 4 variants unique to asthma population.

In summary, the work described in this thesis has identified a novel association between serum soluble cleaved PLAUR and obstructive lung disease, as well defining novel genetic and post-translational regulatory mechanisms for PLAUR, importantly defining isoform specific PLAUR regulation for the first time. This work has also identified novel isoform specific roles for PLAUR, which have significant modulatory effects on bronchial epithelial cell function, and has through next generation sequencing furthered knowledge on universal and asthma specific PLAUR variation.

PUBLICATIONS

Portelli M, Sayers I. **Genetic basis for personalized medicine in asthma**. Expert Rev Respir Med. 2012 Apr;6(2):223-36.

ABSTRACTS

<u>**Portelli MA**</u> & Sayers I. **miRNA regulation of PLAUR in bronchial epithelial cells**. *Poster presented at the Biochemical Society Workshop: MicroRNAs and their targets: promises and pitfalls, London UK, 2nd November 2010.*

<u>**Portelli MA**</u>, Stewart CE, Koppelman GH et al. **Investigating the soluble cleaved urokinase plasminogen activator receptor as a biomarker in asthma and COPD** *Poster presented at the American Thoracic Society Annual Coference, Denver Colorado, May 13-18 2011.*

<u>**Portelli MA**</u>, Hall IP & Sayers I. **Cigarette Smoke Modulates PLAUR Expression In Bronchial Epithelial Cells Via A 3`UTR Mechanism**. *Poster presented at the American Thoracic Society annual conference, San Francisco California, May 18-23 2012.*

<u>**Portelli MA**</u>, Sliedinski M, Postma DS, Nieuwenhuis M, Vonk JM, Altmuller Jet al. **GWAS Identifies That A Human Plasma Kallikrein Single Nucleotide Polymorphism Regulates Serum PLAUR Levels In Asthma And COPD**. *Poster presented at the American Thoracic Society annual conference, San Francisco California, May 18-23 2012.*

<u>**Portelli MA**</u>, Hall IP & Sayers I. **Cigarette smoke induces a soluble uPAR splice variant that can increase bronchial epithelial cell proliferation**. *Poster presented at the Biochemical Society Workshop: Delivering and phenotyping mouse models for the respiratory community, London UK, 4th December 2012.*

ORAL COMMUNICATIONS

Portelli MA, Hall IP, Sayers I. **Investigating soluble cleaved uPAR as a biomarker in COPD**. *Oral Communication by invitation, University of Malta Scientific Seminar Series, 10th October 2011.*

Portelli MA, Sliedinski M, Postma DS, Nieuwenhuis M, Vonk JM, Altmuller Jet al. **GWAS identifies a KLKB1 promoter SNP that regulates serum PLAUR levels in asthma and COPD**. *Oral Presentation at the 12th Annual ILH respiratory science research meeting, Holywell Park Loughborough, 2nd May 2012.*

Portelli MA, Sliedinski M, Postma DS, Nieuwenhuis M, Vonk JM, Altmuller Jet al. **A protein based GWAS identifies KLKB1 as a novel proteolytic regulator of scuPAR**. *Oral Communication by invitation, University of Malta Scientific Seminar Series, 7th January 2013.*

ACKNOWLEDGMENTS

TABLE OF CONTENTS

ABBREVIATIONS

1B10	Mouse Fibroblast Surface Protein antibody
3`UTR	Three prime untranslated region
5`UTR	Five prime untranslated region
AAT	α_1-antitrypsin
Amp^{100}	Solution of 100µg/ml Ampicillin
APS	Ammonium PerSulphate
ATF	Amino-Terminal Fragment
ATS	American Thoracic Society
AUGOSA	Genome-Wide Association Study To Identify Genetic Determinants Of Severe Asthma
BALF	Bronchiolar Lavage Fluid
BEBM	Bronchial Epithelial Basal Media
BEGM	Bronchial Epithelial Growth Media
BEWM	Bronchial Epithelial Wounding Media
BHR	Bronchial Hyper-Responsiveness
bp	Base Pairs
CC26	Rabbit Anti-Nonselenium Glutathione peroxidase antibody
cDNA	Complimentary DNA
CEU	Caucasian European Population
CK-14	Anti-cytokeratin 14 antibody
C_t	Cycle threshold
COPD	Chronic Obstructive Pulmonary Disease
CSE	Cigarette Smoke Extract
CSM	Cigarette Smoke Media
$D_{I/II/III}$	Domain I/II/III
DL	Dual Luciferase Assay
DMEM	Dulbecco's Modified Eagle's Medium
DMSO	Dimethyl Sulphoxide

DNA	Deoxy Ribose Nucleic Acid
ECL	Enhanced Chemiluminescence
ECM	Extracellular Matrix
EDTA	Ethylenediaminetetraacetic acid
EGFR	Epidermal growth factor receptor
ELISA	Enzyme linked immunosorbent assay
ENCODE	Encyclopaedia of DNA Elements
eQTL	Expression Quantitative Trait Locus
ERS	European Respiratory Society
FBAT	Family Based Association Tests
FCS	Foetal Calf Serum
FENO	Fractional exhaled nitric oxide
FEV_1	Forced Expiratory volume in 1 second
FEV_1pp	Forced Expiratory volume in 1 second (percentage predicted)
FITC	Fluorescein isothiocyanate antibody
FGF2	Fibroblast Growth Factor
fMLP	N-formyl-methionine-leucine-phenylalanine
FSGS	Focal Segmental Glomerulosclerosis
FVC	Forced Vital Capacity
GAPDH	Glyceraldehyde 3-phosphate dehydrogenase
GPI	Glycosylphosphatidylinositol
GINA	Global Initiative for Asthma
GOLD	Global Initiative for Chronic Obstructive Lung Disease
GPCRs	G-protein coupled receptors
GWAS	Genome-Wide Association Studies
HASM	Human Airway Smooth Muscle
HAT	Human Airway Trypsin-like protease
HGF/SF	Hepatocyte Growth Factor/Scatter Factor
HIV	Human-Immunodeficiency Virus
HK	High-molecular-weight-kininogen

hnRNPC	Heterogeneous Nuclear Ribonucleoproteins C1/C2
HPRT	Hypoxanthine Phosphoribosyltransferase 1
HRP	Horse Radish Peroxidase
HWE	Hardy-Weinberg Equilibrium
Indels	Insertion/Deletions
Kan^{50}	Solution of 50μg/ml Kanamycin
kb	kilobases
kDa	kiloDalton
KLKB1	Human Plasma Kallikrein
LAR	Luciferase Assay Reagent
LB	Lysogeny Broth
LD	Linkage Disequilibrium
LDL	Low-Density-Lipoprotein
LPS	Lipopolysaccharide
LRP	LDL-Receptor-Related Protein
Ly-6	Lymphocyte Antigen 6
mAB	Monoclonal Antibody
MAF	Minor Allele Frequency
miRNA	Micro RNA
MMP	Matrix Metalloproteinase
MRC-5	Normal Human Foetal Lung Fibroblast
MS-1	Mesothelioma cells
MTT	3-(4,5-Dimethylthiazol-2-yl)-2,5-diphenyltetrazolium bromide
NHBEC	Normal Human Bronchial Epithelial Cell
NHLBI	National Heart, Lung, and Blood Institute
pAB	Polyclonal Antibody
PAGE	Polyacrylamide gel
PAS	Plasminogen Activation System
PEF	Peak Expiratory Flow
PBS	Phosphate Buffered Saline

PBS-T	PBS + 0.05% v/v Tween
PBST	PBS + 0.1% v/v Tween
PCR	Polymerase Chain Reaction
PDAR	Pre-Developed Assay Reagents
PGK	Phosphoglycerate kinase
PLAUR	Urokinase Plasminogen Activator Receptor
PMA	Phorbol-12-myristate 13-acetate
qPCR	Quantitative PCR
RLuc	Relative Luciferase
rPLAUR	Recombinant PLAUR
RT-PCR	Reverse Transcription PCR
r.t.p	Room temperature and pressure
SAM	Sequence Alignment/Map
SBS	Sequencing by Synthesis
scPLAUR	Soluble Cleaved PLAUR
SDS	Sodium Dodecyl Sulphate
SHP2	Tyrosine-protein phosphatase non-receptor type 11
SNP	Single Nucleotide Polymorphism
SOC	Super Optimal broth with Catabolite repression
TAE	Tris base, acetic acid and EDTA
TDT	Transmission Disequilibrium Test
TF	Transcription Factor
Tm	Melting temperature
TRITC	Goat anti Rabbit IgG Rhodamine antibody
TSS	Transcriptional Start Site
uPA	Urokinase
uPAR	Urokinase Plasminogen activator receptor
VCF	Variant Call Format
VN	Vitronectin
WHO	World Health Organisation

CHAPTER 1

GENERAL INTRODUCTION

CHAPTER 1: GENERAL INTRODUCTION

The coagulation and fibrinolytic pathways have been shown to play a role in obstructive lung disease and provide potential novel therapeutic targets for both asthma and chronic obstructive pulmonary disease (COPD). The fibrinolytic pathway involves the urokinase plasminogen activator receptor (PLAUR), which has independently been implicated with asthma and COPD pathogenesis both at the gene and protein level. The regulation and role of the receptor within the bronchial epithelium, an important part of the airway involved in airway remodelling, is however poorly understood. This thesis furthers our understanding of the regulation of different PLAUR isoforms in the periphery and in bronchial epithelial cells. This allows for further understanding of the gene architecture with regards to variation, with a focus on differences in variation between asthmatics and controls, and allows for the identification of novel roles for different receptor isoforms in bronchial epithelial cells.

1.1 ASTHMA

Asthma is a chronic inflammatory disorder of the airways (Levy et al., 2012) which results in recurrent episodes of wheezing, breathlessness, chest tightness and cough which occur particularly at night and in the early morning. These episodes are usually associated with widespread but variable airway obstruction, which is often reversible spontaneously or with treatment (Toelle et al., 1992). Asthma induced inflammation also results in increased airway sensitisation by causing an associated increase in bronchial hyper-responsiveness (BHR) to a variety of stimuli (Toelle et al., 1992). Therefore, asthma can be defined as a complex disease involving inflammation, hyper-responsiveness, and bronchoconstriction (Lowhagen, 2012).

1.1.1 PATHOLOGY OF ASTHMA

The inflammatory cascade in asthma involves infiltration of a number of inflammatory cells (eosinophils, neutrophils, B- and T-lymphocytes, macrophages, mast cells, dendritic cells and basophils) into the airway and the release of inflammatory mediators such a leukotrienes, histamine, cytokines and chemokines by airway structural cells (epithelial, smooth muscle, endothelial and fibroblast cells) (Fig. 1.1). However, the degree of inflammation in asthma is not directly related to asthma severity, suggesting that other factors, such as structural changes in the airway also play a role in disease modulation and progression (Barnes PJ, 2002). These structural changes have been termed as airway remodelling and may exist in the presence or absence of inflammatory mechanisms in the airway (Kermode et al., 2011). Airway remodelling is further discussed in Section 1.4.

The inflammatory response in asthma is a result of excessive activation of mast cells in the airway, where in the early response to allergen challenge, degranulation of mast cells results in the release of a number of pro-inflammatory factors such as IL-4, leukotrienes and histamine. This causes an immediate hypersensitivity response which in turn leads to airway bronchoconstriction. The concomitant release of other inflammatory factors such as cytokines and chemokines from the same mast cells provides an optimal environment for the recruitment of other inflammatory cells such as eosinophils, basophils, neutrophils and T-lymphocytes to the airways. Once in the airways these cells act in tandem with allergen activated macrophages, resulting in what is termed as the late asthmatic response (occurring at 4 to 8 hours post challenge). Here, via the release of a number of potent bronchoconstrictors including TNFα, and Interleukines 3, 4, 5 and 13, airway narrowing occurs which may last for a period longer than 24 hours. Of the inflammatory cells involved in the asthmatic response, it is the infiltration of eosinophils that is considered to be characteristic of

the asthmatic phenotype, particularly that of mild/moderate allergic atopic asthma. Therefore the presence of high levels of eosinophils aids in the differentiation between the asthmatic airway and the COPD airway, where neutrophilic infiltration is more prevalent (Barnes, 2000, Lacoste et al., 1993). However, this is not a clear cut distinction, with increasing neutrophilic infiltration occurring with increasing severity (Wenzel et al., 1997).

Although inflammation in asthma has been extensively studied, the relationship between inflammation and clinical symptoms of asthma is still unclear. This may be partially explained by a study that has shown evidence that inflammation is loosely related to airway hyper-responsiveness (Brusasco et al., 1998), where the airways become more susceptible to sensitising agents that would not usually trigger an airway response, due to the increased release of mediators such as histamine and leukotrienes, abnormal smooth muscle behaviour and thickening of the airways.

As mentioned above, airway remodelling (see Section 1.4) also plays an important role in asthma pathogenesis. The airway structural changes characteristic of airway remodelling occur due to prolonged airway inflammation. Here, prolonged release of inflammatory factors results in:

- Thickening of the smooth muscle bronchial walls, leading to airway narrowing
- Denudation of the bronchial epithelium
- Hyperplasia and hypertrophy of the airway smooth muscle
- Hyperplasia and hypertrophy of the epithelial goblet cells resulting in the formation of large mucus plugs that are liable to occlude the airway and increased airway hyper-responsiveness (Douglas and Elward, 2011).

Airway remodelling also involves changes occurring in the extracellular matrix and its constituent proteins (collagen I/III/IV, fibronectin and laminin) (Bai et al., 2000) and

other structural changes such as angiogenesis, vasodilation, increased airway blood flow (Kumar et al., 1998) and changes in autonomic neurological function (Barnes, 1995).

Asthma is a highly heterogeneous disease consisting of a number of disease variants such as severity, disease history, disease comorbidities and therapeutic efficacy, with different underlying pathophysiologies (Lotvall et al., 2011, Wenzel, 2006). Historically the issue of asthma heterogeneity has been tackled by classifying different forms of asthma according to the sensitising agents, allowing sub-classification of the disease into; allergic asthma (triggered by multiple allergens including but not exclusive to pollen, house dust mite and animal dander), exercise-induced asthma (characterised by bronchoconstriction and other asthma symptoms that develop during and/or after exercise) and nocturnal asthma (where the Forced expiratory volume in 1 second [FEV_1] decreases by 15% or more from bedtime to waking up in the morning). However, this classification is problematic when large cohorts of patients with asthma are studied as all defining characteristics may overlap or may not all be present. In order to try and broach this problem, Lötvall *et al.* have proposed a new classification sytem based on 'endotypes', i.e. different subtypes of a condition defined by a distinct pathophysiological mechanism (Lotvall et al., 2011). Classification spanned a number of known asthma phenotypes such as eosinophilic asthma, exercise-induced asthma and adult-onset asthma, splitting the disease into 6 endotypes (Lotvall et al., 2011):

i)   Aspirin-Sensitive

ii)   Allergic pulmonary mycosis

iii)   Allergic

iv)   Asthma predictive indices positive (preschool wheezer)

v)   Severe late-onset

vi)   Asthma in cross country skiers

Correct identification of the relevant endotype to use in research allows for an improved approach to asthma research as it provides the basis for the stratification of a mixed asthma cohort in order to separate datasets based on phenotypes, such as atopic status, which may confound the investigative outcome. In this thesis the specific endotype investigated is 'Allergic asthma' which is classified on the basis of atopy, with non-atopic asthmatics defined as those with negative skin tests and no clinical or family history of allergy. These patients are usually older than their allergic counterparts and have onset of symptoms in later life, often with a more severe clinical course (Rackemann, 1947, Humbert et al., 1999).
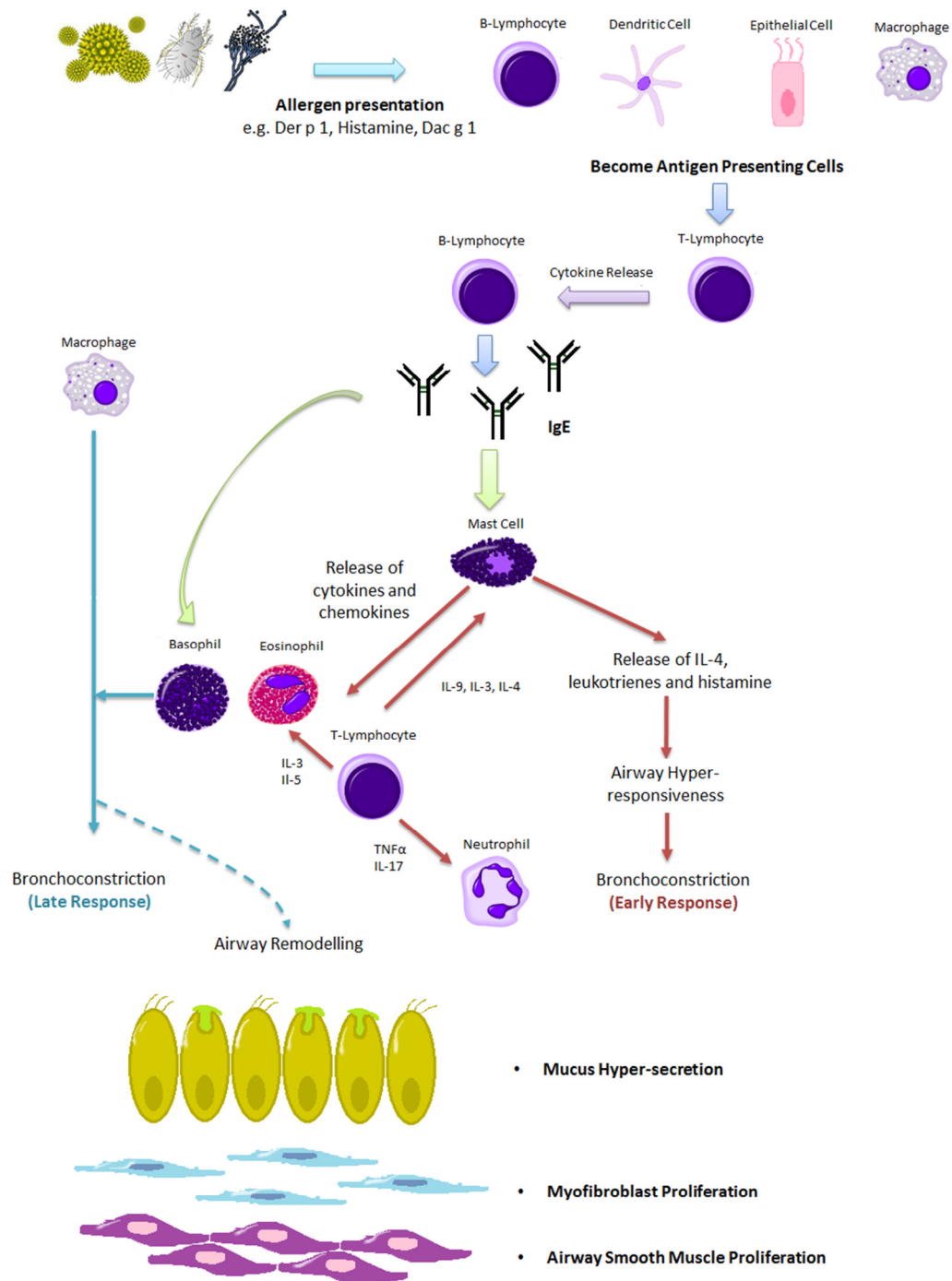
Figure 1.1: The asthma inflammatory cascade. Exposure to allergens; e.g. *Dermatophagoides pteronyssinus* 1 (Der p 1), histamine and *Dactylis glomerata* (Dac g 1) originating from various sources including pollen, house dust mite and mould, are up taken by dendritic cells, B-lymphocytes, epithelial cells and Macrophages, which present the antigens to T-lympocytes. This activates the T-lymphocytes to produce cytokines that regulate immunoglobulin (Ig) E production by the B-lymphocytes. Bound IgE activates mast cells in the airways. Activated mast cells initially release a number of factors including IL-4, leukotrienes and histamine that cause airway hyper-responsiveness and result in the early-response to allergen stimulus via bronchoconstriction. The concurrent release of cytokines and chemokines from the mast cell recruits eosinophils, basophiles and T-lymphocytes to the airway. These cells in association with T-cell activated neutrophils and with antigen stimulated macrophages, release chemokines and leukotrienes over an extended period of time resulting in the late-response to allergen stimulus via bronchoconstriction. Prolonged stimulation of the late-response factors ultimately leads to the airway structural changes such as mucus hypersecretion, myofibroblast and airway smooth muscle proliferation, which are common to the asthmatic lung.

1.1.2 ASTHMA SEVERITY

Asthma can vary in intensity from mild, where assessment of lung function by spirometry may be extremely hard, to severe and unremitting (*status asthmaticus*). Changes in asthma severity are important for correct patient evaluation, treatment and research, where correct classification of a subject is essential for accurate phenotype based investigations. Severe asthma is defined by the World Health Organization (WHO) as "*Uncontrolled asthma which can result in risk of frequent severe exacerbations (or death) and/or adverse reactions to medications and/or chronic morbidity*" (Bousquet et al., 2010), and differs from mild asthma in that it exhibits increased neutrophil infiltration, which may actually be absent in the milder forms of asthma (Jatakanon et al., 1999, Caramori et al., 2005).

In asthma, the term severity has been variably used to indicate the degree of current symptoms (such as the frequency of exacerbations and nocturnal awakenings), the resistance of symptoms to standard treatment (i.e. at which step of the management scale the patient is), and the future risk of death or exacerbations. Since it is difficult for any single one of these factors to correctly define asthma on its own, due to the disease's complex and heterogeneous nature, international guidelines attempt to define severity based on different combinations of these factors.

In this thesis, the guidelines published by the Global Initiative for Asthma (GINA) were used to define asthma severity. This severity scale is based on a combination of the prevalence of day/night time symptoms, airflow limitation and pulmonary function variability (Table 1.1).

	Symptoms/Day	Symptoms/Night	PEF or FEV_1	PEF variability
STEP 1 Intermittent	< 1 time a week Asymptomatic and normal PEF between attacks	</= 2 times a month	>/= 80%	< 20%
STEP 2 Mild Persistent	> 1 time a week but < 1 time a day Attacks may affect activity	> 2 times a month	>/= 80%	20-30%
STEP 3 Moderate Persistent	Daily Attacks affect activity	> 1 time a week	60%-80%	> 30%
STEP 4 Severe Persistent	Continuous Limited physical activity	Frequent	</= 60%	> 30%

Table 1.1: GINA classification of asthma severity. Here, multiple factors including prevalence of day/night time symptoms, airflow limitation and pulmonary function variability, are utilised to place a patient in that category. PEF: Peak Expiratory Flow; FEV_1: Forced Expiratory Volume in 1 second.

1.1.3 DIAGNOSIS AND TREATMENT OF ASTHMA

As described by GINA, asthma diagnosis can be prompted by symptoms such as episodic breathlessness, wheezing, cough and chest tightness. Episodic symptoms after allergen exposure, seasonal variability of symptoms and a positive family history of asthma/atopic disease are also helpful first line diagnostic aides (GINA, 2011).

Clinical testing however plays an important part in correct asthma diagnosis, with measurements of lung function and demonstration of the reversibility of lung function abnormalities adding confidence to initial asthma diagnosis. Lung function testing occurs through spirometry, which is the measurement of the forced expiratory volume in one second (FEV_1) and Forced vital capacity (FVC), or peak expiratory flow (PEF) testing. Asthma diagnosis regularly makes use of the FEV_1/FVC ratio for a more specific asthma diagnosis, as decreases in FEV_1 alone can occur in other lung diseases (GINA, 2011). For this purpose, a normal FEV_1/FVC ratio is considered to be >0.75 to

0.80, with lower ratios identifying airflow limitation (GINA, 2011). A confirmation of asthma diagnosis then occurs if the patient provides a minimal 12% or 200ml increase from pre-bronchodilator readings (Vollmer et al., 1999). This spirometric based asthma diagnosis can then be confirmed with a 60L/min or 20% reversibility in PEF from the pre-bronchodilator reading and recording a diurnal variation in PEF of >20% (GINA, 2011).

In addition to spirometric lung function testing, fractional exhaled nitric oxide (FENO) has recently emerged as an additional potential diagnostic aide for asthma (Stewart and Katial, 2012, Schneider et al., 2012, Ludviksdottir et al., 2012), providing additional information on a number of different aspects, including phenotyping, corticosteroid response and disease control (Ludviksdottir et al., 2012). However FENO cannot be used as a standalone diagnostic test for asthma due to its association with the eosinophilic sub-type of asthma, with guidelines suggesting that its use be limited to the diagnosis of eosinophilic airway inflammation, determining the likelihood of steroid responsiveness and to support the diagnosis of asthma in situations where objective evidence is needed (Dweik et al., 2011).

The therapeutic response to asthma involves multiple drug therapies including long and short acting β_2-adrenoreceptor agonists, leukotriene receptor antagonists and inhaled and/or oral corticosteroids. Asthma treatment is based on a step-wise approach where treatment is started at the step most appropriate to the degree of asthma severity and increased or decreased as necessary to achieve and maintain adequate control (Fig. 1.2) (BTS, 2011).

However, although current asthma therapeutics are able to successfully treat 90-95% of the asthmatic population, there remains 5-10% of patients who do not respond well to conventional treatments. These account for ~50% of the health care costs of asthma (Caramori et al., 2008). This, together with the need to move away from chronic

glucocorticosteriod therapy and its associated side-effects (e.g. adrenal suppression, osteoporosis and increased risk of infection) in severe asthmatics, highlights the need for novel therapies targeting new pathways in asthma therapeutics.

Patients should start treatment at the step most appropriate to the initial severity of their asthma. Check concordance and reconsider diagnosis if response to treatment is unexpectedly poor.

MOVE UP TO IMPROVE CONTROL AS NEEDED

MOVE DOWN TO FIND AND MAINTAIN LOWEST CONTROLLING STEP

STEP 1
Mild intermittent asthma

Inhaled short-acting β_2 agonist as required

STEP 2
Regular preventer therapy

Add inhaled steroid 200-800 mcg/day*

400 mcg is an appropriate starting dose for many patients

Start at dose of inhaled steroid appropriate to severity of disease.

STEP 3
Initial add-on therapy

1. Add inhaled long-acting β_2 agonist (LABA)
2. Assess control of asthma:
   - good response to LABA - continue LABA
   - benefit from LABA but control still inadequate - continue LABA and increase inhaled seroid dose to 800 mcg/day* (if not already on this dose)
   - no response to LABA - stop LABA and increase inhaled steroid to 300 mcg/day.*If control still inadequate, institute trial of other therapies, leukotriene receptor antagonist or SR theophylline

STEP 4
Persistent poor control

Consider trials of:
- increasing inhaled steroid up to 2000 mcg/day*
- addition of a fourth drug e.g. leukotriene receptor antagonist, SR theophylline, β_2 agonist tablet

STEP 5
Continuous or frequent use of oral steroids

Use daily steroid tablet in lowest dose providing adequate control

Maintain high dose inhaled steroid at 2000 mcg/day*

Consider other treatments to minimize the use of steroid tablets

Refer patient for specialist care

* BDP or equivalent

Figure 1.2: Step-wise therapy for asthma. Therapeutics for asthma follows a step-wise approach with the strength and number of medications increasing as one attempts to achieve control on exacerbation, followed by down-stepping therapy on resolution of symptoms to attempt to achieve control using the minimal amount of medication. Therapy involves the use of inhaled short and long acting β_2-adrenoreceptor agonists (bronchodilators) as reliever and preventer medication respectively, inhaled and oral steroids (anti-inflammatory), oral β_2-agonists and Theophylline (bronchodilators) and oral Leukotriene receptor antagonists as preventers. Figure obtained from BTS British Guideline on the Management of Asthma (BTS, 2011).

1.2 CHRONIC OBSTRUCTIVE PULMONARY DISEASE

COPD is defined by both the American Thoracic Society (ATS) and the European Respiratory Society (ERS) as *a preventable and treatable disease state characterised by airflow limitation that is not fully reversible* (Celli et al., 2004), where the airflow limitation is progressive resulting from an abnormal inflammatory response of the lungs to noxious particles and gases such as cigarette smoke (Vestbo et al., 2012).

COPD usually presents in the sixth and seventh decade of life and is generally classified as a disease of smoking adults, although other sensitizing factors such as air pollution, poor diet and occupational exposure can substitute cigarette smoke, especially in less developed countries (Barnes PJ, 2002, Barnes et al., 2003).

1.2.1 PATHOLOGY OF COPD

Pathologically COPD, as asthma, is classified as an inflammatory disease. However, in reality COPD is a term which includes a number of separate and distinct diseases:

1. Bronchitis: Inflammation of the bronchial mucous membranes, which results in mucus hyper secretion. In COPD, bronchitis is chronic which usually develops due to recurrent airway injury caused by inhaled irritants.

2. Emphysema: Destruction of alveolar walls causing the collapse of the small airways during forced exhalation and resulting in dyspnoea. Inhaled irritants are once again major causes of emphysema. (Currie, 2007, Barnes et al., 2003)

In addition to the mucus hypersecretion and tissue destruction caused by bronchitis and emphysema, inflammation in COPD results in the disruption of the normal repair and defence mechanisms of the airway epithelium causing destruction of the lung parenchyma, loss of lung elasticity and closure of the small airways (bronchiolitis)

(Currie, 2007, Barnes et al., 2003). In patients with COPD, emphysema, bronchitis or bronchiolitis or any combination of the three may be present. However, the relative contribution of each to the disease process is often difficult to discern.

Inflammation in COPD differs strikingly from that in asthma in that it is characterised by a predominance of macrophages, cytotoxic (CD8+) T-lymphocytes and neutrophils (Barnes PJ, 2002). Exposure to cigarette smoke (or other irritants) results in activation of airway epithelial cells and macrophages, resulting in the release of a number of chemotactic factors, cytokines and inflammatory mediators such as LTB4, IL-8 and related CXC chemokines, that attract CD8 T-lymphocytes, monocytes and neutrophils to the area. The CD8 cells and neutrophils in turn activate airway fibroblasts, resulting in abnormal airway repair processes and bronchiolar fibrosis (Currie, 2007). Increased release of proteases such as Cathepsin G, Neutrophil Elastase and matrix metalloproteinases (MMP)-8 and -9 by neutrophils and macrophages in the airway results in mucus hypersecretion, ciliary dysfunction and increased alveolar wall destruction, i.e. airway remodelling (see Section 1.4) (Currie, 2007, Barnes PJ, 2002, Barnes et al., 2003).

Direct oxidative stress through cigarette smoke (and other irritants) can also affect the airway through the release of oxidants (free radicals). These oxidants have a dual effect on the airway; primarily they inhibit anti-proteases that would otherwise regulate the increased secretion of proteases by macrophages and neutrophils and secondly they directly cause airway remodelling by causing alveolar wall destruction, ciliary dysfunction and mucus hypersecretion through squamous metaplasia, increased proliferation of goblet cells and increased size of bronchial sub-mucosal glands (Barnes PJ, 2002, Currie, 2007).

Epithelium

Macrophage

Oxidative stress

Eosinophil

Basophil

Neutrophil

Release of chemotactic factors, cytokines and inflammatory factors

e.g. CXCL1/8 LTB$_4$

e.g. CXCL1/9/11

T-Lymphocyte

Neutrophil

Anti-Proteases

Leukocyte Recruitment

Activation

Oxidants

Fibroblast

Proteases
e.g. Cathepsin G

Mucus Hypersecretion & Ciliary Dysfunction

Abnormal repair & Bronchiolar fibrosis

Alveolar Wall Destruction

Figure 1.3: The COPD inflammatory cascade. Exposure to airway irritants such as cigarette smoke results in the release of a number of chemotactic factors (e.g. CCL2, CXCL9/10/11), cytokines (e.g. IL-8, MCP-1, IL1β) and inflammatory factors (e.g. TNFα) from both the airway epithelial cells and macrophages which recruit T-lymphocytes and neutrophils respectively, to the airways. Both the neutrophils and the T-lymphocytes activate lung fibroblasts resulting in abnormal repair and bronchiolar fibrosis. Proteases released from neutrophils result in alveolar wall destruction (emphysema) which is compounded by oxidants released by oxidative stress from the inhaled irritant and other Leukocytes recruited to the airways. Oxidants cause alveolar wall destruction both directly and by inhibiting anti-proteases that would counter-act the neutrophil released proteases.

1.2.2 COPD SEVERITY

COPD can vary in intensity from almost undetectable (mild COPD) to severe and unremitting (very severe COPD). As in asthma, changes in disease severity are important for patient evaluation, treatment and research, where correct classification of a subject is essential for accurate phenotype based investigations. In the case of COPD, severity is classified according to the guidelines laid out by the Global Initiative for Chronic Obstructive Lung Disease (GOLD) which utilises post-bronchodilator lung

function tests (spirometry) to classify increasing COPD severity (Table 1.2) (Vestbo et al., 2012, GOLD, 2011).

COPD Severity	Spirometry
I. Mild	$FEV_1/FVC < 0.7$ $FEV_1 \geq 80\%$ predicted
II. Moderate	$FEV_1/FVC < 0.7$ $50\% \leq FEV_1 < 80\%$ predicted
III. Severe	$FEV_1/FVC < 0.7$ $30\% \leq FEV_1 < 50\%$ predicted
IV. Very Severe	$FEV_1/FVC < 0.7$ $FEV_1 < 30\%$ predicted *or* $FEV_1 < 50\%$ predicted plus chronic respiratory failure

Table 1.2: GOLD classification of COPD severity. COPD severity diagnosis is based on spirometry readings utilising the FEV_1/FVC ratio in conjunction with FEV_1 percentage predicted.

1.2.3 DIAGNOSIS AND TREATMENT OF COPD

According to GOLD, and as in asthma, the diagnosis of COPD is based on an initial diagnosis of phenotypic changes, which is then confirmed through spirometry. Initial phenotypes which may indicate the presence of COPD and which warrant spirometry testing include dyspnoea, chronic cough, and chronic sputum production, a history of exposure to risk factors such as tobacco smoke and a family history of COPD. The detection of a post-bronchodilator FEV_1/FVC of <0.70 via spirometry then confirms the presence of persistent airflow limitation and therefore of COPD (GOLD, 2011). Patients with severe COPD can additionally present with fatigue, weight loss and anorexia (Schols et al., 1993).

The first aim of COPD treatment is smoking cessation (or prevention of inhalation of other irritating substances), usually requiring the aid of nicotine replacement therapy in various forms such as inhalers, sprays, gum and patches. Direct pharmacological therapy for COPD is aimed at reducing the symptoms of COPD as well as the frequency and severity of exacerbations along with improving health status and exercise

tolerance (GOLD, 2011). At the time of writing, no therapy is available that has successfully improved the long term decline in lung-function that is symptomatic of COPD identifying that current therapy is still far from optimal and that further development of novel COPD therapies is essential for optimal COPD therapy.

Pharmacotherapy in COPD is, as in asthma, also based on exacerbations and the degree of breathlessness. Therapy involves the use of bronchodilators (e.g. long and short acting β_2-agonists, short and long acting anti-muscarinics, methylxanthines), glucocorticosteroids (anti-inflammatories) as well as the phosphodiesterae-4 inhibitor Roflumilast for exceptionally severe COPD. Therapy is administered in a step-wise approach similar to asthma, with different types of medication administered either alone or in combination (GOLD, 2011) (Table 1.3).

Therapy	
Short-acting β_2-agonist inhaler or **Short-acting antimuscarinic inhaler** As required	First Symptoms
Long-acting anti-muscarinic inhaler or **Long- acting β_2-agonist inhaler**	FEV$_1$≥50pp
Long- acting β_2-agonist +corticosteroid inhaler	FEV1≥50pp & still symptomatic with long-acting β_2-agonist inhaler
Long-acting anti-muscarinic inhaler or **Long- acting β_2-agonist +corticosteroid inhaler**	FEV$_1$≤50pp
Long-acting anti-muscarinic inhaler and **Long- acting β_2-agonist +corticosteroid inhaler**	FEV$_1$≤50pp and still symptomatic
Oral Theophylline/Aminophylline	Still symptomatic
Phosphodiesterae-4 inhibitors (Roflumilast)	Severe chronic obstructive pulmonary disease associated with chronic bronchitis and a history of frequent exacerbations

Table 1.3: Step-wise pharmaceutical therapy in COPD. Management of COPD follows a step-wise approach with the strength and number of medications increasing as one attempts to achieve symptomatic control, followed by down-stepping therapy on resolution of symptoms to attempt to achieve control using the minimal amount of medication. Therapy involves the use of inhaled bronchodilators (short and long acting β_2-agonists, short and long acting anti-muscarinics and methylxanthines), inhaled glucocorticosteroids (anti-inflammatory) in combination therapy with long-acting β_2-agonists, while use of the phosphodiesterase-4 inhibitor Roflumilast is limited to severe exacerbations of COPD. Data obtained from the British National Formulary (BMA., 2012)

1.3 THE GLOBAL BURDEN OF ASTHMA AND COPD

Both asthma and COPD are global problems. The WHO estimates that asthma affects around 235 million people worldwide while COPD affects 64 million people worldwide (2004 figures).

In the UK around 5.4 million people currently receive treatment for asthma (1.1 million children (1 in 11) and 4.3 million adults (1 in 12)), with 1,131 asthma related deaths reported in 2009. Asthma cost the UK economy up to 1.1 million working days in 2008/9 and also presents a burden to the NHS, with an estimated 79,794 emergency hospital admissions occurring in 2008/9 and costing the NHS £1 billion per year for treatment and care (AsthmaUK, 2012). Currently around 1 million people are known to suffer from COPD in the UK resulting in approximately 30,000 COPD related deaths per year, however this may be a gross underestimation as around 2 million people are thought to be living with the disease but are currently undiagnosed (HSE, 2011, NHS, 2010). The rate of mortality in the UK is double the European average, being the fifth leading cause of death in the UK. COPD, like asthma, presents a burden to the NHS, with 1 in 8 (*circa.* 130,000) emergency hospital admissions being for COPD, making it the second largest cause of emergency admission in the UK, and one of the most costly inpatient conditions treated by the NHS (BLF, 2008). Economically, the total cost of COPD to the NHS was estimated, in 2000-01, to be around £500 million for direct costs and around £1 billion when including indirect costs (NICE, 2010).

1.4 AIRWAY REMODELLING IN ASTHMA AND COPD

As discussed in Sections 1.1.1 and 1.2.1, the development of both asthma and COPD results in a degree of airway remodelling, where although an amount of overlap occurs between both diseases, airway remodelling remains distinct between asthma and COPD (see below and Table 1.4) (Dournes and Laurent, 2012). The structural changes that define airway remodelling are an important feature in the airways of asthmatics and COPD patients (Postma and Timens, 2006), where even in newly diagnosed asthma patients, a degree of structural changes can be identified on the bronchial wall (Laitinen et al., 1993). Airway remodelling can be defined as a process of sustained disruption and modification of structural cells and tissues leading to the development of a new airway wall morphology (O'Donnell et al., 2002). The main airway structural changes common to both asthma and COPD are airway fibrosis, elevated smooth muscle mass, mucous metaplasia and glandular hypertrophy (O'Donnell et al., 2002, Elias et al., 1999). In both cases, airway remodelling is initiated either through various inflammatory pathways, highlighting the importance of the inflammatory pathway in both diseases (Jeffery, 1998), or through bronchial hyper-responsiveness, where airway remodelling occurs independently of inflammation (Grainge et al., 2011). Initiation of airway remodelling differs between asthma and COPD, with initiation stemming from deregulated injury and/or repair mechanisms in the asthmatic airway leading to permanent changes in the airway physiology. In COPD on the other hand, initiation is almost an exclusive reaction to the toxic effects of cigarette smoke. The outcomes of airway remodelling also differ between disease states. In asthma, structural changes involve the sloughing and denudation of the airway epithelium with thickening of the sub-epithelial basement membrane, diffuse excess matrix deposition in the large airways and increased vascularity in the large airway wall. In COPD however, there is squamous metaplasia of the epithelium and diffuse excess matrix

deposition in the small airways with no effect on the sub-epithelial basement membrane and large airway vascularity (O'Donnell et al., 2002). These structural changes ultimately lead to increased bronchial hyper-reactivity and therefore a worsening of the disease state (Chetta et al., 1997).

	Asthma	COPD
Initiation	Deregulated injury/repair mechanisms	Inhaled Irritants (e.g. Cigarette Smoke)
Airway smooth muscle	Hyperplasia	
Mucus layer	Hyperplasia and Hypersecretion	
Fibrosis	Fibrosis of the airway walls	
Airway Epithelium	Sloughing and denudation	Squamous Metaplasia
Extracellular Matrix	Excess deposition in the large airways	Diffuse excess deposition
Airway Vascular system	Increased Vascularity	No effect
Basement Membrane	Thickening	No effect

Table 1.4: **Airway structural changes defining airway remodelling in asthma and COPD.** Although certain aspects such as hyperplasia of the airway smooth muscle layer, the presence of fibrosis on the airways and hyperplasia of epithelial cells resulting in mucus hypersecretion are common to both asthma and COPD, differences in changes occurring in the airway epithelium, extracellular matrix, basement membrane and airway vascular system makes airway remodelling in asthma separate and distinct from that in COPD.

1.5 GENETICS OF ASTHMA AND COPD

Genetics plays an important role in both asthma and COPD, as identified by the strong hereditary component present in asthma (approximately 25% of the offspring of an asthma patient will have asthma (Panhuysen et al., 1998)) and the lack of consistency between smoking and COPD, i.e. not all smokers contract COPD and not all COPD sufferers are smokers (Mannino, 2002). Multiple genetic studies have been carried out in asthma and COPD throughout the years, confirming the role of genetics in asthma and COPD and identifying and investigating a number of disease relevant genes (see Table 1.5).

Gene Family	Examples
Controlling the development and regulation of the immune response	*GATA3, TBX21, IL4, IL4RA, STAT6, and IL12B*
Involved in inflammation	*ALOX-5, IL-1825 and IL18R126*
Involved in the detection of pathogens and allergens	*TLR2, TLR4, TLR6, TLR10, and NOD1/CARD4*
Involved in mediating the response to allergic inflammation and oxidant stress on the tissue level	*ADAM33, COL6A5, DPP10 and GPRA*
Involved in the constriction of the airways	*PDE4D, CHRNA3/5 and NOS1*
Involved in the catalysation of enzymatic reactions	*AGPHD1, IRES2*
Involved in signal cascades	*CHRNA3, HHIP*

Table 1.5: **Examples of genes associated with asthma and COPD.** Genes known to be involved with obstructive respiratory disease come from various pathways and regulate various outcomes. Data obtained from (March et al., 2013, Siedlinski et al., 2013, Cho et al., 2012).

An important example is the association of α_1-antitrypsin (AAT) deficiency to early onset emphysemia, making it a genetic risk factor for COPD (DeMeo and Silverman, 2004, Janciauskiene et al., 2011). Here absence of the α1 band following electrophoresis is associated with the development of emphysemia (probably through an increase in levels of neurophil elastase), with severe pulmonary impairment expected if the levels of serum AAT go below the protective threshold of 35% of the

normal mean value (≤0.8 mg/ml or ≤ 11 μmol/L) (Janciauskiene et al., 2011). Although used clinically as a diagnoistic test, this mutation is only present in around 1-2% of COPD patients highlighting that obstructive lung disease has multiple genetic contributions to its development (DeMeo and Silverman, 2004).

Initial genetic studies into asthma and COPD have utilised familial aggregation and twin studies, studies which are useful in determining whether a trait has a suitable genetic component. The familial aggregation of asthma and COPD has been described in a number of early studies (Higgins and Keller, 1975, Sibbald and Turner-Warwick, 1979, Silverman et al., 1998, McCloskey et al., 2001) as was the higher concordance of asthma in monozygotic twins when compared to dizygotic twins (Edfors-Lubs, 1971, Duffy et al., 1990).

Early segregation studies led investigations into whether a major gene affects the distribution of a given phenotypic trait as well as defining the Mendelian mode of inheritance. Via these segregation studies, a strong familial component to asthma (Martinez and Holberg, 1995) and COPD (Wang et al., 2008) was identified, where, within these studies, the genes for the plasminogen activator (*PLAU*), the urokinase plasminogen activator receptor (*PLAUR*), and thrombospondin (*THBS1*) were identified as being genes associated with the obstructive lung diseases. Candidate gene studies on genes to either have a role in disease (functional) or linked to a region of interest (positional) provide information on the genetic role in modulating disease severity, progression and therapy. Examples include studies on the β2-adrenergic receptor gene (*ADRB2*) and on 5-lipoxygenase inhibitors (5LOIs) in asthma (Reihsaus et al., 1993, Drazen, 1998) and on the *MMP1* and *IL13* genes in COPD (Joos et al., 2002, van der Pouw Kraan et al., 2002).

More recent genetic studies have involved the use of genome-wide association studies (GWAS). This form of analysis allows for a hypothesis free mapping of asthma and

COPD genes and has identified among others, hits on chromosomes 2, 4, 5, 9, 12 and 15 as novel polymorphisms associated with asthma (CSGA, 1997, Moffatt et al., 2010, Himes et al., 2013, Hao et al., 2012) and hits on chromosomes 2, 4, 5, 12, 19 and 22 as novel polymorphisms associated with COPD (Silverman et al., 2002, Palmer et al., 2003, DeMeo et al., 2004, Soler Artigas et al., 2011). GWAS investigations have also identified hits on chromosomes 2, 3, 4, 5, 6, 12 and 15 to be associated with changes in lung function, identifying further potential targets for interventions to alleviate respiratory disease (Repapi et al., 2010).

Genetic based investigations of asthma and COPD does not only allow for the furthering of our understanding on diseases function, but also provides a medium for the detection of novel diagnostic tests and novel therapeutic targets for disease management. This emphasises the importance of genetics based investigations into the disease as laid out in this thesis.

1.6 COAGULATION AND FIBRINOLYSIS IN ASTHMA & COPD

The coagulation pathway describes the laying down of fibrin clots through the activation of Thrombin via an activation cascade of blood factors, which in turn activate fibrinogen to form fibrin (Fig. 1.4). The fibrinolysis system is the complementary degradation pathway to the coagulation system where activation of the enzyme plasmin from its precursor plasminogen, mainly driven by the urokinase plasminogen activator and its receptor, results in the digestion of fibrin into fibrin degradation products (Fig. 1.4).
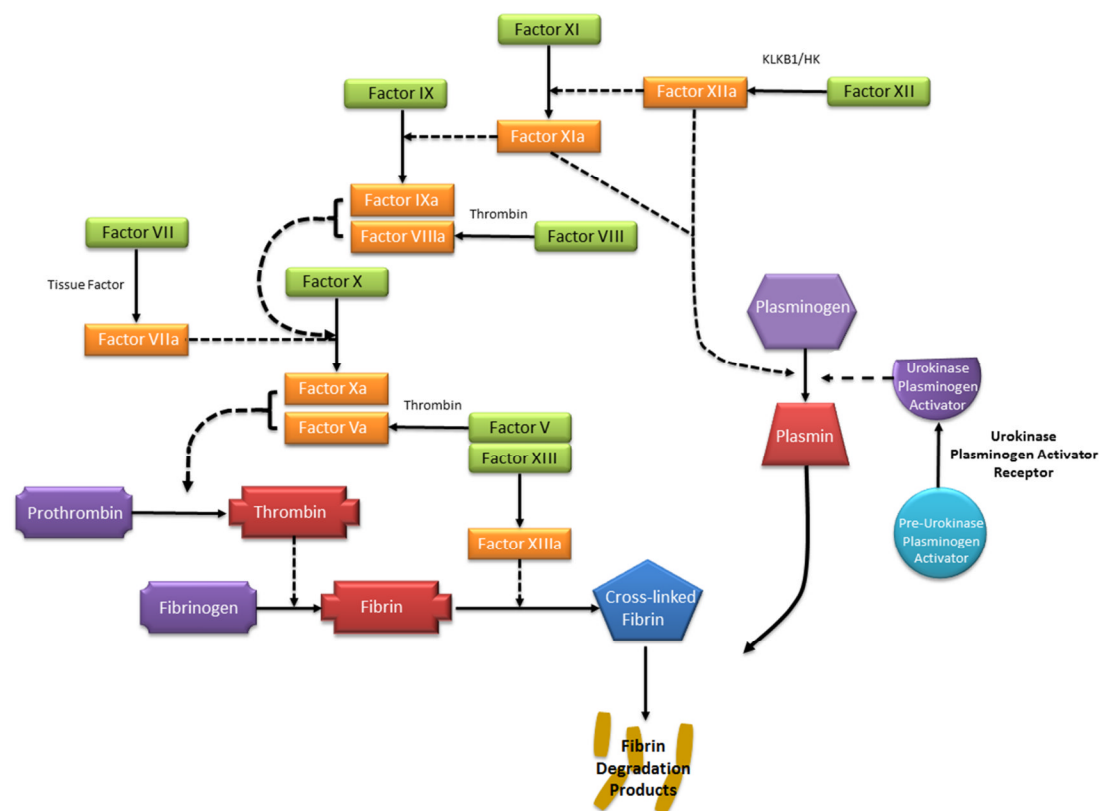
Figure 1.4: The coagulation/fibrinolysis pathway. These pathways concentrate on the formation and degradation of fibrin plaques in the body. Activation of thrombin from its precursor prothrombin via the intrinsic (Factor VII) and extrinsic (Factors V-XIII) coagulation cascades results in the formation of cross-linked fibrin plaques. These plaques are susceptible to fibrinolysis by plasmin which is activated from its precursor plasminogen via activated factors XI and XII as well as by the urokinase plasminogen activator, which is activated via its receptor (PLAUR). KLKB1: Human Plasma Kallikrein; HK: High molecular weight kininogen.

Although the respiratory and coagulation/fibrinolysis system have historically been considered to be separate compartments within the body, the human airways are now considered as a respiratory organ where plasma exudation from the bronchial microvasculature occurs (Rogers and Evans, 1992, Persson, 1986) and in which coagulation and anticoagulation mechanisms can be initiated and regulated locally (de Boer et al., 2012). This coagulation/fibrinolytic system has been implicated in both asthma and COPD (Polosa et al., 2011, de Boer et al., 2012) with pro-coagulant activity and impaired fibrinolysis being described as important early findings in the distal airspaces of patients with lung injury, predisposing the airways to fibrin deposition and alveolar epithelial injury (Idell, 2002, Ware et al., 2003). Indeed cardiovascular events such as deep vein thrombosis and pulmonary emboli have been shown to be a major cause of morbidity and mortality in COPD and asthma (Curkendall et al., 2006, Huiart et al., 2005, Sidney et al., 2005).

However, the risk in asthma and COPD due to effects driven by the blood coagulation/fibrinolysis pathway is not limited to the increased risk in cardiovascular events. Pulmonary coagulation and fibrinolysis arising from crosstalk between epithelial, endothelial and inflammatory cells has been shown to have a major impact on the pathophysiology of both COPD and asthma. In COPD, Polosa *et al.* identified that fibrinolytic markers such as von Willebrand factor and prothrombin fragments 1 and 2 were elevated during disease exacerbation (Polosa et al., 2011), while an imbalance between blood coagulation and anticoagulation factors versus oxidative stress has been reported in COPD patients suffering from acute exacerbations (Huang et al., 2011). In asthma, activated Factor X has been shown to be involved in airway remodelling in an ovalbumin-induced asthma mouse model through the stimulation of mucin production, regulation of amphiregulin expression and collagen deposition (Shinagawa et al., 2007), while activated Factor VII has been shown to function in the

allergic asthmatic response via stimulating lung eosinophilia and airway hyper-responsiveness (Shinagawa et al., 2009).

Studies have suggested that the major effects of the coagulation/fibrinolysis pathway on obstructive airway disease are abnormalities that result in greater fibrin deposition and/or reduced fibrinolysis. This hypothesis was suggested by Wagers *et al.* on discovery that increased fibrin deposition on the luminal surface of the airway epithelium was apparent in a patient who died in *status asthmaticus* and that increasing airway hyper-responsiveness was apparent in 'wild type' mice challenged with aerosolised fibrinogen and thrombin, with the authors concluding that increased fibrin in the airways significantly contributed to airway hyper-responsiveness in asthma (Wagers et al., 2004). This hypothesis was supported by a study carried out by Brims *et al.*, which identified that severe asthmatics had higher levels of various components of the coagulation/fibrinolysis pathways in their sputum than control subjects. These included tissue factor, which activates fibrin deposition, as well as plasminogen activator inhibitor 1 and thrombin activatable fibrinolysis inhibitor, which inhibit fibrinolysis (Brims et al., 2009). The discovery that mice deficient in thrombin activatable fibrinolysis inhibitor, an important regulator of fibrinolysis, had enhanced airway hyper-responsiveness and lung injury in an ovalbumin-induced asthma model (Fujiwara et al., 2012) further suggests that deregulation of the fibrin/fibrinolytic pathways is important to changes occurring within the lung.

Apart from the effects caused by increased fibrin deposition in the airways, the fibrinolytic system is also able to affect obstructive respiratory disease through its effect on airway remodelling, which occurs via the molecule plasmin (Kucharewicz et al., 2003). The effect of plasmin on airway remodelling is driven by direct degradation of the extracellular matrix (ECM) and indirect degradation through the regulation of a

number of other molecules such as the activation and inhibited of deactivation of MMPs (Cho et al., 2000) and the release of leukotriene B4 (Weide et al., 1994).

Therefore, through its effect both on fibrin deposition and airway remodelling the coagulation/fibrinolytic pathway plays an important role in the development and modulation of the obstructive airway diseases asthma and COPD. Therefore a better understanding of different components of these pathways would potentially further aid our understanding of the development and modulation of asthma and COPD. It could also potentially identify novel targets for asthma and COPD therapeutics, especially with regards to airway remodelling, which is not adequately targeted using current therapeutics. This thesis has focussed on the plasminogen activator receptor (PLAUR; also known as uPAR, CD87 & MO3), an important receptor involved in the fibrinolysis pathway through the activation of pro-urokinase to active urokinase, which leads to the formation of plasmin from its precursor plasminogen and subsequent fibrinolysis (see Section 1.7.1) (Blasi and Carmeliet, 2002). Apart from its involvement in the fibrinolytic pathway, selection of PLAUR was based on other supporting evidence outlined in Section 1.6.

1.7 PLAUR IN OBSTRUCTIVE RESPIRATORY DISEASE

Apart from the suggested importance of the fibrinolytic pathway in the obstructive respiratory diseases asthma and COPD (see Section 1.5), interest in PLAUR stems from work carried out by colleagues in the Therapeutics and Molecular Medicine laboratory, which identified *PLAUR* as an asthma susceptibility gene in 587 asthma families (Barton et al., 2009). The same study identified that single nucleotide polymorphisms (SNPs) across the *PLAUR* gene and its 5`UTR and 3`UTR were associated with asthma, BHR susceptibility, baseline lung function and lung function decline in populations originating from multiple centres as well as serum levels of PLAUR (Barton et al., 2009). A follow on study on the same 25 SNPs in a population of 992 smokers identified association with baseline lung function (Stewart et al., 2009). Association with an alternate obstructive lung disease, i.e. COPD, was determined in an independent study by Wang *et al.*, where through gene expression profiling and lung function studies in 43 COPD subjects, *PLAUR* was found to be involved in lung tissue remodelling and repair and was determined to differentially express *PLAUR* in the COPD lung when compared to controls (Wang et al., 2008). Interestingly, the association of PLAUR to COPD was found to be independent of the smoking pack/year status (Wang et al., 2008).

Further evidence for the role of PLAUR in obstructive lung disease has been published in a number of *in vitro* and *ex vivo* studies. While membrane PLAUR has been shown to be standardly expressed in the apical membrane of the airway epithelium (Drapkin et al., 2000), levels were elevated in the inflamed asthmatic epithelium when compared to healthy controls (Stewart et al., 2012, Beaufort et al., 2007) and in COPD subjects when compared to controls (Wang et al., 2008) (Fig. 1.5). PLAUR was also elevated in the lungs of patients who died of *status asthmaticus* when these were compared to the airways obtained from 7 lung donors without a diagnosis of asthma (Chu et al., 2006).

In an *in vitro* study using normal human bronchial epithelial cells (NHBECs), mechanical stimulation of cells in order to mimic the process that occurs in the lung during bronchoconstriction, an important event in both asthma and COPD, resulted in a 16.2 fold increase in the expression of PLAUR mRNA in conjunction with the elevation of other molecules involved in the fibrinolytic pathway, such as PLAU and PAI-1 (Chu et al., 2006). This evidence suggests that PLAUR may be involved in asthma and COPD pathogenesis, where elevated PLAUR levels could cause changes in the airways synonymous with both asthma and COPD, a hypothesis supported by Brooks *et al.* who identify PLAUR as a potential marker of airway disease severity (Brooks et al., 2006).
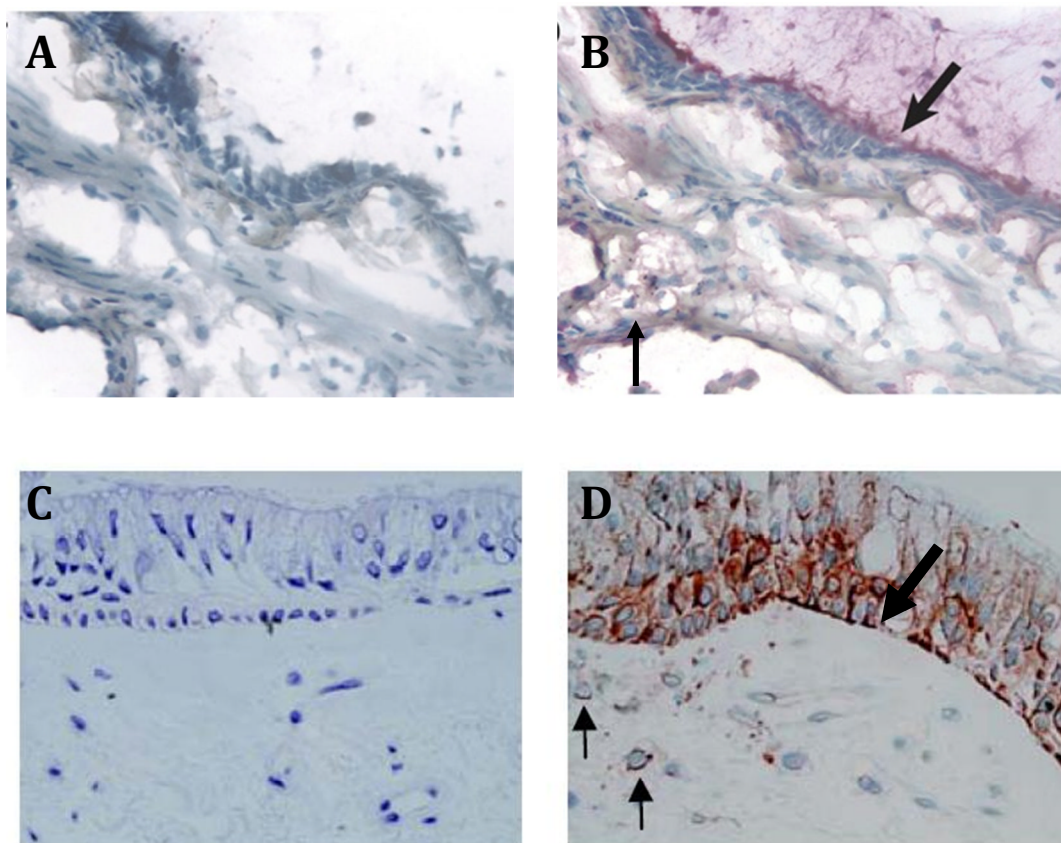
Figure 1.5: Elevated levels of PLAUR are present in the asthmatic and COPD lung. Immunohistochemistry identifies elevated levels of PLAUR in the epithelial layer (identified by the large arrows) of the COPD (Panel B) and asthmatic (Panel D) lung when compared to their respective controls (Panels A & C). Elevations can also be identified in the lamina propia (submucosal layer; small arrows Panels B & D). Figure adapted from (Wang et al., 2008, Stewart et al., 2012).

Although evidence has identified that the expression of PLAUR by structural cells in the airways is altered in asthma and COPD, it is pertinent to mention that elevated levels of

the receptor have also been identified in other peripheral cells. In COPD subjects, levels of membrane bound PLAUR expressed on neutrophils and macrophages were found to be significantly elevated when compared to controls (Jiang et al., 2010). Interestingly, this elevation occurred in COPD patients irrespectively of their smoking history, a result also identified by another group (Wang et al., 2008), suggesting that PLAUR is not simply elevated due to exposure by disease initiating factors such as cigarette smoke but rather is likely to play a direct role in disease pathophysiology.

A direct role for PLAUR in obstructive respiratory disease has in fact been suggested by Wang *et al.*, where the authors identify that PLAUR is involved in lung tissue remodelling and repair in COPD subjects. This hypothesis that PLAUR is involved asthma and COPD pathophysiology through a direct role in airway remodelling is further supported by a number of other studies. Elevated PLAU and PAI-1 in the airways post injury (Heguy et al., 2007), the discovery that PLAUR is critical for efficient bronchial wound repair *in vitro* and that inhalation of PLAU protects against sub-epithelial fibrosis and airway hyper-responsiveness in an asthma mouse model (Kuramoto et al., 2009), identifies that the pathway involving PLAUR is likely important in airway injury. Airway injury and the dysregulation of repair are prevalent in asthma and COPD and are known to have a role in airway remodelling during disease development.

Although most studies have concentrated on membrane bound PLAUR, there has also been interest in the role of the soluble cleaved form of the receptor (see Section 1.8.3.2) in asthma and COPD. However as of writing, this has been a limited interest, with only two studies carried out. Both these studies identify elevated soluble cleaved PLAUR (scPLAUR) in the induced sputum of asthmatic and COPD patients (Xiao et al., 2005, Jiang et al., 2010), with levels associated with airflow limitation, health status and exercise tolerance in COPD patients (Jiang et al., 2010). This suggests that identified

PLAUR dependant effects may be at least partially driven by the soluble cleaved form of the receptor, a situation previously hypothesised in a human bronchial epithelial cell population (Stewart et al., 2012).

1.8 PLAUR ACTIVITY

Since the discovery of PLAUR in 1985 (Vassalli et al., 1985), a substantial amount of literature has accumulated, identifying a role for the membrane bound and soluble cleaved form of this protein in a range of biochemical processes. PLAUR is known to carry out this role through either the regulation of pericellular plasminogen activation (Ellis et al., 1992) or through various non-proteolytic functions through the interaction with a number of cell bound processes (Ploug, 2003).

1.8.1 PROTEOLYTIC FUNCTIONS

PLAUR binds the serine protease PLAU or its zymogen pro-PLAU with very high affinity (1nM) and specificity (Ploug, 2003, Smith and Marshall, 2010, Blasi and Carmeliet, 2002) through utilisation of PLAU's amino-terminal fragment (ATF) (Huai et al., 2006, Llinas et al., 2005). Binding of PLAU to PLAUR results in the conversion of the inactive single-chain pro-PLAU into the active two-chain PLAU by a single proteolytic event (Blasi and Carmeliet, 2002) (Fig. 1.6). Therefore cell functions regulated by PLAU come under indirect regulation by PLAUR via its proteolytic role on this molecule.

In the lung, PLAU is primarily involved in chemotaxis and airway remodelling through the activation of the plasminogen activation pathway (Kucharewicz et al., 2003). Once activated, PLAU converts plasminogen into plasmin (Blasi and Carmeliet, 2002) and so in turn activates the plasminogen activation system (PAS). Activation of the PAS then results in:

- Fibrin degradation (Connolly et al., 2010)
- Activation of a number of growth factors and pro-inflammatory cytokines such as TNFα, IL-1α & IL-1β (Rabbani and Mazar, 2001, Syrovets et al., 2001)
- Chemoattraction resulting in neutrophil infiltration (Rijneveld et al., 2002)

- Remodelling of the extracellular matrix (ECM) through the removal of ECM glycoproteins

- Activation of MMPs (Behrendt, 2004, Kjaergaard et al., 2008, Kucharewicz et al., 2003)

- Phagocytic clearance of apoptotic cells (D'Mello et al., 2009, Park et al., 2009)

The activation of the PAS therefore has an important effect on cell and tissue, function especially in the case of airway remodelling (Kucharewicz et al., 2003), highlighting the importance of PLAUR in the modulation of asthma and COPD (see Section 1.6).
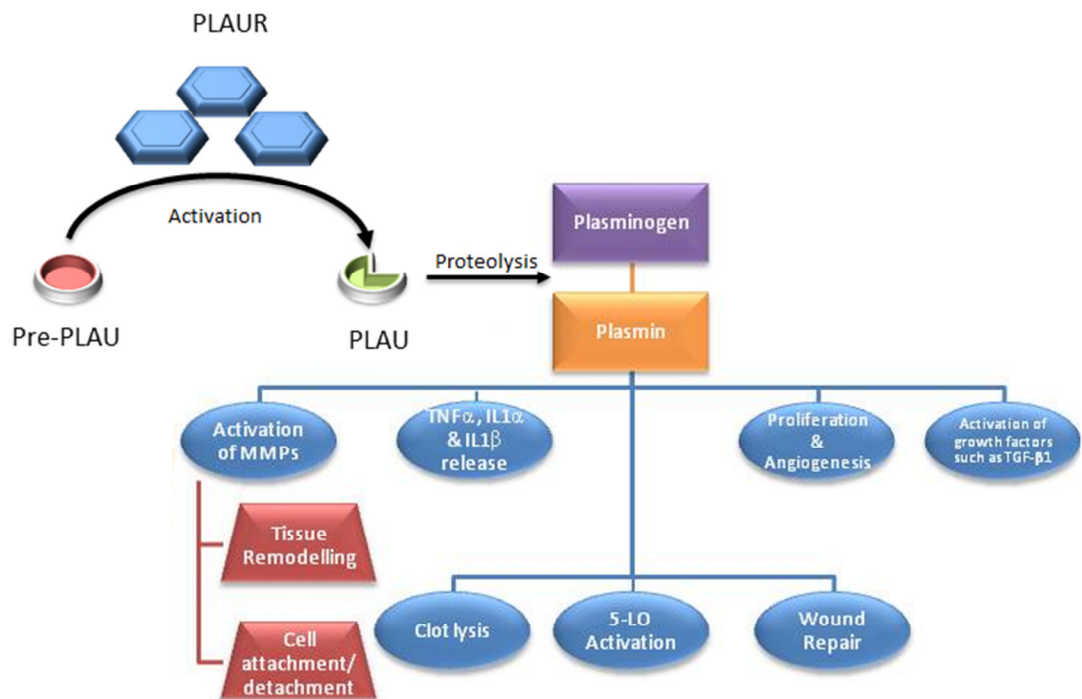
Figure 1.6: PLAUR activates urokinase from pre-urokinase, which proteolytically cleaves plasminogen to form plasmin, thereby activating the plasminogen plasmin cascade. Activation of the plasminogen-plasmin cascade results in a number of downstream functions such as the activation of MMPs, release of inflammatory factors including TNFα, IL1α and IL1β and activation of growth factors such as TGFβ1 as well as the regulation of a number of downstream effects such as fibrinolysis, wound repair, cell proliferation and angiogenesis.

1.8.2 NON-PROTEOLYTIC FUNCTIONS

Since PLAUR is attached to the outer leaflet of the phospholipid bilayer of the cellular membrane via a glycosylphosphatidylinositol (GPI) anchor, the receptor has no part of its protein structure exposed to the cellular cytoplasm (Kjaergaard et al., 2008). This

therefore means that PLAUR *a priori* is unable to elicit transmembrane responses without the aid of other cell-membrane bound proteins (Ploug et al., 1991b).

However, PLAUR is still able to elicit other responses independent of the PAS by also interacting with a number of other cell factors, such as:

- Vitronectin (VN) (Wei et al., 1994, Hoyer-Hansen et al., 1997a)

- Integrins, including the β_1 β_2 β_3 families, Mac1, $\alpha_M\beta_2$ and $\alpha_v\beta_5$ (Wei et al., 1996, Xue et al., 1997, Xue et al., 1994, Blasi and Carmeliet, 2002)

- G-protein coupled receptors (GPCRs) such as formyl peptide receptor-like 1 (FPRL1) (Resnati et al., 1996, Resnati et al., 2002)

- Epidermal growth factor receptor (EGFR) (Resnati et al., 2002)

- High molecular-weight kininogen (HKa) (Colman et al., 1997, Chavakis et al., 2000)

The importance of these cell associated factors in relation to PLAUR is twofold. Primarily the independent activities of these cell factors are regulated by PLAUR, and secondarily, they also help transduce PLAUR mediated intracellular signal-transduction pathways that involve cytosolic and transmembrane kinases and cytoskeletal components among others (Fig. 1.7) (Blasi and Carmeliet, 2002).

PLAUR binding to cell-associated factors leads to important downstream events such as the increased cellular proliferation on interaction with the $\alpha_5\beta_1$ integrin (Aguirre Ghiso et al., 1999) and regulation of the chemotactic activity of the full length receptor and D_{II}/D_{III} fragment of PLAUR via FPRL1 (Resnati et al., 2002, Blasi and Carmeliet, 2002). Stimulation of cell signalling pathways plays an important role in the non-proteolytic function of PLAUR with stimulation of pathways such as ERK1/2 and the JAK1/STAT1 pathway resulting modulation of cell proliferation (Aguirre Ghiso et al.,

1999, Koshelnick et al., 1997) and downstream up-regulation of various early response oncogenes such a c-myc, c-fos and c-jun (Mazar et al., 1999) (Fig.1.7).
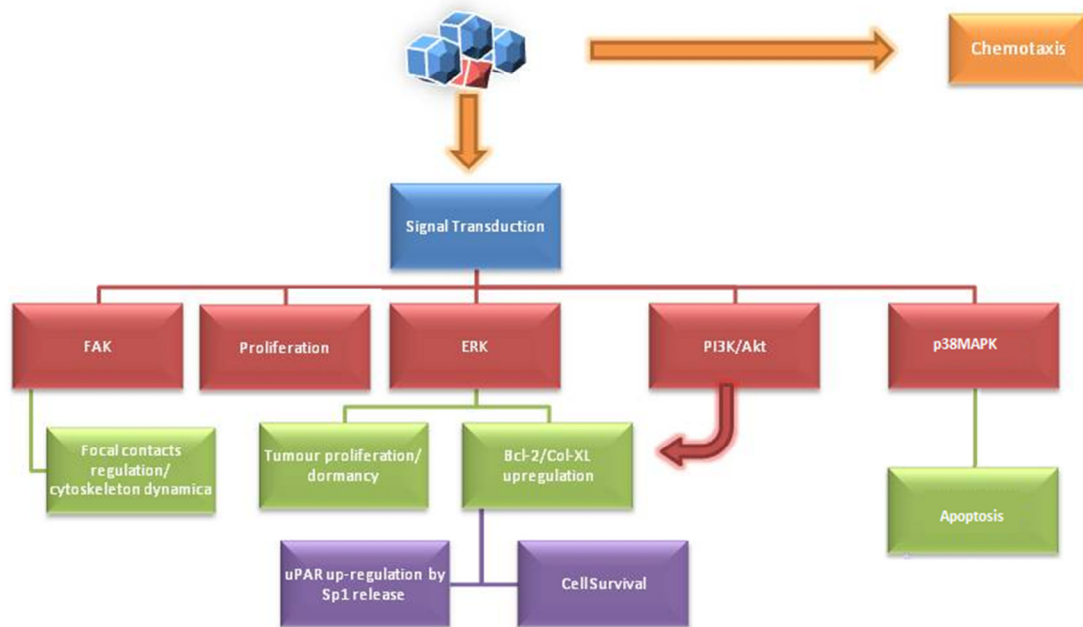
Figure 1.7: Cell signalling cascades regulated via PLAUR. PLAUR activates cell signalling cascades through the interaction of the receptor with a number of cell co-factors including integrins, GPCRs and high molecular weight kininogen. Activation of these cell signalling pathways (FAK, ERK, PI3K) results in the regulation of a number of cellular processes such cytoskeleton dynamics, proliferation and cell survival.

1.8.3 NATURAL PLAUR INHIBITORS

PLAUR has been shown to be regulated by two specific receptor inhibitors, namely plasminogen activator inhibitor type-1 (PAI-1) and type-2 (PAI-2) (Irigoyen and Nagamine, 1999, Kruithof, 1988). These are mainly synthesised by the endothelium, platelets, megakaryocytes, neutrophils, monocytes, mast cells, smooth muscle cells and fibroblasts (Sillaber et al., 1999, Simpson et al., 1991, Kim et al., 2011, Cho et al., 2004). Both PAI-1 and PAI-2 are members of the Serpine Family (Loskutoff et al., 1999) differing in terms of secretion, localisation and stability (Blasi and Verde, 1990, Vassalli et al., 1991), with PAI-1 having an efficiency 20 to 100 times greater than that of PAI-2 (Kruithof et al., 1986).

PAI-1 and PAI-2 both inhibit binding of the pro-PLAU zymogen and therefore inhibit activation of the plasminogen activation pathway and antagonise the proteolytic function of PLAUR (Kruithof, 1988, Irigoyen and Nagamine, 1999). However, PAI-1 also regulates other PLAUR mediated cell effects, such as chemotaxis, through the active competition with VN for its binding site (Stefansson and Lawrence, 1996) and the promotion of internalisation of the PLAU-PLAUR complex. This internalisation occurs via the low-density lipoprotein (LDL)-receptor-related protein (LRP) with the resulting immunoprecipitation of PLAU and recycling of free PLAUR to the cell surface (Czekay et al., 2001). Therefore the plasminogen activator inhibitors have a dual role in not only antagonising PLAUR's proteolytic functions but also antagonising its non-proteolytic ones, by making the receptor unavailable to cell bound factors such as GPCRs and integrins.

The role of PAI-2 however is poorly understood (Lee et al., 2011, Medcalf, 2011). Studies have been limited to downstream function, identifying that PAI-2 is a modulator of monocyte adhesion, proliferation and differentiation (Yu et al., 2002) while protecting cells from cytolysis and apoptosis (Kumar and Baglioni, 1991, Dickinson et al., 1995, Fish and Kruithof, 2006) and providing a control mechanism for PLAU dependant ECM degradation (Montemurro et al., 1999).

1.9 THE UROKINASE PLASMINOGEN ACTIVATOR RECEPTOR

1.9.1 GENE STRUCTURE AND RECEPTOR SPLICE VARIANTS

PLAUR is encoded by a gene located on chromosome 19q13 and is present on the anti-sense strand of the human genome (Casey et al., 1994). Its transcriptional start site (TSS) was determined in a number of cells and tissues and shown to vary between -45 and -69 base pairs relative to the translation start site (ATG) (Wang et al., 1995, Stewart and Sayers, 2009). The *PLAUR* gene in its full form consists of 7 exons; of these, exon 1 encodes the five prime untranslated region (5`UTR) and a signal peptide, while exons 2-3, 4-5 and 6-7 respectively encode the homologous protein domains D_I, D_{II} and D_{III} (Casey et al., 1994) (Fig. 1.8).

Various splice variants of the receptor are known to exist. The splice variant causing the greatest change in protein structure is the relocation of the terminal exon (Exon 7 to form alternate Exon 7b; see Fig. 1.8). While still encoding for a structure containing 3 globular domains, in this splice variant the amino acid sequence from position 254 is completely different to that of the full length receptor. This translates into a structurally different terminal domain (D_{III}) which is different to that of the full-length membrane PLAUR (mPLAUR). The amino acid sequence is also significantly shorter, having a full length of 281 amino acids compared to the 335 amino acid length of mPLAUR. The significantly shorter length of the Exon 7b splice variant means that this splice variant lacks the GPI anchor (Pyke et al., 1993) and so results in the formation of an alternate soluble form of the receptor (soluble spliced PLAUR: ssPLAUR). This soluble spliced receptor is expressed in various human cell lines and tissues (e.g. human airway smooth muscle cells (HASMs) and NHBECs) and is up-regulated by phorbol ester in A549 cells (Pyke et al., 1993, Stewart and Sayers, 2009). Alteration of

one of the receptor's globular domains will also affect the PLAUR ligands specific to this region (Colman et al., 1997). However, by retaining an intact D_I region, it is probable that some PLAU binding activity is retained (Luther et al., 2003), albeit not at the same affinity as offered by mPLAUR (Blasi and Carmeliet, 2002). At the time of writing work has been limited on the soluble spliced PLAUR and the function of this receptor remains relatively unknown.
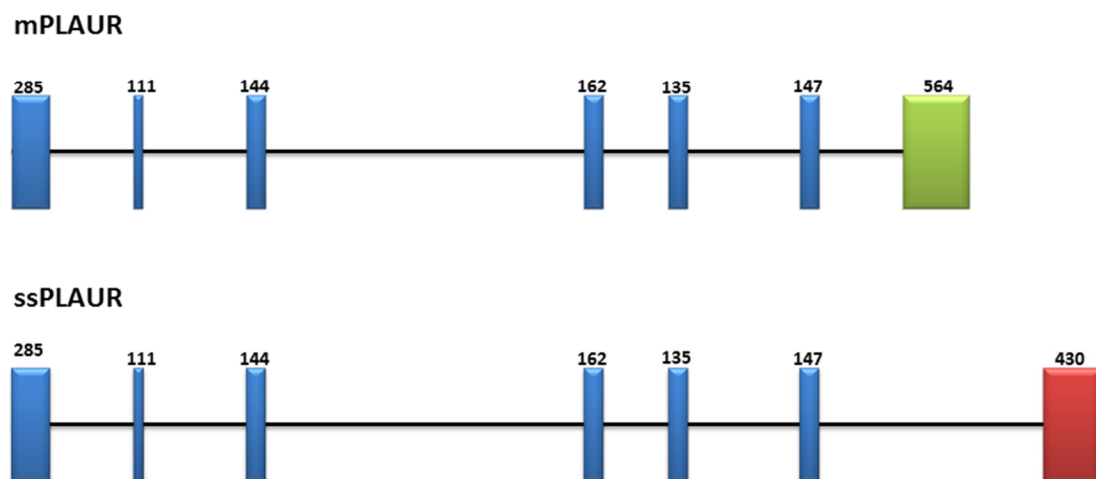
Figure 1.8: Alternate gene structures for the most common variants of the PLAUR gene (mPLAUR & ssPLAUR). THE *PLAUR* gene consists of 7 exons containing one of two terminal exons (Exon 7). The standard Exon 7 (Exon 7a; 564bp) codes for the membrane bound protein, while the smaller alternate exon (Exon 7b; 430bp) is located at a further distal region than Exon 7a and codes for an alternate D_{III} and 3`UTR. The resulting protein also lacks a GPI anchor and so forms the soluble spliced form of the receptor ssPLAUR. These two forms were determined to be the most abundant in the lung (mPLAUR: 24%; ssPLAUR: 57%), in human airway smooth muscle cells (mPLAUR: 15%; ssPLAUR: 74%) and in human bronchial epithelial cells (mPLAUR: 7%; ssPLAUR: 77%) (Stewart and Sayers, 2009). Other splice variants exist in either form, namely Exon 3, Exons 4 & 5, Exon 5 and Exon 6 deletions.

Other identified splice variants include those lacking exon 3, exons 4 & 5, exon 5 and exon 6 (Stewart and Sayers, 2009, Luther et al., 2003, Casey et al., 1994). The exon 6 deletion variant has been found to be the most common deletion variant, along with the exon 7b variant, expressed (>5%) in peripheral cells (polymorphonuclear leukocytes & peripheral blood mononuclear cells) (Stewart and Sayers, 2009). Exon deletion results in structural changes in the receptor structure, which suggests that these splice variants have different PLAUR ligand binding affinities and different

degrees of PLAUR driven chemotaxis when compared to the 'wildtype' receptor. However, apart from the exon 4/5 deletion variant, which has been identified as a putative prognostic marker in breast cancer and soft tissue sarcoma patients (Luther et al., 2003, Kotzsch et al., 2005, Kotzsch et al., 2011), these splice variants have also not been extensively investigated, with their effect on cellular functions as yet unknown.

1.9.2 MOLECULAR STRUCTURE

The urokinase plasminogen activator receptor is a highly glycosylated GPI anchored cell membrane protein (Ploug et al., 1991b, Roldan et al., 1990, Plesner et al., 1994a, Hoyer-Hansen and Lund, 2007) translated from a 1.4kb mRNA (Plesner et al., 1994a, Behrendt et al., 1991) encoded on chromosome 19q13 (Ploug et al., 1991b, Ploug et al., 1991a, Sayers et al., 2008). PLAUR is a member of the lymphocyte antigen 6 (Ly-6) superfamily, which consists of a large group of GPI-anchored, secreted and transmembrane proteins with a diverse number of biological functions (Ploug, 2003). The Lys-6 superfamily is characterised by Ly-6 and PLAUR domains (LU-domains), which are orientated in what is known as the three finger fold (Kjaergaard et al., 2008), forming 3 globular structures with 5-6 antiparallel β-strands each linked by 4-5 disulphide bonds (Kjaergaard et al., 2008). This protein folding results in the formation of 3 structurally homologous globular domains, annotated as domain 1 (D_I), domain 2 (D_{II}) and domain 3 (D_{III}), each separated by a 15 residue inter-domain linker sequence and each covering approximately 80-90 residues including either 8 or 10 cysteine residues (Fig. 1.9) (Blasi and Carmeliet, 2002, Ploug, 2003, Beaufort et al., 2007, Behrendt et al., 1991).
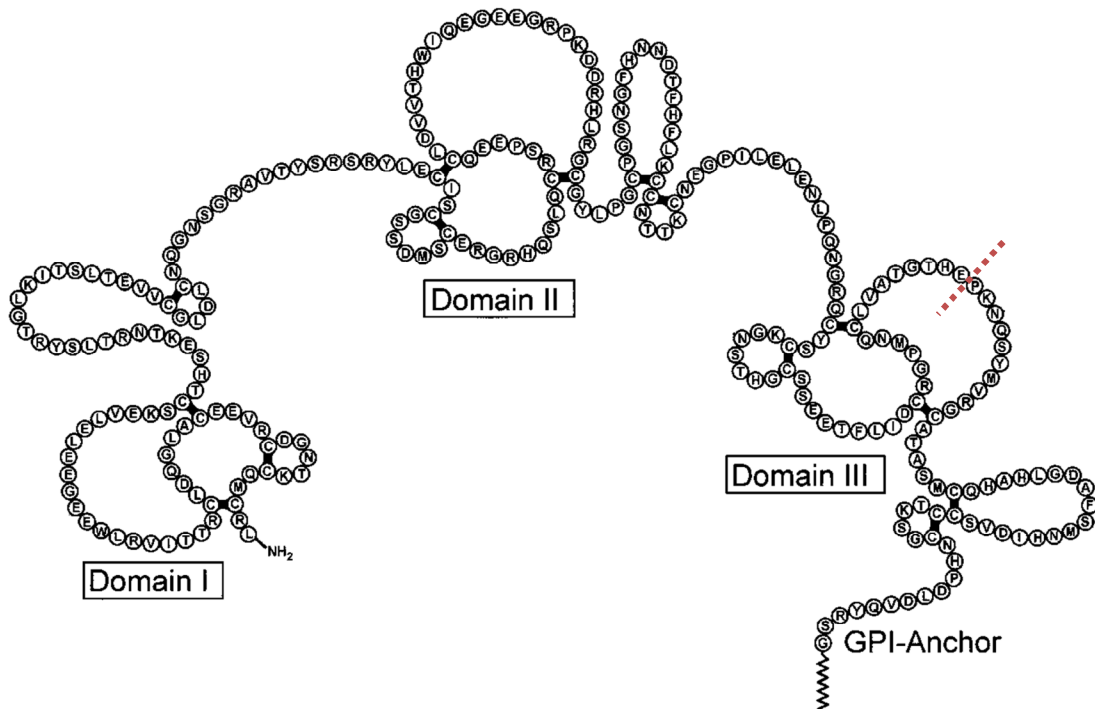
Figure 1.9: The multidomain structure of PLAUR. The two dimensional cartoon of PLAUR identifies protein folding to form the 3 receptor globular domains (numbered from the NH2-terminus) that together form the receptor's ligand binding site. Black bars identify the disulphide connections within the protein structure which give rise to the globular domain loops required for PLAUR ligand binding. The red dotted line identifies the region at which the amino acid sequence changes in the soluble spliced form of the receptor (ssPLAUR). In ssPLAUR the amino acid sequence is changed to 'RSLWGSWLPCKSTTALRPPCCEEAQATHV' which alters the conformation of domain III and does not form the GPI-anchor. Adapted from (Hansen et al., 2004).

The PLAUR GPI anchor has been found to be extended and able to undergo oscillatory movements relative to the cell membrane (Chevalier et al., 2006, Chevalier et al., 2005) resulting in PLAUR being a flexible molecule. This enables the receptor to adopt more favourable orientations to bind with its ligands and cell-membrane bound factors.

X-ray crystallography has identified that the receptor's 3 structural domains pack together into a concave structure with a large central cleft, presenting residues, necessary for urokinase (PLAU) binding at its amino-terminal growth factor (ATF) domain, from all 3 domains (Blasi and Carmeliet, 2002, Liang et al., 2001) with the D_I to D_{III} domain likely facing towards the cell membrane (Xu et al., 2012) (Fig. 1.10).
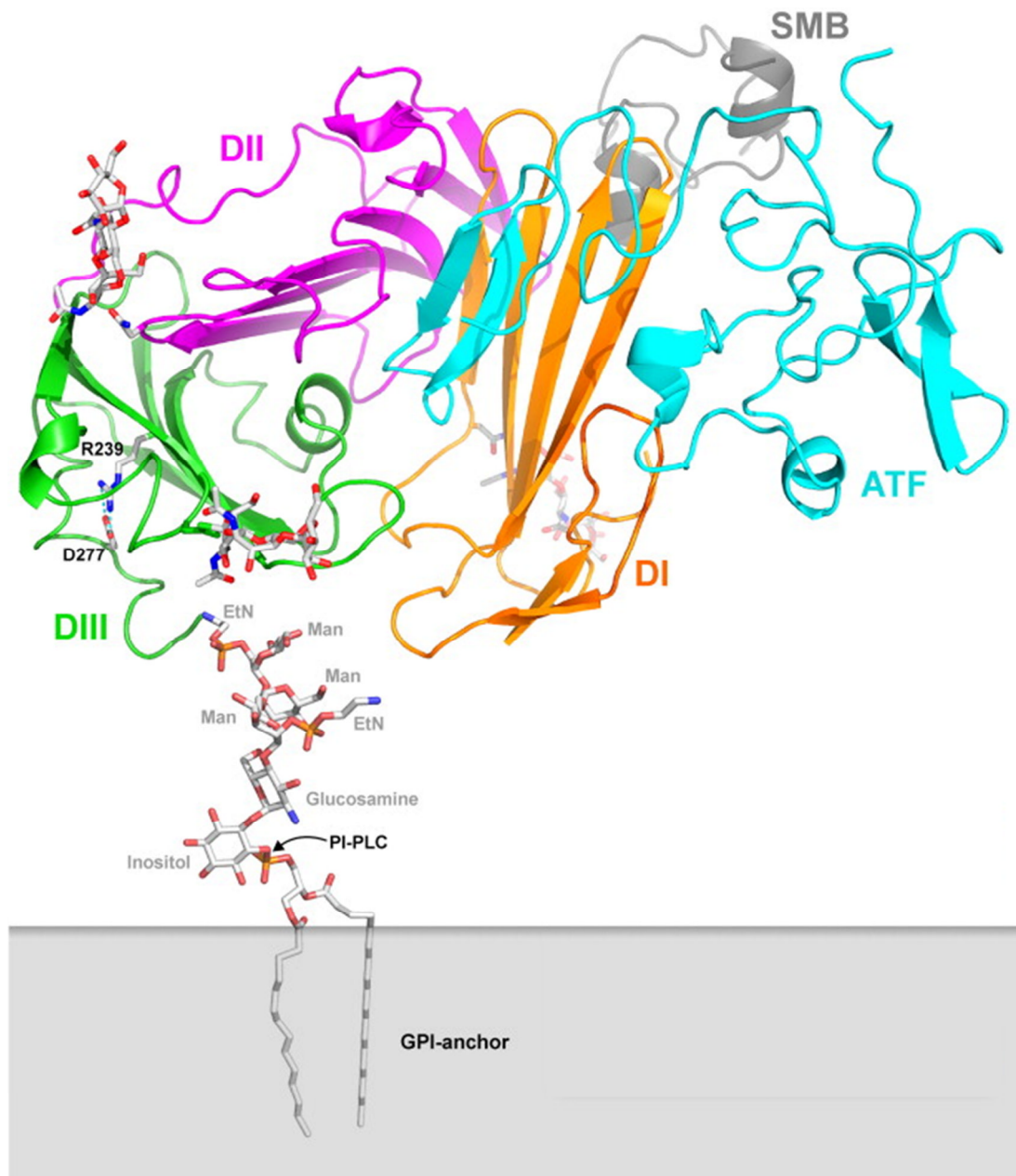
Figure 1.10: The three dimensional structure of PLAUR bound with PLAU. This three dimensional structure allows for visualisation of the orientation of the membrane bound globular domains ready to receive the amino terminal fragment (ATF) of the ligand urokinase and Vitronectin (SMB). The individual domains in PLAUR are colour coded as follows: D_I, orange; D_{II}, magenta; and D_{III}, green. Structures shown in the stick representation (GPI anchor, carbohydrates linked to Asn52, Asn162, and Asn200 as well as residues Arg239 and Asp277) are colour coded according to their atomic elements [nitrogen (blue), oxygen (red), carbon (white), and phosphor (orange)]. Man, mannose; Etn, ethanolamine; PI-PLC, phosphatidylinositol phospholipase C. Figure derived from (Xu et al., 2012).

The structure of PLAUR suggests that all 3 globular domains are required for optimal ligand binding and that receptor structural integrity is necessary for PLAU driven effects, based on:

1. The presence of ligand binding sites within each of these distinct structural globular domains (D_{I-III} – see Fig. 1.10),

2. The dynamic role of a correctly folded D_{II} (regions 130-140) during ligand loading and unloading (Xu et al., 2012),

3. The close spatial proximity between D_I and D_{III} present in intact PLAUR might be required for the assembly of the composite binding site (Blasi and Carmeliet, 2002).

The final point is of special importance when considering the structural differences between ssPLAUR and the alternate soluble form of PLAUR, scPLAUR (see Section 1.8.3.2), where ssPLAUR does not have an intact D_{III}. This suggests that ssPLAUR may not fully interact with PLAU and any effects driven by this receptor (as yet undefined) would be independent of the plasminogen-plasmin pathway.

1.9.3 CLEAVAGE OF PLAUR

PLAUR is susceptible to cleave at multiple sites, including the linkage region between D_I and D_{II} and at the receptor's GPI anchor. This gives rise to multiple forms of the receptor such as a soluble D_{II}/D_{III} fragment and a full length soluble receptor, of which some retain some activity such as chemotaxis (D_{II}/D_{III} fragment) and integrin binding (soluble cleaved receptor), whilst others such as the soluble D_I fragment have, to date, no known effects.

1.9.3.1 CLEAVAGE OF THE DOMAIN I/II LINKER

Studies by limited proteolysis clearly identify that the linker region between D_I and D_{II}, corresponding to residues 83 to 89, as being particularly susceptible to enzymatic hydrolysis by a number of different proteases including Pepsin, MMP-12, Chymotrypsin, human airway trypsin-like protease (HAT), Cathepsin G and PLAU (Fig. 1.11) (Behrendt et al., 1991, Andolfo et al., 2002, Hoyer-Hansen et al., 1997b, Koolwijk et al., 2001, Beaufort et al., 2004).
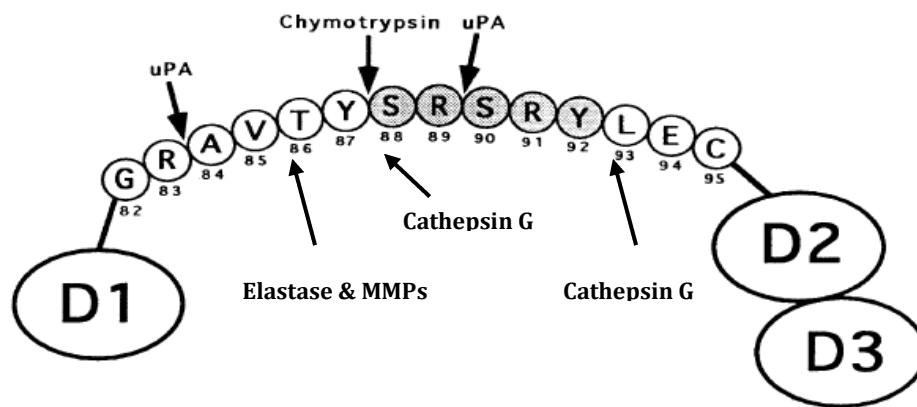
Figure 1.11: PLAUR $D_I/_{II}$ cleavage. The PLAUR DI/DII linker sequence indicating the various protease sensitive sites which results in the loss of globular domain DI. This results in the formation of a DII/DIII fragment which, provided that the urokinase-sensitive SRSRY sequence is left intact, has chemotactic activity. Figure adapted from (Fazioli et al., 1997).

This results in the loss of D_I (Fig. 1.11) resulting in the loss of the high affinity domain for PLAU and VN binding (Ploug et al., 1994, Hoyer-Hansen et al., 1997a, Sidenius and Blasi, 2000). Subsequent studies identified that cleavage in this region also abolished PLAUR's lateral interactions with integrins, its ability to regulate integrin adhesive functions as well as PLAUR driven effects on cellular proliferation and migration (Montuori et al., 2002). Cleavage at the D_I/D_{II} linker therefore acts as a regulatory procedure for PLAUR driven processes. Since this is driven by PLAU itself (Hoyer-Hansen et al., 1997b), it suggests that a PLAUR-PLAU interaction exists whereby PLAU self-regulates PLAUR levels in a negative-feedback mechanism.

The resulting D_{II}/D_{III} fragment however, has been reported to retain a chemotactic neoepitope that allows the fragment to retain a role in cell migration and stem cell mobilisation (Resnati et al., 1996, Resnati et al., 2002, Selleri et al., 2005). This fragment has been detected *in vitro* and *in vivo* in monocytes, basophils and ovarian tumours (Wahlberg et al., 1998, Beaufort et al., 2004, de Paulis et al., 2004).

1.9.3.2 GPI ANCHOR CLEAVAGE

The PLAUR's GPI-anchor is also susceptible to glycolytic and lipolytic cleavage, most significantly by the enzymes phospholipase C and D (Ploug et al., 1991b, Wilhelm et al., 1999). This results in the release of the entire protein moiety from the cell surface, forming a soluble form of the receptor (soluble cleaved PLAUR: scPLAUR) (Fig. 1.12).
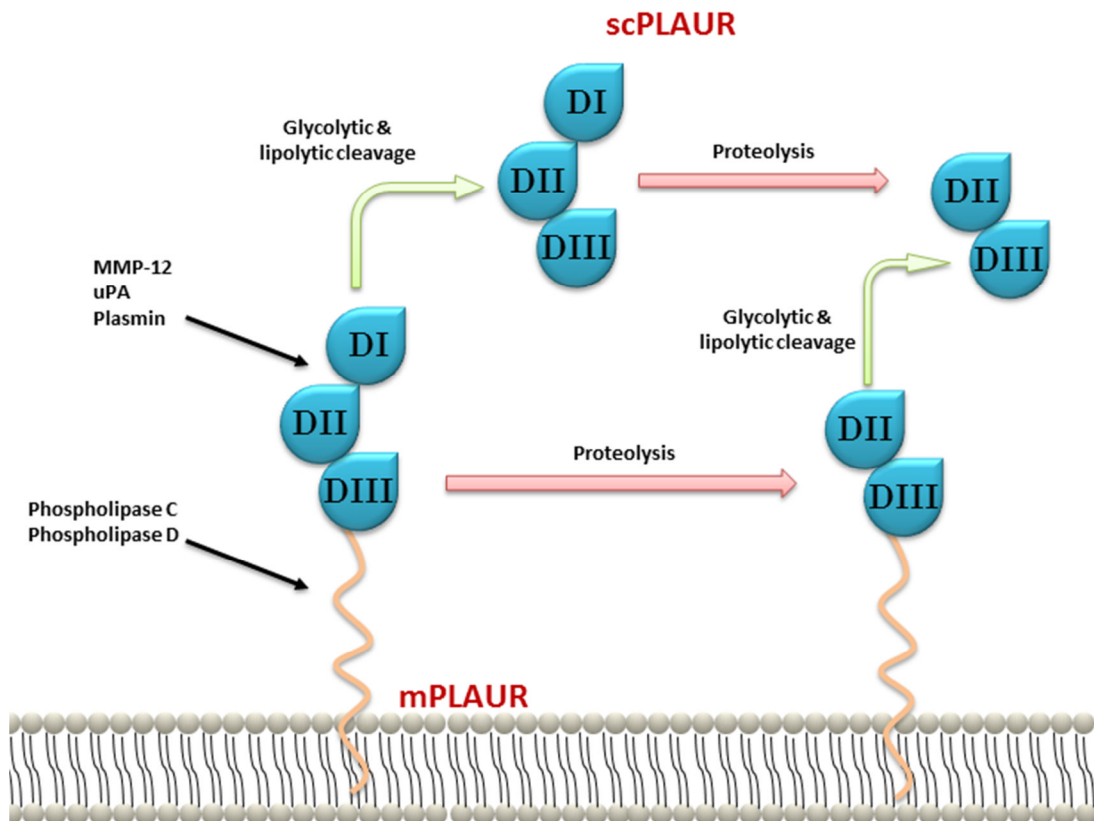
Figure 1.12: PLAUR cleavage products. PLAUR is a 3 globular domain protein attached to the cellular membrane. Cleavage occurring on the membrane bound receptor can either be proteolytic or glyco/lipolytic. Glycolytic and lipolytic cleavage occurs at the GPI anchor by substances such as Phospholipase C & D, and results in the formation of a soluble form of the receptor which structurally mirrors the corresponding membrane bound receptor. Proteolytic cleavage occurs in the linker region between D_I and D_{II} and results in the loss of D_I to form a D_{II}/D_{III} fragment which has chemotactic activity.

Soluble cleaved PLAUR has been detected in plasma, urine, blood, serum and cerebrospinal fluid (Sorio et al., 2011, Zimmermann et al., 2012, Haupt et al., 2012, Terracciano et al., 2011, Sporer et al., 2005). High levels (800–2000pg/ml) of scPLAUR have been recorded *in vitro* in supernatants from a human bronchial epithelial cell line (BEAS2B) and a human acute monocytic leukemia cell line (THP1), with lower levels present in supernatants from HASMs and NHBECs (50-800pg/ml) (Stewart and Sayers, 2009). Cleavage at the GPI anchor allows the protein to retain an intact PLAUR moiety and therefore scPLAUR is still able to interact with the ligands and cell factors which are involved with the membrane bound receptor, such as PLAU, VN and the β_1 and β_2 integrins (Hoyer-Hansen et al., 1997a, Behrendt and Dano, 1996, Wei et al., 1996, May et al., 1998). Interestingly however, scPLAUR lacks the ability to bind with the N-formyl-methionine-leucine-phenylalanine (fMLP) receptors (Resnati et al., 2002), identifying that cleavage of the GPI anchor does result in some conformational change to the receptor and that the function of scPLAUR may not be identical to that of the membrane bound receptor. Therefore, although scPLAUR may be able to carry out some functional effects identical to mPLAUR, it may have a role independently of the membrane bound receptor. This is due to conformational changes in receptor structure and the ability to interact with co-factors located distally from PLAUR expressing cells.

The soluble cleaved receptor can also function by competing with mPLAUR for extracellular ligands due to its identical nature to mPLAUR. Here, competition for PLAU would reduce PLAU driven proteolysis (see Section 1.7.1) and cell adhesion to VN. Therefore, scPLAUR could be defined as a decoy for these extracellular ligands, dampening the effect of over expression of the aforesaid ligands (Montuori et al., 2005) at their target site. However, scPLAUR cannot be solely classified as a decoy receptor as reports have also identified an active role for scPLAUR due to its ability to bind cell surface ligands (e.g. the β_1 integrins - see above). This identifies that while increased production of scPLAUR may reduce PLAUR's proteolytic functions by its sink-like

activities, it will not affect its non-proteolytic ones. Interestingly, it has been suggested that increased scPLAUR generation may be a way of transferring excess PLAUR from one cell type to another, where it is then taken up by endocytosis. This process having already been described to occur between neutrophils and eosinophils (Mizukami and Todd, 1998, Mustjoki et al., 2000),

Cleavage at the GPI anchor can also release PLAUR that has been previously cleaved at the D_I/D_{II} linker, which interacts in the same fashion as the membrane bound D_{II}/D_{III} fragment as discussed in Section 1.8.3.1.

1.10 PLAUR AND NON-RESPIRATORY DISEASE

Although this thesis specifically deals with asthma and COPD, it is important to note that PLAUR has a role in other human diseases, especially where disease causes tissue remodelling (Solberg et al., 2001) and in diseases associated with stress, injury and inflammation (Smith and Marshall, 2010).

Associations with disease have not been limited to the membrane bound form of the receptor. Multiple studies have highlighted the importance of the soluble cleaved form of the receptor either as a biomarker of disease or disease progression or as being directly involved in disease progression/modulation. Diseases to which PLAUR (and ergo scPLAUR) have been associated with include various types of cancer, cardiovascular disease, diabetes, human-immunodeficiency virus (HIV) infected patients and neuromuscular disease (Eugen-Olsen et al., 2010b). However associations with other types of diseases have also been reported.

In a multi-disease study, Eugen-Olsen *et al.* identified elevated levels of scPLAUR in the blood of disease specific patients, associating baseline scPLAUR to an increased risk of development of diseases with low grade inflammation, such as cancer, cardiovascular disease and Type II *Diabetes Mellitus*. An increased risk of disease-related mortality was also reported (Eugen-Olsen et al., 2010b). This argues in favour of scPLAUR as a biomarker of disease, especially with regards to disease involving an inflammatory cascade, a relationship also identified in chronic liver disease patients (Zimmermann et al., 2012). The findings from the Eugen-Olsen study where mirrored in a study by Haupt *et al*. were scPLAUR levels in plasma were associated with diabetes, cancer, cardiovascular disease and liver disease as well as an increased degree of mortality in disease in general (Haupt et al., 2012). The relationship between scPLAUR and disease risk and mortality was further replicated by Savva *et al.* and Sidenius *et al.* in disease

specific patient cohorts of patients with ventilator-associated pneumonia and sepsis or HIV (Savva et al., 2011, Sidenius et al., 2000) as well as by Zimmermann *et al.* who identified that elevated scPLAUR was associated with higher mortality rates or need for transplantation in patients suffering from chronic liver disease, while also identifying a correlation between circulating scPLAUR, liver function, fibrosis markers and renal function (Zimmermann et al., 2012).

PLAUR has also been of interest in multiple forms of cancer, including but not limited to breast, lung, colon, gastric and prostate carcinomas (Laufs et al., 2006), with PLAUR differentially expressed and activated on invading tumour cells (Mazar et al., 1999). A recent analysis by Andres *et al.* has identified a correlation between overall PLAUR levels in breast tissue biopsies and overall survival rates (Andres et al., 2012) and recently soluble cleaved PLAUR has been found to be involved in chondrosarcoma cell mobilisation (Bifulco et al., 2011).

The multiple studies highlighting a relationship between the soluble cleaved form of the receptor and disease prognosis identifies that this form may be independently important in PLAUR disease modulation apart from it being a useful diagnostic severity marker in multiple disease states.

The association of PLAUR with multiple diseases may be partially explained through its effects on the coagulation/fibrinolysis pathway (see Sections 1.5 and 1.7.1). However, the direct effect of PLAUR on cell homeostasis due to modulation of cell migration, proliferation, adhesion and differentiation, which would regulate tissue remodelling, also plays an important role. The effect of PLAUR on cellular homeostasis is described below.

1.11 ROLE OF PLAUR IN CELLULAR HOMEOSTASIS

PLAUR is expressed in a wide variety of cells and tissues with only a limited number of cells identified that do not express the receptor. These include non-activated B- and T-lymphocytes , CD34+ hematopoietic stem cells (Plesner et al., 1994b) and human embryonal kidney cells (HEK-293) (Wei et al., 1996). The near universal expression of PLAUR as well as the potential regulation of a number of different cell functions through the receptors proteolytic and non-proteolytic functions, suggests that PLAUR is involved in cellular homeostasis. This hypothesis is strengthened by the classification of PLAUR as an activation antigen in T-lymphocytes and monocytes, where its expression appears to be relevant to cell function (Fazioli et al., 1997).

Indeed, PLAUR has been implicated in a number of cellular mechanisms including cellular adhesion, proliferation and migration, as well as being involved in ECM and basement membrane proteolysis (Mekkawy et al., 2012). Pathways regulating changes in these cellular outcomes that are affected by PLAUR tend to overlap between the different outcomes, suggesting a complex system of cell function regulation. Examples include the regulation of extracellular signal related kinases/p38 signalling, which affects cellular migration and proliferation, as well as the PLAUR dependant elevation of HS-1-associated protein X-1 which augments cellular proliferation, migration and adhesion (Xue et al., 2009, Mekkawy et al., 2012). Recent studies have also implicated the MEK/ERK arm of the MAPK signalling pathway in the regulation of PLAUR driven cell migration and proliferation (Whyte et al., 2012, Nowicki et al., 2011).

PLAUR can also interact with other receptors to influence cell functions. An example of which is the cooperation with the epidermal growth factor receptor to mediate cellular mitogenesis (Jo et al., 2005). This is of special interest since increased cellular mitosis may go part way to explain the PLAUR dependant increase in cellular proliferation.

1.11.1 CELLULAR INVASION AND MIGRATION

PLAUR plays a central role in tissue invasion via cell migration (Andreasen et al., 2000) and is strongly associated with cell motility (Lijnen, 2001). This is highlighted by the strong correlation between cellular invasive and migratory potential with mPLAUR levels (Ossowski et al., 1991) and by increased PLAUR expression at the leading edge of re-epithelising wounds (Fig. 1.13) (Romer et al., 1994, Stewart et al., 2012).
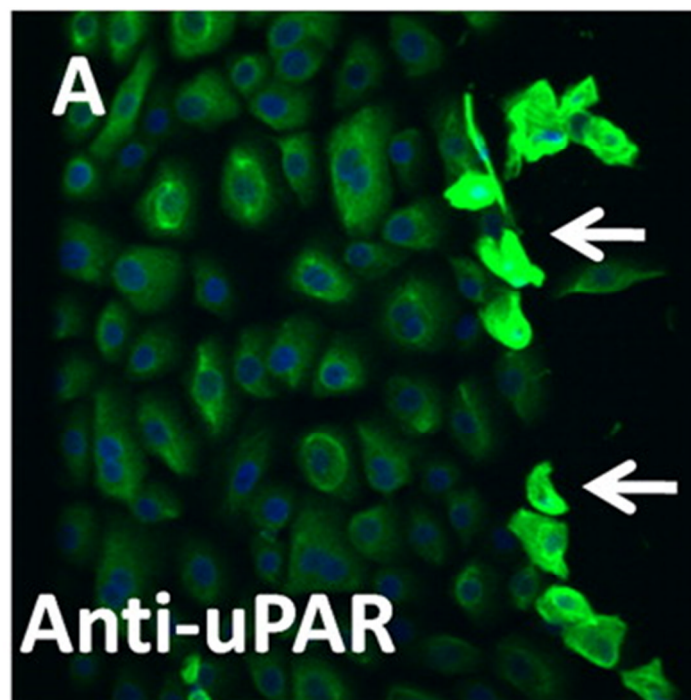
Figure 1.13: Elevation of PLAUR at the wound edge of re-epithelising wounds. PLAUR specific staining identifies a striking elevation in PLAUR expression at the wound edge of a scratch wound model when compared to the remaining population of primary epithelial cells. Image obtained from (Stewart et al., 2012).

Other more direct studies have confirmed this association with over-expression of PLAUR in human pleural mesothelial cells causing an increase in the rate of cell migration *in vitro* (Tucker et al., 2010), while PLAUR levels on monocyte cells were associated with the degree of monocyte migration *ex vivo* (Chen et al., 2012). Suppression of PLAUR inhibited the migration of pancreatic and bronchial epithelial cells (Xue et al., 2009), while the granulocytes and monocytes of PLAUR knockout mice had severely impeded migratory and chemotactic capacity (May et al., 1998).

This PLAUR mediated regulation of cell migration is thought to occur through either the activation of latent growth factors or their release from the ECM, following ECM degradation through PLAUR activation (Preissner et al., 2000). Examples include the cleavage of the ECM protein fibronectin (Quigley et al., 1987), activation of transforming growth factor beta (TGFβ) (Odekon et al., 1994) and activation of the pro-hepatocyte growth factor (Naldini et al., 1995).

More recent studies however have suggested alternate methods of PLAUR mediated cellular migration. Some studies have identified that an interaction between PLAUR and VN regulates cellular migration (Kjoller and Hall, 2001, Madsen et al., 2007, Smith et al., 2008) through integrin signalling resulting in p130Cas-Crk and DOCK180 dependant Rac activation (Smith et al., 2008, Kjoller and Hall, 2001). Other studies have identified a direct method by which PLAUR effects cell migration through its own innate chemotactic properties. The chemotactic activity is driven by a region located between D_I and D_{II} in the PLAUR globular structure (SRSRY; amino acids 88 to 92), which happens to also be the protease sensitive region of the receptor that results in the loss of the D_I domain. This epitope drives chemotaxis through the activation of the p56/p59[hck] tyrosine kinase and via interaction with GPCRs (Fazioli et al., 1997).

1.11.2 CELLULAR ADHESION

PLAUR is known to affect the adhesion of leukocytes such as neutrophils (Chavakis et al., 1999, Brooks et al., 2006). It has been proposed that PLAUR modulates cell adhesion either directly as a cell-linked adhesion protein or counter-receptor, or indirectly via integrins (e.g. β_2 integrins) in association with other cytoskeletal and signalling proteins (Preissner et al., 2000). The direct method of cell adhesion mainly refers to VN dependant adhesion, where cells use PLAUR to bind soluble, multimeric VN and a number of factors such as α_v-integrins and zinc ions and thus cause cell

attachment (Wei et al., 1994, Kanse et al., 1996, Chavakis et al., 1999). However, a study by Brooks *et al.* have suggested that a multiprotein complex consisting of integrins ($\alpha_M\beta_2$ and $\alpha_4\beta_1$), PLAUR, PLAU and the GPCR fMLP is involved in the promotion of cell adhesion in leukocytes (Brooks et al., 2006).

The indirect method on the other hand refers to the release of other pro-adhesion molecules from the cell surface or the ECM through PLAUR driven degradation. Examples include the activation of plasminogen to plasmin and the activation of cell signalling cascades through PLAUR-integrin interaction (Preissner et al., 2000).

1.11.3 CELLULAR PROLIFERATION

Over-expression of PLAUR in human pleural mesothelial cells identified an increase in the rate of cell proliferation *in vitro* and subsequently the rate of tumour formation *in vivo* (Tucker et al., 2010), while suppression of PLAUR was found to inhibit the proliferation rate of pancreatic cells (Xue et al., 2009).

As in its other cellular activities, PLAUR driven modulation of proliferation occurs through either a direct (proteolysis dependant) or indirect (proteolysis independent) method. In the first instance, plasmin activated from plasminogen through the action of the PLAUR-PLAU complex, can release and activate a number of growth factors from the extracellular matrix. Examples include activation of TGFβ and hepatocyte growth factor/scatter factor (HGF/SF), both of which are known to increase the rate of proliferation in epithelial cells (Mazzieri and Blasi, 2005). Independently and through its proteolytic effect, PLAUR increases cellular proliferation through signalling cascades. For example, PLAUR constitutively activates the epidermal growth factor receptor (EGFR) inducing an imbalance between p38 and p42/44 and so shifting the balance between the proliferation activating ERK1/2 signalling cascade and the pro-apoptotic p38MAPK signalling cascade towards the ERK1/2, thereby indirectly

increasing the rate of cellular proliferation (Liu et al., 2002a). However, an increase in the rate of proliferation of the embryo fibroblasts of PLAUR knockout mice identifies that the role of PLAUR in cellular proliferation must be cell specific and is more complex than anticipated (Mazzieri et al., 2006).

1.11.4 CELLULAR GROWTH AND DIFFERENTIATION

PLAUR is involved in the differentiation of mesenchymal stem cells to vascular smooth muscle cells, the differentiation of monocytes to macrophages and the differentiation of fibroblasts to myofibroblasts (Vallabhaneni et al., 2011, Bernstein et al., 2007, Blasi and Carmeliet, 2002). As described above, PLAUR influences cellular growth and differentiation indirectly through cell factors such as $\alpha_5\beta_1$, which in turn increases ERK activity, causing an imbalance between the ERK^{MAPK} to p38^{MAPK} ratio, increasing cell growth (Aguirre-Ghiso et al., 2001).

Interestingly, PLAUR can also affect cellular growth and differentiation via the direct modulation of gene expression. Here PLAUR undergoes cellular internalization and nuclear transport in vascular smooth muscle cells, mediated by the platelet-derived growth factor receptor and SUMOylated RanGAP1. Once in the nuclear region, PLAUR associates with myocardin, which is then recruited to the promoters of serum response factor target genes and undergoes proteasome degradation. This then initiates a change in the vascular smooth muscle phenotype that contributes to adverse vascular remodelling after injury *in vivo* (Kiyan et al., 2012).

Remarkably, there is evidence that the shift from full length PLAUR to the D_{II}/D_{III} fragment is crucial to the role of PLAUR in fibroblast to myofibroblast differentiation. Berstein *et al.* identify that full length PLAUR was down-regulated in myofibroblasts when compared to fibroblasts, the originating cell type, with retention of the full-length form appearing to prevent the transition from fibroblast to myofibroblast (Bernstein et

al., 2007). The authors suggest a model where lack of stimulus by fibroblast growth factor (FGF2) at the end of wound healing results in a reduction in the recycling of the D_{II}/D_{III} cleaved PLAUR to full length PLAUR, which in turn results in increased cellular adhesion. This increase in cellular adhesion then provides the tension required between the ECM and the cell surface required for the assembly of α-SMA stress fibres that are characteristic of myofibroblasts.

1.11.5 CELLULAR APOPTOSIS

It has been suggested that PLAUR may confer protection to cells against induced apoptosis, with a decrease in PLAUR, in conjunction with MMP-9 down-regulation, shown to increase apoptosis (Gondi et al., 2008, Chetty et al., 2010, Nalla et al., 2010, Nagaraju et al., 2011). This relationship was further defined by *in vivo* experiments carried out in wildtype and p53-, PLAU-, PLAUR-, and PAI-1-deficient mice following Bleomycin induced acute lung injury (Bhandary et al., 2012).

Regulation of cellular apoptosis occurs through an indirect method via multiple pathways. These include the MAPK signal pathways, where RNA silencing of the *PLAUR* gene results in a decrease in ERK activity and therefore an elevated p38 to pERK activity ratio (Li et al., 2010) and the STAT3 and NF-κB related signalling pathways, where RNA silencing of *PLAUR* and *MMP-9* genes inhibited activation of these pathways through EGFR (Kotipatruni et al., 2012).

1.12 REGULATION OF PLAUR EXPRESSION

Modification of gene transcription is thought to be the main mediator of PLAUR expression. In general modification of *PLAUR* gene transcription can be brought about by a number of factors and pathways including, but not exclusive to:

i)   Epidermal growth factor

ii)   TGFβ1

iii)   Protein kinase C and

iv)   The MAPK and JNK-pathways (Laufs et al., 2006).

Indeed, *PLAUR* gene expression is known to be influenced by:

i)   Tumour promoters

ii)   Hormones

iii)   Growth factors

iv)   Cytokines

v)   Hypoxia (Ganne et al., 1999, Graham et al., 1998).

1.12.1 PROMOTER TRANSCRIPTIONAL REGULATION

At the gene level, regulation of gene expression is brought about by modulation of gene transcription through *cis-* and *trans-* acting factors (Lewin, 2004). *Cis*-acting factors are regulatory elements existing proximally to the gene, which together are commonly termed as the gene's promoter region. *Trans*-acting factors however are regulatory elements that are located elsewhere (distally) in the genome, which includes transcription factors, suppressors and enhancers. These *cis-* and *trans-* activating factors work together in order to regulate expression levels of the gene.

The promoter for the *PLAUR* gene was first described simultaneously by two groups in 1994 and 1995 in colon cancer and U937 lymphoma cells (Soravia et al., 1995, Wang et al., 1994). Both groups identified that the minimal promoter in these cell lines lies within the first 200bp from the major TSS. Wang *et al.* identify that this promoter lacks both TATA and CAAT boxes and contains a GC-rich proximal sequence that contains multiple Sp-1 consensus elements that regulate basal expression of the gene (Soravia et al., 1995). Other studies carried out on colon cancer cells confirmed the location of a minimal promoter within the first 200bp upstream of the TSS, identifying that a region between 190 to 171 base pairs upstream of the TSS was required for PLAUR expression via the induction of the MAPK- and JNK-pathways (Lengyel et al., 1997, Gum et al., 1998). This region contains an AP-1 consensus motif that was bound to the c-Jun, c-Fos and Fra-1 oncogenes (Lengyel et al., 1996), which when deleted resulted in a severe reduction of promoter activity (Allgayer et al., 1999). The importance of the AP-1 transcription factor motif in PLAUR transcription was confirmed by Okan *et al*,. where an AP-1 motif at 70bp upstream of the TSS was required for transcription activation, along with a c-Jun binding motif at 184bp upstream of the TSS (Okan et al., 2001).

Other transcription factors known to affect *PLAUR* transcription include PEA3/Ets, KLF4, Sp-1, NFκB, HIF-1 and AP-2 (Lengyel et al., 1996, Hapke et al., 2001, Schewe et al., 2005, Schewe et al., 2003, Wang et al., 2000, Wang et al., 2004, Buchler et al., 2009). Here, experiments using a negative AP-2 expression construct also inhibited PLAUR mediated proteolysis as well as inhibiting PLAUR transcription, thereby identifying that inhibition at the transcriptional level can be applied to suppress and/or modify PLAUR mediated effects such as proteolysis, cellular invasion and metastasis (Laufs et al., 2006).

The PLAUR promoter has also been determined to regulate gene expression through gene silencing. Gene-silencing was driven by the β_3 integrin via the promoter region between 398 and 197 base pairs upstream of the TSS, particularly with the PEA3 motif located at 248bp upstream of the transcriptional start site (Laufs et al., 2006).

However, although all the above studies suggest that the first 200bp upstream of the *PLAUR* TSS is the minimal region required for *PLAUR* transcription, a study in transgenic mice has identified that the 1.5kb region upstream of the TSS to be required for optimal expression, with a region spanning between 1295 and 1192 base pairs upstream of the TSS proposed as a novel regulatory region (Wang et al., 2003). Therefore it is suggested that further *PLAUR* regulatory regions still remain to be discovered.

1.12.2 POST TRANSCRIPTIONAL MODIFICATION

PLAUR expression can also be regulated through post-transcriptional mechanisms which alter PLAUR mRNA stability. The first reports of post-transcriptional regulation of PLAUR expression were published in 1995, where Lund *et al.* identified that phorbol-12-myristate 13-acetate (PMA) and TGFβ1 increased expressed levels of PLAUR through increasing the stability of PLAUR mRNA in addition to their direct effects on *PLAUR* transcription (Lund et al., 1995). Further studies were then forthcoming, with a study identifying that T-lymphocyte engagement through the β_2 integrin lymphocyte function-associated antigen-1 ($\alpha_L\beta_2$) resulted in PLAUR stabilisation through a *cis*-acting AU-rich region present in the 3`UTR of the gene (Wang et al., 1998). Shetty later identified a novel binding protein (Heterogeneous nuclear ribonucleoproteins C1/C2 [hnRNPC]) that bound to a 110bp region of the gene's 3`UTR, resulting in increased *PLAUR* mRNA stability (Shetty, 2005). A second study identified p53 as a novel protein that bound to a 37bp region of the gene's 3`UTR

that destabilised the *PLAUR* mRNA (Shetty et al., 2007a), confirming the 3`UTR's importance in *PLAUR* regulation through stabilisation and destabilisation functions.

Post-transcriptional regulation of the gene is however not limited to the gene's 3`UTR. Over multiple studies Shetty *et al.* identified, in mesothelioma (MS-1) and human lung carcinoma cells, a 50kDa *PLAUR* binding protein, later identified to be Phosphoglycerate kinase (PGK), which when selectively bound to a 51bp fragment of mRNA that corresponded to the PLAUR coding region resulted in destabilisation of *PLAUR* mRNA (Shetty et al., 1997, Shetty and Idell, 1999, Shetty et al., 2004) and thereby reduced the expressed levels of PLAUR. This activity was found to be independent of PGK's previously known enzymatic activity (Shetty et al., 2005). A later study then identified PGK regulation of *PLAUR* mRNA stability to be part of a system of regulation involving hnRNPC and the Tyrosine-protein phosphatase non-receptor type II (SHP2). Here, inhibition of protein tyrosine phosphatase-mediated dephosphorylation, partly driven by PLAU, results in SHP2 phosphorylation. This subsequently increases *PLAUR* mRNA stability through a decrease in the degree of interaction between PLAUR and PGK, alongside a simultaneous enhancement of the interaction of hnRNPC with the *PLAUR* 3`UTR (Shetty et al., 2007b), a process linked to Lipopolysaccaride (LPS) induced PLAUR elevations (Bhandary et al., 2009).
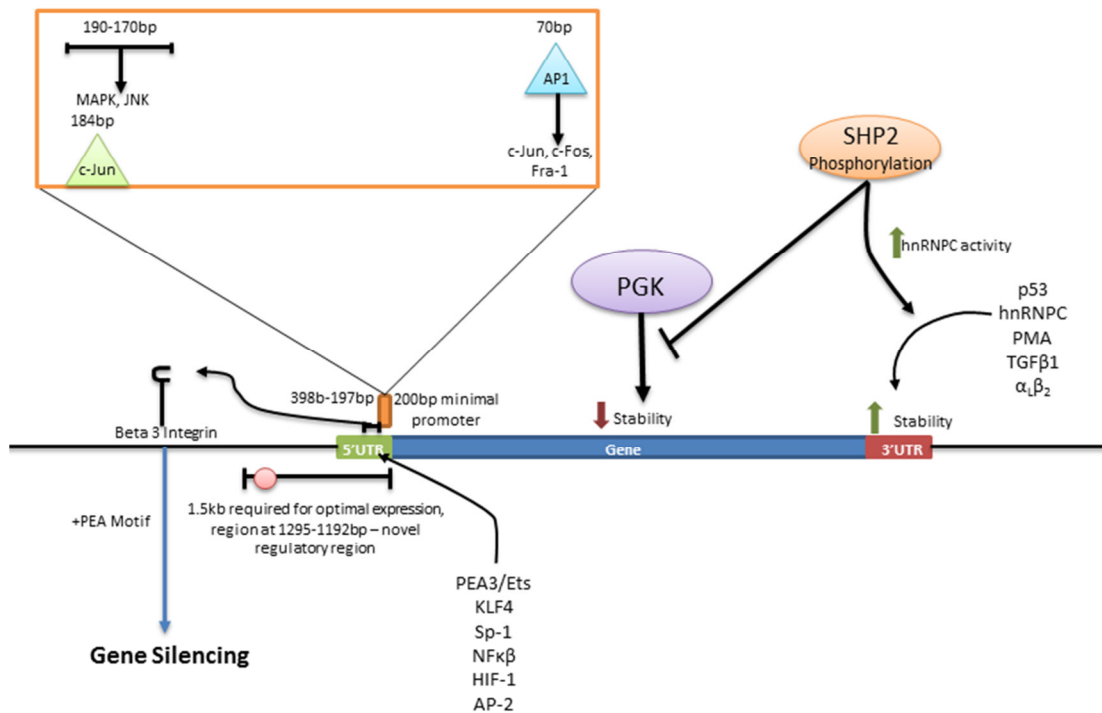
Figure 1.14: Known regulatory mechanisms for PLAUR mechanisms. At the 5`UTR the gene minimal promoter was determined to be located within the first 200bp upstream of the gene transcriptional start site. Here, regulation involves an AP-1 and c-Jun motif as well as the c-Fos, Fra-1, MAPK and JNK pathways. Other transcription factors involved in PLAUR regulation include PEA3/Ets, KLF4, Sp-1, NFκβ, HIF-1 and AP-2. Although the minimal promoter region lies in the first 200bp upstream of the gene, the region up to 1.5kb upstream of the gene has also been determined to be crucial for optimal gene expression. Here the region at 398bp-197bp is known to interact with the β3 integrin causing gene silencing, while the region at 1295-1192bp has been proposed as a novel regulatory region. Post transcriptionally, p53, hnRNPC, PMA, TGFβ1 and αLβ2 have been found to increase PLAUR mRNA stability while PGK, through interaction within the gene's coding region (region not specified) decreases PLAUR gene stability. Post-transcriptional modification is known to involve the tyrosine-protein phosphatase non-receptor type 11 (SHP2), where on phosphorylation SHP2 increases heterogeneous nuclear ribonucleoproteins C1/C2 (hnRNPC) activity while simultaneously inhibiting phosphoglyserate kinase (PGK) activity, thereby increasing the amount of stable PLAUR mRNA.

1.13 AIMS

Although limited studies have been carried out investigating PLAUR regulation and function in the airways, a more in depth analyses of general PLAUR regulation and function is still outstanding, especially with regards to the regulation of specific forms of the receptor and in primary human airway cells, where previous associations with obstructive lung disease (asthma and COPD) have been described.

Therefore, the aims of the work described in this thesis were:

1. To investigate the relationship between scPLAUR and obstructive lung disease (asthma & COPD) diagnosis and clinical parameters.
2. To identify novel genetic mechanisms regulating scPLAUR levels.
3. To define the relative contribution of proximal PLAUR regulatory regions in determining gene expression.
4. To determine the functional role of different PLAUR forms in primary bronchial epithelial cells.
5. To identify both rare and common genetic variants spanning PLAUR and to identify which of these are relevant to asthma.

CHAPTER 2:

GENERAL MATERIALS & METHODS

CHAPTER 2: GENERAL MATERIALS AND METHODS

This Chapter describes methodologies used in multiple Results Chapters. Methodologies specific to a particular Chapter are explained within that Chapter's methodology section.

Room temperature is considered to be an ambient temperature of circa. 25°C.

2.1 MATERIALS

2.1.1 GENERAL MATERIALS

All materials used in this thesis are listed below, except for mammalian cells and their culture material (see Section 2.1.2) and plasmids (see Sections 4.5.6 & 5.4.2.2).

• Agarose	Invitrogen, 15510-027
• Ampicillin	Sigma-Aldrich, A9518
• Anti-beta Actin antibody	Abcam, ab8227
• Acrylamide (30%)	Sigma-Aldrich, A3699
• APS (ammonium persulphate)	Promega, V3131
• BigDye® Terminator 3.1 Cycle Sequencing Kit	Applied Biosystems, 4337456
• BetterBase	Microzone, 3BBR
• β-mercaptoethanol	Sigma-Aldrich, M6250
• Bio-Rad protein assay standard II	Bio-Rad 500-0007
• Bovine Serum Albumin (BSA), protease-free	Sigma-Aldrich, A3059
• Complete Mini Protease Inhibitor Tablets	Roche, 11836153001
• DAPI	Sigma-Aldrich, D9542
• DEPC-treated water	Invitrogen, 75-0024
• Dithiothreitol	Sigma-Aldrich, D9779
• Donkey Anti-Goat HRP	R&D, HAF 109
• DMSO	Sigma-Aldrich, 154958
• DNA Engine Tetrad 2 Cycler	Bio-Rad PTC-240
• DNase I, amplification grade	Invitrogen, 18068-015
• dNTP Set	Bioline, BIO-39026
• ECL Western blotting Detection Reagents kit	GE Healthcare, RPN2209
• EcoRI restriction enzyme	Promega, R6011
• EDTA	Sigma-Aldrich, ED
• EndoFree® Plasmid Maxi Kit	Qiagen, 12362
• Ethanol	Sigma-Aldrich, 32221
• Ethidium Bromide	Invitrogen, 15585-011
• E-Toxate™ Water (endotoxin-free)	Sigma-Aldrich, 2107
• FuGENE® 6 Transfection Reagent	Roche, 11814443001
• GeneGenius Gel Doc system	
• Glacial acetic acid	Fisher Scientific, A/0400/PB17
• Glycerol	Fisher Scientific, BPE229-1
• Glycine	Sigma-Aldrich, G8790
• Goat Anti-Mouse HRP	R&D, HAF 007
• Goat Anti-Rabbit HRP	R&D, HAF 008

- Goat serum — Sigma-Aldrich, G6767
- HRP-Streptavidin conjugate — Fisher, 43-8323
- Human Duoset® ELISA — R&D Systems DY807
- Iso-Butanol — Fisher, 15828-0010
- IsoPropanol — Sigma-Aldrich, 190764
- Kanamycin — Sigma-Aldrich, K4378
- Kodak® GBX Developer/Replenisher — Sigma-Aldrich, P7042
- Kodak® Fixer — Sigma-Aldrich, P8307
- KpnI restriction enzyme — Promega, R6341
- LB agar, Miller — Fisher Scientific, BPE1425-500
- LB broth, Miller — Fisher Scientific, BPE1426-500
- MAX Efficiency® DH5α™-T1R Competent Cells — Invitrogen, 12297-016
- Methanol — Fisher Scientific, M/4000/17
- MTT — Sigma-Aldrich, M5655
- NanoDrop Technologies NanoDrop® ND-1000 Spectophotometer
- NheI restriction enzyme — Promega, R6501
- NotI restriction enzyme — Promega, R6431
- Orange G dye — Sigma-Aldrich, O1625
- PBS (1x) [Sterile] — Sigma-Aldrich, D8662
- PBS (Dulbecco A) — Oxoid BR0014G
- Photographic film (Hyperfilm) — GE Healthcare, 28906837
- Platinum® Taq High Fidelity DNA Polymerase — Invitrogen, 11304-011
- Precision Plus kaleidoscope marker — Bio-Rad, 161-0375
- Protein Reagent Dye Concentrate — Bio-Rad, 500-0006
- PVDF Membrane (Immobilon-P) — Millipore, IPVH00010
- QIAPrep® Spin Miniprep Kit — Qiagen, 27106
- QIAquick Gel extraction kit — Qiagen, 28704
- QIAshredder® Spin Columns — Qiagen, 79654
- Restriction Buffer H, 10x — Promega, R008A
- Restore Stripping buffer — Fisher scientific, 21059
- RNase-Free DNase Set — Qiagen, 79254
- RNase ZAP™ — Sigma-Aldrich, R2020
- RNeasy® Mini Kit — Qiagen, 74104
- Sodium acetate — Sigma-Aldrich, S2889
- Sodium dodecyl sulphate — Sigma-Aldrich, L5750
- Superscript™ First-Strand Synthesis System for RT-PCR kit — Invitrogen, 11904-018
- Sulphuric Acid (2N) — Sigma-Aldrich, 35276
- TaqMan® Universal PCR Master Mix (2x) — Applied Biosystems, 4304437
- TEMED — Sigma-Aldrich, T9281
- TOPO TA Cloning® Kit for Sequencing — Invitrogen, K4575-J10
- TOPO XL PCR cloning kit — Invitrogen, K4510-20
- TRIS-base — Fisher scientific, 15504-020
- Triton X-100 — Sigma-Aldrich, 9002-93-1
- Tween® 20 — Sigma-Aldrich, P7949
- T4 DNA Ligase (HC) — Promega, M180A
- VectaShield™ Hard+Set Mounting Media with DAPI — Vector Laboratories, H-1500
- XhoI restriction enzyme — Promega, R6161
- 1Kb DNA ladder — Invitrogen, 15615-016
- 100bp DNA ladder — Invitrogen, 15628-019

2.1.2 MAMMALIAN CELLS AND CELL CULTURE MATERIAL

- BEAS-2BR1 cell line   A kind gift from Prof Ray Penn, University of Maryland, Baltimore, USA
- BEGM BulletKit   Lonza/Clonetics, CC-3170
- Cigarettes (3R4F)   University of Kentucky, Reference Cigarette Program
- DMEM culture medium   Sigma-Aldrich, D5796
- Foetal calf serum (FCS)   Sigma-Aldrich, F-7524
- HBEC (primary cells; Donors 7F3158 & 7F3206)   Lonza/Clonetics, CC-2540
- MRC-5 cell line   ECACC, 84101801
- Trypan Blue solution, 0.4%   Sigma-Aldrich, T8154
- Trypsin-EDTA solution (1x)   Sigma-Aldrich, T3924
- Trypsin Inhibitor   Invitrogen, 17075-029

2.2 MOLECULAR BIOLOGY METHODS

2.2.1 POLYMERASE CHAIN REACTION

A Polymerase Chain Reaction (PCR) is a technique by which a segment of DNA is exponentially replicated *in vitro* through a process of denaturation, annealing and extension. Amplification of the region of interest, using the original strand as a template, occurs on the addition of oligonucleotides (Primers) complimentary to either of the terminal ends of the region of interest, along with single nucleotides (dNTPs), Magnesium and an amplification enzyme. Successive cycles of amplification produce increasing amounts of the required fragment on an exponential scale.

Primers used for specific amplifications are referenced in their respective Chapters (see Sections 2.2.12, 4.5.6 & 5.4.2) and were designed according to the standard rules (Dieffenbach et al., 1993). However, certain primers used in this thesis were larger than the recommended length of ~20bp. This was due to necessary design elements for plasmid construction e.g. restriction sites. In general all primers were about 28–40bp long, contained *circa* 50% GC content to avoid mispriming in GC rich DNA regions and contained a melting temperature (Tm) between 60°C and 80°C. Palindromes, repeats and runs were avoided. All primers were designed manually and validated (including detection of stable hairpins, dimers and cross-dimers) using the online tools NetPrimer[1] and Primer-BLAST[2] (Ye et al., 2012).

All PCRs carried out used the amplification enzyme Platinum *Taq DNA* Polymerase along with other constituents as outlined in Table 2.1.

---

[1] http://www.premierbiosoft.com/netprimer/index.html
[2] http://www.ncbi.nlm.nih.gov/tools/primer-blast

Reagent	Stock Concentration	Final Concentration	Volume
Water			36.75 µl
Enzyme buffer	10 X	1 X	5 µl
Mg^{2+}	50 mM	2 mM	2 µl
dNTP	5 mM	200 µM	2 µl
Platinum Taq	5 U/µl	0.03 U/µl	0.25 µl
Forward Primer	10 µM	0.2 µM	1 µl
Reverse Primer	10 µM	0.2 µM	1 µl
Sample Template			2 µl
Total Volume			*50 µl*

Table 2.1: Polymerase Chain Reaction mix. This table identifies the constituent materials required to carry out a PCR as well as the required volume and concentration.

A heated lid DNA Engine Tetrad 2 Cycler was used to carry out all PCRs using cycling parameters as outlined below.

Initial Denaturation	94°C	1min	
Denaturation	94°C	30 sec	**X 35 cycles**
Annealing	55°C	30 sec	
Extension	68°C	1 min per kb (minimum 1min)	
Final Extension	72°C	10 min	
	4°C	hold	

2.2.2 AGAROSE GEL ELECTROPHORESIS OF DNA

Agarose gel electrophoresis is a process by which DNA fragments are separated according to the fragment's size. DNA is formed of negatively charged nucleotides, which uniformly migrate towards a positive charge. Fragments separate based on size due to smaller fragments passing more readily through the gel matrix than larger fragments. DNA fragments are visualised using the intercalating agent Ethidium Bromide (0.5µg/ml). This emits luminescence on exposure to UV light. A number of gel concentrations were used according to the size of fragment to be resolved. A 1% w/v gel was used for fragments between 200bp and 1kb while a 1.5% w/v gel was used for fragments between 1.5kb and 10kb. Gels were created by heating agarose powder dissolved in 1xTAE buffer (50ml) (from 50X stock – see Appendix I). Samples were loaded using 6x Orange G loading dye (Appendix I) to a final concentration of 1x, while

the required DNA ladder(s) (Appendix I)) were included on each gel. Gels were run in 50ml 1x TAE buffer at approximately 80Volts for 30 minutes. Bands of DNA fragments were visualised under UV light using a Syngene GeneGenius Gel Doc system and GeneSnap v6.08 software (Syngene).

2.2.3 GEL PURIFICATION OF DNA BANDS

The Qiagen QIAquick Gel extraction kit was used to purify all PCR products. Here a specialised silica membrane selectively retains DNA and washes clear any contamination, followed by elution of the DNA with sterile water.

Briefly, the required DNA fragments are excised, using a sterile single-use scalpel, from the agarose gel while visualised on a Ultra-Violet Transilluminator. The pieces are dissolved into the DNA extraction buffer by incubation at 50°C for 10 minutes. The resulting solution is then passed through the silica membrane in microspin cups by centrifugation. The resulting bound DNA is washed with wash buffer + 50% Ethanol and eluted by passing 50µl of sterile water through the membrane (following a one minute incubation at room temperature). The extraction procedure is quality controlled by gel electrophoresis (see Section 2.2.2).

2.2.4 TOPO TA AND TOPO XLCLONING

Both the TOPO TA and the TOPO XL (for fragments >2.5kb) kits have been used to form large copy numbers of a particular sequence of DNA via cloning (Fonte et al., 2002, Liu et al., 2002b). This results in the duplication of DNA with a lower degree of error than that provided by PCR. Cloning involves the use of a single Adenosine overhang introduced at the terminal end of a PCR fragment by the *Taq* enzyme. *E.coli* cells provided by the kit are then transformed with the kit specific plasmid (Fig. 2.1), where the bacteria form multiple copies of the plasmid through their reproduction.
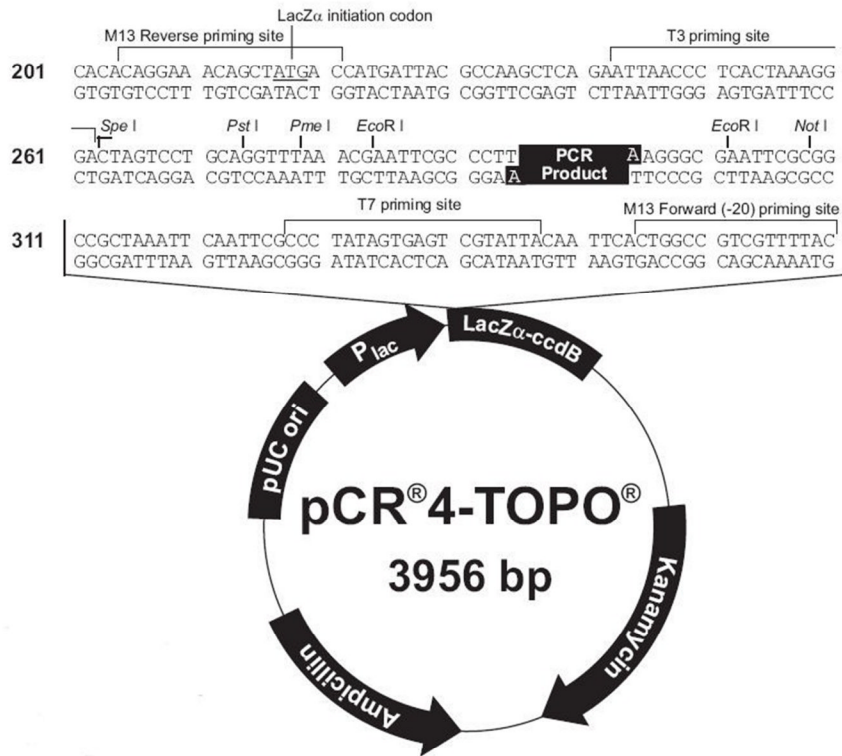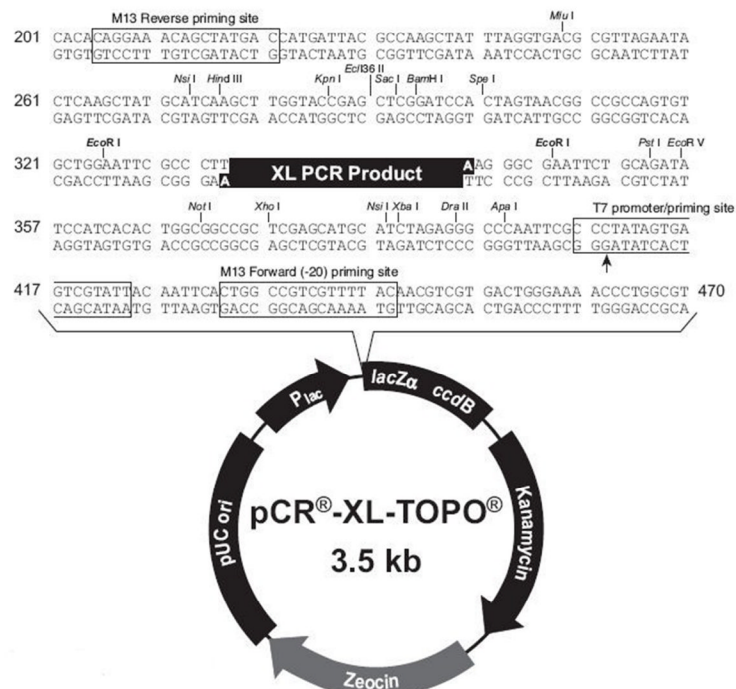
Figure 2.1: Vectors used in TOPO cloning. The pCR4-TOPO vector (Panel A) was used to clone all fragments smaller than 1000 base pairs while the pCR-XL-TOPO (Panel B) was used to clone fragments larger than 1000 base pairs.

2.2.4.1 TOPO TA CLONING KIT FOR SEQUENCING

The TOPO TA Cloning® kit for Sequencing provides a highly efficient single step cloning strategy directly for *Taq* polymerase-amplified PCR products. The protocol involves:

1. Incubation of a mix of 4µl of the freshly prepared PCR product (see Section 2.2.3), 1µl of the kit's salt solution and 1µl of the pCR-4-TOPO vector at 23°C for five minutes.

2. Addition of 2µl of the TOPO® Cloning reaction into a vial of One Shot® TOP10 Chemically Competent *E. coli.*

3. Incubation of the mix on ice for thirty minutes.

4. Heat-shocking the cells for thirty seconds at 42°C without shaking and immediately transferring the tubes to ice.

5. Addition of 250µl of kit provided SOC medium warmed to room temperature followed by shaking the tube horizontally at 200 rpm at 37°C for one hour.

The bacterial broth was then used to culture transformed bacteria to form sizable colonies that could be used for plasmid prepping (Section 2.2.6). For a detailed procedure please refer to Section 2.2.5.

2.2.4.2 TOPO XL PCR CLONING KIT

TOPO® XL PCR Cloning is modified for the cloning of long PCR products. This kit differs from the TOPO TA Cloning® kit in the inclusion of a different plasmid vector (pCR-XL-TOPO; Fig. 2.1b) and has a kit specific methodology for the gel purification of the PCR constructs that is different to those outlined in Sections 2.2.2 & 2.2.3. In brief the procedure is as follows:

1. **Running the gel**

Gels were prepared by dissolving 50mg of agarose into 50 mL of 1X TAE buffer and 40µL of the kit provided 2mg/mL Crystal Violet solution. A total of 40µl of the PCR product with 8µl of the 6X Crystal Violet Loading Buffer was loaded into the gel, which was run in 1X TAE buffer. The DNA band should be visible in normal light.

2. **Gel Purification**

The band was excised using a sterile single-use scalpel and then dissolved in 2.5x volume of sodium iodide by heating at 50°C. Following the addition of 1.5x volume of binding buffer the product was passed through the membrane in the filter tubes by centrifugation and washed with 1x Wash Buffer. Following 1 minute incubation at room temperature, the DNA was then eluted by passing 50µl of sterile water through the membrane.

3. **TOPO Cloning**

Similar to the TOPO TA method, 4µl of the gel purified PCR product was added to 1µl of the pCR-XL-TOPO vector and left to incubate for five minutes at room temperature. Following this, 1µl of the 6x TOPO® Cloning Stop Solution was added, which increased the yield of transformants by an average of 2-fold. The kit then follows a procedure identical to that for the TOPO TA Cloning kit (see Section 2.2.4.1).

2.2.5 BACTERIAL CELL CULTURE

Bacterial strains cultured in this thesis included the TOP 10 *E.coli* cells provided in the TOPO TA and TOPO XL cloning kits as well as the MAX Efficiency® DH5α™ Competent Cells. Transformation (see Section 2.2.4.1) and culturing procedures were identical for both types of cells.

All transformed cells were cultured on Lysogeny Broth (LB) agar plates (Appendix I) inoculated with 100μg/ml Ampicillin (Amp[100]) at 37°C for 16-18 hours, apart from those containing the pCR-XL-TOPO vector, which were similarly treated but on LB agar plates inoculated with 50μg/ml Kanamycin (Kan[50]). Following incubation, single transformed colonies were propagated in 5ml Amp[100] or Kan[50] LB broth (Appendix I) in a heated orbital incubator at 37°C for 16-18 hours at 200rpm. A 100μl aliquot of the broth was used to streak a new Amp[100] or Kan[50] LB agar plate, with the procedure described above repeated to form an LB broth with a colony originating from a single bacterial cell. Broths were then used to either extract plasmid DNA (see Section 2.2.6) or to form glycerol stocks for long-term storage.

Glycerol stocks were formed by mixing 700μl of the LB broth culture (cell density: ~3-4.10[9] cells/ml) with 500μl of autoclaved 50% w/v glycerol. These stocks were then stored at -80°C.

2.2.6 PURIFICATION OF PLASMID DNA

Plasmid purification was carried out using the QIAprep® Miniprep kit unless larger and endotoxin free stocks of plasmid for mammalian cell transfection were required were the Endofree® Plasmid Purification kit was used. Both kits use alkaline lysis, neutralisation and solution adjustment to high salt-binding conditions. Plasmid DNA is then bound to a silica-based membrane, and washed to remove both contaminants and endonucleases followed by elution under low salt conditions, all via centrifugation.

2.2.6.1 QIAPREP® MINIPREP KIT (YIELDS 5 –15MCG DNA)

This kit was used to create plasmid stocks with a resulting concentration of ~200ng/μl and a maximum volume of 50μl. In brief 1400μl of the LB broth (Section 2.2.5) was centrifuged at 6800xg to form a bacterial pellet. The resulting bacterial pellet was

re-suspended in 250µl of Buffer P1 with RNase A, lysed using 250µl of Buffer P2 and neutralised within five minutes of the addition of Buffer P2 by adding 350µl of Buffer N3. The resulting mixture was then centrifuged for 10 min at 13,000rpm to form a compact white pellet consisting of organelles and other cell debris. The supernatant was then applied to a QIAprep spin column, where the DNA was bound to the silica based membrane, washed using 500µl of Buffer PB and 750µl of Buffer PE +80% v/v Ethanol and eluted in 50µl sterile water following a one minute incubation.

2.2.6.2 ENDOFREE® PLASMID PURIFICATION KIT (YIELDS 300–500MCG DNA)

As this kit was solely used for the formation of plasmids to be transfected into mammalian cells it is important that the solution is endotoxin free. This is since endotoxins can reduce the transfection efficiency of mammalian cells with plasmid DNA (Weber et al., 1995), cause nonspecific activation of the immune system, stimulate cytokine production and induce the characteristic shock syndrome associated with bacterial infections (Heid et al., 1996).

The principle through which this kit functions is similar to that of the QIAPrep® Spin Miniprep Kit. Due to the larger scale of this preparation, plasmid DNA is bound to an anion-exchange resin by gravity flow where it is washed and eluted via centrifugation, with the resulting DNA pellet concentrated through isopropanol precipitation and re-pelleted by centrifugation. This resulting pellet was re-suspended in endotoxin-free water.

2.2.7 DIDEOXYNUCLEOTIDE TRIPHOSPHATE CHAIN TERMINATOR SEQUENCING

Also known as the Sanger method, this DNA sequencing method denatures target DNA and anneals it to an oligonucleotide primer, which causes 5` to 3` chain extension similar to that in PCR (Section 2.2.1). Addition of the chain-terminating dideoxynucleotide triphosphates (ddNTPs), which lack a 3' OH group, forms short DNA chains of varying size (Suzuki et al., 2005). In this way, each nucleotide in the investigated sequence is presented as a terminal nucleotide in the resulting solution. In the dye terminator version of this technique, the ddNTPs are labelled with different fluorescent dyes allowing, following separation based on fragment length by gel electrophoresis, nucleotide detection on exposure to laser excitation of the relevant wavelengths. This allows for accurate determination of the DNA sequence.

All ddNTP sequencing was exclusively carried out on plasmids, using the BigDye® Terminator v3.1 Cycle Sequencing Kit. All utilised sequencing primers are listed below in Table 2.2.

Plasmid	Type	Primer	Tm	Percentage GC
pGL4	Forward	CTAGCAAAATAGGCTGTCCC	60	50
	Reverse	TACCAACAGTACCGGA	68	50
psiCHECK-2	Forward	TCAAGAGCTTCGTGGAGCGCG	75	61
TOPO (M13)	Forward	GTAAAACGACGGCCAG	49	56
	Reverse	CAGGAAACAGCTATGAC	42	47

Table 2.2: Sequencing primers utilised in this thesis. Each primer was used individually to sequence their relative plasmids using dideoxynucleotide triphosphate chain terminator sequencing. Primers for pGL4 and psiCHECK-2 were designed by the investigator, while the M13 primers were provided with the TOPO and TOPO XL kits.

2.2.7.1 SEQUENCING REACTION

The sequencing reaction was carried out in a mastermix set up as shown in Table 2.3.

Substance	Volume per sample (µl)
Plasmid DNA	0.5 (~100ng)
BigDye premix	0.5
BetterBase	3.5
1µM primer	1.5
Sterile Water	4.0

Table 2.3: Reaction mix for dideoxynucleotide triphosphate chain terminator sequencing. All sequencing reactions carried out in this thesis utilised the same mix as listed above.

A heated lid DNA Engine Tetrad 2 Cycler was used to carry out all sequencing reactions using the template outlined below:

Denaturation	96°C	30 sec	**X 25 cycles**
Annealing	50°C	15 sec	
Extension	60°C	4 min	
Final Extension	28°C	1 min	
	10°C	hold	

2.2.7.2 PURIFICATION AND ANALYSES OF SEQUENCING REACTIONS

The resulting DNA fragments were then precipitated using the following method:

1. Pipette the resulting PCR mixture into a 500µl microcentrifuge tube containing 2µL of 3M sodium acetate, pH 5.2 and 2µl of 125mM EDTA (pH 8.0) and incubate at 28°C for 15 min.

2. Add 50µl of 100% Ethanol to each tube and centrifuge for 30 min at 13000xg.

3. Aspirate and discard the resulting solution and rinse the pellet with 250µl of 70% ethanol followed by centrifugation for 5 min at 13000xg.

4. Carefully aspirate all of the supernatant and air dry the pellet.

The resulting pellet was then sent to the Post-Genomic Technologies Facility, School of Molecular Medical Sciences, University of Nottingham UK, where sequencing was carried out using an Applied Biosystems 3130 Genetic Analyser.

2.2.7.3 ANALYSIS

DNA sequences were visualised and converted to FASTA format using Chromas Lite version 2.10 (Technelysium Pty Ltd, Australia). Standard IUPAC DNA ambiguity codes were assigned.

Sequences were first screened for vector contamination by the online tool VecScreen[3] and then aligned using the online sequence alignment tool Nucleotide BLAST[4] against the human genome (Build 37). Any apparent variation on the BLAST output was investigated in Chromas Lite by chromatogram peak verification at relevant positions.

2.2.8 RESTRICTION DIGEST

Restriction enzymes recognize short DNA sequences and cleave double-stranded DNA within or adjacent to these sequences allowing for specific extraction of DNA fragments from a larger DNA sequence. Restriction sites were identified using the online tool WEBCutter[5]. The use of restriction enzymes for cloning is outlined in the plasmid design sections of this thesis (Section 4.5.6 & 5.4.2).

In brief, restriction digests were carried out using Promega UK restriction enzymes and other constituents as outlined in Table 2.4.

---

[3] http://www.ncbi.nlm.nih.gov/VecScreen/VecScreen.html

[4] http://blast.ncbi.nlm.nih.gov/Blast.cgi?PAGE=Nucleotides&PROGRAM=blastn&BLAST_PROGRAMS=megaBlast&PAGE_TYPE=BlastSearch&SHOW_DEFAULTS=on

[5] http://rna.lundberg.gu.se/cutter2/

Substance	Volume (μl)
BSA	0.2
Restriction Enzyme Buffer	2
Restriction Enzymes	0.5 (total; 0.25x2)
DNA sample	2
Sterile water	8.3

Table 2.4: Reaction mix for restriction digests carried out in this thesis. All digests utilised the mix as outlined above. Restriction enzyme buffers changed as follows, according to the enzyme mix; [Promega Multicore: NheI/KpnI] [Promega Buffer D: XhoI/NotI] [Promega Buffer H: XhoI/EcoRI]

A heated lid DNA Engine Tetrad 2 Cycler was used to incubate the mix at 37°C for 60 minutes after which the reaction was terminated by the addition of 2μl of Orange G loading dye. Resulting fragments were visualised on an agarose gel with undigested plasmid as a negative control (Section 2.2.2). DNA to be used in ligation procedures were gel purified as outlined in Section 2.2.3.

2.2.9 T4 LIGATION

Ligation is the process by which two complimentary DNA strands are joined together through the catalysing of the formation of a phosphodiester bond by a ligase enzyme. Ligation was carried out using the T4 DNA Ligase kit (Promega, UK), according to the manufacturer's instructions. In brief, 1μl of gel purified digested vector (100ng) was combined with 3μl of insert to form a molar ratio of 1:3 and other constituents as outlined below (Table 2.5) to form a final volume of 10μl:

Substance	Volume (μl)
Linearized Vector	1
Insert	3
T4 DNA Ligase (5U/μl)	1
Ligase 10X Buffer	1
Sterile water	4

Table 2.5: Mix used to carry out T4 ligations. All ligation carried out in this thesis used the mix as outlined above.

A heated lid DNA Engine Tetrad 2 Cycler was used to incubate the mix at 22°C for 3 hours, followed by incubation at 4°C for 18 hours, thereby allowing enough time for the ATP-dependent ligation to occur. Vector- and insert-only ligations were included as negative controls. One Shot® MAX Efficiency® DH5α™-T1R Competent Cells were then transformed with the ligation mixture as outlined in Section 2.2.5.

2.2.10 TOTAL RNA EXTRACTION

Total RNA extraction was carried out using the Qiagen RNeasy® Mini Kit in conjunction with the Qiagen QIAShredder Kit as per manufacturer's instructions. Here, a specialised high-salt buffer system retains up to 100μg of total RNA of a length greater than 200 bases from disrupted cells to the RNeasy silica membrane. Washes then clear any contamination, followed by elution of the DNA with sterile water. Selection of RNA >200 bases excludes 5.8S rRNA, 5S rRNA, and tRNAs from the resulting solution (Qiagen, 2010).

Briefly, cells cultured in either T25 flasks or 6-well tissue culture plates (area per well 9.60cm^2; expected number of cells at confluence ~300000) were disrupted in 350μl of RLT buffer via mechanical scraping, The solution was then homogenised by placing the lysate directly into a QIAshredder spin column within a 2ml collection tube and passing the solution through by centrifugation at 13000rpm. The resulting homogenised solution was then treated with 1X volume 70% ethanol which was then passed through the silica membrane in a fresh RNeasy spin column by a 15 second centrifugation at 13000rpm. The resulting bound RNA was then washed with 350μl Buffer RW1. DNase I (10μl DNase I enzyme + 70μl Buffer RDD [Qiagen RNase-Free DNase Set]) was then incubated on the membrane at room temperature for 15 minutes in order to degrade any genomic DNA. This was followed by a final wash with 350μl of Buffer RW1 and

500µl Buffer RPE+80% v/v ethanol. The RNA was then eluted in 50µl of RNase-free water directly to the spin column membrane (x2 elutions).

Presence of RNA in the resulting RNA solutions was then detected using agarose gel electrophoresis (Section 2.2.2) and quantified using a NanoDrop Technologies NanoDrop® ND-1000 Spectrophotometer. All RNA samples were stored at -80°C. All work was carried out in an RNAse free environment set up by the use of RNase ZAP™.

2.2.11 SYNTHESIS OF COMPLIMENTARY DNA

Single stranded complimentary DNA (cDNA) was synthesised from the extracted total RNA samples using Invitrogen's Superscript™ First-Strand Synthesis System for RT-PCR kit. All cDNA synthesis was carried out using the kit's random hexamers (6bp oligonucleotides of random sequence) at a concentration of 10ng per 1µg of RNA. This allowed for the priming of multiple random sites on the RNA template. This generated overlapping cDNA fragments of various sizes, thereby ensuring that the whole RNA sequence was represented in the resulting cDNA mix. The resulting single-stranded DNA is treated with RNase in order to remove any RNA template remaining and make it ready for qPCR. A reverse transcriptase (RT) negative control was carried out for each sample synthesised, while a general RT positive control was carried out for the cDNA synthesis experiment *per se*. All cDNA used for comparative analyses was created in one experiment in order to limit batch variation.

Briefly, the following master mix was set up:

Substance	Volume (µl)
10mM dNTP mix	1.00
Random hexamers	0.50
RNA	Equivalent to 2.5µg RNA
DEPC-treated water	To 10

Table 2.6: Reaction mix A for reverse transcription PCR. This mix is the first part of the solution utilised to create cDNA from RNA using the Superscript™ First-Strand Synthesis System.

A heated lid DNA Engine Tetrad 2 Cycler was then used to incubate the RNA/primer mixture at 65°C for 5 minutes, followed by incubation on ice for 1 minute. A total of 9µl of the following solution was then added to the solution (Table 2.7):

Component	Volume (µl)
RT Buffer	2
MgCl2	4
DTT	2
RNaseOUT™ (40 U/µl)	1

Table 2.7: Reaction mix B for reverse transcription PCR. This mix is the second part of the solution utilised to create cDNA from RNA using the Superscript™ First-Strand Synthesis System.

Following a two minute incubation at room temperature, 1µl (50 units) of the SuperScript™ II RT enzyme was added, except in the case of RT negative controls where 1µl of DEPC-treated water was added instead. The solution was then incubated at room temperature for 10 minutes followed by incubation at 42°C for 50 minutes and termination of the reaction at 70°C for 15 minutes using a heated lid DNA Engine Tetrad 2 Cycler. In order to remove any remaining and contaminating RNA, 1µl of RNaseH was added (37°C for 20 minutes). Due to the high concentration resulting from this protocol, the resulting cDNA was diluted 1:10 into sterile water.

Quality control of the synthesis procedure for both successful synthesis and contamination was carried out by reverse-transcription PCR (RT-PCR). This involved carrying out a PCR as described in Section 2.2.1 using primers for Glyceraldehyde 3-phosphate dehydrogenase (GAPDH) (see Table 2.8) in all the samples and the RT negative controls. RT-PCR was not carried out on the RT positive control as this was based on bacterial RNA and therefore lacked the human GAPDH gene. Bands were visualised on an agarose gel with positive detection of GAPDH resulting in a band at the 293bp position.

Name	Sequence	Location
Forward GAPDH Primer	GGTGAAGGTCGGAGTCAACGGA	Exon 1 12:6644008-6644029
Reverse GAPDH Primer	GAGGGATCTCGCTCCTGGAAGA	Exons 3&4 12:6645959-6645969 12:6646099-6646110

Table 2.8: GAPDH primers used in the quality control of qPCR reactions. The reverse primer was designed to cross over two exons which allowed for selective replication of GAPDH mRNA.

2.2.12 QUANTITATIVE PCR

Quantitative PCR is the method of choice for mRNA quantification as a measure of gene activity, addressing the requirement for mRNA quantification in molecular medicine, biotechnology, microbiology and diagnostics (Nolan et al., 2006). For all work addressed, the TaqMan® method was used. This technique utilises a fluorescent DNA probe based on the 5′ to 3′ exonuclease activity of *Taq* polymerase (Holland et al., 1991). Here, a designed gene specific oligonucleotide probe, with a reporter fluorescent dye attached to its 5′ end and a quencher dye attached to its 3′ end, hybridises to the accumulating PCR product. Using primers designed to specific gene exon regions, *Taq* polymerase is able to cleave the quencher dye during PCR amplification via its 5′ nuclease activity (Heid et al., 1996) adding a second layer of

specificity to the reaction. This results in fluorescence accumulation, which allows for the quantitation of gene expression with high degree of specificity and sensitivity (VanGuilder et al., 2008, Suzuki et al., 2005).

The cycle threshold (C_t) can be defined as the point when the degree of fluorescence becomes exponential and moves into the linear phase of a graph where the number of cycles (x-axis) is plotted against fluorescence on a logarithmic scale (y-axis). The relationship between the original concentration of the starting template and the C_t is an inverse one, with the lower the C_t, the greater the starting quantity of template and vice-versa. Relative gene expression was calculated using C_t values as previously described (Livak and Schmittgen, 2001), where a $C_t>40$ is taken as no cDNA present (RT-ve). All C_t values were calculated using MxPro™ QPCR Software v4.01 and Microsoft Excel 2010.

Variation in cDNA levels between samples was corrected using the hypoxanthine phosphoribosyltransferase 1 (HPRT) Pre-Developed TaqMan Assay Reagent (PDAR) as a housekeeping gene. As the PDAR was found to interact with the assays for membrane and soluble PLAUR (Dr Ceri Stewart; unpublished work), these assays were carried out in conjunction with the assay for total PLAUR. In this way the PDAR values obtained from the total PLAUR assay could be utilised in the calculations for the membrane and soluble PLAUR assays.

The primers and probes (Tables 2.9 & 2.10) used to quantify the starting levels of mRNA were designed and validated by Dr Ceri Stewart (University of Nottingham) using Beacon Designer 7.0 software (PREMIER Biosoft International) (Stewart et al., 2009, Stewart et al., 2012). Each assay was validated through the use of standard curves. These were produced by assaying a PLAUR expressing plasmid construct serially diluted 10-fold from 300,000 to 30 copies, as outlined by the Applied Biosystems guide 'Creating Standard Curves with Genomic DNA or Plasmid DNA

Templates for Use in Quantitative PCR'. QPCR efficiency rates were determined at 65.3% for the total PLAUR assay, 85.1% for the mPLAUR assay and 72.0% for the ssPLAUR assay (Fig. 2.2). Assay efficiency was plotted using the MxPro™ QPCR Software v4.01 using the formula:

$$\textit{Assay Efficiency (\%) = [(10-1/slope-1) x 100]}$$

Assay	Target	Forward Primer	Reverse Primer	PDAR
1	Total PLAUR	PLAUR E1 L258 CTGCTGCTGCTCCACACCT	PLAUR E2 R345 ACTCTTCCACACGGCAATCCC	HPRT
2	Membrane PLAUR	PLAUR E1 L258 CTGCTGCTGCTCCACACCT	E7V1 R1118 TGGGTGGTTACAGCCACTTT	None
3	Soluble PLAUR	PLAUR E1 L258 CTGCTGCTGCTCCACACCT	suPAR R1013 TGGCAACCAGCTTCCCCAGAGT	None
All	Probe	uPARall CCAGCCTCTTGGGGCCTGCGGT		

Table 2.9: Primers and Probes used in the TaqMan™ qPCR carried out in this thesis. While the probe and the forward primer are common to all 3 assays, the reverse primer for each assay specifically targets either total PLAUR, membrane PLAUR or soluble spliced PLAUR. Due to interference between the Housekeeper gene HPRT and the assays for membrane and soluble spliced PLAUR, the housekeeper gene was only multiplexed with the total PLAUR assay and so the remaining assays had to be carried out at the same time using the HPRT values from the first assay. PDAR: pre-developed assay reagent, HPRT; hypoxanthine phosphoribosyltransferase 1. The alphanumeric code present in primer names is an experimental cross-reference.

Primer Name	Sequence	Exon	Location
PLAUR E1 L258	CTGCTGCTGCTCCACACCT	1	44174226 - 44174245
PLAUR E2 R345	ACTCTTCCACACGGCAATCCC	2	44171775 - 44171796
E7V1 R1118	TGGGTGGTTACAGCCACTTT	7a	44153162 - 44153181
sPLAUR R1013	TGGCAACCAGCTTCCCCAGAGT	7b	44150672 - 44150694
Probe	CCAGCCTCTTGGGGCCTGCGGT	2	44171861 - 44171839

Table 2.10: Locations of qPCR primers and probe outlined in Table 2.8. Locations refer to chromosome 19 build GRCh37.
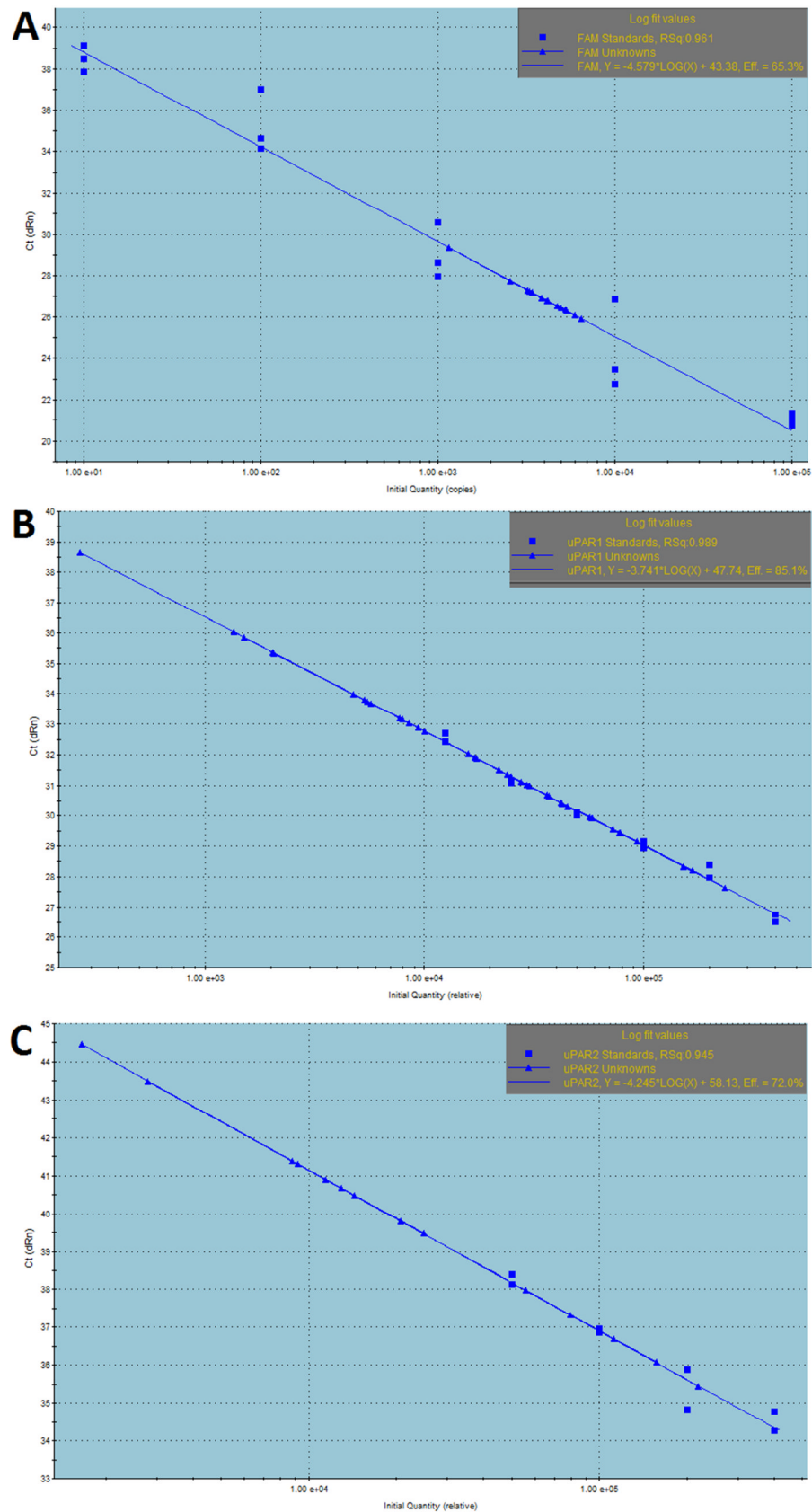
Figure 2.2: Standard curves for total (Panel A), membrane bound (Panel B) and soluble spliced (Panel C) PLAUR qPCR assays. Variation between sample readings and the standard curve determines the efficiency of that qPCR assay. QPCR efficiency rates for the total PLAUR, mPLAUR and ssPLAUR assays were determined to be 65.3%, 85.1% and 72.0% respectively. Data generated in collaboration with Dr Ceri Stewart (University of Nottingham).

2.2.12.1 TAQMAN REACTION

Quantitative PCR was carried out on 4 wells per sample (3x RT positive; 1x RT negative) as well as 3 blank wells per assay, as detailed in Table 2.11:

Component	Volume (µl)
TaqMan Universal PCR Master Mix	10
cDNA (1:10 dilution)	2
10µM Forward Primer	0.6 (0.3µM)
10µM Reverse Primer	0.6 (0.3µM)
5µM Probe	0.4 (0.1µM)
PDAR (HPRT)	1
Sterile Water	To make up 20

Table 2.11: TaqMan™ mastermix for qPCR. This mastermix was used universally for qPCR in this thesis. Reverse primers varied according to the assay used (Table 2.8) while both probe and forward primer remained constant (Table 2.8).

Each assay was then run on the Stratagene™ qPCR machine, collecting data for the ROX™, HEX™ and FAM™ dyes using the cycling procedures listed below:

Total PLAUR:

Temperature	Time	
50°C	2 min	
95°C	10 min	
95°C	15 sec	**X 40 cycles**
60°C	10 min	

Membrane and Soluble spliced PLAUR:

Temperature	Time	
50°C	2 min	
95°C	10 min	
95°C	20 sec	**X 40 cycles**
55°C	20 sec	
65°C	1 min	

2.2.12.2 ANALYSIS

Data analyses were carried out using the MxPro Mx3005P v4.01 software, utilising the following procedure:

1. The reference dye was set to ROX and selected or unselected according to which assay had been carried out

2. Data was treated individually, with fluorescence set to dRN

3. Data was visualised as log10 values and thresholds, determined through manual adjustment of the cycle threshold, were set for each assay:

   a. HPRT: 0.02

   b. Total PLAUR: 0.03

   c. Membrane/Soluble Spliced PLAUR: 0.04

4. The generated data was exported to Microsoft Excel where $deltaC_t$ was calculated by subtracting of the data from each well from the mean HPRT value for that particular sample triplicate

5. In order to correct for the logarithmic scale to which this data is plotted the $deltaC_t$ value is transformed by $[2^{\wedge}(-deltaC_t)]$. This generates values representing the original mRNA concentrations.

2.3 PROTEIN METHODS

2.3.1 BIO-RAD PROTEIN ASSAY

The Bio-Rad protein assay is based on the Bradford assay for solubilised protein quantification (Bradford, 1976). This is a simple and accurate procedure that involves the addition of an acidic dye to a protein solution, where the absorbance spectrum shifts from 465nm to 595nm on binding to protein. This assay was used to normalise protein concentrations prior to carrying out any protein based assay.

Briefly, the protein reagent dye is diluted 1:5 in sterile water and 500μl was added to 10μl of the protein sample in a 96-well plate. The same volume was also added to PBS only wells, used as a negative control, and a set of 6 serial dilutions of BSA (2000μg/ml to 62.5μg/ml) to be used as a standard curve. The solution was left at room temperature for 10 minutes to allow dye-protein binding to occur. 200μl of the solution was then plated into a new 96-well plate and the degree of absorption at 595nm was read using a Flexstation 3 microplate reader. Unknown samples can be extrapolated from the standard curve.

2.3.2 WESTERN BLOTTING

Western Blotting is a procedure that allows for visualisation and quantification of specific proteins from a mix of total proteins through the use of antibodies raised against the protein of interest. For the purpose of this thesis, proteins were separated in a polyacrylamide gel and transferred to a PVDF sheet based on the methodology outlined by Towbin *et al*. (Towbin et al., 1979).

2.3.2.1 CELL LYSATE RECOVERY

Total intracellular protein samples used for western blotting were obtained from cells cultured in 6-well plates. To collect the protein lysate, the cell monolayer was first washed twice with 2ml of PBS. The monolayer was then exposed to 100μl of 1xSDS loading dye followed by manual scraping of the cell monolayer and recovering of the cell lysate to a microfuge tube.

2.3.2.2 SDS PAGE ELECTROPHORESIS

Sodium Dodecyl Sulphate polyacrylamide gel electrophoresis (SDS-PAGE) is a method by which proteins are separated according to their electrophoretic mobility, which is a value that reflects both the length of a protein's polypeptidechain (i.e. size) and its charge. Presence of the anionic detergent SDS linearizes the proteins while also imparting a negative charge to linearized proteins with an even distribution of charge per unit mass, thereby facilitating the separation of the protein according to charge/size.

Briefly, 10% Acrylamide resolving gels (resolves 21-100kDa) (constituted as outlined in Table 2.12) were used with the Bio-Rad Mini-protean III gel electrophoresis apparatus.

Component	Volume
Distilled water	8.0ml
30% Acrylamide	6.6ml
10% SDS	200μl
1.5M TRIS-HCL	5.0ml
10% APS	200μl
TEMED	8.0μl

Table 2.12: Reaction mix to create 10% Acrylamide resolving gels. This gel was used to separate proteins based on their electrophoretic mobility on application of a current as the first step in Western Blotting.

Once this gel had set, a 5% stacking gel (constituted as outlined in Table 2.13) was formed as set out below and placed on the 1cm gap on the top of the stacking gel. A comb was introduced to the gel and left to set.

Component	Volume
Distilled water	6.80ml
30% Acrylamide	1.66ml
10% SDS	100µl
1.0M TRIS-HCL	1.26ml
10% APS	100µl
TEMED	10µl

Table 2.13: Reaction mix to create 5% Acrylamide stacking gels. This gel was used to stack the sample prior to separation on a resolving gel for the Western Blotting procedure.

Samples were loaded onto the gel while submerged in running buffer following denaturation of the samples by heating at 94°C for 5 minutes. Samples were then separated by first running the samples through the stacking gel at 100V followed by the resolving gel at 200V until just before the blue band runs off the bottom of the gel.

2.3.2.3 WESTERN BLOTTING USING THE WET TECHNIQUE

Following successful separation of proteins by SDS-PAGE, proteins are transferred to a PVDF membrane. Transfer utilises electroblotting, where an electric current attracts the proteins from the gel into the PVDF membrane while maintaining the organization they had within the gel. Following protein transfer, non-specific protein binding sites are blocked by incubation in goat serum or milk. Proteins of interest are then probed with a primary antibody raised against a specific protein. A labelled (e.g. Horse Radish Peroxidase [HRP]) polyclonal secondary antibody then binds to the primary antibody and so amplifies the signal. The secondary antibody is then conjugated to a luminescent enzyme that allows visualisation of the target protein using photographic film.

Briefly, following electrophoresis, the resolving gel was equilibrated in 1X transfer buffer for 15 minutes. At the same time PVDF membrane, activated by dipping in 100% methanol, and filter paper cut to the dimensions of the resolving gel (~7x9cm) were also equilibrated in 1X transfer buffer for 15 minutes. The SDS-PAGE separated proteins were then transferred to the PVDF membrane in ice-cold 1X transfer buffer, where the protein transfers towards the positive cathode at 100V over a period of 1 hour. The membrane was washed for 10 minutes in PBS+0.1% v/v Tween (PBST) and blocked using either 10% goat serum in PBST for the anti-PLAUR monoclonal primary antibody IIIF10, or 10% Marvel™ milk in PBST for the anti-PLAUR polyclonal primary antibody BAF807. All blocking was carried out over 4 hours at room temperature. The primary antibodies (Table 2.14) were diluted in the blocking solution and incubated with the membrane at 4°C overnight. This was followed, after a 3X wash in PBST, with incubation with an HRP-conjugated secondary antibody (Table 2.14) diluted in the respective blocking solution and incubated at room temperature for 60 minutes.

Blocking Agent	Primary Antibody	Secondary Antibody
10% Goat Serum	IIIF10 monoclonal (1:400)	Goat Anti-Mouse HRP (1:1000)
10%v/v Marvel Milk	BAF807 polyclonal (1:500)	Donkey Anti-Goat HRP (1:1000)
10%v/v Goat Serum	Anti β-Actin (1:1000)	Goat Anti-Rabbit HRP (1:1000)

Table 2.14: Antibodies used in Western Blotting for PLAUR. Monoclonal antibody IIIF10 specifically binds to PLAUR D_I, while BAF807 is a non-specific polyclonal binding to all parts of the PLAUR protein. Anti β-actin was used as the control antibody, normalising for loading variation, based on total protein loaded into the wells.

2.3.2.4 ECL METHOD OF WESTERN BLOT PROTEIN DETECTION

The Enhanced Chemiluminescence (ECL) method of protein detection was used to detect labelled protein levels. In this method HRP, conjugated to the secondary antibody, catalyses the oxidation of diacylhydrazide luminol present in the ECL

solution, to produce excited luminol which decays to ground state via a light-emitting pathway. Exposure of photographic film to this luminescent blot allows for highly sensitive (<1pg antigen) quantification of the protein of interest.

In brief, following a 3X wash with PBST, the membrane was incubated for one minute at room temperature in 1ml of ECL reagent 1 and 1ml of ECL reagent 2 and then exposed to photographic film (Hyperfilm, GE Healthcare) within a developing cassette. The exposed film was visualised using a 1:5 dilution of Kodak® Developer. Development was terminated by washing the film in tap water and immersing it in a 1:5 dilution of Kodak® Fixer until it turned transparent. The film was rinsed in water and air dried. If a secondary blot was to be carried out on the membrane, primary and secondary antibodies were stripped off the blot by incubating the blot in warmed (37ºC) Restore Western Blot Stripping Buffer (Fisher Scientific, UK) for 15 minutes at 37ºC. The membrane would then be ready for re-blocking and staining.

The relative densities of Western blot bands were calculated using the software Image J 1.4s, with protein densities normalised to the concentration of β-Actin staining when cellular protein lysate was used.

2.3.3 SANDWICH ENZYME-LINKED IMMUNOSORBENT ASSAYS (ELISA)

Measurement of the concentration of circulating soluble cleaved PLAUR was carried out using sandwich Enzyme Linked Immunosorbent Assays (ELISAs) (Martins et al., 2012, Rybakowski et al., 2012, Singh et al., 2012) based on the previous use of sandwich ELISAs to detect circulating levels of soluble cleaved PLAUR (Andres et al., 2012, Barton et al., 2009). Sandwich ELISAs capture the protein in between two layers of antibodies (i.e. capture and detection antibody) using two separate epitopes on the protein (Fig. 2.3). This gives an advantage over other forms of ELISA due to increased sensitivity and removing the need for sample purification.
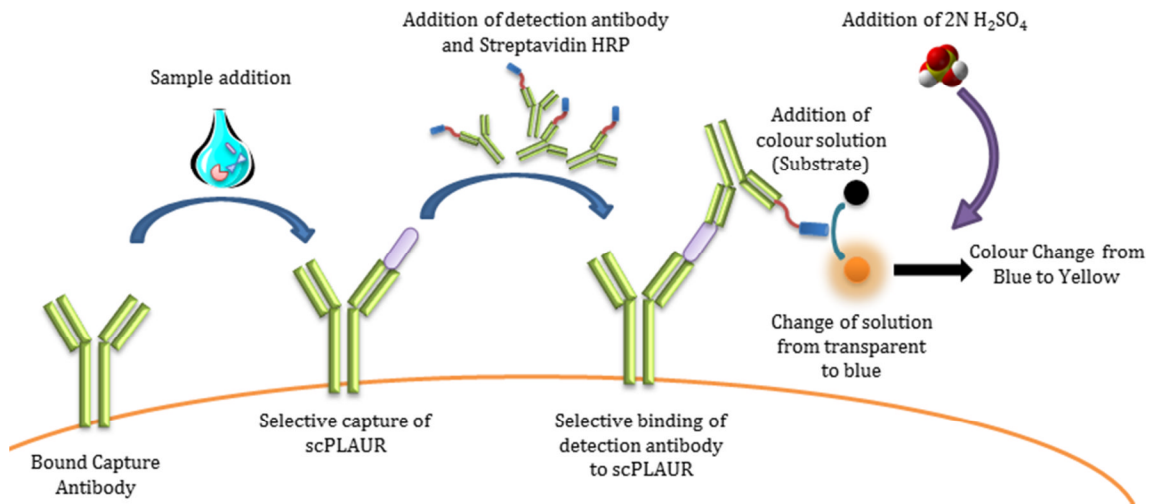
Figure 2.3: Sandwich ELISA procedure. A capture antibody is left overnight to bind to the plastic, which is then blocked using 1% solution of BSA in PBS. Sample then specifically binds to the capture antibody and in turn captures the detection antibody to which the HRP conjugated streptavidin binds. This then allows activation of the colour solution which can be read using a plate reader to quantify the amount of soluble protein in solution when data is read off a standard curve.

The kit used in this thesis was the Human Duoset® PLAUR ELISA, detects scPLAUR and not ssPLAUR (Fig. 2.4).
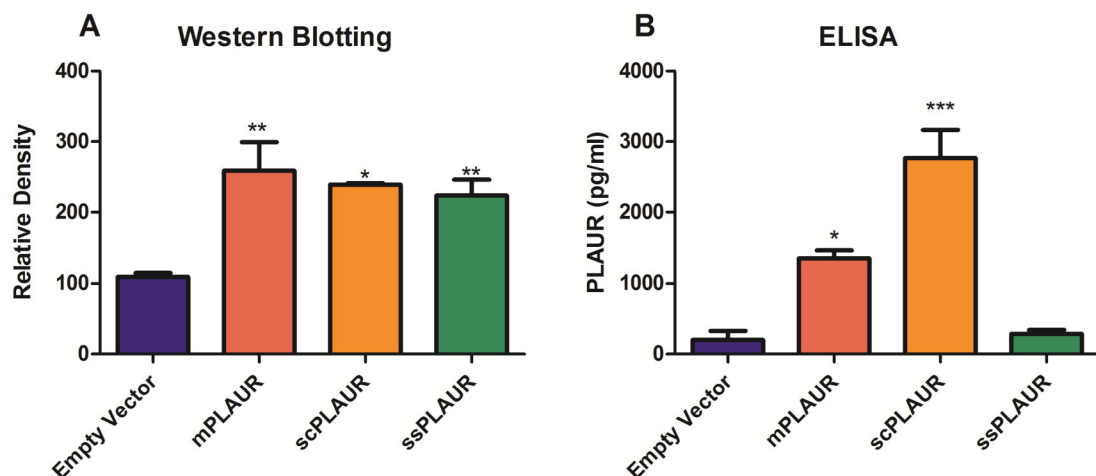
Figure 2.4: The Duoset sandwich ELISA detects scPLAUR but not ssPLAUR. Supernatant was taken from a population of Normal Human Bronchial Epithelial cells shown, via Western Blotting, to be recombinantly over expressing each of the different forms of PLAUR (Panel A) (P=1.3x10^{-3}). A Duoset Sandwich ELISA on these supernatants was able to identify elevated levels of scPLAUR originating from the overexpression of the molecule or from excess shedding due to mPLAUR expression, but was unable to detect overexpression of the soluble spliced receptor (Panel B) (P<1x10^{-4}). (n=4 over 2 donors; Western Blotting data normalised to media only control.)

In brief, a non-sterile 96 well plate was coated overnight with detection antibody diluted in phosphate buffered saline (PBS). Following removal of the remaining solution by 3 PBS+0.05% v/v Tween (PBS-T) washes, the rest of the uncoated plate was blocked with reagent diluent (PBS + 1% w/v BSA) for one hour. Sample, diluted in reagent diluent as required, was then added in duplicate for a period of two hours. This was followed by the addition of the capture antibody diluted in reagent diluent with 2% v/v heat-inactivated Goat Serum for two hours, Streptavidin diluted in Reagent diluent for 20 minutes and Colour Solution. Plates were washed 3 times with PBS-T before the addition of each new solution. Following a 20 minute incubation in the dark, stop solution (2N H_2SO_4) was added and the optical density was read using a Flexstation 3 microplate reader (reading at 450nm and corrected at 570nm). Concentration values were then calculated from standard curve that was included into each plate assay.

2.4 MAMMALIAN CELL CULTURE AND RELATED METHODS

2.4.1 MAMMALIAN CELL LINES

2.4.1.1 BEAS2BR1 CELLS

Beas2BR1 cells, which were originally derived from the bronchial epithelium of non-diseased individuals, were transformed with an Adenovirus12-SV40 hybrid virus that prolongs proliferation and infers TGF-β resistance (Reddel et al., 1988) (Fig. 2.5). Although these cells are routinely used as representative cells of the airway epithelium, in this thesis their use was limited to proof of principle experiments in light of their known atypical karyotype (Ohnuki et al., 1996).

100μm
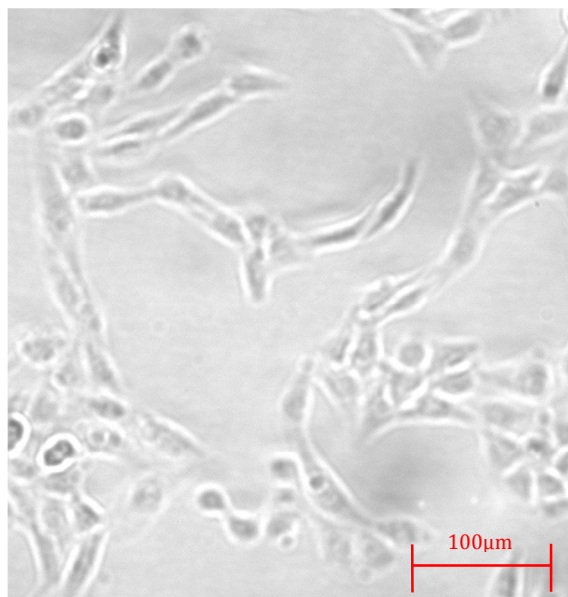
Figure 2.5: A light microscope X20 magnification image of Beas2BR1 cells. Cells are identified to be generally rounded with slightly tapered edges.

2.4.1.2 MRC-5 CELLS

MRC-5 fibroblast cells were originally derived from the normal lung tissue of a 14 week old male foetus (Jacobs et al., 1970) (Fig. 2.6). In this thesis these cells were used as control fibroblast cells for immunostaining experiments.
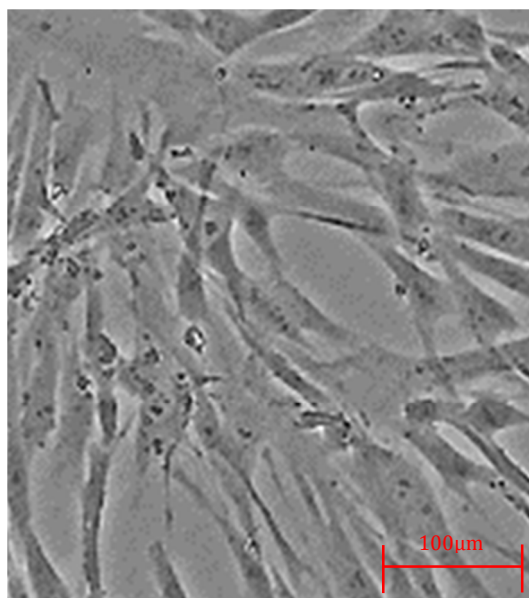
Figure 2.6: A light microscope X20 magnification image of MRC-5 cells. Cells are identified to be thin and highly elongated, which is characteristic of fibroblasts.

2.4.1.3 CULTURING CONDITIONS FOR MAMMALIAN CELL LINES

All cell lines were cultured in Dulbecco's Modified Eagle's Medium (DMEM) supplemented with 10% v/v Foetal Calf Serum (FCS). Cells were detached from culture through trypsinisation, with trypsin de-activated using DMEM+10% FCS.

2.4.2 MAMMALIAN PRIMARY CELLS

2.4.2.1 NORMAL HUMAN BRONCHIAL EPITHELIAL CELLS

Primary cells used in this thesis were human bronchial epithelial cells obtained from the post-mortem lungs of normal male subjects sourced from Lonza® (Castleford, UK) (Fig. 2.7). For further details see Appendix II
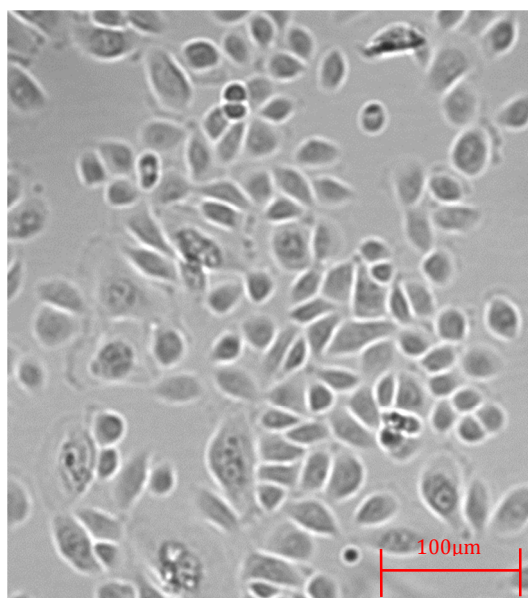
Figure 2.7: A light microscope X20 magnification image of normal human bronchial epithelial primary cells (Donor 7F3158). Cells are identified to be generally rounded with a rice like shape, which is different to that of Beas2BR1 cells.

2.4.2.2 CULTURING CONDITIONS FOR MAMMALIAN PRIMARY CELLS

Normal human bronchial epithelial cells (NHBECs) are cultured in bronchial epithelial basal media (BEBM) supplemented with additives and growth factors to form bronchial epithelial growth media (BEGM) [5μg/ml insulin, 52μg/ml bovine pituitary extract, 0.5ng/ml human recombinant epidermal growth factor, 0.5μg/ml hydrocortisone, 0.5μg/ml epinephrine 9a, 10μg/ml transferrin, 0.1ng/ml retinoic acid and 6.5ng/ml triiodo-L-thyronine (Lonza®). Cells were detached from culture through trypsinisation, with trypsin de-activated using Trypsin Inhibitor. NHBECs were seeded

at specific numbers as laid out in Table 2.15 in order to seed at 3500cells/cm^2 as recommended by Clonetics; Manual - 'Airway Epithelial Systems - Instructions for use'.

Culturing Plastic	Number of cells to seed at 3500cells/cm^2
T75 vented flask	262,500
T25 vented flask	87,500
6-well plate	96,000
48-well plate	7,500
96-well plate	3,200
4-well chamber slide	8,300

Table 2.15: Cell seeding densities for Normal Human Bronchial cells. These cell seeding densities were used to seed at the recommended density of 3500 cells/cm^3, which resulted in a 90% confluent population after five days of culture.

2.4.3 CRYOPRESERVATION OF CULTURED CELLS

In order to be able to store both cell lines and primary cells long-term, cell expansion has to be halted whilst maintaining cell viability (Ryan, 2004). Cells were frozen to a temperature of -180°C by placing them in a cryogenic tank filled with liquid nitrogen. Prior to freezing, cells were suspended in a 10%v/v solution of DMSO in FCS (Cell lines) or BEGM (NHBECs). DMSO acts as a cryoprotective agent reducing the rate of cooling and therefore preventing cell dehydration and the formation of ice crystals that would otherwise lyse the cells. Primary cells were frozen in freezing medium of BEGM+10%v/v DMSO at a concentration of 2.5×10^6 cells/ml (per vial). Cell lines were frozen in freezing medium of FCS+10% v/v DMSO, with one confluent T75 flask split into 8 vials (1ml).

2.4.4 CELL COUNTING

Cell density was determined through cell counting using an improved Neubauer haemocytometer. Briefly a 10µl cell suspension was added under the coverslip of the assembled haemocytometer. Cells were visualised under an inverted light microscope and the average number of cells was counted in the 4 corner squares. This was then multiplied by $1x10^4$ as the volume of each corner square is $0.1mm^3$.

2.4.5 TRANSIENT TRANSFECTION OF MAMMALIAN CELLS

All transient transfections of mammalian cells were carried out using the lipid based transfection reagent FuGENE® 6 (Promega, UK)(Uyttersprot et al., 1998) where the liposome+DNA complex moves into the cell by either endocytosis or fusion with the plasma membrane via the lipid moieties of the liposome (Gao and Huang, 1995). FuGENE® 6 was selected based on its very high transfection efficiency, low cytotoxicity and ability to function equally well in the presence or absence of serum.

Transfection was carried out according to the manufacturer's instructions with transfections carried out when cells achieved 50-80% confluence. Briefly, the FuGENE® 6 Transfection Reagent was first diluted in BEGM, followed by a 5 minute incubation. Plasmid DNA was then added at an experiment specific ratio, allowed to complex with the FuGENE® 6 for 15 minutes and then added to the cells.

2.4.6 MANUFACTURE OF CIGARETTE SMOKE EXTRACT

The use of cigarette smoke extract to stimulate bronchial epithelial cells has been extensively used in the literature to imitate the effect of smoking on the airway epithelium (Liu et al., 2008, Profita et al., 2011, van der Deen et al., 2007). Cigarette smoke extract was formulated as previously described (Carp and Janoff, 1978) using the University of Kentucky Reference Cigarette programme cigarettes version 3R4F

(Roemer E et al., 2012)(*Appendix III*), which were sealed and stored at 4°C until use. Briefly, two 84mm long cigarettes with the filter removed were combusted in a home-made setup (Fig. 2.8) and the smoke bubbled manually through 15ml of BEBM. The resulting solution was then filter sterilised through a 0.22μm filter so as to remove any bacteria or large contaminating particles. In order to normalise different formulations of CSE, the absorbance of a set of CSE serial dilutions was determined (0%v/v, 10%v/v, 20%v/v, 50%v/v and 100%v/v CSE) and corrected at 320nm via the NanoDrop Technologies NanoDrop® ND-1000 Spectophotometer, using its Protein A280 setting. A CSE dilution that gave an absorbance value of 0.15 was considered to be 100% CSE.
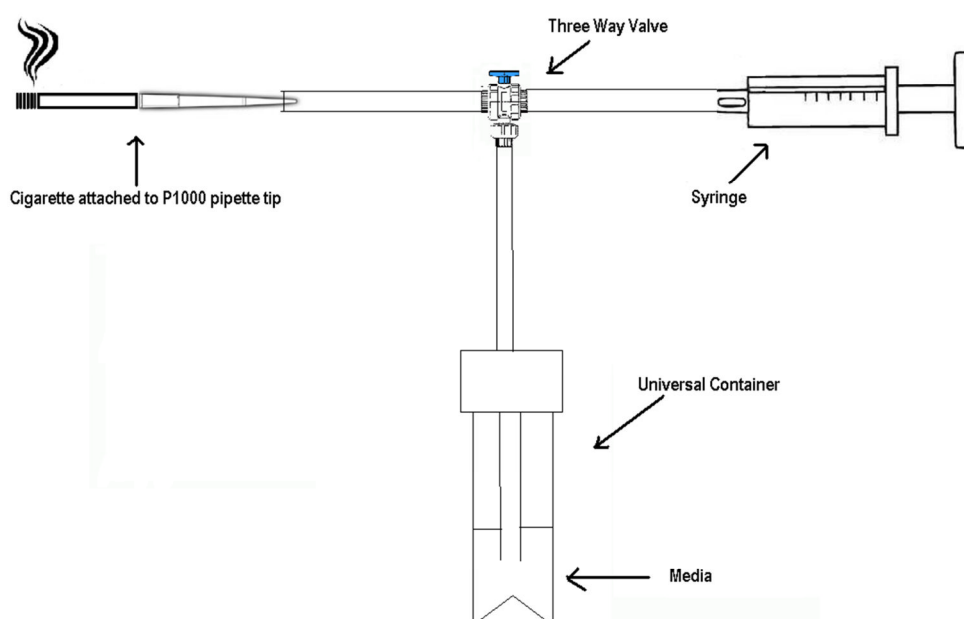
Figure 2.8: In house set-up used to manufacture cigarette smoke extract. Two University of Kentucky 3R4F cigarettes with their filter removed were attached, via a 3 way valve to a 20ml syringe and 15ml of media. Manually smoke was bubbled through the media until both cigarettes were spent creating cigarette smoke media that was then filter sterilised and normalised for use in cell culture.

In order to identify the maximum CSE concentration that could be used with NHBECs without causing significant cell death, increasing concentrations of CSE diluted in BEBM were introduced to NHBECs. NHBECs were then counted using a haemocytometer (see Section 2.4.4) following dilution of the cells with a 1:10 solution of Trypan Blue, a dye which is actively excluded from the cytoplasm of viable cells. This identified a 5% v/v solution of CSE diluted in BEBM as the maximal solution that can be used in NHBECs (Fig. 2.9).
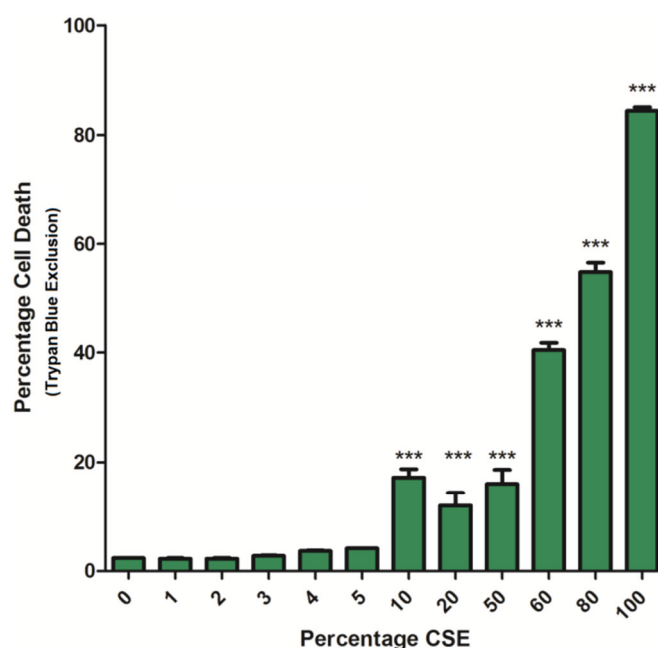
Figure 2.9: Cell death rates on increasing concentrations of cigarette smoke extract. Determination of viable cells using Trypan blue exclusion identified that addition of cigarette smoke extract at a concentration higher than 5%v/v results in substantial cell death ($n=3$). ***: $P<0.001$,

All additions of CSE to NHBECs occurred within 30 minutes of original smoke distillation, in order to prevent precipitation of the dissolved substance.

2.5 CELLULAR OUTCOMES

2.5.1 SCRATCH-WOUND ASSAY

The scratch-wound assay has been previously used as a model for cell injury and as a measure of cell migration/proliferation (Wadsworth et al., 2006, Bove et al., 2008, Loo et al., 2011, Stewart et al., 2012). This assay involves the disruption of a fully confluent NHBEC monolayer in a 6-well plate by dragging the tip of a sterile P200 pipette tip vertically across the well and then allowing cells, while under optimal growth conditions ($37°C+5\%$ CO_2), to attempt to repair the scratch-wound. The scratch wound assay was carried out in bronchial epithelial wounding media (BEWM), which consists of BEGM without Hydrocortisone, Epinephrine or Epithelial growth factor supplements. These supplements were excluded as they or related molecules have previously been shown to modulate wound repair (Wadsworth et al., 2006, Sivamani et al., 2009) and/or PLAUR (the gene under investigation) expression (Baek et al., 2008).

Briefly, 24 hours prior to scratch-wounding, NHBEC culture media was changed to BEWM. NHBECs grown to >90% confluence were then wounded with a sterile P200 pipette tip to form 3 vertical wounds. The cell monolayer was then washed with warmed sterile PBS and fed with fresh warmed BEWM. Wounds were then visualised over 24 hours at 9 sites in each well using a Nikon Diaphot 300 Inverted Phase Contrast Microscope with the 4x objective lens. Wound areas were calculated using CellProfiler cell image analysis software (Kamentsky et al., 2011) using a pipeline specifically designed for NHBECs by Mr Benjamin Willson (University of Nottingham). Data was presented as percentage wound remaining rather than area healed in order to compensate for variation in wound size.

2.5.2 MTT ASSAY

The 3-(4,5-Dimethylthiazol-2-yl)-2,5-diphenyltetrazolium bromide (MTT) assay is a colorimetric assay used to quantify mitochondrial dehydrogenase activity, which reduces MTT to hydrophobic formazan crystals (Mosmann, 1983). These crystals give a quantifiable purple colour when dissolved in alcohol (isopropanol). The assay therefore measures cellular respiration, with the amount of formazan produced being proportional to the number of living cells present in culture. The rate of cellular respiration measured by the MTT assay has been previously extrapolated to represent the rate of cellular proliferation (Mosmann, 1983). However, as this assay is not a true measure of changes in cell number, the resulting data cannot be used with full certainty to determine the proliferation rate of NHBECs in cell culture. Therefore, in this thesis, results from the MTT assay are considered as data relating to mitochondrial activity that may relate to cellular proliferation rates.

Briefly, following removal of BEGM, 200μl of a sterile, 0.22μm filtered, 0.5mg/ml solution of MTT in BEGM was added to NHBECs cultured in a 96-well plate. The culture was then incubated at $37^{\circ}C+5\%$ CO_2 for 4 hours, after which the MTT solution was removed and the resulting formazan crystals dissolved in 200μl of isopropanol. The solutions were then incubated for 10 minutes at room temperature. The degree of absorption was then read using a Flexstation 3 microplate reader at a wavelength of 570nm using a background reduction of 690nm. All samples were assayed in quadruplet and isopropanol only wells were used as negative controls.

2.5.3 CASPASE-3/7 ASSAY FOR CELLULAR APOPTOSIS

The Apo-ONE® Homogeneous Caspase-3/7 Assay is a sensitive measurement of caspase-3 and -7 activities (Promega Technical Bulletin # TB295). These members of the cysteine aspartic acid-specific protease (caspase) family are known to be activated in the apoptotic cell through extrinsic (death ligand) and intrinsic (mitochondrial) pathways (Salvesen, 2002, Ghavami et al., 2009). Therefore, these molecules can be used as a marker of the degree of apoptosis in a cell population. In this assay, a pro-fluorescent substrate (rhodamine 110, bis-(N-CBZL-aspartyl-L-glutamyl-L-valyl-L-aspartic acid amide [Z-DEVD-R110]) diluted in an optimized bifunctional cell lysis/activity buffer (DEVDase) is cleaved by active caspase-3/7. This cleavage results in loss of the DEVD peptide allowing the rhodamine 110 group to fluoresce on excitation at 499nm.

The assay was carried out according to manufacturer's instructions. Briefly, NHBECs cultured in a black walled tissue culture plate were cultured in the presence of either 100μl of BEGM (basal cells) or 100μl of a 300μM solution of H_2O_2 in BEGM (stimulated cells), previously shown to induce NHBEC apoptosis (Bucchieri et al., 2002). Cells were then incubated at 37°C+5% CO_2 for 8 hours, after which they were frozen at -80°C overnight. A 100μl solution of freshly prepared Caspase-3/7 reagent (1:99 solution of 100X Substrate to Buffer) was then added to the cells which were then left to incubate for 8 hours at 37°C+5% CO_2. Using a Flexstation 3 microplate reader, solutions were mixed and fluorescence read using an excitation wavelength of 485nm and an emission wavelength of 530nm. All samples were assayed in triplicate and media only wells were used as negative controls.

2.5.4 IMMUNFLUORESCENCE

Immunostaining was first described in 1941 by Coons *et al.* as a method to detect specific protein in a tissue sample via the use of antibodies (Coons et al., 1941, Coons and Kaplan, 1950). For the purpose of this thesis, staining was limited to that of cultured cells, i.e. immunocytochemistry, where primary antibodies bind to specific peptides or protein antigens within or on the surface of the cultured cells. Visualisation occurs through the binding of a secondary fluorescent-tagged antibody grown against the species of the primary antibody which is excited and detected on an Improvision Spinning Disk Confocal Microscope (PerkinElmer UK).

Briefly, the media was aspirated off NHBECs cultured in 4-well glass chamber slides and washed (X3) in PBS. Cells were then fixed by incubation at room temperature for 45 minutes in 4% formaldehyde, followed by blocking overnight at 4°C with a PBS solution containing 10% v/v goat serum with 0.15% v/v Triton X-100 and 1% v/v BSA. The relevant primary antibody was added and left to incubate overnight at 4°C, followed by the addition, in the dark, of the relevant secondary fluorescent antibody. Finally cells were mounted underneath a glass cover-slip using the VectaShield™ Hard+Set Mounting Media with DAPI. Cells were washed 3 times with PBS between each step. Fluorescence was visualised using the Improvision Spinning Disk Confocal Microscope (PerkinElmer UK).

2.6 METHODS INVOLVED IN POPULATION GENETICS

2.6.1 STUDY POPULATIONS

2.6.1.1 DUTCH ASTHMA AND CONTROL POPULATION

A cohort of 514 Caucasian Dutch asthma patients and 104 Caucasian spouse controls were selected from 2 populations consisting of a) 200 families and b) 407 trios, based on the presence of serum samples. Both populations were ascertained through a proband characterised using a standardized study protocol, with asthma from the northern part of the Netherlands and studies with an identical protocol, as previously described (Koppelman et al., 2009). Control subjects were chosen from spouses of the asthmatic subjects who had no doctor diagnosed respiratory disease. The controls were predominantly female (62.5%), >40 years (mean age=50±8.16) and had a smoking pack-year history mean of 10.50 (±1169). Mean percentage predicted FEV_1 (FEV_1(%Pred)) was 100% (±13.32), FEV_1/VC was 0.82 (±0.04) with a percentage change in FEV_1 post bronchodilator of 3.91% (±4.43). Asthma subjects were evenly distributed along gender (Female: 55.1%) but were generally younger with a mean age of 40 (±12.3) and had a smoking pack-year history mean of 4.95 (±9.58). Mean FEV_1 (%Pred) was 92.42% (±18.73), FEV1/VC was 0.76 (±0.12) with a percentage change in FEV_1 post bronchodilator of 17.44% (±15.82). Ethical approval was obtained by the University of Groningen.

2.6.1.2 UK COPD POPULATION

A cohort of 381 British COPD subjects were recruited from 5 UK centres based on physician and spirometry defined COPD (Stewart et al., 2009). Subjects were Caucasian, predominantly male (62.7%), > 40 years (mean age=68±8.45) and smokers

with > 10 pack-year history (mean = 46.87±18.52). Mean FEV_1 (%Pred) was 41.87 (±18.52), FEV_1/VC was 0.45 (±0.12) with a percentage change in FEV_1 post bronchodilator of 1.16% (±0.15). Ethical approval was obtained from the relevant ethics committees (Nottingham, Sheffield, Manchester, Leicester and Oxford) and informed consent from all subjects was obtained. Of the recruited subjects, 161 had a previous diagnosis of asthma in addition to COPD.

2.6.2 SNP GENOTYPING

All SNP genotyping was outsourced to KBiosciences (Hoddesdon, Hertfordshire, UK), which carried out genotyping in 96-well DNA plates containing 10ng/ml DNA and 4 water control samples. KBiosciences utilises its own patented allele-specific PCR system called KASP (KBioscience Competitive Allele-Specific PCR genotyping system) to carry out genotyping. This involves the use of two allele-specific forward primers, each of which contain a unique unlabelled 5` tail, with a common reverse primer in a competitive genotyping system using Fluorescent Resonance Energy Transfer (FRET). Here two unique quencher cassette oligonucleotides (FAM or CAL Fluor Orange 560) interact with the sequences of the tails of the allele-specific primers allowing fluorescent based detection of the SNP genotype. The KASP system allows for the detection of SNPs without the need for a separation step and has a very high SNP to assay conversion rate (>90% in comparison to ~60% with Taqman®).

2.6.2.1 QUALITY CONTROL OF GENOTYPING DATA

Quality control was initially carried out by KBiosciences using the following criteria:

- Identify whether the genotypes were in distinct genotype clusters for each SNP
- Identify whether all water controls were negative
- Identify if the number of the SNP call was >90% of the genotyped population

I also completed quality control with genotyping data visualised using the KBioscience developed software SNPviewer2[6]. An example of the interface can be seen in Fig. 2.10. Axes correspond to the fluorescence intensity from the two unique quencher cassette oligonucleotides with different colours used to represent the genotype groups (red, green and blue), black for the water control and pink for samples that could not be called by the software. Data was quality controlled by checking that:

- Appropriate clustering was present
- Genotype success rates were >90% of the genotyped population

Any samples that were miscalled and could be identified as a particular genotype with acceptable accuracy were manually re-called on the output data sheet. Analysis identified that genotyping success rates were >91% for all SNPs genotyped and >99% for the majority of the SNPs genotyped.
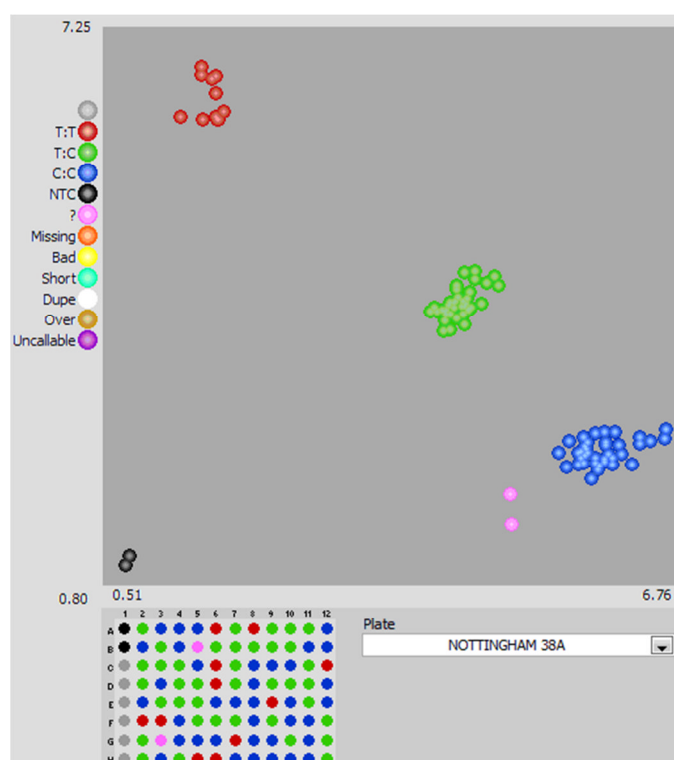
Figure 2.10: Representative image of SNPViewer2 outlay of KASP genotyping by KBiosciences. Axes correspond to the fluorescence intensity from the two unique quencher cassette oligonucleotides with different colours used to represent the genotype groups (red, green and blue), black for the water control and pink for samples that could not be called.

---

[6] http://www.kbioscience.co.uk/software/SNP%20viewer%20intro.html

2.6.2.2 HARDY-WEINBERG EQUILIBRIUM

Under Hardy-Weinberg Equilibrium (HWE), both allele and genotype frequencies in a population remain constant from generation to generation unless specific disturbing influences are introduced. Deviations from HWE may be due to either genotyping error, which tends to be the most common cause in genotyping analyses (Cox and Kraft, 2006, Hosking et al., 2004), non-random mating, small population size, selection bias, mutation or migration or any combination of the above (Salanti et al., 2005).

HWE is modelled using the equation:

$$p^2 + 2pq + q^2 = 1$$

were p^2= AA genotype, 2pq=Aa genotype and q^2=aa genotype.

Genotype data was investigated for variance from HWE using a Chi-squared test, comparing population observed frequencies against expected frequencies. Genotype values were taken from only unrelated individuals (parents) tested. No SNP was found to deviate from HWE in any of the populations genotyped in this thesis ($P<0.05$).

2.6.3 HAPLOTYPE ANALYSES

Linkage Disequilibrium (LD) identifies the degree of non-random association between SNPs across a region, providing a greater insight of DNA regional architecture. Discovery of regions with extensive LD, encompassing a sentinel SNP, identifies alternate polymorphisms that could be the underlying cause of any detected association. This is since SNPs occurring together in a region of high LD are said to occur together in a population at a greater degree than by chance, i.e. are inherited together. Importantly, this form of analysis is therefore able to increase the scope of genotyping experiments through the identification of alternate SNP genotypes that were not included in the original genotyping design.

Haploview[7] (Barrett et al., 2005) was used to provide haplotype data, i.e. LD data, for the population. Here, LD was defined using the R^2 measure. The R^2 value can vary between 0 and 1, where $R^2=0$ denotes linkage equilibrium and $R^2=1$ denotes a perfect correlation between the two alleles at the two SNP markers. Presence of high R^2 values between polymorphisms with similar allele frequencies will therefore identify good tagging SNPs.

Briefly, Haplotype input data was generated using data from the HapMap Project (Frazer et al., 2007, The_International_HapMap_Consortium, 2003) using the procedure outlined below:

1.   HapMap Download was selected from the drop down box

2.   Genome version 3 build, release 27 was selected, followed by the chromosome of interest

3.   The areas of interest adjacent to the SNP of interest was selected

4.   The CEU (Caucasian European Population) from the analyses panel was selected.

5.   The HapMap show info track was selected.

6.   The LD Plot colour scheme was chosen from the display panel.

7.   The show R^2 tab was selected from the display panel

Blocks of linkage disequilibrium were defined as set up by Gabriel *et al.* through the analyses panel (Gabriel et al., 2002).

---

[7] Available at http://www.broadinstitute.org/scientific-community/science/programs/medical-and-population-genetics/haploview/downloads

2.7 STATISTICAL ANALYSES

While two-way ANOVAs were carried out in PRISM v5.04, all remaining statistical analyses were carried out in SPSS v16.

2.7.1 GENETIC ASSOCIATION ANALYSES

2.7.1.1 POWER CALCULATIONS

Power calculations were carried out in QUANTO[8] for association studies of continual traits in the cohorts of non-related individuals. Power calculations were carried out using the following steps:

- Continuous data (change in scPLAUR levels) was selected for outcome/design and 'gene only' was selected as the hypothesis data

- SNP 'minor allele frequency' was inserted for the SNP under investigation and the additive model selected

- The cohort's population mean and standard deviation for the trait analysed were introduced

- The tab 'main effect' was selected and the beta value for the trait (degree of change expected) was also introduced

- Sample size was inputted and an acceptable error rate of 0.05 set

- The calculator button was pressed to run the calculation

---

[8] Available at - http://hydra.usc.edu/gxe/

SNP	MAF	COPD cohort Power Calculation
rs9480227	0.32	>99%
rs7666900	0.14	>99%
rs6988339	0.40	>99%
rs6467459	0.33	>99%
rs4253238	0.48	>99%
rs341119	0.38	>99%
rs2731672	0.29	>99%
rs12200614	0.23	>99%

Table 2.16: Power calculations for genotyping carried out in the COPD cohort based on variation is log$_{10}$scPLAUR levels, identifies a >99% power statistic for all SNPs genotyped. This identifies that all the quality controlled genotyping data is powered to detect variation in log10scPLAUR levels due to changes in SNP genotype via association tests. MAF=Minor Allele Frequency for the analysed population.

2.7.2 TESTS OF NORMALITY

Tests of normality were used in order to determine whether an outcome measure is normally distributed or not and therefore determines which statistical tests can be run on the data. However, in datasets with a small sample size ($n<20$), normality tests are not powered to give confident results on Gaussian distribution. Therefore, as one cannot be sure whether the assumption of normality has been violated and considering that all the analyses in which these datasets were involved in were repeated measurements (data taken from cell culture), all statistical tests in these datasets were carried out using parametric tests.

In datasets where $n\geq100$, distribution was primarily assessed using a histogram graph in SPSS, which identified whether the data fit a 'normal' bell-shaped distribution. Kolomogorov-Smirnov and Shapiro-Wilk tests of normality were also carried out, where the cumulative distribution of the data is compared to an expected cumulative normal distribution. A P-value of <0.05 indicates a non-normal distribution.

2.7.3 LINEAR OUTCOME ANALYSES

2.7.3.1 LINEAR REGRESSION

This thesis is concerned with simple linear regression, where only one continuous exposure variable is considered. Linear regression utilises the equation of a straight line which would best describe how the outcome under investigation (usually plotted on the *y* axis) changes with an increase in the exposure variable (value on the *x* axis). The statistic attempts to plot the best straight line using the method of least squares, with the equation of the regression line being:

$$y = \beta_o + \beta_1 x$$

were β_o is the line intercept and β_1 is the slope of the line. This statistical tool therefore functions on the assumption that the relationship between variables is linear apart from other assumptions including that:

- The outcome variable is normally distributed
- Standard deviation is identical for all points around the regression line
- All data points are independent

Briefly, analysis was carried out in SPSS as described previously (Stewart and Sayers, 2009), by selecting the Univariate analyses drop down menu. The phenotype under investigation (scPLAUR) was placed in the dependant variable box while the exposure variable and further known effectors of the phenotype variable (covariates) were placed either in the covariates box if it was continuous or the Fixed Factor(s) box if they were ordinal, following appropriate coding. The model was specified as 'Custom' and 'Main effects' with factors and co-variates manually moved into the model.

2.7.3.2 CORRELATION ANALYSIS

Correlation analysis estimates the degree of linear association between outcome and exposure variables measured by the correlation coefficient 'r', which can be defined as the number of standard deviations that the outcome 'y' changes for a standard deviation change in the exposure 'x'. The correlation coefficient is always a number between -1 and +1 were r=0 when variables are not associated. Negative values reflect inverse relationships while positive values indicate that the outcome and association variables increase or decrease together. Correlations presented in this thesis are limited to a non-normal (non-parametric) dataset and therefore the non-parametric version of the statistical tool (Pearson's Correlation) was used.

In SPSS, the bivariate button was selected from the Correlations bar in the analyse drop down menu. Pearson's correlation was selected.

2.7.4 CATEGORICAL ANALYSES

2.7.4.1 ANALYSES OF VARIANCE BETWEEN GROUPS

Tests carried out to identify variance in the mean (parametric) or median (non-parametric) occurring between groups can be stratified based on the number of groups analysed. When comparing two groups either a Student's t-test (parametric) or Mann-Whitney test (non-parametric) was used. When variance was investigated across 3 or more groups either a one-way ANOVA (parametric) or a Kruskal-Wallis test (non-parametric) was carried out. Post-hoc tests were carried out in one-way ANOVAs in order to identify the groups that power the significant variance within the analysed population. These consisted of either Tukey's post-hoc test, where all columns were compared to each other or Dunnet's when columns were compared to a selected control column.

112

All tests were carried out as two-tailed, were the null hypothesis is rejected when the value of the test statistic is either sufficiently small or sufficiently large, as opposed to one-tailed were only one of the rejection regions "sufficiently small" or "sufficiently large" is preselected.

In SPSS, the required test was selected from either the Non-Parametric bar or the Compare Means bar in the analyse drop down menu.

2.7.4.2 TWO-WAY ANOVA

A two-way ANOVA is a similar test to the one-way ANOVA used when data can be classified in two ways such as time and effect. This test is useful as it is able to not only determine the main contributory effect of each independent variable but also identify whether there is a significant interaction effect between the independent variables. Briefly in Prism the two-way ANOVA test was selected from the 'analyse' button and the Bonferroni post-hoc test selected from the post-hoc drop-down bar.

CHAPTER 3:

SOLUBLE CLEAVED PLAUR AS A BIOMARKER OF OBSTRUCTIVE RESPIRATORY DISEASE

CHAPTER 3: SOLUBLE CLEAVED PLAUR AS A BIOMARKER OF OBSTRUCTIVE RESPIRATORY DISEASE

3.1 INTRODUCTION

As discussed in Chapter 1, scPLAUR is the remaining structure of the membrane bound receptor, which is formed once cleavage has occurred at the receptor's GPI anchor. Previous studies have identified scPLAUR as a marker of human disease, with elevations in the levels of the expressed protein determined in patients with various types of cancer, including prostate (Almasi et al., 2011), pancreatic (Sorio et al., 2011), colorectal (Halamkova et al., 2011) and lung cancers (Langkilde et al., 2011), as well as other diseases such as liver cirrhosis (Zimmermann et al., 2012), sepsis (Savva et al., 2011), cardiovascular disease (Persson et al., 2012) and other disease with low grade inflammation (Eugen-Olsen et al., 2010a).

Apart from being a biomarker for disease *per se*, disease progression and disease associated mortality, there has been some recent evidence that scPLAUR may act as a direct modulator of disease. High serum levels of scPLAUR have been significantly associated with short overall survival for patients suffering from prostate cancer, (Almasi et al., 2011), while Zimmerman *et al.* have concluded that scPLAUR levels have a high diagnostic power to identify established cirrhosis in chronic liver diseases with a strong prediction of mortality or need for liver transplantation (Zimmermann et al., 2012). Interestingly, a recent study by Shankland *et al.* has gone one step further by identifying that scPLAUR not only acts as a disease biomarker in focal segmental glomerulosclerosis, but also plays a direct role in the development and progression of the disease through the receptor's interaction with the β_3 integrin (Shankland and Pollak, 2011).

Interest in scPLAUR in obstructive lung disease stems from work in the same group reported by Barton *et al.* in 2009, where *PLAUR* was identified as an asthma susceptibility gene (Barton et al., 2009). In this study, single nucleotide polymorphisms (SNPs) present in the gene's intron 3 and 5`UTR, which were associated with asthma, bronchial hyper-responsiveness (BHR) and decline in FEV_1, were also associated with differential serum scPLAUR expression (Barton et al., 2009). Here the presence of the SNP risk allele was associated with elevations in serum scPLAUR.

Other studies provide further evidence of an association between scPLAUR and respiratory disease. Elevated scPLAUR levels were identified in the induced sputum of asthmatics when compared with healthy controls (Jiang et al., 2010, Xiao et al., 2005) and in COPD subjects when compared to both asthmatics and healthy controls (Xiao et al., 2005). Levels of scPLAUR in induced sputum were also found to be associated with the degree of disease severity, with elevations discovered in the sputum of COPD patients with a GOLD classification of III + IV when compared with COPD patients with a classification of I + II (Jiang et al., 2010). Elevated levels of PLAUR were also identified in the airways of patients who had died in *status asthmaticus* when compared to airways from whole lung donors (Chu et al., 2006) and in the bronchial epithelial cells of asthmatic subjects when compared to healthy controls (Stewart et al., 2012).

Therefore it was hypothesised that serum scPLAUR may be elevated in both asthma and COPD, having a potential contribution to disease modulation. In addition it was also hypothesised that serum scPLAUR may be associated with lung function based on the known relationship between PLAUR and lung-function associated *PLAUR* SNPs (Barton et al., 2009).

Identification of a novel serum molecule associated with obstructive airway disease that could reflect changes in the airway, such as airway remodelling and changes in lung function, may be utilised in conjunction with lung function tests to help determine

the degree of asthma/COPD severity and to monitor disease progression. Although previous work has already identified that elevated scPLAUR is associated with asthma and COPD, this has been carried out in the induced sputum of diseased individuals. Procurement of induced sputum is more stressful for the patient than procurement of a simple blood sample. Therefore targeting scPLAUR in serum would be an easier and therefore more clinically relevant medium to use for clinical diagnostics.

3.2 AIMS

1. To determine whether the levels of scPLAUR in serum are elevated in obstructive lung disease and reflect PLAUR driven mechanisms.

2. To determine whether the levels of scPLAUR in patient serum are related to disease severity, lung function and/or bronchial hyper-responsiveness.

3. To replicate associations between a selection of PLAUR SNPs and serum scPLAUR levels.

3.3 METHODS

For general methods including population descriptives and demographics refer to Chapter 2: General Materials and Methods.

3.3.1 ENZYME LINKED IMMUNOSORBENT ASSAY

Before quantifying serum scPLAUR levels, datasets were quality controlled. Related subjects and controls with a percentage predicted FEV_1 of <80% were removed from the dataset. Serum scPLAUR levels were then determined in the Dutch asthma/control (n=514 asthmatics; 96 controls), and Leicester COPD cohorts (n=381) via a Duoset® ELISA for scPLAUR (R&D Systems), with absorbance recorded using a Flexstation 3 microplate reader. A detailed description of this method is found in Section 2.3.3.

3.3.2 GENOTYPING AND QUALITY CONTROL

Genotyping data generation and quality control analysis were carried out by Dr Ian Sayers (University of Nottingham) using procedures as described in Section 2.6.2. Controls from the original dataset were quality controlled by excluding any subjects with a FEV_1 predicted <80%.

3.3.3 STATISTICAL ANALYSES

3.3.3.1 POPULATION STATISTICS

Tests for normality were initially carried out on scPLAUR levels in both datasets using the Kolomogorov-Smirnov and Shapiro-Wilk tests. A detailed description of these tests is available in Section 2.7.2.

3.3.3.2 CORRELATION ANALYSES

As the distribution of scPLAUR levels in both datasets was determined to be non-normalised, Pearson's Correlation was used in this chapter for all the correlation analyses. Correlation was carried out on a number of potential co-variates for scPLAUR levels in serum, namely height, weight, age and smoking pack/years.

Correlation analyses were also carried out on scPLAUR levels with the lung function parameters FEV_1 (L), FEV_1(%Pred), FEV_1/FVC, BHR (assessed through P_C20 [the provocative concentration of a substance such as methacholine required to cause a 20% fall in FEV_1]) and the mean percentage change in FEV_1 post-bronchodilator (reversibility). Analyses were carried out separately in each population. A detailed description of the procedure used is available in Section 2.7.3.2.

3.3.3.3 LINEAR REGRESSION

Linear regression (Univariate analyses of variance test) was used to identify associations between *PLAUR* SNPs and serum scPLAUR levels. Analyses were carried out separately in each population using the additive model. Age, height, weight and smoking pack/years were used as covariates. A detailed description of the procedure used to carry out the test is available in Section 2.7.3.1.

3.3.3.4 COLUMN STATISTICS

As serum scPLAUR levels were defined as non-normally distributed, Mann-Whitney and Kruskal-Wallis tests were utilised to investigate differences in scPLAUR levels between controls, asthmatics, COPD subjects and COPD subjects with a co-morbidity of asthma, as well as differences between COPD severity, nocturnal asthma awakenings and asthma atopic status. The Mann-Whitney test was also utilised to determine

whether gender was a co-variate in the populations. A detailed description of the procedure used to carry out this test is available in Section 2.7.4.

3.4 RESULTS

3.4.1 POPULATION DESCRIPTIVES

For details of the populations used in this study see Sections 2.6.1.1 & 2.6.1.2.

Population descriptives identified significant differences between the different sub-populations used in this study (Table 3.1).

	Control	Asthma	COPD	COPD & Asthma
Number	96	514	220	161
Percentage Male	37.5%	44.9%	62.7%	49.1%
Mean Age* (Years)	50 ±8.16	40 ±12.3	68 ±9.11	66 ±7.65
Mean Height* (Metres)	1.71 ±0.08	1.74 ±0.09	1.67 ±0.09	1.66 ±0.10
Mean Weight* (kg)	76.35 ±12.08	78.12 ±15.67	70.76 ±18.16	73.35 ±16.82
Percentage Never Smokers	29.2	48.7	0	0
Mean Smoking* pack years	10.50 ±11.69	4.95 ±9.58	45.95 ±26.69	41.53 ±24.09
FEV1 pre* (%Pred)	100.94±11.00	80.71±20.70	40.50±16.99	39.51±16.27
FEV1 post* (%Pred)	104.78±11.33	92.42±18.73	47.53±19.39	43.56±16.83
FEV_1/VC pre*	0.80 ±0.05	0.70 ±0.14	0.46 ±0.13	0.44 ±0.12
FEV_1/VC post*	0.82 ±0.04	0.76 ±0.12	0.45 ±0.13	0.44 ±0.13
Percentage Reversibility* (% change in FEV_1 post bd)	3.91 ±4.43	11.72 ±7.16	6.64 ±3.29	3.59 ±0.56
BHR (P_C20 mg/ml)	>32	<32	n/a	n/a

Table 3.1: Population desciptives for cohorts used in this analysis. A star symbol defines parameters that are statistically different across the groups as defined by Kruskal-Wallis tests.

3.4.2 PLAUR SERUM LEVELS ARE NOT NORMALLY DISTRIBUTED

In the combined population of controls, asthmatics, COPD and COPD & asthma subjects (n=991), the Kolmogorov-Smirnov and Shapiro-Wilk tests for normality result in P-values of $P<0.001$. Since a significant P-value negates the null hypothesis of normal distribution this identifies that serum scPLAUR levels are non-normally distributed. This can also be confirmed by eye (Fig. 3.1), where a population curve presents a right-handed skew. This result is also apparent for the control (n=96), asthmatic (n=514), COPD (n=220) and COPD & asthma (n=161) populations, when these were analysed separately ($P<0.01$) (Fig. 3.2). Conversion of the data to log_{10}, x^2 and square root values did not alter the distribution of the data (Table 3.2) and so all analyses were carried out on the non-transformed scPLAUR data using non-normally distributed tests.
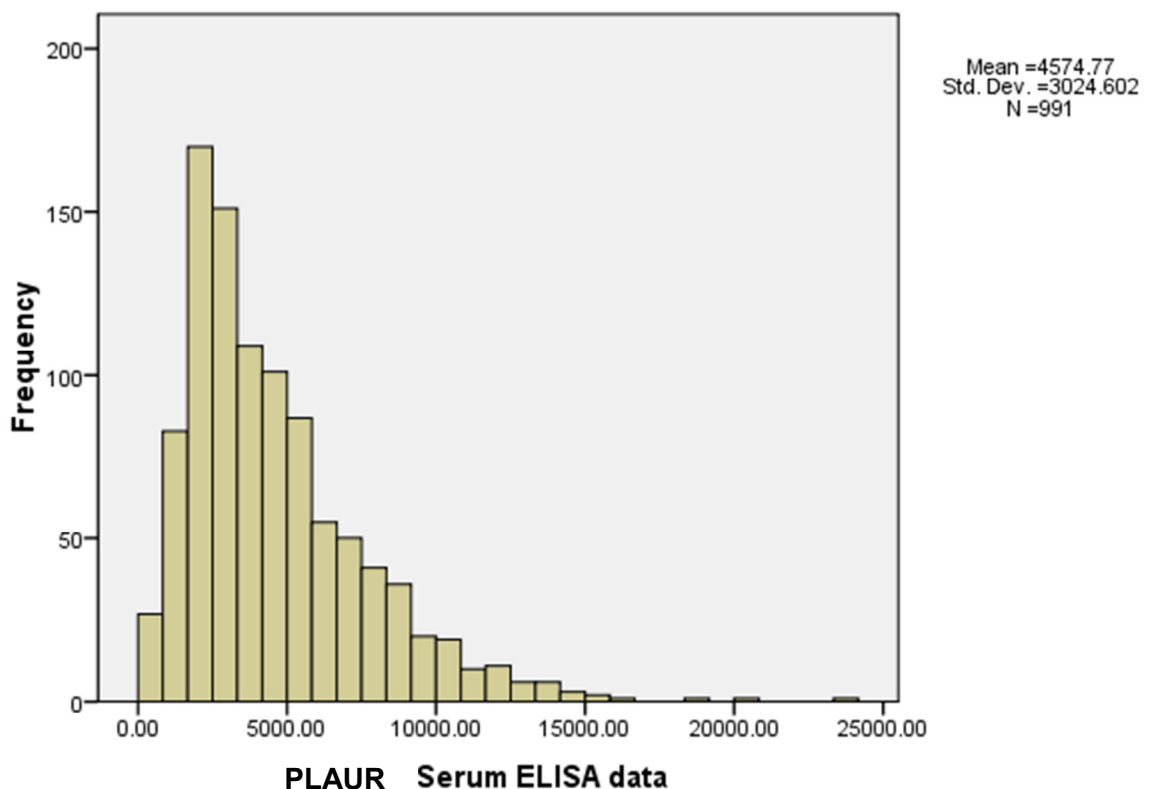
Figure 3.1: The normality curve for the combined population of controls, asthmatics, COPD patients and COPD patients. The curve presents with a right-handed skew, identifying a non-normally distributed population. Analyses of the dataset using Kolmogorov-Smirnov and Shapiro-Wilk tests confirm this finding ($P<0.001$).

123
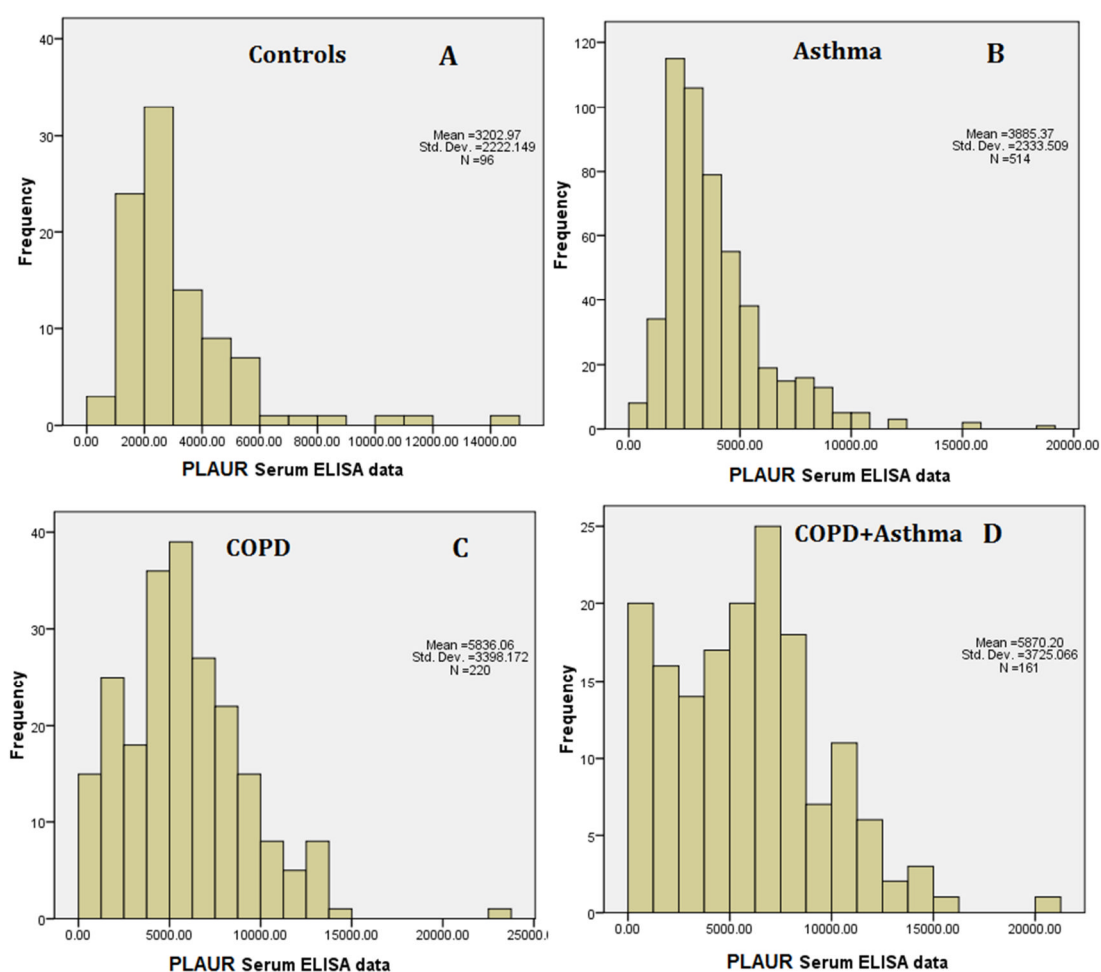
Figure 3.2: Population curves for the individually analysed cohorts. When analysed separately, controls (A), asthmatics (B), COPD patients (C) and COPD patients with a co-morbidity of asthma (D) are also found to produce right-skewed population curves and are therefore considered to be non-normally distributed. Analyses of the datasets using Kolmogorov-Smirnov and Shapiro-Wilk tests confirm this finding *P*<0.01.

PLAUR values	Kolmogorov-Smirnov	Shapiro-Wilk
Raw	<0.001	<0.001
log	0.04	<0.001
x^2	<0.001	<0.001
Square Root	<0.001	<0.001

Table 3.2: Conversion of serum PLAUR data (*n*=991) to log, squared and square root values does not alter significance for the Kolmogorov-Smirnov and Shapiro-Wilk tests of normality. Therefore raw serum PLAUR levels were used and analysed using non-parametric statistical tests.

In the combined population of controls, asthmatics, COPD and COPD & asthma subjects, patient height and weight were both negatively correlated with serum scPLAUR levels, while age and smoking pack/years were positively correlated with serum scPLAUR levels (Table 3.3; Fig. 3.3). Gender was not associated with serum scPLAUR levels (P=0.304). These associations were replicated in the individual datasets (data not shown). Therefore in this chapter, age, height, weight and smoking pack/years were considered as co-variates and included in the tests of association.

Factor	p-Value	Correlated?	R^2
Height	0.001	Yes	0.012
Weight	<0.001	Yes	0.014
Smoking pack/years	<0.001	Yes	0.059
Age	<0.001	Yes	0.036

Table 3.3: Age, height weight and smoking pack/years were defined as covariates for this study. Association was based on significant positive (Smoking & Age) and negative (Height & Weight) correlations with serum scPLAUR levels.
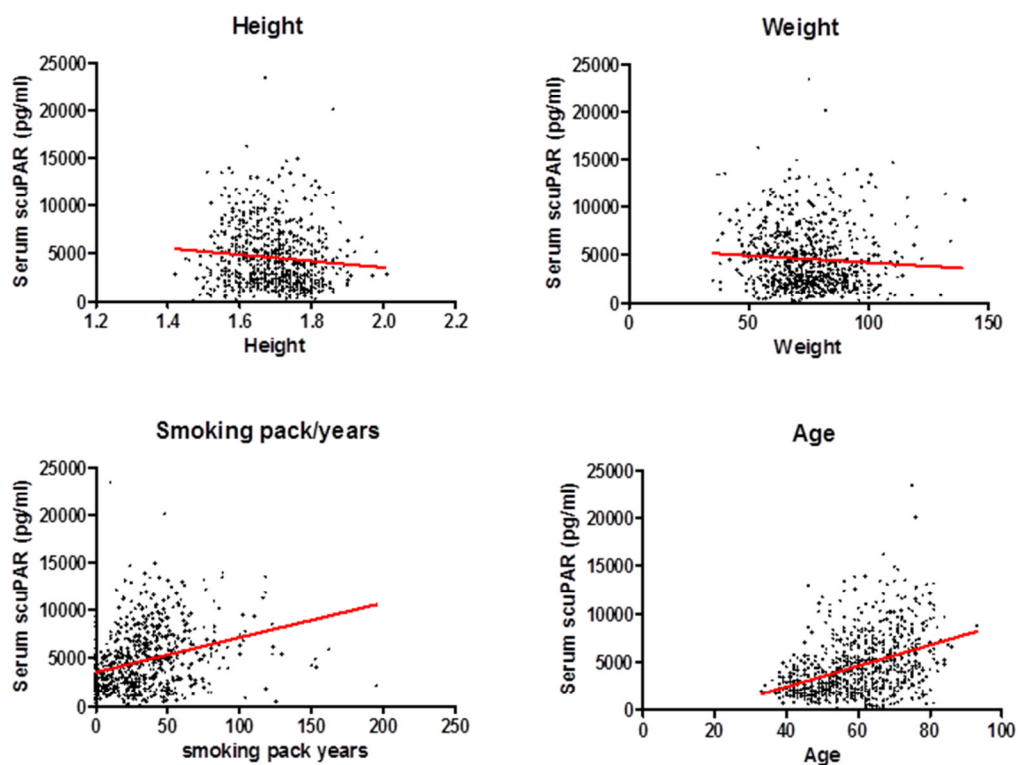
Figure 3.3: Dot plots for the linear variants tested for correlation. In the combined population negative correlations for height (R^2=-0.012) and weight (R^2=0.014) and positive correlations for smoking pack/years (R^2=0.059) and age (R^2=0.036) are identified (P<0.001).

3.4.4 SERUM SCPLAUR LEVELS ARE ELEVATED IN ASTHMA AND COPD

Median levels of serum scPLAUR in asthmatics (3306pg/ml) were elevated when compared to healthy controls (2538pg/ml) ($P<1x10^{-5}$) (Fig. 3.4). Serum scPLAUR levels in COPD patients (5836pg/ml) and COPD with a co-diagnosis of asthma (5870pg/ml) were also elevated when compared to healthy controls, but were also elevated when compared to asthmatics ($P<1x10^{-5}$) (Fig. 3.4). Serum scPLAUR levels did not vary between the COPD patients and the COPD patients with a co-diagnosis of asthma ($P=0.66$) (Fig. 3.4). However, a large distribution of data can be identified in each population, with a significant degree of overlap occurring between them.
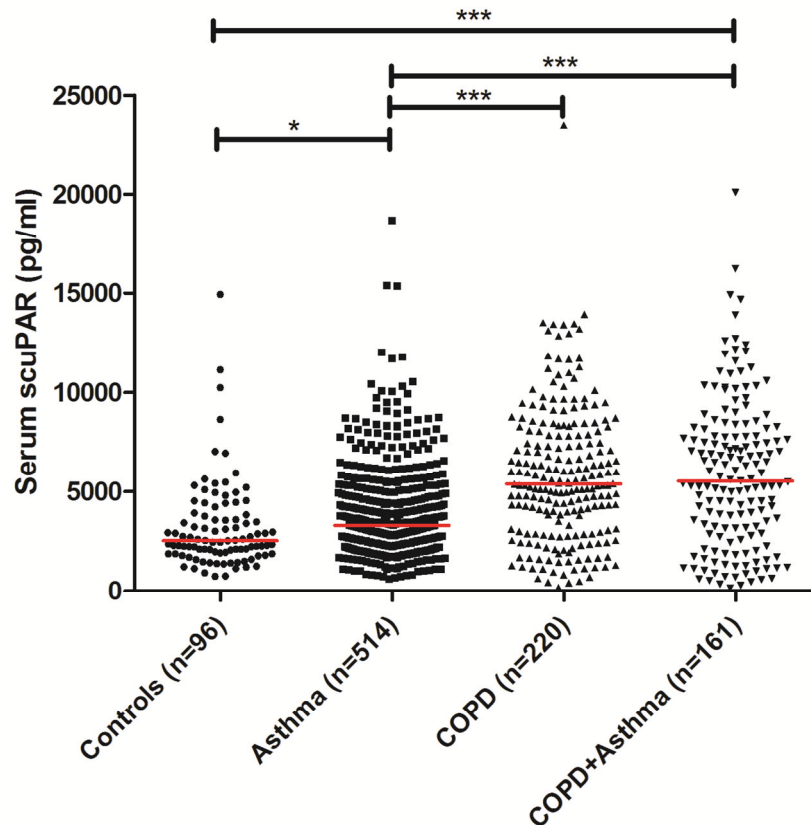
Figure 3.4: A scatter plot of serum scPLAUR levels based on disease phenotype identifies a relationship between receptor levels and disease status. Median levels, indicated by the red horizontal line, are elevated in asthmatics (3306pg/ml), COPD patients (5836pg/ml) and COPD with a co-diagnosis of asthma (5870pg/ml) when compared to controls (2538pg/ml). Levels were also elevated in the COPD patients (with and without asthma) when compared to asthmatics. No difference was identified between the different COPD populations. *** = $P<1x10^{-5}$; *= $P<0.05$.

3.4.5 COPD SEVERITY IS NOT ASSOCIATED WITH SERUM SCPLAUR

Due to the large range of data distribution present in the COPD and COPD+asthma cohorts, it was hypothesised that serum scPLAUR is modulated according to COPD disease severity as defined by the Global Initiative for Chronic Obstructive Lung Disease (GOLD) (GOLD, 2011). Analysis identified that when stratified based on GOLD criteria, no difference exists between median levels of serum scPLAUR in a population consisting of all subjects with COPD (P=0.54) (Fig. 3.5a). This lack of association was replicated in the COPD only (P=0.99) and COPD+asthma (P=0.33) cohorts (Fig. 3.5b&c).
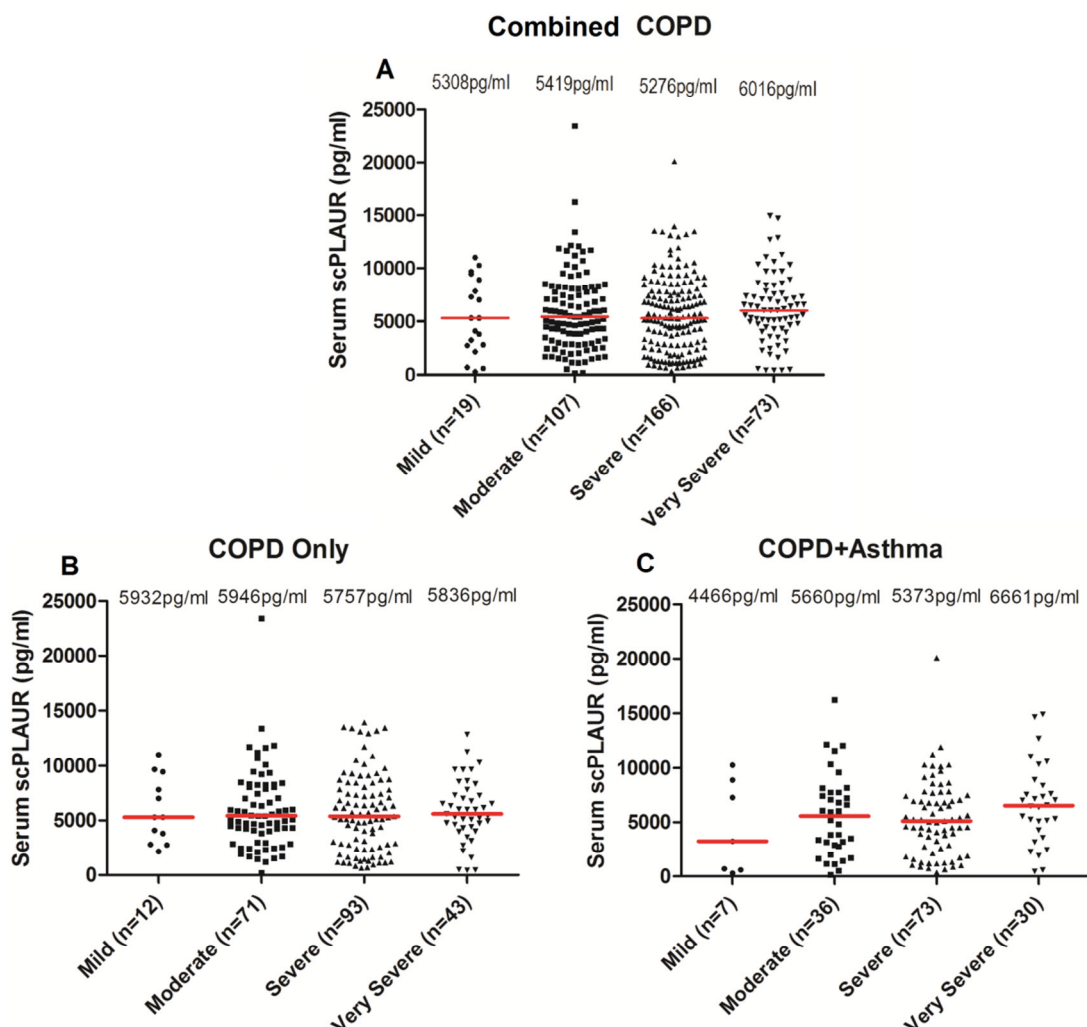
Figure 3.5: A scatter plot of serum scPLAUR levels in the combined COPD (A), COPD only (B)and COPD+asthma (C) populations. Stratification of the total COPD population according to the GOLD criteria for COPD severity identifies no discernible difference in median serum scPLAUR levels (A: P=0.54; B: P=0.99; C: P=0.33).

3.4.6 ELEVATED SCPLAUR IS A FEATURE OF NON-ATOPIC ASTHMA

As data points within the asthmatic population demonstrate a wide distribution, the possibility that the elevation in serum scPLAUR was driven by a specific asthmatic sub-phenotype was investigated. Individuals determined to be atopic (n=324; serum PLAUR=3217pg/ml) or non-atopic (n=124; serum PLAUR=4215pg/ml) were compared (Table 3.4). Atopic status was defined by the Phadiatop™ test, a commercially available variant of serum specific IgE assay (Merrett and Merrett, 1987). Both presented with elevated serum scPLAUR when compared to controls (n=96; serum PLAUR=2538pg/ml) (Fig. 3.6). However, the non-atopic asthmatic population had elevated levels of serum scPLAUR when compared to both atopic asthmatics and controls (P<1x10^{-4}), identifying that atopic status may be a driving force behind asthma serum scPLAUR elevation (Fig. 3.6).

	Atopic Asthma (n=324)	Non-Atopic Asthma (n=124)
Percentage Male	52.5	31.6
Age (Years)	41±11.68	43±13.70
Height* (Metres)	1.75±0.09	1.70±0.08
Weight* (kg)	79.00±15.06	74.63±14.36
Smoking pack/years	5.11±10.17	5.38±9.35
FEV$_1$ pre (%Pred)	80.41±19.98	78.87±25.52
FEV$_1$/VC pre	0.68±0.13	0.68±0.17
Reversibility* (% change in FEV$_1$)	18.81±16.80	16.38±15.51
BHR* (PC20 mg/ml)	6.23±8.45	11.58±11.64

Table 3.4: Population desciptives for asthma cohort stratified on atopy identify mean values and standard deviation. A star symbol defines statistically different parameters across groups as defined by Mann-Whitney tests.
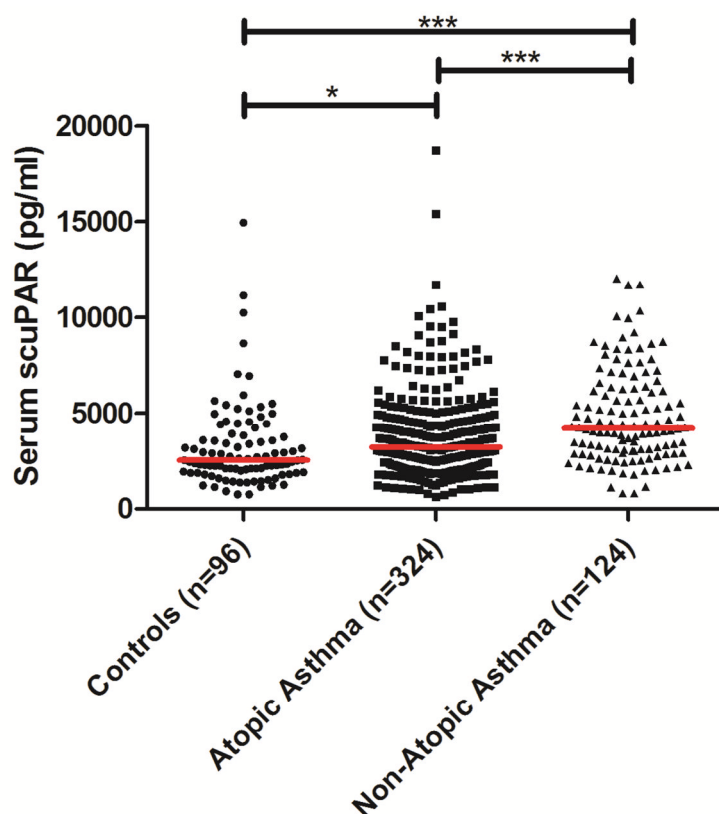
Figure 3.6: Serum scPLAUR levels are associated with atopic status in asthma. Stratification of the asthmatic population according to atopy, identifies that while serum scPLAUR is elevated in both atopic (3217pg/ml) and non-atopic asthmatics (4215pg/ml) when compared to controls (2538pg/ml) ($P=1\text{x}10^{-4}$), the elevation in asthmatics is strongly driven by the non-atopic phenotype ($P=1\text{x}10^{-4}$).

3.4.7 SERUM SCPLAUR IS NOT RELATED TO THE DEGREE OF NOCTURNAL AWAKENINGS IN ASTHMA

Due to the absence of asthma severity scores in the dataset, nocturnal awakening occurring due to asthma was used as a substitute to define poorly controlled asthma. Patient demographics confirm that asthmatics who reported nocturnal awakenings due to an asthma exacerbation within the last 12 months had worse lung function, as defined by pre-bronchodilator percentage predicted FEV_1 and FEV_1/VC, confirming overall less well controlled asthma in this sub-set (Table 3.5).

	No Nocturnal Awakenings (n=55)	Nocturnal Awakenings (n=125)
Percentage Male	69.1	56.6
Age (Years)	52 ±9.52	52 ±7.89
Height* (Metres)	1.75 ±0.09	1.73 ±0.09
Weight* (kg)	81.38 ±13.55	78.12 ±13.59
Percentage Never Smokers*	25.5	40.3
Smoking pack/years*	13.11 ±15.88	7.86 ±11.52
FEV_1 pre* (%Pred)	78.02 ±23.74	66.83 ±25.52
FEV_1/VC pre*	0.64 ±0.15	0.60 ±0.14
Reversibility* (% change in FEV_1)	10.82 ±5.87	14.07 ±7.76

Table 3.5: Population desciptives for the asthma cohort once stratified on reported nocturnal awakenings due to an asthma exacerbation within the last 12 months. Values identify mean values and standard deviation. A star symbol defines statistically different parameters across groups as defined by Mann-Whitney tests.

Serum scPLAUR levels in asthmatics who reported a nocturnal awakening (n=125; 2495pg/ml) were not statistically different to the levels present in asthmatics who reported no nocturnal awakenings (n=55; 2908pg/ml). Therefore serum scPLAUR levels were not associated with the degree of nocturnal awakenings in asthma in a sub-set of the asthma population (n=180) (P=0.11) (Fig. 3.7) and by association with asthma severity.
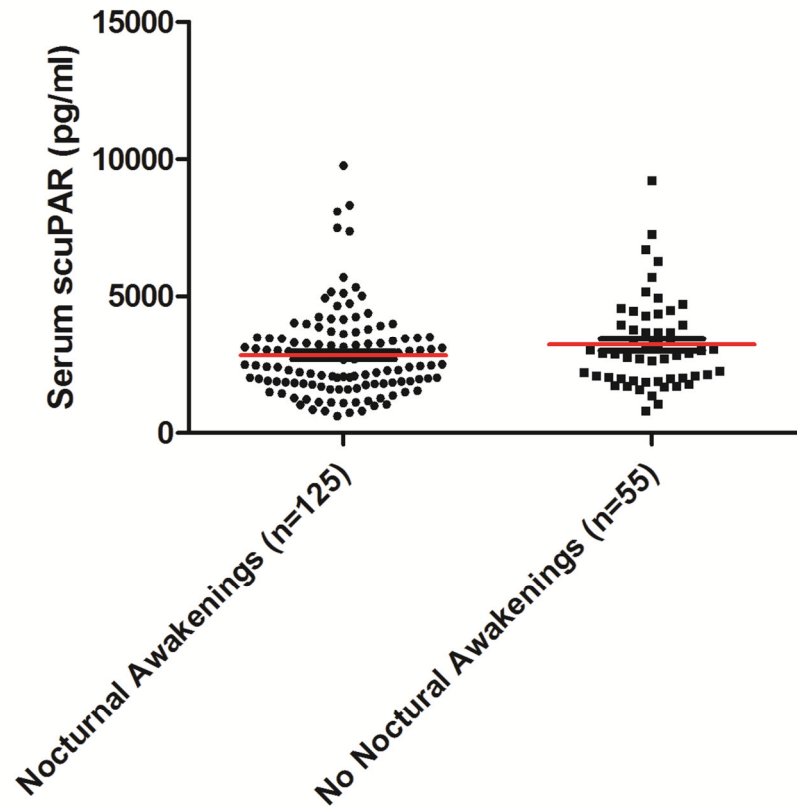
Figure 3.7: Serum scPLAUR levels are not associated with asthma severity as defined by the presence of nocturnal awakenings. A scatter plot diagram identifies that the serum scPLAUR levels in asthmatics who reported no Nocturnal awakenings over 12 months (2908pg/ml) were not statistically significant from those who reported at least one awakening over the past 12 months (2495pg/ml) (P=0.11).

3.4.8 SMOKING IS ASSOCIATED WITH ELEVATIONS OF SERUM SCPLAUR IN NON-ATOPIC ASTHMATICS

Building on the identified correlation between smoking pack/years and serum scPLAUR levels (see Section 3.4.3), as well as recent data obtained by colleagues (unpublished) which identified that PLAUR SNPs are differentially associated with various lung function parameters according to ever/never smoking history, it was decided to stratify the results already presented based on smoking history. Analyses identified that smoking history did not alter serum scPLAUR levels based on the control, asthma, COPD and COPD+asthma phenotypes (Fig. 3.8). However, when asthma was separated based on the atopic phenotype, although a slight elevation in

131

serum scPLAUR levels is still found in never smokers; it is current smokers that are found to drive the majority of the elevation of serum scPLAUR in non-atopic asthmatics (Fig. 3.9a). Interestingly, ex-smokers show no change in serum scPLAUR compared to non-diseased controls, as is the case with all smokers in the atopic phenotype (Fig. 3.9b).
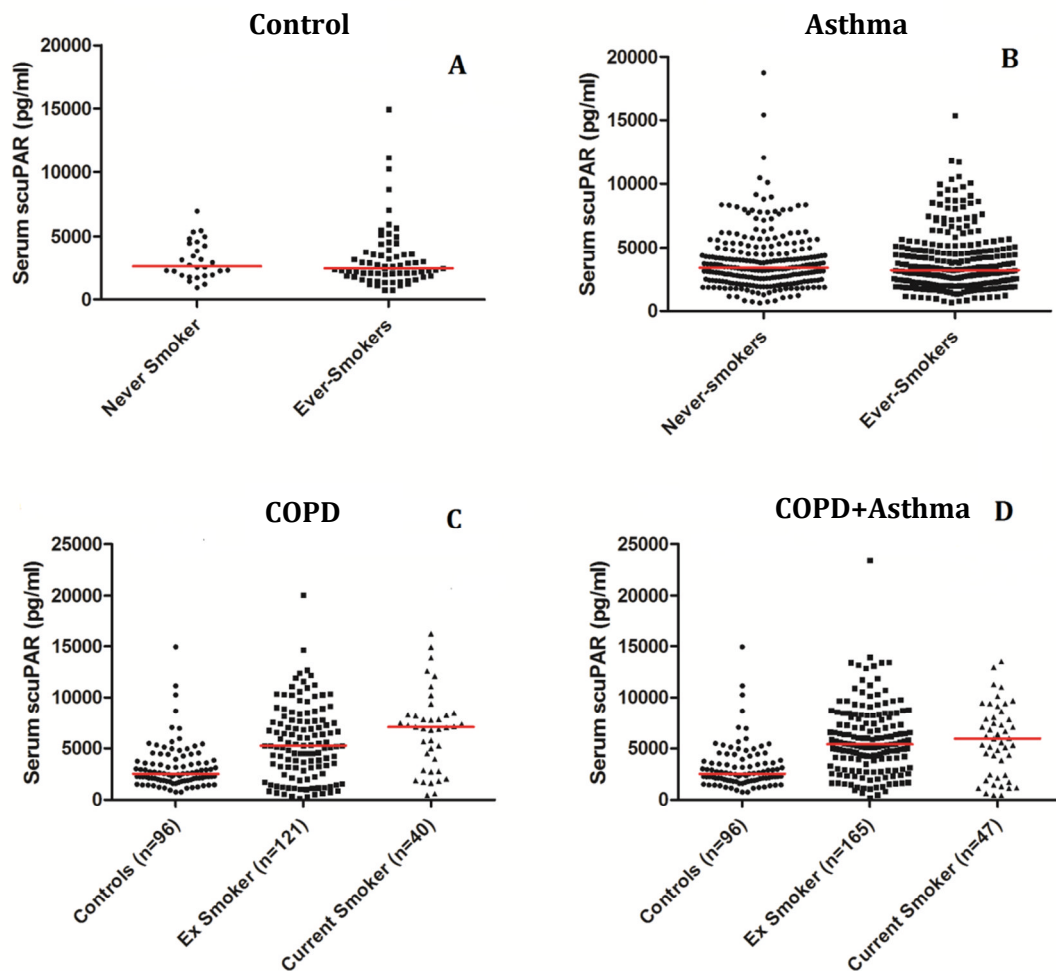
Figure 3.8: Stratification of serum scPLAUR based on smoking status. Median serum scPLAUR levels in the control (A), asthma (B), COPD (C) and COPD+asthma (D) populations, as identified by the red horizontal lines, identify that no difference in the expressed levels of scPLAUR occurs when based on smoking status.. Controls (2628pg/ml VS 2463pg/ml; *P*=0.63); Asthmatics (4547pg/ml vs. 4819pg/ml; *P*=0.42); COPD (5258pg/ml vs. 7071pg/ml *P*=0.07); COPD+asthma (5838pg/ml vs. 5952pg/ml *P*=0.90).
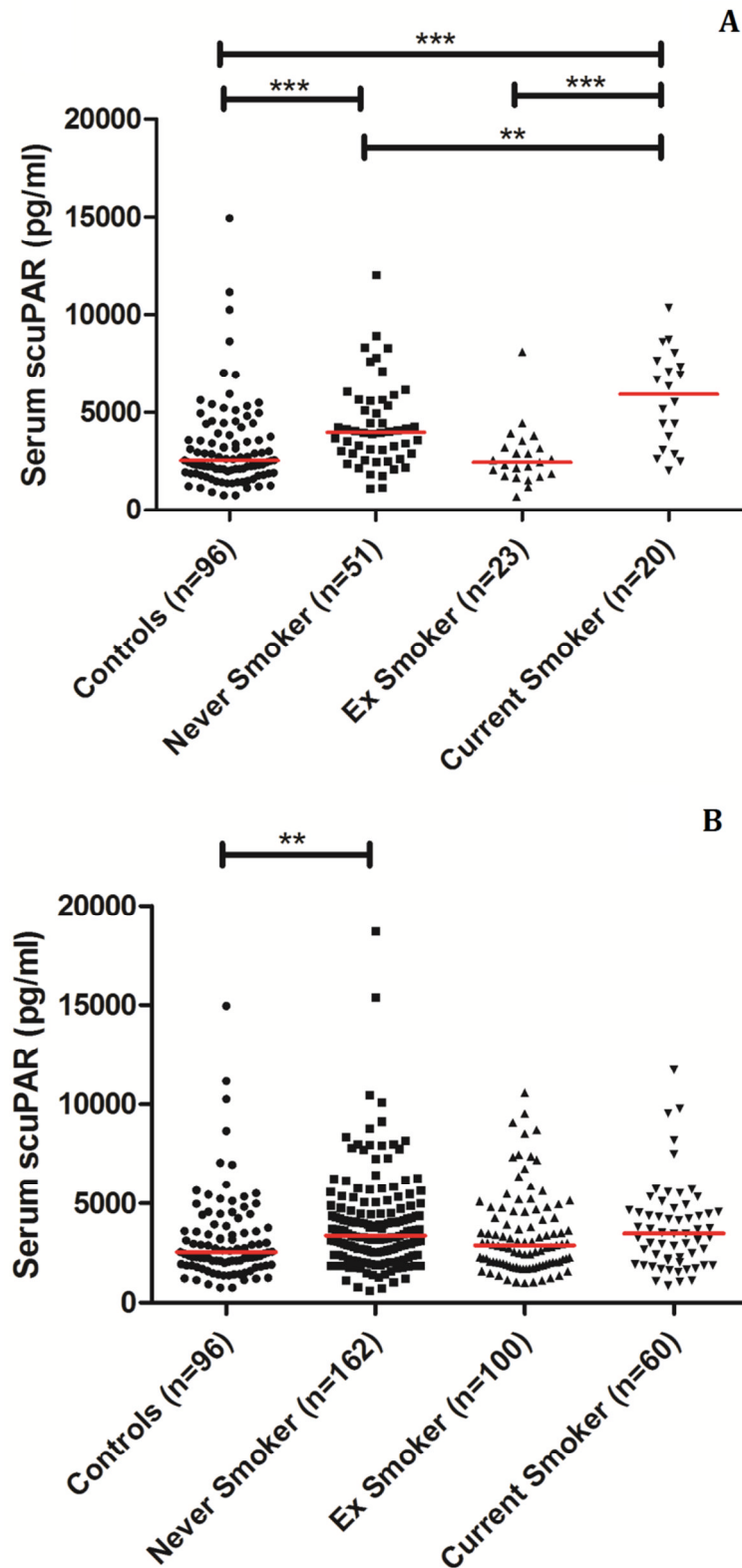
Figure 3.9: Median serum scPLAUR levels stratified based on IgE defined atopy and smoking status. In non-atopic individuals (A), the elevation of serum scPLAUR previously identified in the non-atopic phenotype is shown to be mainly driven by current smokers (2538pg/ml vs. 3975pg/ml vs. 2457pg/ml vs. 5932pg/ml; $P<0.001$). In atopic individuals (B) the slight elevation previously identified is driven by individuals who have never smoked (2538pg/ml vs. 3365pg/ml vs. 2867pg/ml vs. 3478pg/ml; $P=0.03$).

3.4.9 SERUM SCPLAUR LEVELS ARE NOT ASSOCIATED WITH LUNG FUNCTION

In each individual population an overall lack of correlation was identified between serum scPLAUR levels and lung function as defined by the following spirometry values:

i) FEV_1 percentage predicted pre-Salbutamol

ii) FEV_1 percentage predicted post-Salbutamol

iii) FEV_1/VC pre-Salbutamol

iv) FEV_1/VC post-Salbutamol

Suggestive evidence could be identified between serum scPLAUR and FEV_1/VC in the asthma cohort and for percentage change in FEV_1 in the COPD cohort. However, these did not hold once the *P*-value was corrected for multiple testing using Bonferroni's correction, where the corrected *P*-value was defined as $P=2.50 \times 10^{-3}$ (Table 3.6).

	FEV_1pp prbd	FEV_1pp pobd	FEV_1/VC prbd	FEV_1/VC pobd	Change in FEV_1
Control	-0.146	-0.093	-0.154	-0.151	0.150
	0.157	*0.367*	*0.133*	*0.142*	*0.144*
Asthma	0.044	0.024	0.115	0.119	-0.066
	0.321	*0.582*	*0.009*	*0.007*	*0.139*
COPD	0.031	-0.005	0.027	-0.003	-0.161
	0.654	*0.939*	*0.691*	*0.970*	*0.017*
COPD + Asthma	-0.146	-0.180	0.029	-0.029	-0.016
	0.080	0.081	*0.723*	*0.738*	*0.848*

Table 3.6: Serum scPLAUR is not correlated with spirometry defined lung function in any of the studied populations. Using a *P*-value of $P=2.50 \times 10^{-3}$ as defined by Bonferroni's correction for multiple testing, analyses identify that serum levels of scPLAUR are not associated with lung function parameters. In each cohort top values indicate the *Z*-value while italic values identify the *P*-value. FEV_1=forced expiratory volume in 1 second; VC= forced vital capacity; pp= percentage predicted; prbd = pre-bronchodilator; pobd=post-bronchodilator.

3.4.10 SERUM SCPLAUR LEVELS ARE NOT ASSOCIATED WITH BHR IN ASTHMA

In the asthmatic population, no association was identified between serum scPLAUR levels and bronchial hyper-responsiveness as defined by a bronchial challenge test where the amount of histamine required to cause a 20% decline in FEV_1 (P=0.727; Z=0.061).

3.4.11 THE *PLAUR* 5` REGION SNP rs4493171 IS ASSOCIATED WITH SERUM SCPLAUR LEVELS IN COPD PATIENTS

Investigations into whether 6 5`UTR SNPs were associated with serum scPLAUR levels in the asthma and COPD cohort allowed for replication of the association identified by Barton *et al.* between the 6 PLAUR SNPs and serum scPLAUR levels (Barton et al., 2009). A seventh important Lys200Arg asthma associated SNP (rs2302524) located in the gene's Exon 6 was also investigated to identify whether this was also related to levels of serum scPLAUR.

Quality control identified that one SNP in the asthma dataset, two SNPs in the COPD dataset and one SNP in the COPD with asthma dataset were not in Hardy Weinberg equilibrium (P<0.05). Although, due to the high number of comparisons (n=42), it is possible that the significant P-values are due to chance alone, this cannot be distinguished from alleles that are truly out of Hardy Weinberg equilibrium. Therefore none of these highlighted SNPs were used in the analyses (Table 3.7).

SNP	Location	MAF Asthma	Asthma (*n=514*)	MAF COPD	COPD (*n=220*)	MAF COPD + Asthma	COPD +Asthma (*n=161*)
rs346043	5`UTR	0.24	0.18	0.16	0.78	0.22	0.72
rs1994417	5`UTR	0.29	**0.04**	0.22	0.2	0.22	0.77
rs4493171	5`UTR	0.21	0.81	0.17	0.89	0.16	0.58
rs344779	5`UTR	0.31	0.77	0.27	**0.03**	0.26	0.27
rs2356338	5`UTR	0.26	0.3	0.17	**0.04**	0.23	**0.05**
rs2239372	5`UTR	0.45	0.25	0.35	0.75	0.36	0.85
rs2302524	Exon 6	0.15	0.14	0.12	0.32	0.12	0.37

Table 3.7: Identifying whether SNP genotyping lies within Hardy-Weinberg Equilibrium. Analyses identify that a number of SNPs provide significant *P*-values indicating that they are not in Hardy-Weinberg Equilibrium (HWE). SNP rs1994417 is not in HWE in the asthma cohort, while SNP rs344779 is not in HWE in the COPD cohort. SNP rs2356338 is not in HWE in either the COPD or the COPD+Asthma cohorts. These SNPS will therefore not be used in the association analyses in their respective cohorts.

Analyses of the remaining SNPs identified that in the asthma population no association exists between any of the *PLAUR* SNPs and expressed levels of scPLAUR in serum. In the COPD and COPD+asthma populations however, one SNP (rs4493171) was significantly associated with serum scPLAUR levels (Table 3.8). However, the association in the COPD+asthma population did not survive correction for multiple testing, where the Bonferroni corrected *P*–value was calculated at *P*=0.007. The F-statistic of the surviving association identifies that the major allele (C) is associated with an elevation of serum scPLAUR over five times the expected value at the null hypothesis. All analyses were corrected to the identified co-variates for serum scPLAUR (Section 3.4.3). No analysis was carried out in the control population due to the lack of genotyping data in this cohort.

SNP	Asthma (*n*=514)	COPD (*n*=220)	COPD +Asthma (*n*=161)
rs346043	0.828	0.300	0.043
	0.438	*0.741*	*0.958*
rs1994417	n/a	0.267	2.471
		0.766	*0.089*
rs4493171	0.161	**5.339**	3.529
	0.851	***0.005***	*0.032*
rs344779	1.596	n/a	0.195
	0.204		*0.823*
rs2356338	0.186	n/a	n/a
	0.83		
rs2239372	2.341	0.190	0.073
	0.097	*0.828*	*0.929*
rs2302524	0.0812	1.507	2.361
	0.445	*0.225*	*0.099*

Table 3.8: SNP rs4493171 is significantly associated with serum scPLAUR levels in the COPD cohort. Presence of the major allele (C) of rs4493171 was associated with elevated levels of serum scPLAUR. Although the same SNP was associated with the COPD+asthma cohort at the $P<0.05$, this did not survive Bonferroni correction for multiple testing ($P=0.007$) Top values indicate the F statistic, while italic values identify the associated P-values.

3.4.12 A PLAUR EXON 6 SNP (RS2302524) IS ASSOCIATED WITH SERUM SCPLAUR IN ASTHMATICS

PLAUR 5`UTR and gene SNPs investigated in section 3.4.11, were separated based on smoking status in the asthma population. One SNP (rs2302524) located in exon 6 of the *PLAUR* gene, changes a lysine (K) amino acid to arginine (R) at position 220 of the PLAUR protein structure, was found to be significantly associated with serum scPLAUR levels in the never smokers (Table 3.9). This association survived correction for multiple testing, where the Bonferroni corrected P–value was calculated at $P=7 \times 10^{-3}$. The F-statistic identifies that the major allele (T) is associated with an elevation of serum scPLAUR over 5 times the expected value at the null hypothesis. Analyses were not carried out in the COPD cohort, as all subjects were smokers, or in the control cohort, as genotype data was not available.

SNP	Direction of Effect		P-value	
	Ever Smoke	Never Smoke	Ever Smoke	Never Smoke
rs346043	0.072	0.152	0.789	0.697
rs1994417	0.252	0.742	0.616	0.39
rs4493171	0.101	0.002	0.751	0.966
rs344779	3.27	0.599	0.072	0.44
rs2356338	0.812	0.124	0.134	0.14
rs2239372	1.644	3.28	0.201	0.071
rs2302524	1.924	5.342	0.167	**0.002**

Table 3.9: SNP rs2302524 was associated with serum scPLAUR in asthmatics who were never smokers. Presence of the major allele (T) was associated with elevated levels of serum scPLAUR fivefold above the expected value as outlined by the F-statistic.

3.4.13 SMOKING STRATIFICATION IDENTIFIES AN ASSOCIATION BETWEEN SERUM SCPLAUR AND LUNG FUNCTION BUT NOT BHR IN ASTHMATICS

When separated based on smoking status, serum scPLAUR levels were found to be negatively associated with lung function as defined through the FEV_1/VC ratio in ever smokers. The association held with FEV_1/VC ratios taken both pre and post treatment with a bronchodilator (Salbutamol). Serum scPLAUR levels were also associated with percentage airway reversibility post-bronchodilator in the smoking asthma population (Table 3.10). No association was found between serum scPLAUR and BHR regardless of smoking status. There were no associations between serum scPLAUR levels and lung function as defined by spirometry in the control population regardless of smoking status (Table 3.11). All analyses in this section were corrected for the previously identified confounders of age, height and weight.

	Ever Smoke		Never Smoke	
	R^2	*P*-value	R^2	*P*-value
FEV$_1$ pre	0.003	0.324	0.005	0.255
FEV$_1$ post	0.001	0.550	0.007	0.203
FVC pre	1.96×10^{-4}	0.824	1×10^{-6}	0.986
FVC post	0.002	0.483	1×10^{-6}	0.993
FEV$_1$/VC pre	0.017	**0.034**	0.010	0.117
FEV$_1$/VC post	0.015	**0.050**	0.014	0.059
BHR	0.005	0.310	0.006	0.263
FEV$_1$ reversibility	0.018	**0.029**	9×10^{-6}	0.961

Table 3.10: Serum scPLAUR levels are associated with lung function in asthmatic smokers but not in asthmatic never smokers. An association exists between serum scPLAUR and FEV$_1$ reversibility and lung function measured using the FEV$_1$/VC test both pre and post Bronchodilator (Salbutamol) were determined in the asthmatic population. No association could be identified between scPLAUR and BHR.

	Ever Smoke		Never Smoke	
	R^2	*P*-value	R^2	*P*-value
FEV$_1$ pre	1.21×10^{-4}	0.926	0.002	0.836
FVC pre	7.84×10^{-4}	0.818	0.007	0.662
FEV$_1$/VC pre	0.020	0.250	0.045	0.279

Table 3.11: Serum scPLAUR levels are not associated with lung function or BHR in a control population regardless of smoking status. Serum scPLAUR levels were also independent of the degree of airway reversibility in controls.

3.5 DISCUSSION

The aims of this chapter were to determine whether serum scPLAUR is elevated in asthma and/or COPD *per se* and whether it is associated with lung function, airway reversibility and/or bronchial hyper-responsiveness. This chapter also attempted i) to replicate the associations between a selection of *PLAUR* SNPs identified by Barton *et al.* to be associated with serum scPLAUR levels in other subjects, ii) to investigate whether an important exon 6 SNP was associated with changes in serum scPLAUR levels and iii) to extend the study into COPD. In order to correct for multiple testing throughout this chapter, significance thresholds were modified using Bonferroni's Correction to account for false positive results.

Initial findings identified that serum scPLAUR was associated with the obstructive lung diseases asthma and COPD (regardless of asthma co-morbidities), in a relationship pattern similar to the sputum based results reported by Xiao *et al.*, corroborating the hypothesis that scPLAUR has a role in these diseases. The novel identification that circulating levels of scPLAUR are related to obstructive lung diseases mirrors previously reported relationships in other diseases, such as prostate cancer, diabetes Type II and chronic liver disease, where scPLAUR has been defined as a marker of disease progression and disease related mortality (Almasi et al., 2011, Zimmermann et al., 2012, Eugen-Olsen et al., 2010a). Correction of the statistical analyses to identified co-variates gives confidence that the identified associations are true associations rather than an artefact driven by non-related variation within the studied population. Association between scPLAUR and obstructive lung disease highlights a possible role for this molecule in the development and/or maintenance of asthma and COPD. As previously discussed in Chapter 1, recent developments have identified that scPLAUR interacts with β_3 integrin leading to the modulation of the kidney disease, FSGS (Wei et al., 2011). Therefore it is possible that serum scPLAUR elevations in asthma and COPD

are reflective of modulation of the development and/or progression of these diseases through an interaction with a yet undefined co-factor, such as the β_3 integrin family.

An alternate hypothesis for the observed elevation in serum scPLAUR is that elevation is not associated with the presence of asthma and COPD *per se* but rather acts as a marker of low-grade inflammation, given that, as described in Chapter 1, inflammation is an important factor in both asthma and COPD development. Indeed scPLAUR has previously been associated with a number of general inflammatory diseases (Eugen-Olsen et al., 2010a), while a number of other studies have reported positive correlation between scPLAUR and pro-inflammatory biomarkers such as leukocyte numbers, TNFα, and high sensitive C-reactive protein (CRP) (Eugen-Olsen et al., 2010a, Thuno et al., 2009, Andersen et al., 2008). It is however unlikely that this is the underlying reason for the observed association in this study based on lack of association with disease severity, with increasing asthma and COPD severity specifically known to be associated with increasing inflammation in the lung (Turato et al., 2002, Louis et al., 2000). However, investigations into the relationship between serum scPLAUR and asthma severity must be considered in light of the lack of clinical data such as GINA scores and medical history, from which asthma severity is usually defined. This study was limited to using the nocturnal awakening phenotype as a surrogate phenotype for asthma severity based on the National Heart, Lung, and Blood Institute (NHLBI) definition that asthma severity is determined on the basis of both impairment and risk, with impairment defined as a function of the frequency of daytime and nocturnal symptoms (NHLBI, 2007). As subjects in this dataset that reported nocturnal awakenings due to asthma have lower lung function than subjects who had no nocturnal awakenings this increases confidence in the use of this phenotype as a marker of disease severity.

As mentioned in Chapter 1, asthma is not a single homogenous disease but is a group of diseases based on the presence and absence of various phenotypes, including atopy (Lotvall et al., 2011). Atopic asthmatics differ from non-atopics in their triggering mechanism; atopic asthma is triggered by allergens originating from pollen and house dust mite among others, while non-atopic asthma is not directly triggered by any known allergen, but rather through the activation of innate receptors such as those for IL-33 and GM-CSF (Barnes PJ, 2002, Willart et al., 2012). Non-atopic asthma is also regarded as generally manifesting later in life and is often more severe than atopic asthma (Rochat, 2005) as reflected in this dataset where non-atopic asthmatics have less airway reversibility (P=0.042) and less BHR ($P<1x10^{-3}$). Based on these differences, it was decided to investigate whether association with scPLAUR was driven by atopic status as defined by the Phadiatop™ test, a commercially available variant of serum specific IgE assay that was introduced for the screening of allergic sensitization in 1987 (Merrett and Merrett, 1987). Elevated serum scPLAUR levels in non-atopic asthmatics suggest that serum scPLAUR is associated with changes in the airway rather than asthma *per se*, an idea supported by the increased levels of scPLAUR present in COPD, which is by definition an irreversible airway obstructive disease, vastly different from asthma in respect of airway reversibility.

Based on the above data, it is therefore likely that serum scPLAUR may be involved in airway remodelling, causing irreversible changes such as smooth muscle hypertrophy, mucous gland hyperplasia, increased cell proliferation and thickening of the basement membrane (Wilson, 1998, Busse et al., 1999). This hypothesis is supported by the association of serum scPLAUR levels to spirometry defined lung function (FEV$_1$/VC) and airway reversibility post-bronchodilator treatment in an ever smoking population. A serum scPLAUR associated change in the degree of airway remodelling could lead to the progression and/or modulation of airway obstructive disease, especially COPD and non-atopic asthma, identifying an active role for scPLAUR in these disease states.

As a strong positive correlation between serum scPLAUR and smoking pack/years was identified in this chapter and recent data from colleagues in the department (unpublished) identified PLAUR SNPs as being differentially associated with various lung function parameters according to ever/never smoking history, it was decided to investigate whether smoking history was a driving force in any of our phenotype associations. Smoking status did not appear to have any role in the elevation of serum scPLAUR in asthma or COPD, but seems to be the driving force elevating serum scPLAUR in non-atopic asthma. Lack of a role for smoking status in asthma and COPD may be explained due to our grouping of all asthmatics into one single disease state and the uniform high rate of smoking in COPD. A role for smoking in regulating scPLAUR in non-atopic asthma, lends further credence to the hypothesis that serum scPLAUR plays a role in airway remodelling as cigarette smoke has a well-established role in causing structural changes to the airways (Niewoehner et al., 1974, Floreani and Rennard, 1999, Churg et al., 2006).

The second focus of this chapter was to identify whether serum scPLAUR was associated with lung function as defined by spirometry, percentage reversibility of FEV_1 and BHR. A lack of association between serum scPLAUR and lung function was contrary to what was anticipated based on the identification by Barton *et al.* of an association between serum scPLAUR associated SNPs and lung function, albeit in a family based design. The previously derived conclusion that serum scPLAUR plays a role in airway remodelling, would also lead one to expect a relationship between serum scPLAUR and lung function. However, this study was limited in its ability to relate airway remodelling to lung function since airway remodelling is more closely associated with longitudinal FEV_1 (Mahut et al., 2010, Rasmussen et al., 2002), while this study has investigated cross sectional changes. Therefore, the identified lack of association with lung function does not preclude the hypothesis that serum scPLAUR plays a role in airway remodelling. Indeed unpublished work in the same group

associated various PLAUR SNPs with a number of airway remodelling parameters such as epithelial proliferation rates and the rate of Collagen III deposition. Failure to associate with lung function tests may also be explained by the possible masking effect of cigarette smoke on any scPLAUR driven effect on the airways. This is suggested based on the well-established role of cigarette smoke in causing changes in the airways (Niewoehner et al., 1974, Floreani and Rennard, 1999, Churg et al., 2006). Indeed, when stratified according to smoking status, an association with lung function and airway reversibility were identified. Elevations of serum scPLAUR corresponded with a lower FEV_1/VC ratio and a lesser degree of airway reversibility, complimenting the hypothesis that the association of serum scPLAUR with asthma and COPD occurs via an effect on airway obstruction. Although difficult to define, airway remodelling can be thought of as a collective term that encompasses the alterations in structural cells and tissues resulting in airway wall thickening, sub-epithelial fibrosis, increased myocyte muscle mass, as well as myofibroblast and mucus hypersecretion (Elias et al., 1999). Therefore, through possible scPLAUR influenced thickening and fibrosis of the airway, changes should occur in the airway resulting in a lesser degree of airway reversibility and a lower FEV_1/VC ratio, as identified.

The third focus of this chapter was to attempt to replicate the association between the 7 SNPs identified by Barton *et al.* (rs2356338, rs4493171, rs2239372, rs346043, rs344779 and rs1994417) and serum scPLAUR, and to identify any association with the exon 6 SNP rs2302524. Replication and extension of the findings was largely unsuccessful with only a single 5`UTR SNP (rs4493171) found to be associated with serum scPLAUR levels. However, rs4493171, which is located in the gene's 5`UTR (~10kb upstream of the TSS) was associated with serum scPLAUR in the same directional effect as that reported by Barton *et al.*, where presence of the major allele (C) resulted in elevated serum scPLAUR (Barton et al., 2009). This is of interest as Barton *et al*. identify this SNP (T allele) as being protective to asthma. Therefore,

confirmation of the link between the risk genotype and serum scPLAUR levels ties in well with our assertion that elevated serum scPLAUR is associated with the disease. Failure to replicate the remaining SNPs may be due to differences in our populations from the populations used in the Barton *et al.* study. This study was therefore limited by not being a true replication of the original study with regards to patient characteristics, disease and study design. In Barton *et al.*, association was defined using Family Based association tests. These tests are based on analysis of a linear combination of observed offspring genotypes and phenotypes, which is appreciably different from analysing the effect of SNPs on cross-sectional lung function data in a population of non-related adults. Also, lack of association may be due to the low power of association for these datasets. Power calculations identify the probability at which a test will reject the null hypothesis when the null hypothesis is false. In this dataset power ranged from 70% to 45%, identifying that low power of detection exists for some of the associations and may explain why such associations did not achieve a significant *P*-value in these analyses.

Another possible mask for SNP activity would be smoking history. As one can expect, smoking was not present in the child population in the original study where the 7 *PLAUR* SNPs were associated with serum scPLAUR levels. This may explain why no positive association was evident in the remaining 6 non-significant SNPs. However this hypothesis was proved false when the dataset was stratified along the smoking history phenotype and none of serum scPLAUR associated SNPs were found to deviate from the null hypothesis of no association.

Interestingly, the association of rs2302524 with serum scPLAUR in a never smoker population of asthmatics and a combined population of controls and asthmatics identified a novel exon 6 SNP associated with serum scPLAUR. Failure to associate this SNP when not stratifying for smoking status may be explained due to the strong

correlation of cigarette smoke on serum scPLAUR expression. Elevations of serum scPLAUR driven by cigarette smoke are so strongly correlated that they in all likelihood are still able to confound the data and mask the effect of rs2302524, a non-synonymous SNP that alters the PLAUR protein structure by changing a lysine amino acid to arginine within the receptor's Domain III.

In conclusion, this chapter identifies that serum scPLAUR may be involved in the obstructive lung diseases asthma and COPD, with an important effector role played by cigarette smoke, especially in the alteration of lung function and reversibility. This suggests that circulating levels of scPLAUR may either be involved in these disease states via airway remodelling, an effect known to be augmented on exposure to cigarette smoke, or be a marker of processes occurring in the asthmatic/COPD lung associated with cigarette smoke. This study also identifies rs2302524 as a novel regulatory SNP for serum scPLAUR, which however appears to be masked by cigarette smoke but has investigative potential due to its association with asthma and lung function as defined by FEV_1, which may be due to its up-regulation of serum scPLAUR. Replication and extension of the results presented by Barton *et al.* associating 6 SNPs with serum scPLAUR levels were however largely unsuccessful. This however, does not necessarily disprove the authors' results. One must consider that the authors replicated their own results in two separate cohorts (Barton et al., 2009), while this study was severely limited in that the population (unrelated control/diseased adults) differed from the cohorts used in the study (affected sibling pairs). Therefore while this study highlights a significant association between rs4493171 and serum scPLAUR in COPD one cannot either truly define this as a true replication or reject Barton *et al.*'s results.

CHAPTER 4:

IDENTIFICATION OF A NOVEL GENETIC MECHANISM DETERMINING SOLUBLE CLEAVED PLAUR LEVELS USING A GENOME-WIDE ANALYSES

CHAPTER 4: IDENTIFICATION OF A NOVEL GENETIC MECHANISM DETERMINING SOLUBLE CLEAVED PLAUR LEVELS USING A GENOME-WIDE ANALYSES

4.1   INTRODUCTION

As discussed in Chapter 3, scPLAUR is a molecule that is known to be elevated in a number of diseases including various cancers (Eugen-Olsen et al., 2010b), cardiovascular disease (Eugen-Olsen et al., 2010b), HIV (Savva et al., 2011) and kidney disease (Wei et al., 2011). Elevations of the soluble cleaved receptor were associated with increased disease risk and elevated mortality rates in these diseases (Savva et al., 2011, Eugen-Olsen et al., 2010b), while in breast cancer elevated scPLAUR was associated with lower survival rates (Andres et al., 2012). In Chapter 3, results identify that levels of serum scPLAUR are elevated in both asthma (driven by the non-atopic phenotype) and COPD, with a relationship between scPLAUR serum levels to smoking history also identified. Therefore the soluble cleaved form of the receptor may be considered to be an important driver of disease and disease associated mortality, including in the obstructive lung diseases asthma and COPD through possible interactions with cellular cofactors such as β_3 integrins, such as has been described in kidney disease (Wei et al., 2011). It is consequently important that the regulatory processes for the expression of this soluble form of the receptor in human serum is fully understood as this would provide a better understanding of the mechanism of disease and any potential therapeutic targets within. The work in this chapter has attempted to address this question through identification of genetic regulators for serum scPLAUR using a genome-wide association study (GWAS). Although a number of

studies (Stewart et al., 2012, Xiao et al., 2005) have investigated scPLAUR expression and function, such as in the airway epithelium and in induced sputum while other studies have identified associations between *PLAUR* SNPs and serum scPLAUR levels (Barton et al., 2009), there has been to date no genetic based investigation into the underlying genetic mechanism of regulation of scPLAUR levels in serum.

GWAS involves the statistical determination of association of a large number of single nucleotide polymorphisms (SNPs) (7300k) spanning the human genome, with a known outcome or trait, in this case the identified level of scPLAUR in serum. Due to the association of elevated serum scPLAUR in asthma (Chapter 3), analyses were carried out on two distinct pools of individuals, namely a control population with no asthma or obstructive lung disease and a population of doctor diagnosed asthmatics. Using these cohorts the twofold aim of identifying novel genetic mechanisms that regulate serum scPLAUR and determining if this regulation is specific or more relevant in obstructive lung disease were approached. The same sample pool as in Chapter 3, namely the Dutch asthma case and control cohort, was utilised for these analyses.

4.2 AIMS

1. To identify novel genetic mechanisms determining scPLAUR levels in serum using a genome-wide approach.

2. To identify the mechanism of regulation driven by these novel genetic determinants.

3. To identify the functional effects of scPLAUR in primary human bronchial epithelial cells.

4.3 METHODS -GENETICS

For general methods including population descriptives and demographics kindly refer to Chapter 2: General Materials and Methods.

4.3.1 ENZYME LINKED IMMUNOSORBENT ASSAY

Serum scPLAUR levels were determined in the Dutch asthma/control cohort (see Section 2.6.1.1) in 514 asthmatics and 104 controls via a Duoset® ELISA for scPLAUR (R&D Systems), with absorbance recorded using a Flexstation 3 microplate reader. A detailed description of this method is found in Section 2.3.3.

4.3.2 GENOME WIDE ASSOCIATION STUDY

A GWAS was carried out by the Dutch collaborators (Dr Martin Siedinski and Dr Gerard Koppelmann; University of Groningen, the Netherlands) using the Illumina 300 and 370 chips. The control and asthma study populations used in the GWAS analyses were obtained from the same pool of subjects as used in Chapter 3 and outlined in Section 2.6.1.1. Serum scPLAUR levels were log10 transformed prior to the analyses. Quality control of the population dataset led to the exclusion of related subjects using a PI HAT cut off of 0.1875 and the exclusion of ethnic outliers and cryptically related subjects using *smartpca* software. This resulted in two final datasets of 104 controls and 480 asthma cases. Quality Control on SNP data carried out in both asthma subjects and controls identified a SNP call rate of 0.95 and indicated that the population was in Hardy Weinberg equilibrium with regards to the SNPs ($P >1x10^{-7}$). A total of 295,196 SNPs were analysed for each of the 584 individuals and analyses carried out in either cohorts separately and in a combined case/control cohort. Analyses was carried out in PLINK using the additive model (Purcell et al., 2007).

4.3.3 STATISTICAL SIGNIFICANCE TESTING

As a large number of tests of association, such as those carried out in a GWAS, are likely to result in the generation of a number of false positives, the level of significance (significant *P*-values) needs to be corrected for multiple testing. Corrections for multiple testing are based on the requirement of a stronger level of evidence to be observed in order for an individual comparison to be deemed significant, compensating for positive results occurring by chance due to the number of inferences being made. For the multiple testing carried out in the GWA datasets, Bonferroni Correction was used. The Bonferroni correction is derived by observing Boole's inequality (Miller 1981), which states that if n tests are performed, each significant with probability β (where β is unknown), then the probability that at least one of them comes out significant is $\leq n\beta$. If the required significance level for the entire series of tests is equal to α; by solving for β, $\beta = \alpha/n$.

Using the Bonferroni Correction at the 5% significance level, and considering that 295196 SNP associations were made per sample, genome-wide significance was defined using a *P*-value (β) of $P \leq 1.69 \times 10^{-7}$, where $\alpha = 0.05$ and n=295,196. Further suggestive regions of interest were identified based on the detection of a sentinel SNP showing association at a threshold of $P = 1 \times 10^{-4}$ or smaller with at least one additional SNP within 100Kb also reaching a threshold of $P = 1 \times 10^{-4}$ or smaller.

4.3.4 VISUALISATION OF ASSOCIATED REGIONS

To identify whether SNPs in the regions adjacent to the GWA selected regions provide supporting evidence for association through elevated log10 *P*-values, the regions 500Kb upstream and downstream of all the SNPs identified in Section 4.3.2, were investigated. Investigations were carried out *in silico* using the online software tool LocusZoom version 1.1[9] with the original GWAS dataset (Pruim RJ *et al.* 2010).

4.3.5 SNP GENOTYPING IN ADDITIONAL COHORTS AND ANALYSES OF DATA FOR QUALITY CONTROL

In order to be able to carry out experiments to attempt duplication of the association results obtained from the GWAS, the selected GWA SNPs were genotyped in an additional disease cohort. Genotyping was carried out by KBiosciences (Hoddesdon, Hertfordshire, UK) on DNA samples from the COPD cohort (*n*=368). A detailed description of this methodology is available in Section 2.6.2.

4.3.6 HAPLOTYPE ANALYSES

Linkage disequilibrium maps for the combined control and asthma population used in the GWA study were generated by the Dutch collaborators (Dr Martin Siedinski and Dr Gerard Koppelmann; University of Groningen, the Netherlands) using Haploview version 4.224 (Barrett et al., 2005). Linkage disequilibrium maps were also generated for the SNP rs4253238 using HapMap (version 3, release 27 on CEU population; region 4:18737100-18741700) and 1000 genome (Release 9, on the CEU population; KLKB1 gene build ENSG00000164344, region 4:187130133-18717962525) populations. The CEU population is defined as residents of the state of Utah with ancestry from northern

---

[9] http://csg.sph.umich.edu/locuszoom

and western Europe (n=180 & 100 respectively). A detailed description of the method is available in Section 2.6.3.

4.3.7 DETERMINING GENOME-WIDE REGULATORS OF PLAUR MRNA

In order to identify whether the results from the protein based GWAS mirrored association data for PLAUR expression in an mRNA based GWAS, associations for PLAUR expression were identified *in silico* using the mRNA by SNP browser v 1.0.1[10]. The software incorporates a generic eQTL database and provides a graphic interface for browsing association between 54,675 transcript levels and 406,912 SNPs. For each transcript, the browser provides association test statistics ($P<0.001$), estimates of effect size and allele information across the genome. Data is obtained from Epstein-Barr virus–transformed lymphoblastoid cell lines taken from 206 families of British descent selected through a proband of childhood asthma, with cells taken from affected subjects and their sibling pairs regardless of whether the sibling pair had asthma (n=397 sibling pairs; 11 half sibling pairs) (Dixon et al., 2007).

Using the software program, the *PLAUR* gene was selected and the mean transcript level for all 3 independent probes (210845_s_at; 211924_s_at; 214866_at) was selected.

---

[10] Available at http://www.sph.umich.edu/csg/liang/asthma/

4.4 METHODS – PROTEIN ASSAYS & ANALYSES

4.4.1 HUMAN PLASMA KALLIKREIN ACTIVITY ASSAY

Since SNP rs4253238 lies within the promoter region of the gene for Human Plasma Kallikrein (KLKB1), it is of interest to determine whether the SNP genotype affects KLKB1 activity. KLKB1 activity in serum was therefore determined using an in house designed activity assay. The assay is based on the commercially available substrate H-Pro-Phe-Arg-AMC, which is cleaved by KLKB1, releasing the 7-amino-4-methylcoumarin (AMC) fluorogenic moiety. Fluorescent intensity can then be related to the degree of KLKB1 activity. 10 serum samples from each rs4253238 homozygote genotype were randomly chosen from the COPD, Asthma and Control cohorts. 5µl of each serum sample was added, in duplicate, to 50µl of H-Pro-Phe-Arg-AMC substrate in activity buffer. After a 5 minute incubation at room temperature, fluorescence then was recorded using a Flexstation 3 microplate reader for a period of 5 minutes using an excitation wavelength of 380nm and absorbance wavelength of 460nm. Prior to use the levels of all protein samples were corrected to 500µg/ml using a Bio-Rad assay (see Section 2.3.1).

4.4.2 DEFINING THE RELATIONSHIP BETWEEN KLKB1 AND SCPLAUR IN EPITHELIAL CELLS USING ELISA AND WESTERN BLOTTING

NHBECs were exposed to commercially obtained human derived KLKB1 at a concentration of 50µg/ml. Supernatant levels of scPLAUR were determined via ELISA while total protein levels of PLAUR were determined via Western blotting using the monoclonal antibody IIIF10, correcting for changes in protein levels by staining for β-actin. A detailed description of both methods is found in Sections 2.3.2 & 2.3.3.

4.5 METHODS – CELLULAR BASED WORK

4.5.1 CULTURING OF NHBECS

Cell based experiments in this chapter were carried out on passage 4 NHBECs cultured in 6-well plates. A detailed description of this method is found in Section 2.4.2.1.

4.5.2 DETERMINING WHETHER KLKB1 DRIVES A CHANGE IN PLAUR mRNA EXPRESSION

Quantitative PCR (qPCR) was used to determine whether PLAUR total mRNA levels are modulated on exposure to KLKB1. A concentration of 50μg/ml KLKB1 was added to HBECs cultured in 6-well plates for a period of 4 or 24 hours. Cells were collected by mechanical scraping and RNA extracted using the Qiagen RNeasy Kit as described in Section 2.2.10. RNA stocks were reverse transcribed to form complimentary DNA (cDNA), using the SuperScript™ First-Strand Synthesis System for RT-PCR as outlined in Section 2.2.11. The resulting cDNA, diluted to 1:10, was used in a qPCR as outlined in Section 2.2.12, using HPRT Pre-Developed TaqMan Assay Reagent (PDAR) as the housekeeping gene and the primers and probes for total PLAUR outlined in Tables 2.9 & 2.10.

These primers and probe were designed and validated by Dr Ceri Stewart (University of Nottingham) and the assay had a 65.3% efficiency rate. Analyses were carried out using the MxPro® software and Microsoft Excel. Further details and cycling parameters are available in Section 2.2.12.

4.5.3 DETERMINING THE RELATIONSHIP BETWEEN KLKB1 AND PLASMIN ACTIVITY IN AN EPITHELIAL CELL MODEL

The plasmin activity assay kit (Cambridge Bioscience; ANA72124) determines the rate of activation of plasminogen into plasmin, a process that occurs in the presence of KLKB1. Neat cell supernatant (50μl) from the cell based experiment outlined in Section 4.5.2 was added in duplicate to a black clear bottomed plate with 50μl of BEGM added as a negative control. The plate was pre-incubated for 10 minutes at 37°C in a hotbox followed by the addition of 50μl pre-warmed plasmin substrate solution into each well. The reagents were mixed completely by shaking the plate gently for 30 seconds, followed by incubation at 37°C for 90 minutes, keeping the plate away from direct light. Fluorescence was then read using an excitation wavelength of 380nm and an emission wavelength of 500nm using a Flexstation 3 microplate reader for a period of 5 minutes.

4.5.4 USING A CELL-FREE SYSTEM TO IDENTIFY A PLAUR PROTEOLYTIC ROLE FOR KLKB1

In order to investigate the role of KLKB1 on PLAUR in a cell-free system, 20μl of recombinant PLAUR (rPLAUR) (R&D Systems 807-UK [10μg/ml]) was incubated with 5μl of commercially obtained human derived KLKB1 (50μg/ml) in 175μl of sterile water at 37°C for 24 hours,. The following controls were used; rPLAUR only [20μl+180μl water]; rPLAUR + Chymotrypsin (Roche 11418467001, reconstituted to 60ng/ml) [20μl+180μl]; rPLAUR + KLKB1 + Protease Inhibitor (Roche 11836153001) [20μl+5μl+100μl+78μl water]. Following incubation, rPLAUR levels were determined via ELISA and Western Blotting, the latter using the mAB IIIF10 and the pAB BAF807. A detailed description of both methods is found in Sections 2.3.2 and 2.3.3.

4.5.5 DETERMINING THE SITE OF KLKB1 MEDIATED CLEAVAGE VIA N-TERMINAL SEQUENCING

N-terminal sequencing was carried out from a digested sample (Section 4.5.4) by Cambridge Peptides, Birmingham UK, using the Edman degradation technique. In this technique, phenylisothiocyanate reacts with the sequence's terminal uncharged amino group under mildly alkaline conditions, forming a cyclical phenylthiocarbamoyl derivative. This terminal amino acid derivative is then cleaved to form a thiazolinone derivative, under acidic conditions, which is then selectively extracted into an organic solvent and treated with acid to form the more stable phenylthiohydantoin-amino acid derivative. This final derivative can then be identified by using chromatography or electrophoresis (Edman, 1949). Using this technique the first 5 terminal amino acids at the site of KLKB1 mediated cleavage in the large remaining PLAUR fragment were identified. The amino acid sequence was compared to the PLAUR protein sequence on http://www.uniprot.org/, protein reference Q03405.

4.5.6 MANUFACTURING AN OVER-EXPRESSING VECTOR FOR SCPLAUR

In order to be able to investigate the role of scPLAUR in NHBECs, an over-expressing vector for scPLAUR was manufactured. The open reading frame of membrane PLAUR (NM_002659.3) minus the sequence coding for the GPI anchor, i.e. amino acids 1 to 293 of the mPLAUR protein structure, was amplified as described in Section 2.2.1, using primers including a consensus Kozak sequence and restriction enzyme sites:

- 5`primer: ACTTGAATTCGCCACCATGGGTCACCCGCCGCT; spacer-EcoRI-Kozak-ATG.
- 3'primer: ACTTCTCGAGTTAACAGCCACTTTTAGTACAGC; spacer-XhoI-stop (TAA).

The resulting PCR product was gel extracted (Sections 2.2.2 and 2.2.3), ligated into pCR®4-TOPO® (see Section 2.2.4) and then subcloned into pcDNA3 using the EcoRI and

XhoI restriction enzymes and T4 ligase (Section 2.2.9). The plasmid was then purified (Section 2.2.6.2) and sequence verified (Section 2.2.7) prior to transfection.

4.5.7 TRANSFECTING NORMAL BRONCHIAL EPITHELIAL CELLS

In order to investigate the role of scPLAUR in the processes of cellular migration, mitochondrial activity and apoptosis in comparison to the role played by mPLAUR and to identify whether any effects are reversible in the presence of KLKB1, a cell system over-expressing scPLAUR and mPLAUR is required. NHBECs cultured in 6-well plates were transfected as described in Section 2.4.5 with the over-expression vector pcDNA3 (empty vector), a pcDNA3 construct for the over-expression of mPLAUR (Designed and tested by Dr Ceri Stewart (Stewart et al., 2012)) and a pcDNA3 construct for the over-expression of scPLAUR (Section 4.5.6). Cells over-expressing scPLAUR were also treated with 2µl KLKB1.

4.5.8 DETERMING THE CHANGES IN BRONCHIAL EPITHELIAL CELL MIGRATION ON OVER-EXPRESSION OF SCPLAUR WITH AND WITHOUT THE PRESENCE OF KLKB1

Cells transfected as described in Section 4.5.7, were investigated using a scratch-wound assay (Section 2.51). Here cells were wounded 24 hours post-transfection and the wound measured at 0, 4, 8 and 24 hours post-wounding. Data analysis was carried out in Cellprofiler™ using a pipeline designed by Mr Benjamin Wilson (University of Nottingham).

4.5.9 DETERMING CHANGES IN BRONCHIAL EPITHELIAL CELL MITOCHONDRIAL ACTIVITY ON OVER-EXPRESSION OF SCPLAUR IN THE PRESENCE AND ABSENCE OF KLKB1

A sterile solution of 0.5mg/ml MTT (3-(4,5-Dimethylthiazol-2-yl)-2,5-diphenyltetrazolium bromide) was added to a cell population 24 hours post-transfection as described in Section 4.5.7. The cells were then incubated at 37°C for 4 hours before the solution was aspirated. On addition of 200µl of isopropanol to each well, absorbance at a wavelength of 570nm was recorded using a Flexstation 3 microplate reader. A detailed description of the MTT method is found in Section 2.5.2.

4.5.10 DETERMING CHANGES IN THE RATE OF APOPTOSIS OF BRONCHIAL EPITHELIAL CELLS ON OVER-EXPRESSION OF SCPLAUR WITH AND WITHOUT THE PRESENCE OF KLKB1

Cells were transfected as described in Section 4.5.7. A 100µl solution of filter sterilised 300µM H_2O_2 in BEGM was then added to one set of transfections (a concentration known to induce apoptosis in NHBECs (Bucchieri et al., 2002)), while 100µl of BEGM was added to an identical set of transfections. The solutions were left to incubate at 37°C for 8 hours and then frozen overnight at -80°C. Using the Apo-ONE® Homogenous Caspase 3/7 assay the rate of apoptosis was determined after an 8 hour incubation at 37°C, through fluorescence readings taken using the Flexstation 3 microplate reader. A detailed description of the method is found in Section 2.5.3.

4.6. STATISTICAL ANALYSES.

4.6.1 LINEAR REGRESSION

Analysis of the COPD cohort was carried out using linear regression. The additive model (outlined in Section 2.7.3.1) and $\log_{10}$ values of serum scPLAUR were used in order to replicate the methodology used in the original GWAS (Section 4.3.2). Although a number of co-variates for serum scPLAUR have been identified in this thesis (Section 3.4.3), since the GWAS was carried out without the inclusion of co-variates, initial analyses were also carried out in this way. Following initial analyses, the statistical analyses were repeated using the known co-variates for serum scPLAUR levels; age, height, weight and smoking pack/years (Section 3.4.3) in order to confirm any positive associations. A detailed description of the method is available in Section 2.7.3.1.

4.6.2 CORRELATION ANALYSES

Spearman's Correlation was used to determine association between KLKB1 activity levels and scPLAUR levels in serum. A detailed description of the procedure used is available in Section 2.7.3.2.

4.6.3 COLUMN STATISTICS

Paired two-tailed Student t-tests and Repeated Measures ANOVA were utilised to investigate differences in scPLAUR supernatant levels, total intracellular PLAUR levels and NHBEC mitochondrial activity rates in this chapter. Pairing was used to address inter-experimental variation. A detailed description of the procedure used to carry out these tests is available in Section 2.7.4.1.

4.6.4 TWO-WAY ANOVA

A two way ANOVA was used to investigate the effect of different categorical variables, i.e. over-expression have on the rate of wound repair as presented by a scratch-wound model in NHBECs and to concurrently determine whether this effect was modulated over time. A detailed description of the procedure used to carry out these tests is available in Section 2.7.4.2.

4.7 RESULTS

4.7.1 LOCI IDENTIFIED BY THE GENOME WIDE ASSOCIATION STUDY

Quantile-Quantile plots for the observed *P*-values in controls (n=104) and asthmatics (n=480) identified a modest deviation from the expected *P*-values (Fig. 4.1). In these individual datasets, no SNP achieved a genome-wide significant *P*-value of $P<1.69\times10^{-7}$ (Bonferroni Correction). Quantile-Quantile plots for the combined analysis carried out on the control/asthma dataset (n=584) identified a stronger deviation from the expected *P*-values (Fig. 4.2), identifying an increase in effect in the combined asthma/control population.
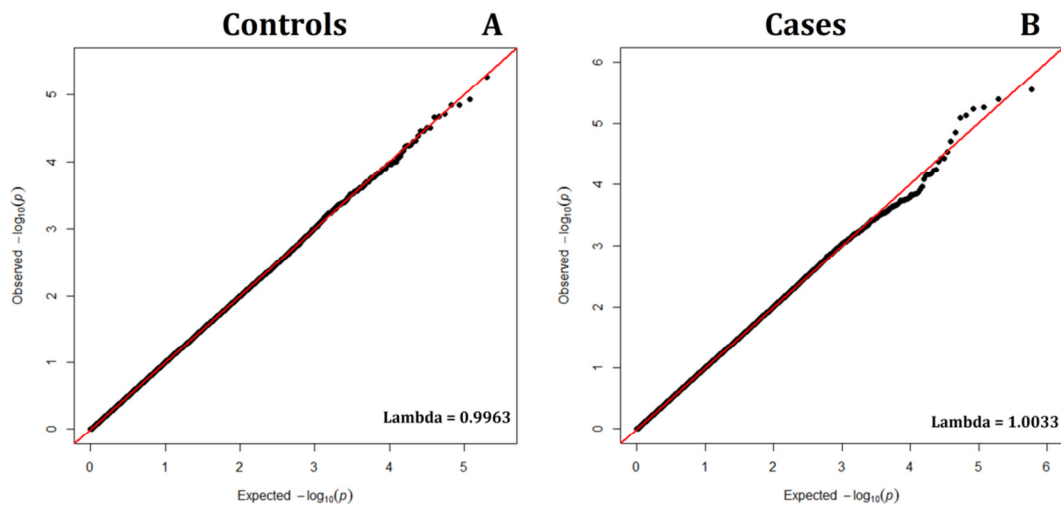
Figure 4.1: QQ-Plot for genome-wide analyses in control (n=104) (Panel A) and asthma (n=480) (Panel B) populations. The QQ-plots identify that measured SNP $\log_{10}$ *P*-values do not deviate from the expected trend in the control population, while there is a modest deviation in the disease (asthma) population suggesting a greater role for genetic regulation.
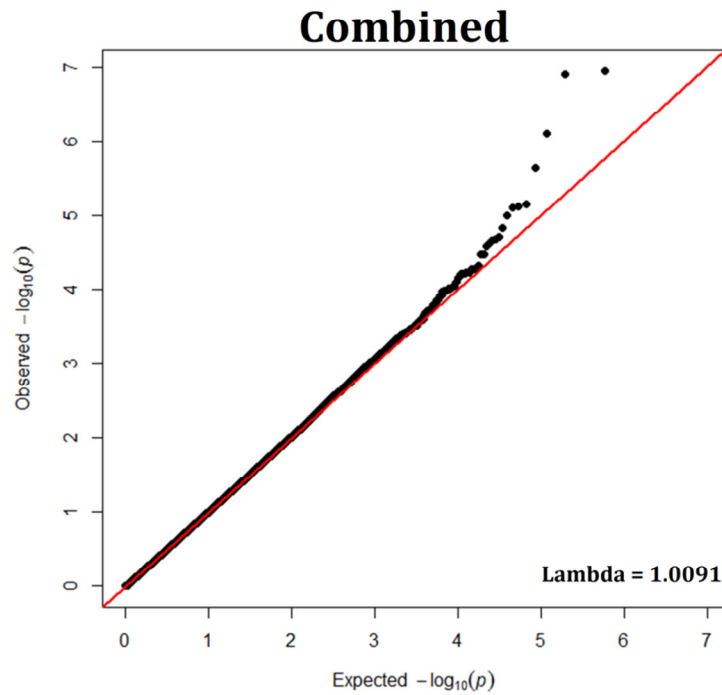
Figure 4.2: QQ-Plot for the combined asthma and control populations (n=584). The QQ-plot identifies that measured SNP log *P*-values deviate significantly from the expected trend denoted by the black trendline. This identifies that potential regulatory SNPs for soluble PLAUR exist within the combined dataset.

Statistical analyses in PLINK, using the additive method identified 2 genome-wide significant SNPs (rs4253238 and rs1912826) located at 4q35 (*P*=1.13x10^{-7}, B=0.0733) (Fig. 4.3). As the 2 SNPs in this region are in near complete linkage disequilibrium (LD) (LOD=99; R^2=94) (Fig. 4.4) they were consequently considered as a single genome-wide significant locus. SNP rs4253238 was selected to act as the sentinel SNP for this locus. The 4q35 region corresponds to the promoter/coding region of the gene for human plasma kallikrein (KLKB1; previously known as KLK3).
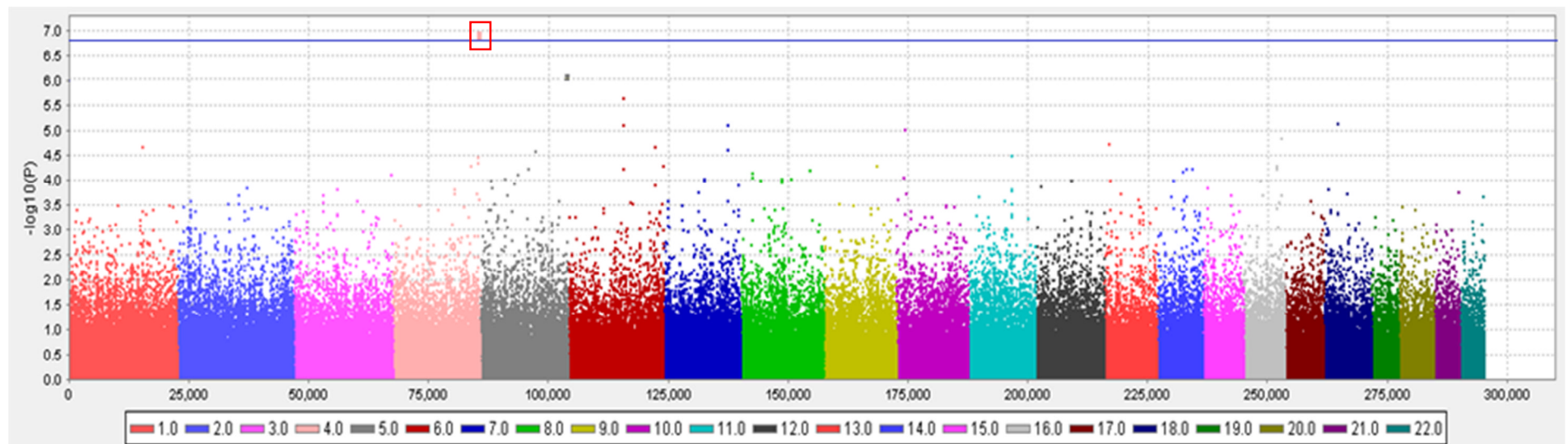
Figure 4.3: Manhattan plot identifies a single chromosome 4 region as genome-wide significant in a combined asthma/control population. This region (identified by a red box) consists of two SNPs; rs4253238 and rs1912826, which achieve a genome-wide significance with a *P*-value of <1.69x10^{-7}. These SNPs lie in the promoter and coding region of the Human Plasma Kallikrein (*KLKB1*) gene.
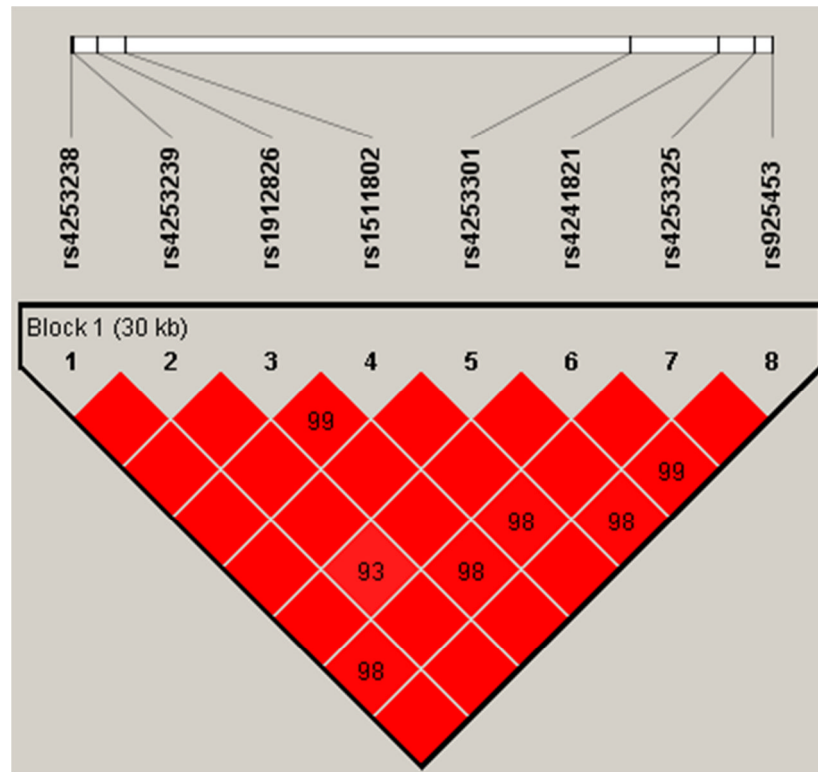
Figure 4.4: Linkage disequilibrium map of the region determined to be Genome-wide significant. Using SNP data from the GWA study the SNPs rs425328 and rs1912826 are shown to be in high linkage disequilibrium (LOD=99; R^2=94). Therefore these SNPs are considered to be a single scPLAUR associated region.

4.7.2 ADDITIONAL POTENTIAL SCPLAUR ASSOCIATED LOCI

Using the less stringent criteria of a *P*-value threshold of 1×10^{-4} or less with an additional SNP with a *P*-value of 1×10^{-4} or less within 100kb to identify potential loci with *P*-values below the Bonferroni corrected *P*-value threshold in the combined GWAS dataset, 7 further regions with potential scPLAUR regulatory SNPs were identified (Table 4.1). Region plots identified supporting evidence in the form of surrounding SNPs with low *P*-values in LD with the sentinel SNP for 6 of the 7 selected loci (Fig. 4.5c-h) similar to the layout for the genome wide significant loci (Fig. 4.5a). Although no supporting evidence was identified for SNP rs2731672, this region was still considered based on its *P*-value being close to the significance threshold (*P*=7.83x10-7; Fig. 4.5b).

SNP	Chromosome	Position	MAF	Beta	*P*-value	Gene
rs4253238 rs1912826	4	187148387	(C) 0.37	0.0733	1.13E07	KLKB1/FXI/CYP4VA2
rs2731672	5	176842474	(T) 0.43	0.0782	7.83E07	FXII
rs12200614	6	96544414	(C) 0.14	-0.0764	2.25E06	FUT9
rs6988339	8	32545916	(G) 0.35	-0.06757	2.92E05	NRG1
rs6467459	7	132692468	(T) 0.29	-0.0658	7.58E06	CHCHD3
rs9480227	6	156198945	(C) 0.47	-0.06615	5.75E05	mIR1202
rs7666900	4	146414333	(T) 0.18	-0.08533	8.39E05	RAB33B / SETD7
rs341119	6	158861618	(A) 0.23	-0.0601	2.19E05	TULP4

Table 4.1: 8 SNPs selected from the GWA study. SNPs were selected using less stringent criteria than achieving a genome wide significant *P*-value of possessing a *P*-value of 1x10-4 or smaller with at least 1 other SNP with a *P*-value of 1x10-4 in the 100kb flanking region and supporting evidence from region plots visualised using the LocusZoom software. MAF = Minor Allele Frequency; OR = Odds Ratio (Minor Allele); KLKB1 = Human Plasma Kallikrein gene; FXI = Factor XI gene; CYP4VA2 = Cytochrome 4VA2; FXII = Factor XII gene; FUT9 = Fucosyltransferase 9 gene; NRG1 = Neuregulin 1 gene; CHCHD3 = Coiled-coil-helix-coiled-coil-helix domain containing 3 gene; mIR1202 = microRNA 1202; RAB33B = Ras-related protein Rab-33B gene; SETD7 = SET domain containing (lysine methyltransferase) 7 gene; TULP4 = Tubby like protein 4 gene. Genome positions refer to Genome Assembly GRCh37.p5, Genome Build 37.3.

Plotted SNPs

C

rs12200614

$P=2.25$x10-6

$FUT9\rightarrow$

Position on chr6 (Mb)

Plotted SNPs

D

rs6988339

$P=2.92$x10-5

$NRG1\rightarrow$

Position on chr8 (Mb)

169

E

rs6467459

P=7.58x10-6

$-\log_{10}$(p-value)

Recombination rate (cM/Mb)

r^2
- 0.8
- 0.6
- 0.4
- 0.2

←PLXNA4   ←CHCHD3   EXOC4→

132   132.2   132.4   132.6

Position on chr7 (Mb)

F

rs9480227

P=5.75x10-5

$-\log_{10}$(p-value)

Recombination rate (cM/Mb)

r^2
- 0.8
- 0.6
- 0.4
- 0.2

156   156.2   156.4   156.6

Position on chr6 (Mb)

170
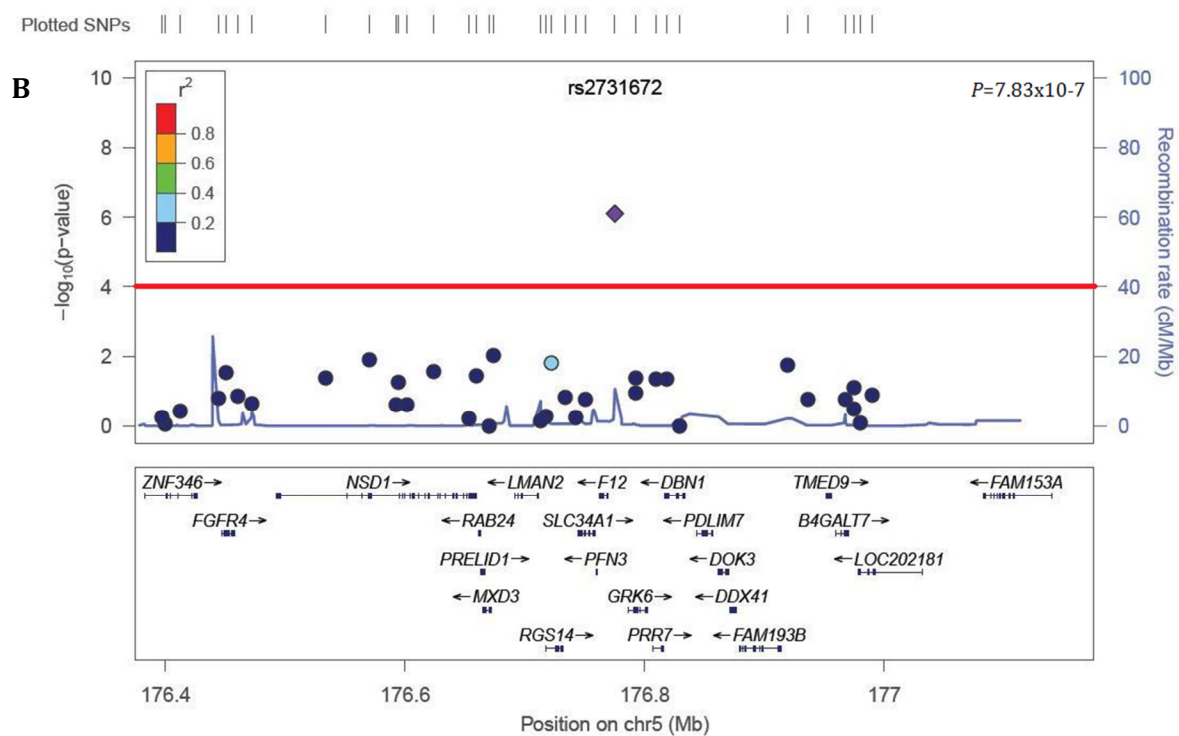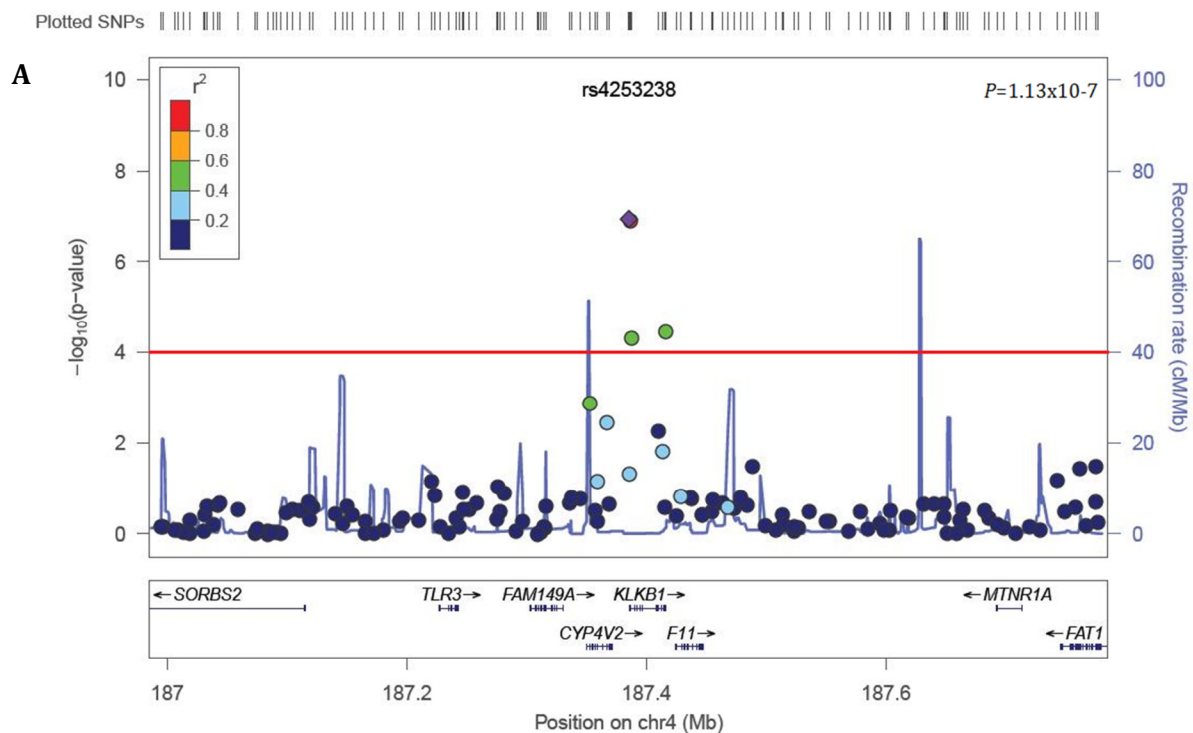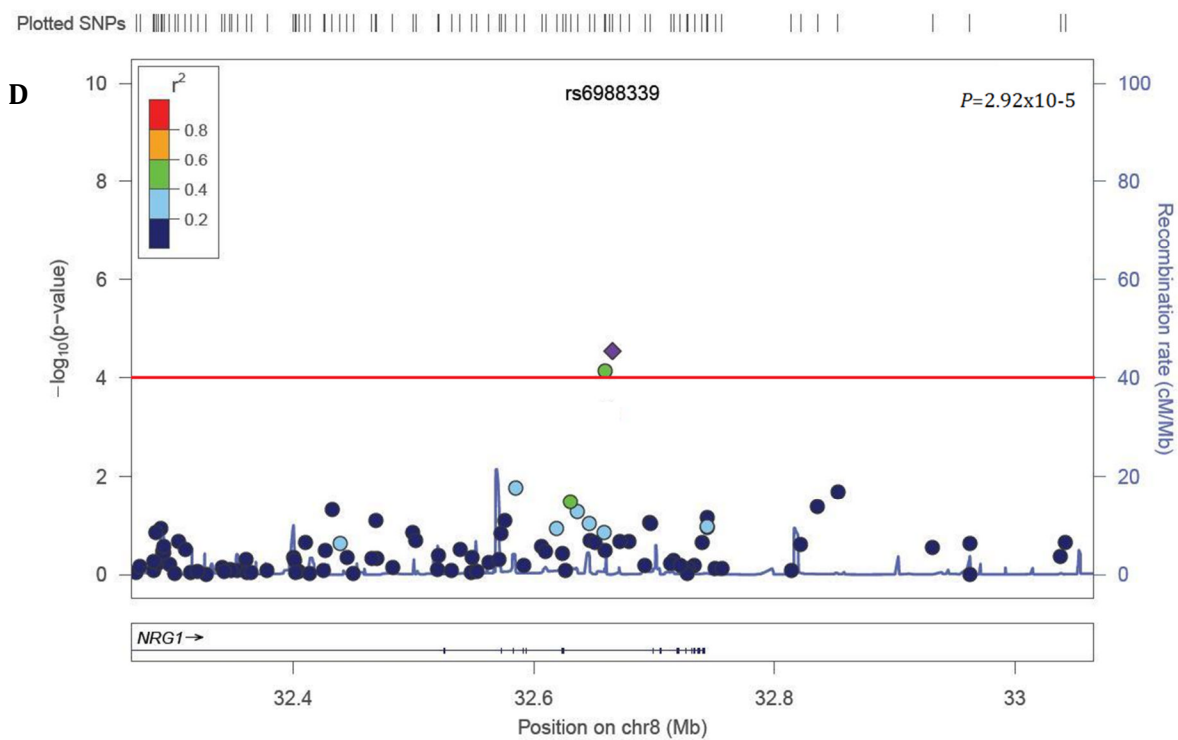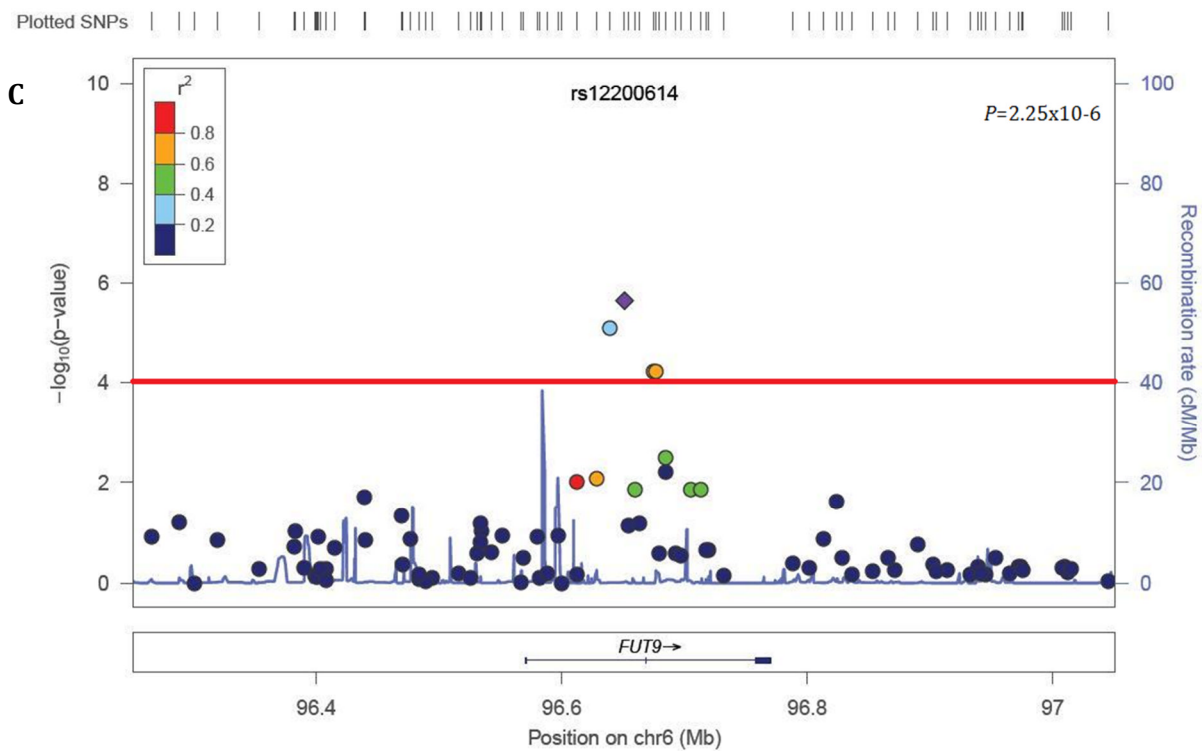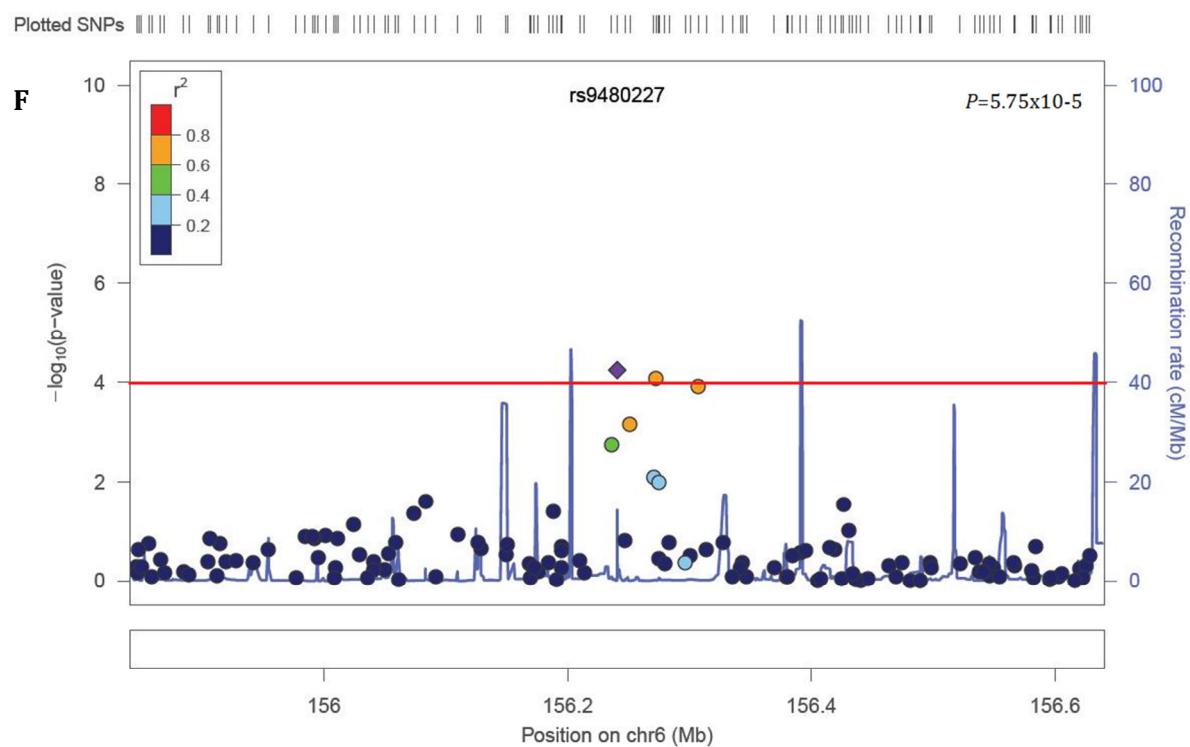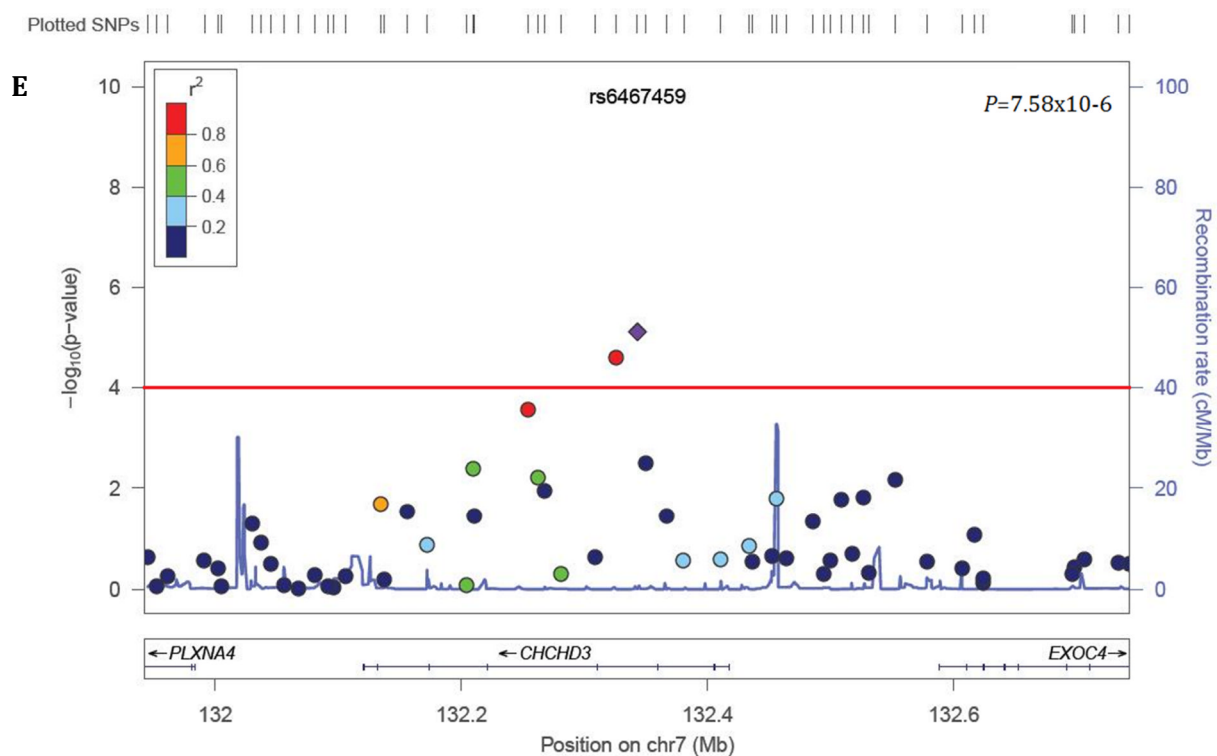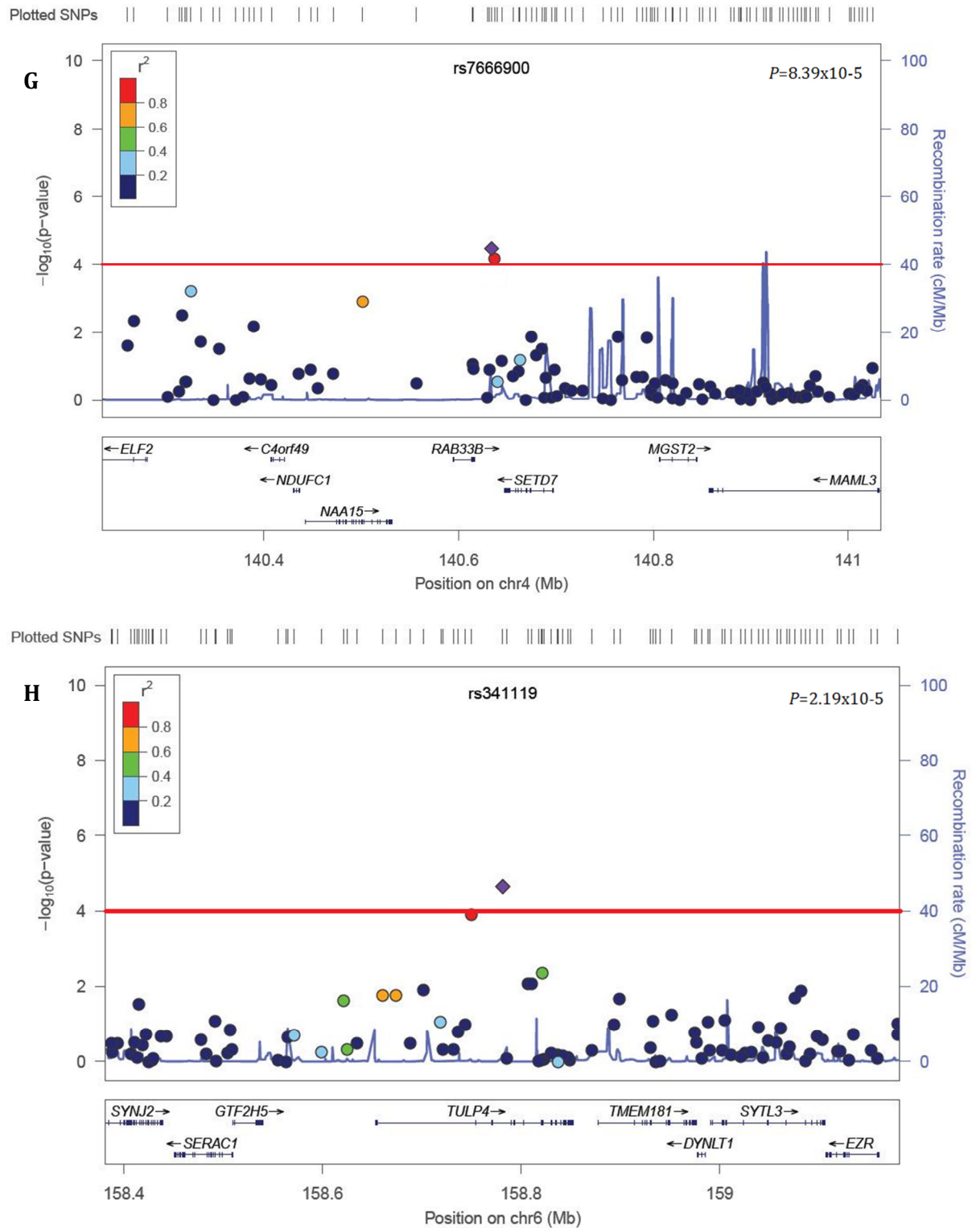
Figure 4.5: Region plots for potential scPLAUR associated SNPs from the GWAS dataset. Statistical significance of each SNP on the $-\log_{10}$ scale is shown as a function of chromosome position (NCBI build 37). The sentinel SNP is shown in purple and the correlation (R^2) of each of the surrounding SNPs shown by their colour (see key). Fine scale recombination rate is plotted in blue. The red line denotes the lower stringency cut off point of $P=1\times10^{-4}$. All SNPs had one SNP $P>1\times10^{-4}$ with one other SNP in 100kb at $P=1\times10^{-4}$ apart from rs2731672 which was selected as it nearly achieved genome-wide significance with $P=7.83\times10^{-7}$.

171

4.7.3 *IN SILICO* MRNA GWAS RESULTS DO NOT MIRROR THE PROTEIN BASED GWAS

In the mRNA by SNP Browser, no SNP achieved genome-wide significance. The top 10 associated SNPs (Table 4.2) did not match the 8 selected SNPs from the protein based GWAS. A comparison of the tagged SNPs in the *in silico* mRNA study and the protein GWAS identified only 9 associations that were present in both studies and had the same direction of effect on PLAUR expression (Table 4.3). Of these associations one (RAB9B) belonged to a pseudo gene.

Marker	Chromosome	Position	MAF	Beta	*P*-value	Gene
rs2528650	7	107194508	(T) 0.34	0.150	1.3×10^{-6}	LAMB1
rs3766027	1	87518821	(G) 0.12	-0.203	4.8×10^{-6}	LMO4
rs1375317	2	168407701	(T) 0.14	0.146	8.9×10^{-6}	B3GALT1
rs1014766	9	75504442	(G) 0.37	-0.138	1.4×10^{-5}	PCSK5
rs10241241	7	98176534	(T) 0.34	-0.162	1.8×10^{-5}	TRAAP
rs3774700	3	62291434	(G) 0.13	0.217	1.9×10^{-5}	C3orf14
rs2147351	13	4235769	(T) 0.29	0.132	2.2×10^{-5}	EPSTI1
rs2969998	18	46284902	(T) 0.08	0.173	2.3×10^{-5}	MAPK4
rs4814111	20	1240988	(T) 0.04	0.233	2.3×10^{-5}	SDCBP2
rs3850590	12	66484825	(C) 0.16	-0.132	2.4×10^{-5}	DYRK2

Table 4.2: Top 10 hits from the *in silico* mRNA GWAS. These hits do not relate to the hits identified in the protein based GWAS. LAMB1 = Human laminin beta 1 precursor; LMO4 = LIM domain only 4; B3GALT1 = Galactosylgalactosylxylosyl protein 3-beta-glucuronosyltransferase 1 Gene; PCSK5 = Proprotein convertase subtilisin/kexin type 5; C3orf14 = hypothetical protein LOC57415; EPSTI1 = epithelial stromal interaction 1; SDCBP2 = Syndecan binding protein 2; MAPK4 = Mitogen-activated protein kinase 4; DYRK2 = dual-specificity tyrosine-(Y)-phosphorylation.

SNP	Chr	Position	MAF	Beta GWAS	P-value GWAS	Beta mRNA	P-Value mRNA	Gene
rs11894671	2	10100000	(T) 0.17	0.059	9.52×10^{-4}	0.109	9.10×10^{-4}	NPAS2
rs1430043	2	16557593	(C) 0.36	-0.078	3.10×10^{-3}	0.172	7.6×10^{-4}	FAM49A
rs7598792	2	23355914	(T) 0.48	0.027	4.00×10^{-3}	-0.106	6.60×10^{-4}	KLHL29
rs2675301	3	2717999	(A) 0.23	-0.040	0.008543	-0.128	8.5×10^{-4}	CNTN4
rs1217461	5	104214088	(G) 0.13	-0.030	5.27×10^{-3}	-0.131	1.40×10^{-4}	RAB9B
rs3860938	9	83337581	(T) 0.20	0.060	4.94×10^{-3}	0.146	6.70×10^{-4}	FRMD3
rs10842777	12	26737511	(A) 0.49	0.031	5.32×10^{-3}	0.105	7.30×10^{-4}	ITPR2
rs1012004	16	22819248	(A) 0.48	-0.044	2.71×10^{-3}	0.106	3.6×10^{-4}	HS3ST2
rs371500	19	45172763	(A) 0.20	0.013	7.42×10^{-3}	-0.210	6.80×10^{-4}	PSMC4

Table 4.3: 9 regions were found to be associated with both the mRNA GWAS and the protein based GWAS and had the same effect on PLAUR expression. None of the associations were genome wide significant in either GWAS. NPAS2: neuronal PAS domain protein 2; FAM49A: Family with sequence similarity 49, member A; KLHL29: kelch-like protein 29; CNTN4: contactin 4; RAB9B: ras-related protein Rab-9B; FRMD3: FERM domain containing 3; ITPR2: inositol 1,4,5-trisphosphate receptor, type 2; HS3ST2: heparan sulfate (glucosamine) 3-O-sulfotransferase 2; PSMC4: proteasome (prosome, macropain) 26S subunit, ATPase, 4.

4.7.4 ASSOCIATION BETWEEN GWAS IDENTIFIED SNPS AND SCPLAUR IN A COPD COHORT

Analysis of the COPD cohort identified that the *KLKB1* promoter SNP rs4253238 was associated with serum scPLAUR levels when analysed without the inclusion of any covariates ($P < 1.00 \times 10^{-3}$). This association held when corrected for age, height, weight and smoking pack/years ($P < 1.00 \times 10^{-3}$) (Table 4.4). The association displayed the same direction of effect on median scPLAUR levels as that identified in the genome-wide association study with the presence of a positive F-value. The F-value also identifies a large change in scPLAUR levels dependant on scPLAUR genotype with over 11 fold difference in scPLAUR levels identified in the uncorrected analyses and nearly 10 fold difference in the corrected analyses in the presence of the minor allele (C) (Table 4.4). This can also be appreciated by eye in a scatter dot diagram where presence of the minor allele (C) was also associated with higher scPLAUR levels (C:C(6654pg/ml)>T:C(5435pg/ml)>T:T(4412pg/ml)) (Fig. 4.6). The scatter dot

diagram identifies however that a degree of overlap between the genotyping groups is present. None of the other 7 SNPs were found to be associated with serum scPLAUR levels in this cohort.

Later analyses of the data using PLINK by Dr Mateusz Siedlinski (University of Groningen, The Netherlands) reproduced the association in the COPD cohort with rs4253238 (P=5.34x10^{-07}; B=0.16812 for log$_{10}$-transformed PLAUR levels and additive allele coding). A meta-analysis including the control, asthma and COPD populations (n=803) further confirmed the association between rs4253238 and serum scPLAUR (P=5.037x10^{-12}; B=0.0879). A significant degree of heterogeneity of the effect between the studies (P=0.02) was observed and reflected a more pronounced effect by rs4253238 on serum scPLAUR in COPD (B=0.16812) than in asthmatics (B=0.06972) or controls (B=0.09129).

SNP	F-value	Uncorrected *P*-value	F-value	Corrected *P*-value
rs4253238	11.348	***<0.001***	9.687	***<0.001***
rs12200614	1.026	0.301	N/A	N/A
rs6988339	0.884	0.414	N/A	N/A
rs9480227	0.255	0.775	N/A	N/A
rs7666900	0.149	0.861	N/A	N/A
rs2731672	0.069	0.934	N/A	N/A
rs6467459	0.724	0.486	N/A	N/A
rs341119	2.248	0.107	N/A	N/A

Table 4.4: A significant association between the GWAS identified SNP rs4253238 and serum scPLAUR levels in the COPD Cohort. This significance holds both when the analyses is carried out with (Corrected) and without (Uncorrected) correction for the known covariates, age, height, weight and smoking pack/years.
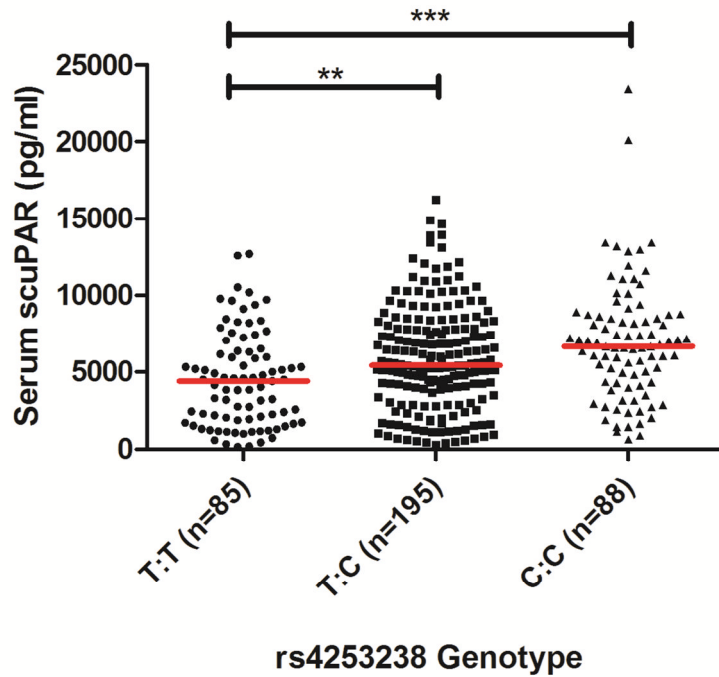
Figure 4.6: The Chromosome 4 SNP rs4253238 significantly alters serum scPLAUR levels in a COPD cohort (n=368). The scatter diagram identifies that the same direction of effect as reported in the GWAS exists, i.e. C:C(6654pg/ml)>T:C(5435pg/ml)>T:T(4412pg/ml), were C is the Minor allele (R²=0.056). These differences were determined to be statistically significant (*P*<0.001) even when corrected to age, height, weight and smoking pack/years.

4.7.5 rs4253238 IS IN LINKAGE DISEQUILIBRIUM WITH KLKB1 SNPS

Two blocks of linkage disequilibrium including the *KLKB1* gene and 5`UTR regions were identified when LD was defined by the association R² values. The first block of LD, which encompassed the KLKB1 5`UTR and gene regions, included the GWAS identified SNP rs4253238. Inclusion of SNP rs4253238 in this block of LD, identified that this SNP is inherited with 4 other *KLKB1* 5`UTR SNPs and 10 *KLKB1* gene SNPs. Specific R² values for LD for rs4253238 range from R²=9 to R²=98, with the majority having an R²>55, therefore identifying that the GWAS tagged SNP is itself in high LD with KLKB1 gene and 5`UTR SNPs independently of the identified block of LD (Fig. 4.7).

Figure 4.7: SNP rs4253238 is in linkage disequilibrium (LD) with SNPs in the *KLKB1* gene and promoter regions. The LD heat map identified LD according to colour which in turn represents D' values as identified by the key. Values define LD based on R² data. SNP rs4253238 is present in a strong block of LD that spans 4 other 5`UTR and 10 gene SNPs.

4.7.6 KLKB1 ACTIVITY IS REGULATED BY rs4253238 GENOTYPE, IS DECREASED IN ASTHMA AND COPD AND IS INVERSLY CORRELATED TO SERUM SCPLAUR LEVELS

The KLKB1 activity assay identified that human plasma kallikrein (KLKB1) protein activity is related to the rs4253238 genotype in serum, i.e. presence of the major allele (T) was associated with increased KLKB1 activity. Presence of the T allele resulted in increased activity in the control ($P<0.01$), asthma ($P<0.01$) and COPD populations ($P<0.001$) (Fig. 4.8). KLKB1 activity was also found to be lower in both asthmatic and COPD patients when compared to the control population *per se* ($P<0.001$) regardless of SNP genotype (Fig. 4.8). This suggests a negative relationship between KLKB1 and scPLAUR and potential regulation of scPLAUR function in disease. Correlation analyses of the KLKB1 activity data from all 3 cohorts, with previously determined scPLAUR levels (see Section 3.3.1), confirmed that KLKB1 activity is inversely correlated to serum scPLAUR ($P<1 \times 10^{-4}$; $R^2 = -0.5277$) (Fig. 4.9).
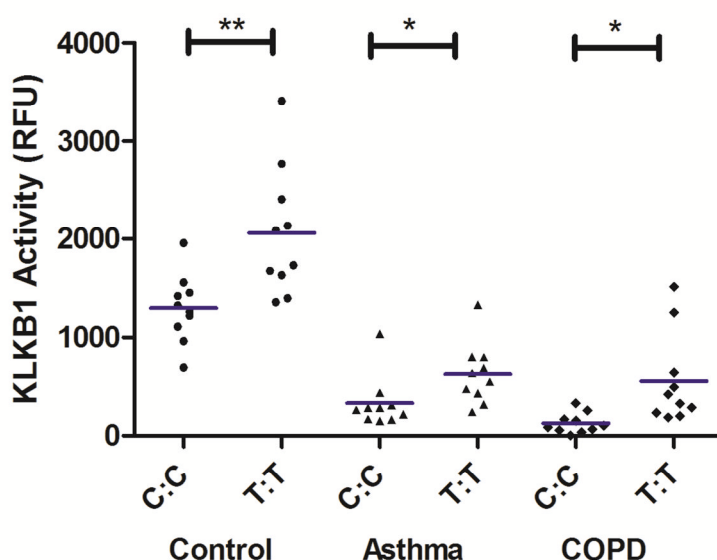
Figure 4.8: KLKB1 activity is related to rs4253238 genotype and disease phenotype. KLKB1 activity was elevated in with the T:T genotype in the control ($P<0.01$), asthma ($P<0.01$) and COPD populations ($P<0.001$). KLKB1 activity is also elevated in controls when compared to asthma and COPD subjects, regardless of the genotype ($P<0.001$). Each column represents data obtained from10 randomly selected subjects. RFU = Relative Fluorescent units.
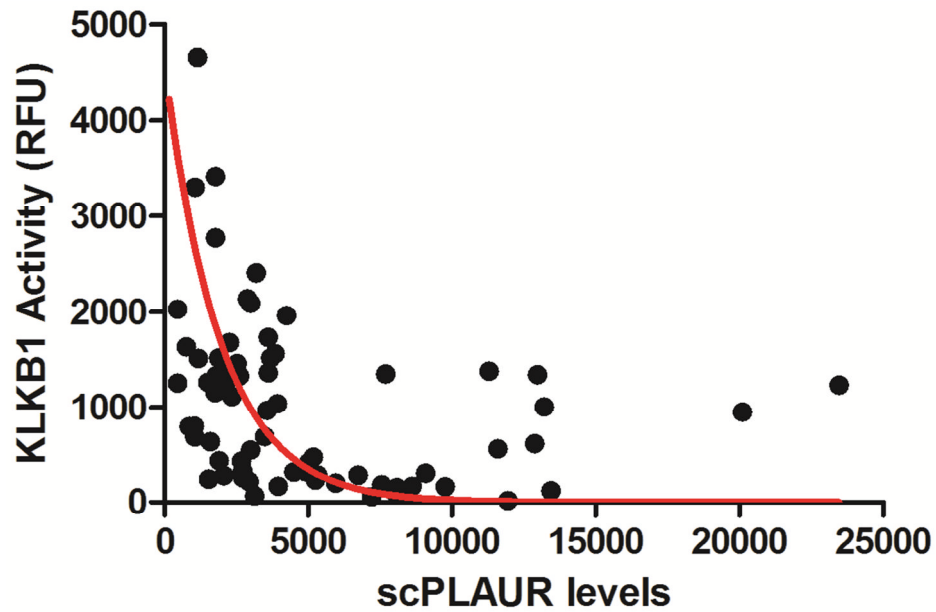
Figure 4.9: KLKB1 activity is correlated to serum scPLAUR levels. In the combined control/asthma/COPD population, increased KLKB1 activity is associated with a decrease in scPLAUR levels ($P<1\times10^{-4}$; $R^2=0.278$) suggesting a relationship between KLKB1 activity and circulating levels of scPLAUR in serum exists.

4.7.7 KLKB1 DETERMINES SCPLAUR LEVELS IN A CELL-BASED SYSTEM

In normal human bronchial epithelial cells (NHBECs) cultured *in vitro* (*n*=3 in Donor 7F3158; *n*=3 in Donor 7F3206), the addition of human derived KLKB1 under normal growth conditions leads to a decrease in the detectable levels of *scPLAUR* in the cell supernatant after both the 4 (*P*=0.015) and 24 hour (*P*=0.029) incubations (Fig. 4.10). At 4 hours levels decreased to 141pg/ml from a basal level of 236pg/ml (40%) while at 24 hours levels decreased to 148pg/ml from a basal level of 268pg/ml (45%). Although no changes could be detected in the levels of total intracellular PLAUR after a 4 hour incubation with KLKB1, a 21% decrease in the levels of total PLAUR intracellular protein was apparent following a 24 hour incubation (*P*=0.05) (Fig. 4.11), suggesting that KLKB1 is more efficient at targeting soluble/extracellular protein.
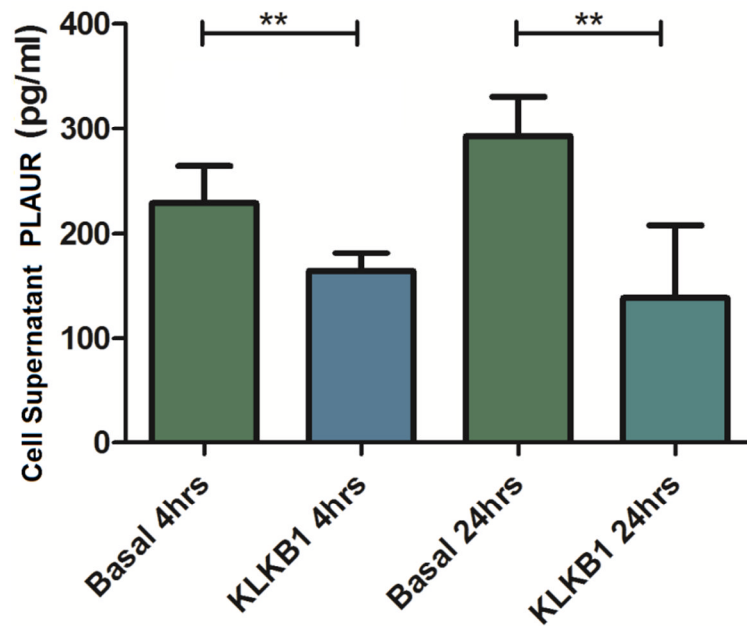
Figure 4.10: KLKB1 decreases levels of scPLAUR in NHBEC cell supernatants. Exposure of 50μg/ml KLKB1 to NHBECs decreases scPLAUR levels in the cell supernatant after a 4 and 24 hour incubation. HBECs were grown under normal conditions. Graphs represent mean values, bars represents the standard error of the mean, *n*=6 carried out in 2 Donors.
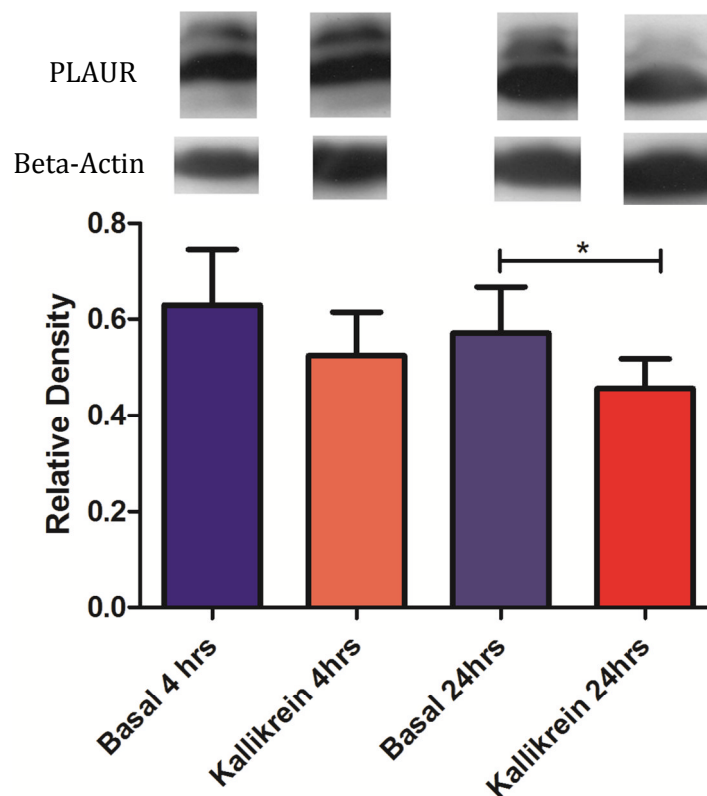
Figure 4.11: KLKB1 decreases levels of total PLAUR whole cell protein. Exposure of KLKB1 to HBECs resulted in a modest decrease in the levels of total intracellular PLAUR only after a 24 hour incubation identifying that the major mechanism of KLKB1 does not involve suppression of PLAUR expression and/or production. HBECs were grown under normal conditions. Graphs represent mean values of D_I specific staining corrected to beta-actin expression, bars represent the standard error of the mean, *n*=6 carried out in 2 Donors.

4.7.8 KLKB1 DOES NOT ALTER PLAUR mRNA EXPRESSION IN BRONCHIAL EPITHELIAL CELLS

As KLKB1 was found to reduce the detectable levels of scPLAUR, but not modify total intracellular PLAUR to a high degree, a qPCR assay was carried out on total PLAUR expression to investigate the hypothesis that KLKB1 affects scPLAUR levels independently of both PLAUR protein and mRNA levels.

Quantitative PCR carried out in a population of normal human bronchial epithelial cells (HBECs), was successful, with clean results obtained from the RT negative controls. On correction of sample readings to the house keeping gene (HPRT), PLAUR mRNA expression was found to be unaltered on exposure of the cell monolayer to KLKB1 after both a 4 (P=0.449) and a 24 hour (P=0.089) incubation period (Fig. 4.12). Unaltered PLAUR mRNA levels confirm the total intracellular protein results and thereby validate the hypothesis that KLKB1 alters scPLAUR levels using a mechanism that is independent of cell driven gene expression and does not target novel gene expression. Therefore it was hypothesised that KLKB1 either directly interacts with scPLAUR altering its circulating levels or drives the expression of an alternate intermediate that itself directly alters the circulating levels of scPLAUR.
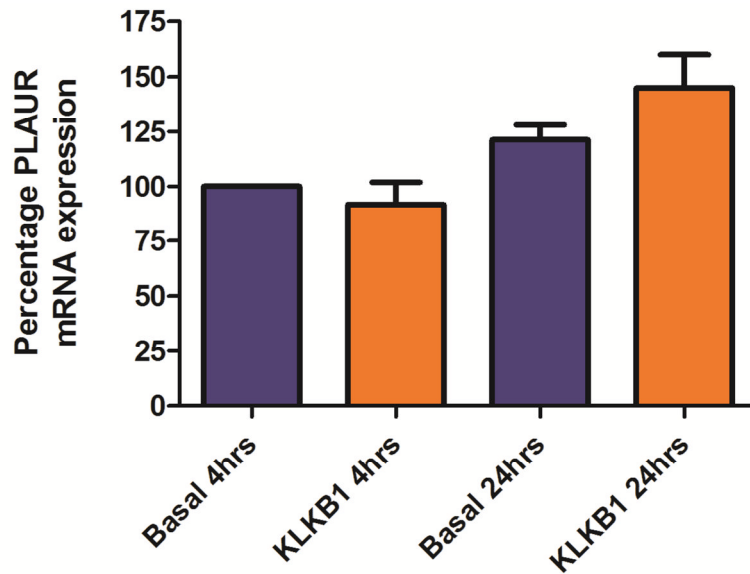
Figure 4.12: Total PLAUR mRNA expression is unaltered on addition of KLKB1. Data from NHBECs corrected to the housekeeping gene HPRT identifies that while total PLAUR mRNA is elevated unilaterally at 24 hours there is no change in expression on exposure to KLKB1 at either time point (P=0.449 (4hrs), P=0.084 (24hrs), n=6 carried out in 2 Donors.

4.7.9 KLKB1 ALTERS THE RATE OF CONVERSION OF PLASMINOGEN TO PLASMIN IN BRONCHIAL EPITHELIAL CELLS

Since KLKB1 is known to increase the rate of plasmin activation from plasminogen *in vivo* (Miles, L. A. *et al.* 1983), and activated plasmin is known to cleave PLAUR in the D_I/D_{II} linker region, disrupting the PLAUR structure (Hoyer-Hansen et al., 1992), it was hypothesised that plasmin may be acting as an intermediary molecule in the observed KLKB1 driven changes in scPLAUR expression. Therefore experimentation was carried out to determine whether KLKB1 dependant plasmin activation was present in the cell (NHBEC)-based system for investigating KLKB1 effects on scPLAUR. A plasmin activity assay carried out on supernatants taken from NHBECs treated with 50μg/ml KLKB1 (see Section 4.5.2), identified that plasmin activity triples within the first 4 hours of addition of KLKB1 (P=3x10^{-3}; n=6 in two donors), with levels returning back to baseline after 24 hours (Fig.4.13). This identifies that KLKB1 mediated effects in the cell-based experiments may be due to KLKB1 regulated activation of plasmin.
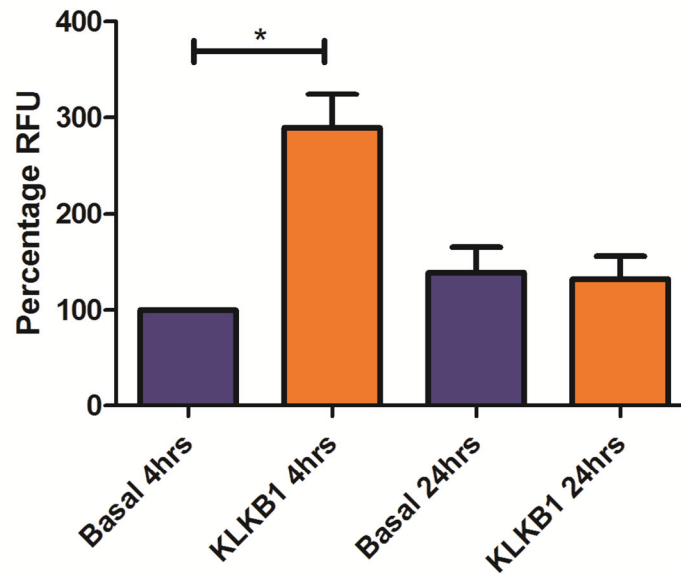
Figure 4.13: Plasmin activity is elevated on addition of KLKB1 but later returns to baseline. Levels of activated plasmin triple following a 4 hour incubation in the presence of KLKB1 ($P=3 \times 10^{-3}$), returning back to baseline at 24 hours, identifying that KLKB1 mediated activity may be due to plasmin activation. Bars represent relative fluorescent units normalised to basal activity at 4 hours, with error bars representing the standard error of the mean. (*n=3), RFU*=Relative Fluorescent units.

4.7.10 KLKB1 IS FOUND TO PROTEOLYTICALLY CLEAVE SCPLAUR IN A CELL FREE SYSTEM

Since it has been identified in Section 4.7.9 that KLKB1 may be driving changes in the expressed levels of scPLAUR through plasmin activation (Fig.4.13), experiments in a cell-free system were carried out so as to identify whether KLKB1 has an as yet unknown direct effect on PLAUR. This experiment utilised commercial recombinant PLAUR (rPLAUR), which mimics scPLAUR in that it is a soluble form of the full length receptor. Incubation of a 1μg/ml solution of recombinant PLAUR with a 1.25μg/ml solution of KLKB1 formed cell-free system independent of other cellular processes that might influence scPLAUR release, formation or degradation, such as activated plasmin. Analysis of the rPLAUR+KLKB1 solution versus the equivalently diluted rPLAUR solution identified that addition of KLKB1 results in complete loss of PLAUR detection (3307pg/ml vs. 0pg/ml) (Fig. 4.14). This identifies that KLKB1 has a direct effect on

PLAUR, altering expression levels through probable disruption of protein integrity, preventing the ELISA capture/detection antibodies from binding.
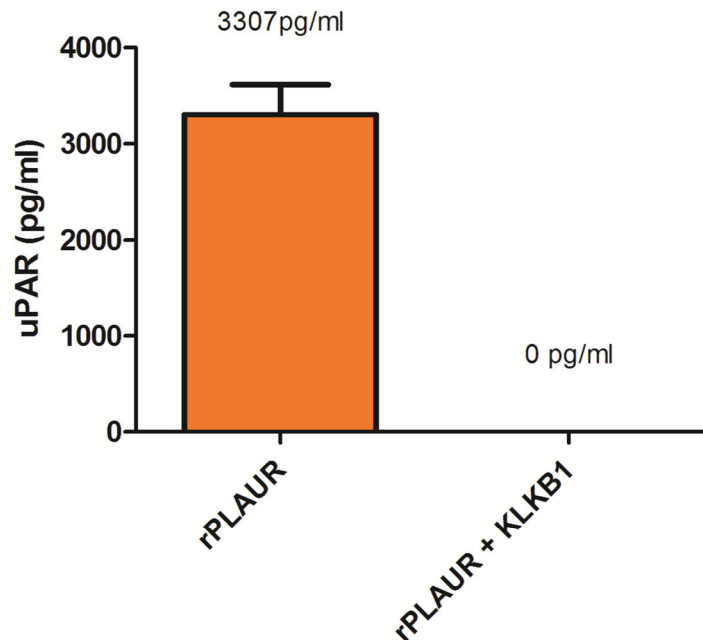
Figure 4.14: Recombinant PLAUR is rendered undetectable by ELISA on exposure to KLKB1. Addition of 1.25µg/ml KLKB1 to 1µg/ml recombinant PLAUR solution results in the complete loss of detection of the recombinant protein, identifying that a direct interaction with KLKB1 is the likely reason for the association between KLKB1 and scPLAUR levels. Bars represent mean data of 3 experiments with error bars identifying the standard error of the mean.

Using western blotting, both the D_I specific (Fig. 4.15A) and polyclonal (Fig. 4.15B) antibodies rPLAUR formed a band at 40-45kDa which identified the rPLAUR protein. On addition of KLKB1 to rPLAUR, no rPLAUR was detected with the mAB IIIF10, indicating that KLKB1 disrupts scPLAUR's Domain I. A smaller fragment (around 30kDa in size) was detected with the pAB BAF807. This identifies that while KLKB1 causes major degradation of rPLAUR, it leaves behind a protein big enough to still be detected using a pAB. No smaller fragments were visualised on either blot. Addition of the known PLAUR proteolytic enzyme Chymotrypsin to the rPLAUR solution did not result in any change in protein composition as defined by the D_I mAB, while staining with the pAB identified that while a rPLAUR representative band remained at 40-

45kDa, a small amount of a smaller ~30kDa fragment was also formed. Importantly, addition of the protease inhibitor mix to the PLAUR/KLKB1 incubation solution resulted in identical results to that formed with untreated rPLAUR, identifying that the effects of KLKB1 can be inhibited. Results were fully replicated in 3 independent experiments.
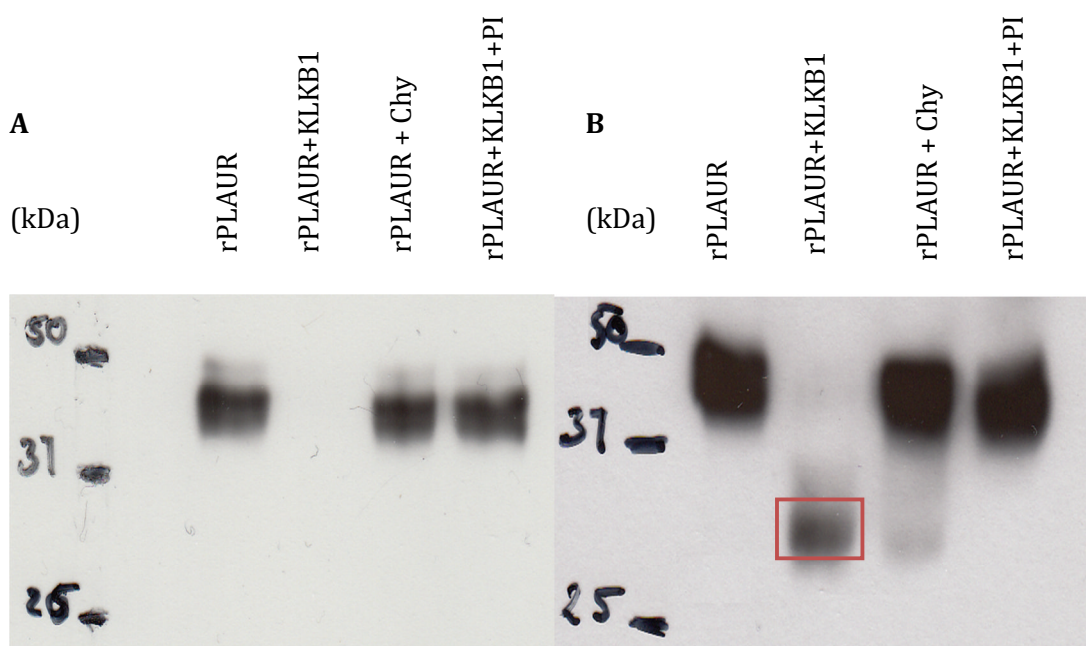
Figure 4.15: Western Blotting identifies a direct proteolytic role for human plasma kallikrein on PLAUR. Staining of recombinant human PLAUR (rPLAUR) digested with human plasma kallikrein (KLKB1) at 37°C for 24 hours with the D_I specific mAB IIIF10 (Panel A) and the pAB BAF 807 (Panel B) identifies that KLKB1 proteolytically cleaves the rPLAUR molecule at the D_I region (Panel A) leaving behind a fragment of around 30kDa in weight, comparable to that formed following digestion with the known PLAUR proteolytic enzyme, chymotrypsin. The ~30kDa region subsequently sequenced is highlighted in the red box. kDa = kiloDalton.

4.7.11 KLKB1 CLEAVES SCPLAUR IN THE VICINITY OF DOMAIN 3

So as to determine the site of cleavage for the identified large ~30kDa fragment formed following incubation of rPLAUR with KLKB1 (Fig.4.15B), N-terminal sequencing was carried out by Cambridge Peptides, directly from solution, on the ~30kDa fragment identified in Fig. 4.15 (*n*=2). This identified that the first 5 amino acids at the cleavage site of this ~30kDa fragment were: Aspartic Acid (D) – Threonine (T) – Histidine (H) – Glutamic Acid (E) – Proline (P). The protein sequence THEP is unique to amino acids 250-253 of the mPLAUR (and ergo the scPLAUR) protein, which lies within D_{III} of the

receptor (Fig. 4.16). The amino acid next to Threonine however is not Aspartic Acid, but rather Glycine (G), which does not correspond to the sequencing results.

```
  1 mghppllpll lllhtcvpas wgLRcmgckt ngdcrveeca lggdlcrtti vrlweegeel
 61 elvekscths ektnrtlsyr tglkitslte vvcgldlcng gnsgravtys RSrylecisc
121 gssdmscerg  rhqslgRSp eeqcldvvth wiqegeegrp kddrhLRgcg ylpgcpgsng
181 fhnndtfhfl kccnttkcne gpilelenlp gngrqcysck gnsthgcsse etflidcrgp
241 mnqclvatgt hepknqsymv rgcatasmcq hahlgdafsm nhidvscctk sgcnhpdldv
301 gyRSgaapgp gpahlsltit llmtarlwgg tllwt
```

Green: **Domain 1**
Blue: **Domain 2**
Yellow: **Domain 3**

Figure 4.16: PLAUR protein sequence. This sequence is identical for human mPLAUR and scPLAUR. Green denotes the sequence that makes up D_I, blue D_{II} and yellow D_{III}. Intermittent regions are the domain liker sequences while the area terminal to D_{III} makes up the GPI anchor. Red areas mark potential proteolytic sites for human plasma kallikrein based on known target sequences of the molecule. The red box denotes the D_{III} cleavage sites identified through N-terminal sequencing.

4.7.12 SCPLAUR ATTENUATES WOUND REPAIR AND INDUCES MITOCHONDRIAL ACTIVITY IN NHBECS WHICH IS REVERSED ON INCUBATION WITH KLKB1

Scratch-wound and MTT assays were carried out to identify whether both scPLAUR and KLKB1 have a functional role in

i)   airway epithelial wound repair, in which scPLAUR has been previously implicated (Stewart et al., 2012), and

ii)   proliferation, which would alter the rate of cellular respiration, based on the previous hypothesis (Chapter 3) that scPLAUR is involved in airway remodelling

Data from scratch-wound assays carried out on NHBECs over-expressing recombinant scPLAUR and mPLAUR, was normalised to the reading from cells transfected with the empty vector (pcDNA3) taken at 8 hours, in order to remove donor dependant variation. Analysis of the data identified that scPLAUR attenuated the rate of wound repair comparable to that caused by mPLAUR at 4 and 8 hours post-wounding

(scPLAUR; 4hrs: $P<0.001$, 8hrs: $P<0.05$; mPLAUR; 4 and 8hrs $P<0.01$) (Fig. 4.17). Addition of 50µg/ml KLKB1 resulted in loss of the scPLAUR driven effects (Fig. 4.17).

Data from the MTT assay was normalised to the rate of mitochondrial activity of cells transfected with the empty vector (pcDNA3). This removed donor dependant variation and corrected for variation caused by differences in mitochondrial activity across different groups (data not shown). Analysis of the combined dataset identified that over-expression of scPLAUR by NHBECs resulted in a near doubling of the rate of cellular mitochondrial activity ($P=2\text{x}10^{-4}$) (Fig. 4.18). Addition of 50µg/ml KLKB1 resulted in complete loss of the scPLAUR driven effects (Fig. 4.18). Over-expression of mPLAUR did not have a significant effect on NHBEC mitochondrial activity.
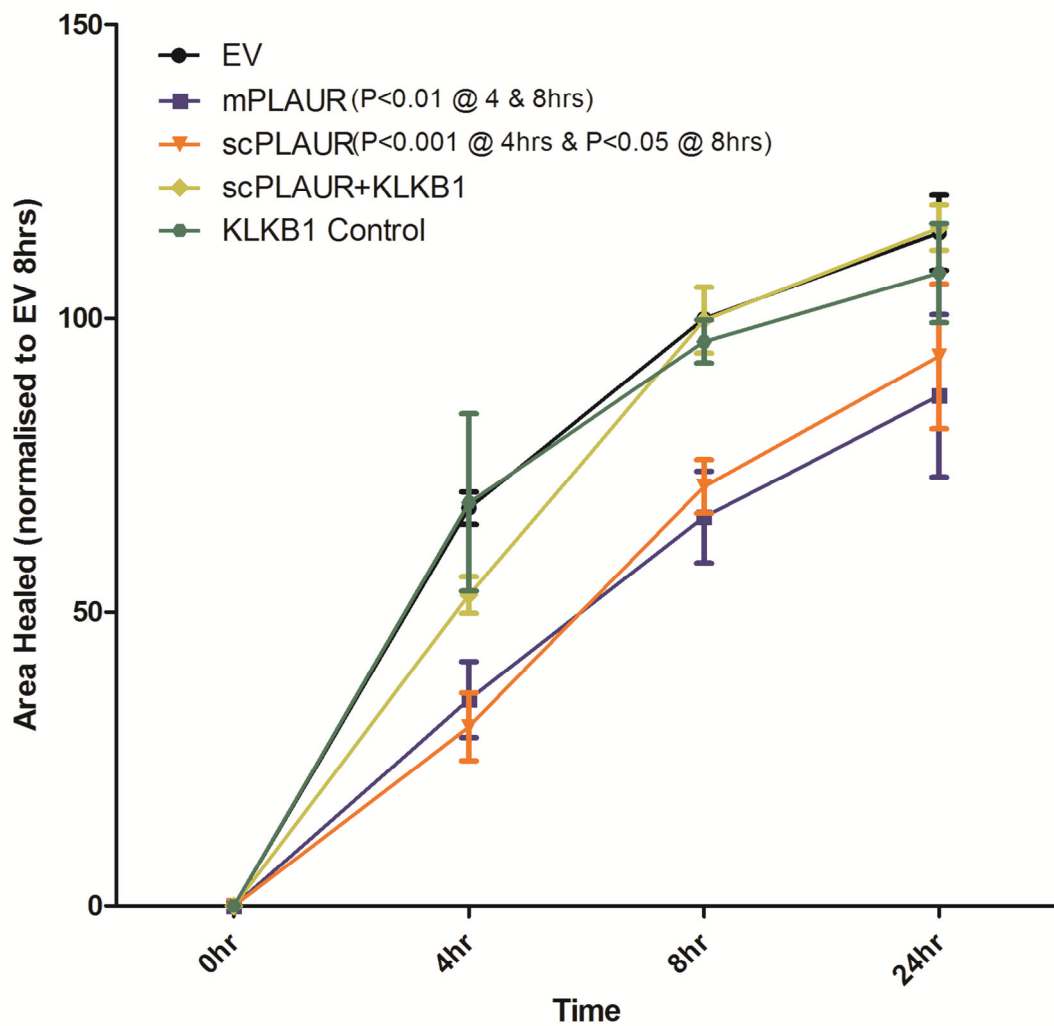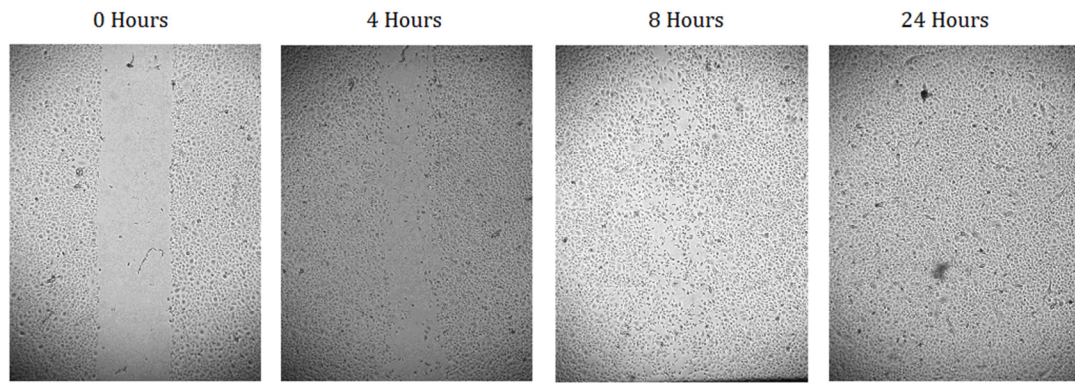
Figure 4.17: Elevated expression of both mPLAUR and scPLAUR attenuate epithelial wound repair in a scratch wound model and is modulated by KLKB1. The rate of mPLAUR driven attenuation appears to be equivalent to the rate driven by scPLAUR (scPLAUR; 4hrs: $P<0.001$, 8hrs: $P<0.05$; mPLAUR; 4 and 8hrs $P<0.01$). Addition of 50μg/ml KLKB1 reverses the effect driven by scPLAUR, increasing the rate of wound repair equivalent to the empty vector control, while KLKB1 on its own did not have and discernible effect on the rate of wound healing. Data points represent the mean area healed normalised to cells transfected with the empty pcDNA3 vector at 8 hours ($n=4$ carried out in two donors). Normalisation to the pcDNA transfected cells was carried out since wound sizes were not constant across different groups.

187
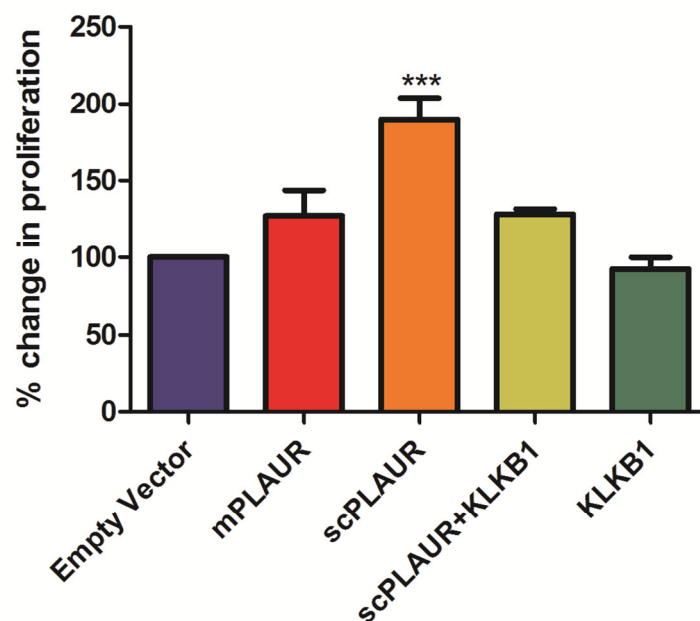
Figure 4.18: scPLAUR increases the rate of NHBEC mitochondrial activity independently of mPLAUR and is modulated by KLKB1. The increase in mitochondrial activity is double that of cells transfected with the empty vector (pcDNA3) at 24 hours post-transfection ($P=2x10^{-4}$). Addition of 50µg/ml KLKB1 results in a reduction of the rate of mitochondrial activity back to background. KLKB1 has no independent effect on cellular mitochondrial activity. Data points represent the mean rate of mitochondrial activity normalised to cells transfected with the empty pcDNA3 vector ($n=4$ carried out in 2 donors).

4.7.13 SCPLAUR DOES NOT AFFECT THE DEGREE OF APOPTISIS IN NHBECS

In order to identify whether both scPLAUR and KLKB1 have a functional role in airway epithelial apoptosis, an important function in airway remodelling, in which scPLAUR has been hypothesised to have a role (see Chapter 3), an Apo-ONE® Homogenous Caspase 3/7 assay was carried out.

Over-expression of scPLAUR did not alter the rate of apoptosis of NHBECs under either basal conditions ($P=0.75$) (Fig. 4.19A) or when stimulated using a 300µM solution of H_2O_2 ($P=0.07$) (Fig. 4.19B). Membrane PLAUR also had no effect on apoptosis in basal cells and while showing a trend for a decrease in the rate of apoptosis in stimulated cells, this was not statistically significant to the rate expressed by NHBECs transfected

with just the empty vector (pcDNA3) ($P=0.29$). Addition of 300μM H_2O_2 resulted in a

100 fold increase in the rate of apoptosis when compared to NHBECs at baseline.
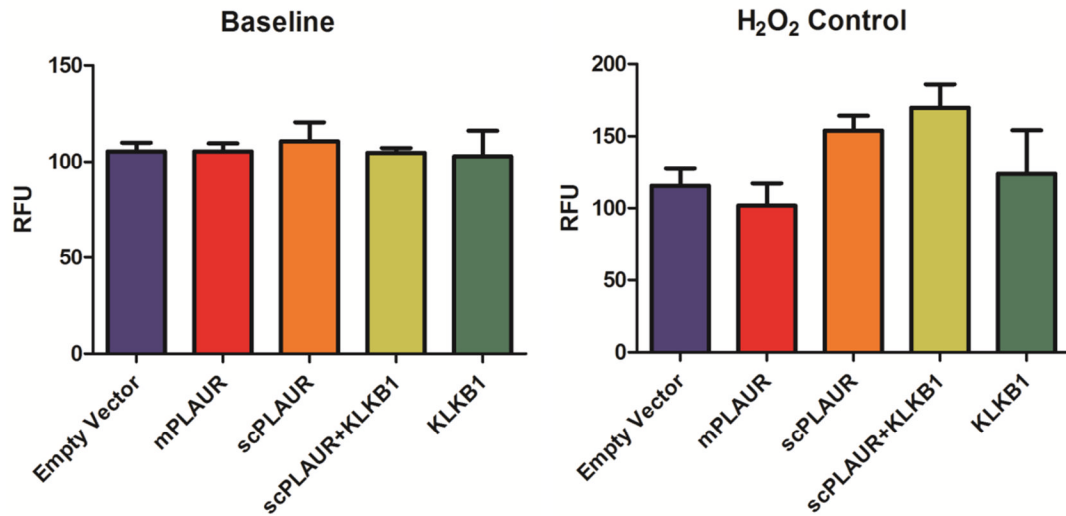
Figure 4.19: Neither mPLAUR or scPLAUR affect the rate of epithelial apoptosis. No change in the rate of apoptosis is discerned in basal NHBECs ($P=0.75$) or in a system were 300μM of H_2O_2 was added to the cell system to stimulate apoptosis ($P=0.07$). A trend identifying a reduction in the rate of apoptosis on over-expression of mPLAUR is apparent in the stimulated cells but this was not statistically different ($P=0.29$) from cells transfected with the empty vector (pcDNA3). The rate of apoptosis in stimulated cells was a 100 fold higher than that of basal cells ($n=4$ carried out in 2 donors).

4.8 DISCUSSION

This chapter has successfully tackled its aims, i.e. i) to identify novel genetic mechanisms determining scPLAUR levels in serum using a genome-wide approach; ii) to identify the mechanism of regulation driven by these novel genetic determinants; and iii) to identify the functional effects of scPLAUR in primary human bronchial epithelial cells. In summary, KLKB1 has been identified as a novel regulator of scPLAUR, cleaving the receptor at D_I and in the vicinity of D_{II} and thereby negating scPLAUR driven effects on bronchial epithelial wound healing and mitochondrial activity (Fig. 4.20).
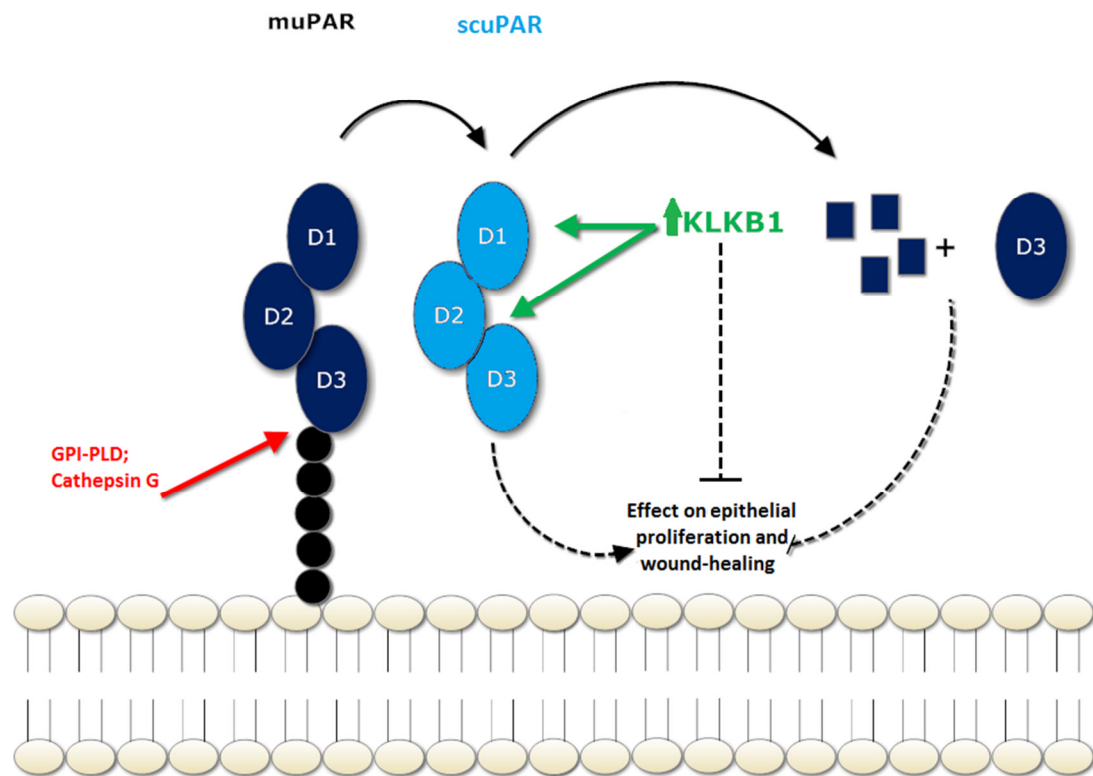
Figure 4.20: The role of KLKB1 in regulating scPLAUR. Membrane bound PLAUR (mPLAUR) is a 3 globular domain (D_I, D_{II} and D_{III}) protein attached to the cell membrane via a GPI anchor. D_I and D_{II} bind to the ligand urokinase while D_{III} is known to interact with cell bound integrins. The GPI anchor is susceptible to both glycolytic and lipolytic cleavage, resulting in the release of a cleaved full-length soluble receptor, soluble cleaved PLAUR, in which all Domains are intact. Proteolytic action carried out by KLKB1, which is elevated in carriers of the rs4253238 T allele, disrupts the receptor's globular domains inhibiting receptor driven effects on bronchial epithelial cell mitochondrial activity (labelled as proliferation) and wound-healing. GPI-PLD: Glycosylphosphatidylinisotol specific phospholipase D; KLKB1: Human plasma kallikrein; mPLAUR: Membrane bound urokinase plasminogen activator receptor; scPLAUR: soluble cleaved urokinase plasminogen activator receptor.

This chapter set out to identify the underlying genetic regulation of elevated scPLAUR in obstructive airway disease identified in Chapter 3 of this thesis, by carrying out two separate GWA studies in asthma and control populations. When analysed separately, no SNP was found to be genome-wide significant in either the populations using a Bonferroni corrected P-value of 1.69×10^{-7}. As this is likely due to the low number of asthmatic (n=480) and control (n=104) subjects used, the number of analysed subjects was increased in a meta-analysis of both populations (n=584). Although this gives the advantage of a larger population increasing the power, combining both populations is not without its limitations. As an association between scPLAUR and asthma has been identified (see Chapter 3) it is possible that the presence of disease may act as a confounder in the analysis. It was in order to increase confidence in the results from the combined dataset that the GWAS results were investigated in an independent dataset (COPD Cohort). Duplication of results in this cohort, where all subjects are matched based on disease phenotype, increases confidence that the associations identified in the combined dataset are due to changes in scPLAUR levels driven by genotype rather than due to disease.

Quantile-Quantile plots identify the likelihood of detecting regulatory loci with deviation of the plotted result from the predicted distribution of P-values occurring for a small number of SNPs. Although only 1 region actually achieved a Bonferroni P-value of 1.69×10^{-7} or smaller, the presence of a larger number of SNPs with effects above the line in the QQ-plots, suggested further regions regulating scPLAUR expression in serum. It is probable that these SNPS did not achieve genome-wide significance due to population size, which remains small for a GWAS and may result in a number of false negative results. Therefore less stringent selection criteria were employed, as used previously (Wan et al., 2011), to capture SNPs that may have failed to achieve genome-wide significance but may however be functionally relevant.

Of the 8 loci identified using the protein based GWAS or secondary criteria, 3 are present in regions associated with candidate genes previously identified with PLAUR or its signalling pathways.

a. Human plasma Kallikrein (*KLKB1*) (Chr:4, rs4253238) and Factor XII (Chr:6, rs2731672) are known to be involved in the plasmin/plasminogen activation cycle (fibrinolytic pathway), which is actively regulated by PLAUR mediated PLAU activation(Crippa, 2007).

b. Neuregulin 1 (*NRG1*) (Chr:5, rs6988339), also known as transcript variant HRG-beta1 (*HRGβ1*) is known to decrease the activity of the PLAUR associated PLAU and MMP 9 (Mazumdar et al., 2001, Puricelli et al., 2002).

The presence of associations in regions associated with candidate genes previously identified with PLAUR or its signalling pathways, further adds confidence to the use of a combined case/control dataset to identify novel regulators for scPLAUR expression.

The remaining identified loci present in chromosomal regions 6q16, 6q25, 4q31.1, 7q33 and 6q25 are in novel regions, having no known association with scPLAUR or its signalling pathways.

Interestingly, failure to replicate associations, especially the rs4253238 association, in the *in silico* mRNA GWAS highlights that a dependence on mRNA levels to identify novel genome wide regulators for gene expression is likely to miss a number of important protein regulatory factors. This was further highlighted when exposure of KLKB1 to NHBECs did not alter PLAUR mRNA levels. As of writing, all published GWA studies have exclusively utilised mRNA levels as an output for gene expression. This identifies that a number of potential gene expression regulators have been missed globally. Although 9 genes had the same directional effect in both the *in silico* and protein GWAS, none fell into our selection criteria and so were not investigated further. However,

presence of the *in silico* associations in the protein GWAS, exhibiting the same directional effect, suggests that although these associations are not significant they may play a role in scPLAUR expression and should be investigated in future work. All of the identified *in silico* regions are in novel regions, having no known association with scPLAUR, however MAPK has been shown to be involved in PLAUR signalling pathways (Baek et al., 2010, Park et al., 2011).

So as to confirm the association of the 8 regions detected by the protein based GWAS and serum scPLAUR levels, an attempt was made to duplicate the results through the genotyping of the 8 selected SNPs in a COPD population. Although SNP rs4253238 was the only successfully replicated SNP, other SNPs were shown to have the same directional effect on scPLAUR levels; namely rs9480227 (chr6:156198945), rs7666900 (chr4:140414333) and rs2731672 (chr5:176842474). This identifies the possibility that failure to reach significance may be due to limited sample numbers, even though the study was powered to detect these variations (see Table 2.16). However, since these SNPs did not replicate, investigations were focussed to the *KLKB1* SNP rs4253238. Interestingly the degree of association between rs4253238 and serum scPLAUR levels was stronger in COPD subjects than in asthmatic and/or controls, which ties in well with deductions made in Chapter 3 of this thesis, where serum scPLAUR was associated to a higher degree with COPD subjects than asthmatics and control subjects.

SNP rs4253238 is a promoter polymorphism for the *KLKB1* gene, a 31kb long gene located on chromosome 4q34-35 that codes for the protein pre-kallikrein (Fink et al., 2007). Pre-kallikrein is cleaved by activated Factor XII, with high molecular weight kininogen as a co-factor, to form the activated protein human plasma kallikrein (KLKB1)(Fink et al., 2007). KLKB1 is a 80kDa serine protease synthesised in the liver that normally circulates in serum at a concentration of 50µg/ml(Lilla et al., 2009), and

is known to participate in the contact activation system of coagulation through the activation of high molecular weight kininogen into bradykinin (Baumgarten et al., 1986, Motta et al., 1998, Schmaier et al., 1999, Rojkjaer and Schmaier, 1999). KLKB1 also activates plasminogen into plasmin *in vitro* at a less efficient rate than that catalysed by either PLAU or tissue plasminogen activator (tPA) (Miles et al., 1983). KLKB1 differs both structurally and catalytically from the large family of tissue kallikreins, which activate both high and low weight kininogen into an alternate form of bradykinin (Lima et al., 2008).

The presence of the rs4253238 minor (T) allele results in the loss of 3 transcription factor binding domains, namely those for:

a) Neurogenic differentiation 1 (NeuroD1), also called β2 transcription factor

b) Binding domain for Kruppel-like C2H2 zinc finger transcription factors

c) Binding domain for the PAR/pZIP family of transcription factors

Haplotype analysis identified that rs4253238 is in strong LD with other SNPs that span the entire *KLKB1* gene, including but not exclusive to SNPs present in the gene exon regions. The rs4253238 SNP has also previously been identified to be in LD with rs3733402, which causes a Arginine to Serine amino acid change at position 124 of the KLKB1 protein, which causes a in the catalytic effect of KLKB1 (Katsuda et al., 2007). This identifies that although an association has been identified between this SNP and scPLAUR expression, it may not be rs4253238 that is the driving force of the association but rather may be a marker for an alternate *KLKB1* SNP that regulates *KLKB1* activity.

An activity assay confirmed that changes in rs4253238 genotype also drove changes in KLKB1 activity with the minor allele associated with a lower level of KLKB1 activity (⇧C:C, ⇩T:T) therefore deducing, as confirmed by correlation analyses, that KLKB1 had an inverse relationship to serum scPLAUR levels. Based on its detection in each cohort,

the relationship between rs4253238 genotype, KLKB1 activity and serum scPLAUR levels was deduced to be a universal relationship regardless of disease state. However, closer inspection of the KLKB1 activity assay data identifies a striking difference in KLKB1 activity between the control and obstructive lung disease populations, suggesting that KLKB1 may, through scPLAUR regulation, play a role in the progression of obstructive lung disease. This is based on the supposition that scPLAUR is a functional molecule that affects cell function and may drive the disease phenotype as has been previously described in FSGS (Wei et al., 2011). The validity of this relationship, identified in an artificial set-up, was confirmed at the protein level using a living *in vitro* system (NHBECs).

Quantitative PCR identified that the mechanism underlying the relationship between KLKB1 activity and serum scPLAUR was independent of changes at the mRNA level of mPLAUR, the progenitor of scPLAUR. This is suggestive of a protein based mechanism of action. First to be investigated was plasmin, a known PLAUR D_I/D_{II} protease (Hoyer-Hansen et al., 1992), based on published data showing an elevation of activated plasmin through modulation of the plasminogen-plasmin pathway by KLKB1. Here, KLKB1 activates PLAU (Ichinose et al., 1986) and plasminogen (Miles et al., 1983), indirectly increasing the overall levels of circulating activated plasmin. However, although elevations in activated plasmin levels were identified on addition of KLKB1 to a NHBEC population, these returned to baseline at 24 hours, an effect not replicated when measuring scPLAUR levels. This suggests that KLKB1 affects scPLAUR levels by an alternate mechanism to that of plasmin activation.

Since KLKB1 has a known proteolytic role, it was hypothesised that KLKB1 affects scPLAUR levels by proteolytically cleaving scPLAUR and so rendering it unable to carry out any of its biological functions. A proteolytic role for KLKB1 ties in well with a previously published investigation into relationships between a different kallikrein,

human tissue kallikrein (hK4) and PLAUR (Beaufort et al., 2006). This study identified that hK4 acts as a proteolytic enzyme on the PLAUR molecule in the D_I-D_{II} linker region and within the carboxyl terminus of D_{III}. However such a proteolytic role for KLKB1 was not a certainty, based on the determination that KLKB1 is non-homologous to any of the other members of the kallikrein family and therefore may not have the same functional roles (Yousef and Diamandis, 2001).

Experimentation carried out in a cell-free based system to remove any influence of the plasminogen-plasmin pathway, identified that exposure to KLKB1 resulted in the loss of PLAUR's D_I epitope as well as loss of full length PLAUR forming a smaller ~30kDa fragment, confirming a plasmin independent proteolytic role for KLKB1. Lack of PLAUR detection by mAB IIIF10 identifies a cleavage site within D_I of the receptor structure while N-terminal sequencing suggests that the KLKB1 mediated cleavage of PLAUR involves a site adjacent to D_{III}. However, the presence of a mismatched allele at position 249 of the rPLAUR protein structure does not allow for confident determination of the D_{III} cleavage site. This is since although this substitution of Glycine to Aspartic Acid at position 249 has been previously described (Zhu, F. X., *et al.* 2000), no SNP has been validated in this region. Also, this sequence does not match the sequence reported by the manufacturing company (R&D Systems), leaving us unable to explain this substitution. Therefore it is likely that KLKB1 regulates PLAUR levels by acting as a proteolytic enzyme on the PLAUR protein, in a plasmin-independent regulatory system. Although detected in the scPLAUR form of the receptor, this regulatory mechanism should be equally valid for the membrane bound receptor, which has the same molecular structure as scPLAUR.

The identification of a novel system of scPLAUR regulation by KLKB1 has important implications for scPLAUR driven disease mechanisms, as regulation of scPLAUR expression may be fundamental to disease progression and development. This

argument is based on scPLAUR association with increased disease mortality rates (Eugen-Olsen et al., 2010b) and recent publications identifying the receptor as having a direct role in the modulation of kidney disease (FSGS) (Wei et al., 2011). Suggestion of the importance of the KLKB1/scPLAUR interaction in disease is hinted at in this chapter by the identification of greater association between rs4253238 and serum scPLAUR in the COPD population and the presence of significantly lower KLKB1 activity in both asthmatics and COPD patients.

Since this thesis set out to investigate PLAUR as a gene/receptor involved in obstructive lung disease, investigations of the role of KLKB1 in disease focussed on scPLAUR driven changes in the lung. Since earlier on (see Section 3.5) it was argued that scPLAUR may modulate disease directly by affecting airway remodelling and mPLAUR has been shown to dyseregulate wound healing through attenuation of repair in NHBECs partly due to the increased scPLAUR shedding (Stewart et al., 2012), it was prudent to identify whether the KLKB1/scPLAUR mechanism effects the rate of migration, proliferation and apoptosis in NHBECs. These outcomes were chosen as dysregulation of epithelial cell turnover (defined by dysregulation of the rates of cellular migration, proliferation and apoptosis) plays an important role in airway remodelling in asthma (Chung, 2005). In this thesis, the MTT assay was used in order to determine the effect of KLKB1/scPLAUR on cellular proliferation. However, one must keep in mind that as previously discussed; results of the MTT assay only indirectly measures cellular proliferation through the measure of cellular respiration (mitochondrial activity). Therefore, while it is likely that changes detected in cellular respiration in this chapter relate to changes in proliferation, a definte link to cellular proliferation cannot be concluded.

Scratch-wound assay results confirm and extend previous suggestions that scPLAUR is the active molecule driving mPLAUR attenuation of epithelial cell migration (Stewart et

al., 2012). In addition scPLAUR increased the rate of NHBEC cellular respiration independently of mPLAUR, lending weight to the argument, stemming from results in Chapter 3, that scPLAUR modulates obstructive airway disease through airway remodelling on over-expression by causing an alteration in normal bronchial epithelial repair and through a possible modulation of cellular proliferation. Complete loss of the effects caused by scPLAUR on addition of KLKB1 further consolidates the conclusion that KLKB1 plays an important role through the regulation of scPLAUR. Therefore it can be hypothesised that a loss of active KLKB1 in obstructive respiratory diseases (asthma and COPD) results in a build-up of active scPLAUR, which in turn modulates changes in the airway by causing a possible increase in epithelial proliferation, while simultaneously inhibiting epithelial cell migration.

In summary, in this chapter, a GWAS study identified genetic determinants (rs4253238) of serum scPLAUR. Importantly, this finding was also observed in an independent population of COPD subjects with a meta-analysis including the control, asthma and COPD populations further confirming the association and identifying a more pronounced effect in COPD subjects than in asthmatics or controls (B=0.09129). The rs4253238 associated protein KLKB1 regulates scPLAUR levels through proteolytic cleavage at the protein's D_I and D_{III} regions, which prevents scPLAUR binding to either PLAU (Blasi and Carmeliet, 2002) or other membrane bound integrins (Wilcox-Adelman et al., 2000, Wei et al., 2007). This renders scPLAUR inactive to its known processes (Fig. 4.17 & Fig. 4.18). It must be noted however, that this process may not be unique to scPLAUR as mPLAUR possesses an identical protein structure. Although common to the general population, KLKB1 mediated regulation of PLAUR may play a role in scPLAUR associated disease, where loss of scPLAUR interaction with membrane bound integrins and its role in sequestering freely circulating PLAU will have an effect in the modulation of associated diseases such as asthma and FSGS. Indeed, this chapter confirmed that KLKB1 regulation of PLAUR is able to prevent

scPLAUR mediated changes in bronchial epithelial cells, which may prevent changes in the airway epithelium such as dysregulation in the process of wound repair and cellular proliferation, which would have an effect on the process of airway remodelling. SNP rs4253238 has a minor allele frequency (MAF) of 0.32 in a Caucasian population, which identifies that the SNP is a relatively prevalent one in a general Caucasian population, making it a potentially widespread regulator of scPLAUR with implications for scPLAUR driven disease.

CHAPTER 5:

DEFINING MOLECULAR MECHANISMS DETERMINING PLAUR MRNA EXPRESSION

CHAPTER 5: DEFINING MOLECULAR MECHANISMS DETERMINING PLAUR MRNA EXPRESSION

5.1 INTRODUCTION

As previously discussed in Chapter 1, different forms of PLAUR exist. These different forms exist via either receptor cleavage or through the presence of different gene splicing. The most common of these and the ones tackled by this thesis are the membrane bound PLAUR (mPLAUR), the soluble cleaved PLAUR (scPLAUR) and the soluble spliced PLAUR (ssPLAUR), which arises from a splice form of the *PLAUR* gene that results in an alternate terminal exon and the lack of a GPI anchor (Pyke et al., 1993, Stewart and Sayers, 2009). A number of recent investigations have suggested that changes in the level of *PLAUR* expression are important in obstructive lung disease. Increases in the expression of total PLAUR were identified in the epithelium of asthmatics (Stewart et al., 2012) and COPD patients (Wang et al., 2008) when compared to non-diseased controls. *In vitro* increases in the level of expressed PLAUR were associated with a reduction in the rate of epithelial cell migration and therefore attenuation of wound repair in bronchial epithelial cells, as well as being up-regulated at the epithelial wound edge (Stewart et al., 2012). This highlights that PLAUR has a probable role in the modulation of tissue remodelling within the airways, through the dysregulation of epithelial migration and wound repair, important constituents of airway remodelling. Furthermore, results discussed in Chapter 3 of this thesis identify an association between scPLAUR (and by its association mPLAUR) and the obstructive lung diseases asthma and COPD, as well an association with the degree of reversibility of fixed airway obstruction in never smokers.

The specific association between scPLAUR and reversibility of fixed airway obstruction in smokers highlights a probable relationship between exposure to cigarette smoke and the role of PLAUR in obstructive lung disease. This hypothesis is further supported by the high degree of correlation between serum levels of scPLAUR and smoking pack/year history identified in Chapter 3 as well as the association defined in literature and in Chapter 3 of this thesis between PLAUR and COPD, a disease whose main causative factor is exposure to cigarette smoke. Therefore, considering the increased expression of PLAUR in obstructive lung disease, its association with cigarette smoke and its role in modulating the rate of wound repair, regulation of the rate of gene expression both basally and under stimulation of wound repair and cigarette smoke, with focus within the airway epithelium, could be an important determining factor for the role of PLAUR in the regulation of cell functional effects.

Although a genome-wide regulator for scPLAUR has been identified (see Chapter 4), the potential genetic regulatory elements within the PLAUR gene itself have not yet been defined in bronchial epithelial cells, the key functional cell type identified in previous work (Stewart et al., 2012, Stewart and Sayers, 2009). Initial genetic based investigations have however identified the 5`UTR/promoter and 3` distal regions as potential important regulatory regions for PLAUR. Colleagues within the same group have determined that SNPs within the 5`UTR/promoter, which is identical for both mPLAUR and ssPLAUR, regulate serum scPLAUR levels as well as asthma risk, the rate of FEV_1 decline in asthma, changes in baseline lung function and protection in COPD (Barton et al., 2009, Stewart et al., 2009). SNPs within the 2 distinct 3 prime distal regions, that give rise to the 2 different terminal exons for the 2 PLAUR isoforms (mPLAUR and ssPLAUR), were also associated with an increased risk in asthma as well as the rate of FEV_1 decline in asthma (Stewart et al., 2009).

Literature on *PLAUR* 5`UTR driven transcription has generally been limited to the discovery and further understanding of the minimal basal gene promoter. Investigations in colon cancer and U937 lymphoma cells have identified that the minimal *PLAUR* promoter lies within the first 200bp of the TSS (Wang et al., 1994, Soravia et al., 1995) and that while this minimal promoter lacks both TATA and CAAT boxes, it contains a GC-rich proximal sequence that contains multiple Sp-1 consensus elements that regulate basal gene expression (Soravia et al., 1995). This 200bp minimal promoter was also found to contain a number of transcriptional elements including but not limited to AP-1, c-Jun, c-Fos and Fra-1, which contributed to *PLAUR* transcriptional regulation (Okan et al., 2001). Investigations into other regulatory areas outside the minimal promoter region have been minimal. A region between 398 and 197 base pairs upstream of the TSS was identified to be essential for *PLAUR* gene silencing occurring through the β_3 integrin in conjunction with the PEA3 motif at 248bp (Laufs et al., 2006), while a study in transgenic mice has identified that the 1.5kb region upstream of the TSS to be required for optimal expression, with a region spanning between 1295 and 1192 base pairs upstream of the TSS proposed as a novel regulatory region (Wang et al., 2003).

Investigations into *PLAUR* post-transcriptional regulation by the gene's 3`UTR have also been limited to a few studies to the 3`UTR of the membrane bound receptor. However, these studies highlight that the 3`UTR has an important role in *PLAUR* regulation through stabilisation and destabilisation functions. PMA, TGFβ1 and hnRNPC have been defined as stabilisers of PLAUR mRNA (Lund et al., 1995, Shetty et al., 2005), while a cis-acting AU-rich region present in the 3`UTR of the gene (Wang et al., 1998) was defined as an important 3`UTR regulatory region for mRNA stability. A destabilising agent for *PLAUR* mRNA (p53) was also discovered (Shetty et al., 2007a).

Therefore, there remains scope for further investigation into *PLAUR* regulation, not only to understand gene regulation in bronchial epithelial cells (the key functional cell type identified in previous work (Stewart et al., 2012, Stewart and Sayers, 2009)) but also to better understand general regulation of this disease important receptor. Specifically it is important to understand how the extended 5 prime distal region, which contains disease associated polymorphisms (see above), affects gene transcription and how 3`UTR regulation of the soluble spliced receptor, which has not yet been investigated, differs from that of the membrane bound receptor. How *PLAUR* transcriptional regulation alters under conditions known to affect PLAUR expression, i.e. smoking and scratch-wounding, will help further our understanding of the driving force behind the changes in receptor expression (including the as yet uninvestigated ssPLAUR). This may highlight potential targets for future manipulation of receptor expression such as micro RNAs, regulators that bind to complementary sequences on 3`UTR transcripts resulting in translational repression or target degradation and gene silencing (Bartel, 2009, Kusenda et al., 2006).

In this chapter, the regulatory potential of the immediate 3`UTR and 5`UTR was investigated using *in silico* identification of regions with high inter-species homology and ergo a high potential for gene regulation and *in silico* prediction of the regions potential gene regulatory elements. These gene regulatory elements were specific to the region investigated, with transcription factors affecting the 5` region and micro RNAs (miRNAs) affecting the 3` region. Transcription factors promote or inhibit the recruitment of the RNA polymerase enzyme to the 5`UTR/promoter regulating the levels of gene transcription to mRNA. Micro RNAs on the other hand are short ($\sim$22 nucleotides) RNAs that bind to and act on mRNA transcripts that regulate gene expression through translational repression, mRNA degradation, gene silencing or a degree of each.

These investigations were then followed by experimental investigations into the role of the untranslated regions in regulating PLAUR expression in bronchial epithelial cells. This built upon previous investigations which identified the minimal *PLAUR* promoter within the first 200 base pairs from the ATG in a number of oncogenic cell lines (Dang et al., 1999, Soravia et al., 1995). To this aim transcriptional regulation by the 5`UTR and 3`UTR was investigated under basal conditions and under stimulation by cigarette smoke extract and scratch-wounding, based on the relationship between PLAUR and cigarette smoke previously identified in this thesis (see Chapter 3) and the previously identified role of mPLAUR and scPLAUR on the rate of scratch-wound repair (see Chapter 4) (Stewart et al., 2012).

5.2 AIMS

1. To investigate the potential regulatory motifs and regions of the *PLAUR* gene's 3` distal region and 5`UTR *in silico*.

2. To determine the relative contribution of the immediate *PLAUR* 5`UTR in transcriptional regulation of the gene.

3. To determine the role of the *PLAUR* 3`UTR in the regulation of *PLAUR* isoform specific expression.

4. To determine the contribution of core *PLAUR* 5`UTR and 3` distal regions to cigarette smoke extract and scratch wound induction of *PLAUR*.

5.3 METHODS - BIOINFORMATICS

5.3.1 IN SILICO PREDICTION OF INTER-SPECIES VARIATION

The use of inter-species homology reports allows for the identification of conserved regions across different species. A high degree of conservation across different species identifies that that region has been conserved through evolution and therefore has a higher probability of containing gene regulatory elements. The further down the evolutionary tree that the conservation is maintained, the higher the probability that gene regulatory elements are present. Inter-species homology reports were set-up using the following databases:

a) VISualization Tools for Alignments, using the Human February 2009 build of the Human genome - http://genome.lbl.gov/vista/index.shtml (Mayor et al., 2000).

b) USCS Genome Browser, using the Human February 2009 build of the human genome - http://genome.ucsc.edu/cgi-bin/hgGateway (Kent et al., 2002).

Analyses were carried out with respect to the genetic sequence in higher Primates (Orang-utan, Chimp, Rhesus Monkey and Gorilla) and Mouse by selected their respective boxes in each software package. The region of interest, encompassing the *PLAUR* gene its 5`UTR and 3` distal regions (chr19:44,145,247-44,179,498 of the February 2009 gene build) were placed into the gene region box and the select button was pressed in order to analyse the region.

In order to determine whether the gene inter-species also occurs at the amino acid level the human (Q03405) protein was aligned with the Mouse (P35456), Rat (P49616) and Chimpanzee (Q9GK80) protein at http://www.uniprot.org/align.

5.3.2 IN SILICO PREDICITION OF 5`UTR TRANSCRIPTION FACTORS

Transcription factors (TF) are proteins which bind to complimentary DNA sequences either alone or in a complex. Through binding, transcription factors control gene transcription by activating or repressing the recruitment of RNA polymerase (Latchman, 1997, Nikolov and Burley, 1997, Lee and Young, 2000). Therefore in order to fully understand the 5`UTR and promoter driven transcription of the gene it is important to identify putative transcription factor binding motifs for this region.

As investigations were carried out *in silico,* TF calls are prone to database dependant errors. Therefore, TFs were only selected if they were present in at least two of the databases used to carry out TF calling.

The sequence up to 2584bp upstream of the *PLAUR* TSS (NC_000019.9: c44184671-44174298) which corresponds to the region investigated later on in this chapter, was analysed as a FASTA sequence, in 3 separate transcription factor databases:

a) MatInspector TF Mining tool – available at: www.genomatix.de (Cartharius et al., 2005).

b) Transcription Element Search System (TESS) – available at: www.cbil.upenn.edu/cgi-bin/tess/tess (Schug, 2008).

c) PROMO - available at: http://alggen.lsi.upc.es/cgi-bin/promo_v3/promo/promoinit.cgi?dirDB=TF_8.3 (Messeguer et al., 2002).

Analyses were done exclusively for human transcription factors. Data were transferred to a Microsoft Excel spread sheet and common transcription factors were identified.

5.3.3 IN SILICO PREDICITION OF POTENTIAL 3`UTR EFFECT MODIFYING miRNAS

In order to identify possible miRNA binding sites the online database http://www.microrna.org/microrna/home.do (Betel et al., 2008) containing a 16228619 predicted microRNA target sites in 34911 distinct 3'UTR from isoforms of 19898 human genes, was used. Target predictions are based on a development of the miRanda algorithm, incorporating miRNA target rules and a compendium of mammalian microRNAs and scored for likelihood of mRNA down-regulation using mirSVR, a regression model that is trained on sequence and contextual features of the predicted miRNA-mRNA duplex.

Under the target mRNA tab, the PLAUR gene was entered into the target mRNA field and *Homo sapiens* selected from the species drop down menu. By selecting the go button links to the alignment details of both *PLAUR* 3`UTRs, originating from the gene's alternate terminal exon and coding for mPLAUR or ssPLAUR, were made available. Calling of miRNAs was done by selecting miRNAs with good miRSRV values from the drop down menu of the display options bar.

5.4 METHODS – MOLECULAR BIOLOGY

5.4.1 DETERMINING CHANGES IN *PLAUR* MRNA EXPRESSION

Quantitative PCR (qPCR) was used to determine changes in *PLAUR* mRNA expression levels. NHBECs in culture were collected by mechanical scraping and total cellular RNA was extracted using the Qiagen RNeasy Kit as described in Section 2.2.10. and used to form complimentary DNA (cDNA) as outlined in Section 2.2.11. The resulting cDNA, diluted to 1:10, was used in qPCR analysis as outlined in Section 2.2.12, using the HPRT gene targeting Pre-Developed TaqMan Assay Reagent (PDAR) as the housekeeping gene and the primers and probes for total or specific forms of *PLAUR* as described in Tables 2.9 and 2.10 (see Section 2.2.12). All primers and probes were designed and validated by Dr Ceri Stewart (University of Nottingham). Analyses were carried out using the MxPro software and Microsoft Excel. Further details and cycling parameters are available in Section 2.2.12.

When correcting stimulated mRNA expression across donors, data were normalised to a 100% with respect to the mRNA values expressed by the cells at baseline.

5.4.2 CONSTRUCTION OF A PLASMID LIBRARY FOR 5`UTR AND 3`UTR TRANSCRIPTIONAL ACTIVITY STUDIES.

5.4.2.1 IDENTIFICATION OF A SUBJECT CARRYING PLAUR SNP COMMON ALLELES WHOSE DNA WILL BE USED AS A CONSTRUCT TEMPLATE

DNA from a number of asthmatics from the Nottingham asthma cohort (*n*=37) was considered as a template to construct the plasmid vectors. The genotype of 17 5`UTR SNPS (reported (Stewart et al., 2009)and unreported), for each of these samples were placed in Excel 2010$^{®}$ and colour coded according to overall genotype. The DNA from the individual (A073) containing the most common haplotype was selected as a template for promoter constructs.

5.4.2.2 GENERATION OF 5`UTR AND 3`UTR CONSTRUCTS FOR USE IN TRANSCRIPTIONAL ACTIVITY STUDIES.

General methods used in plasmid construction through molecular cloning can be found in Sections 2.2.4, 2.2.8 & 2.2.9. The steps involved in the construct of this particular plasmid library are outlined in Fig. 5.1. Where relevant, the concentration and purity of PCR products and plasmid DNA were measured using a NanoDrop Technologies NanoDrop® ND-1000 Spectrophotometer, as outlined in Section 2.2.10. Additional details specific to the construct of plasmids used in this chapter are provided below.
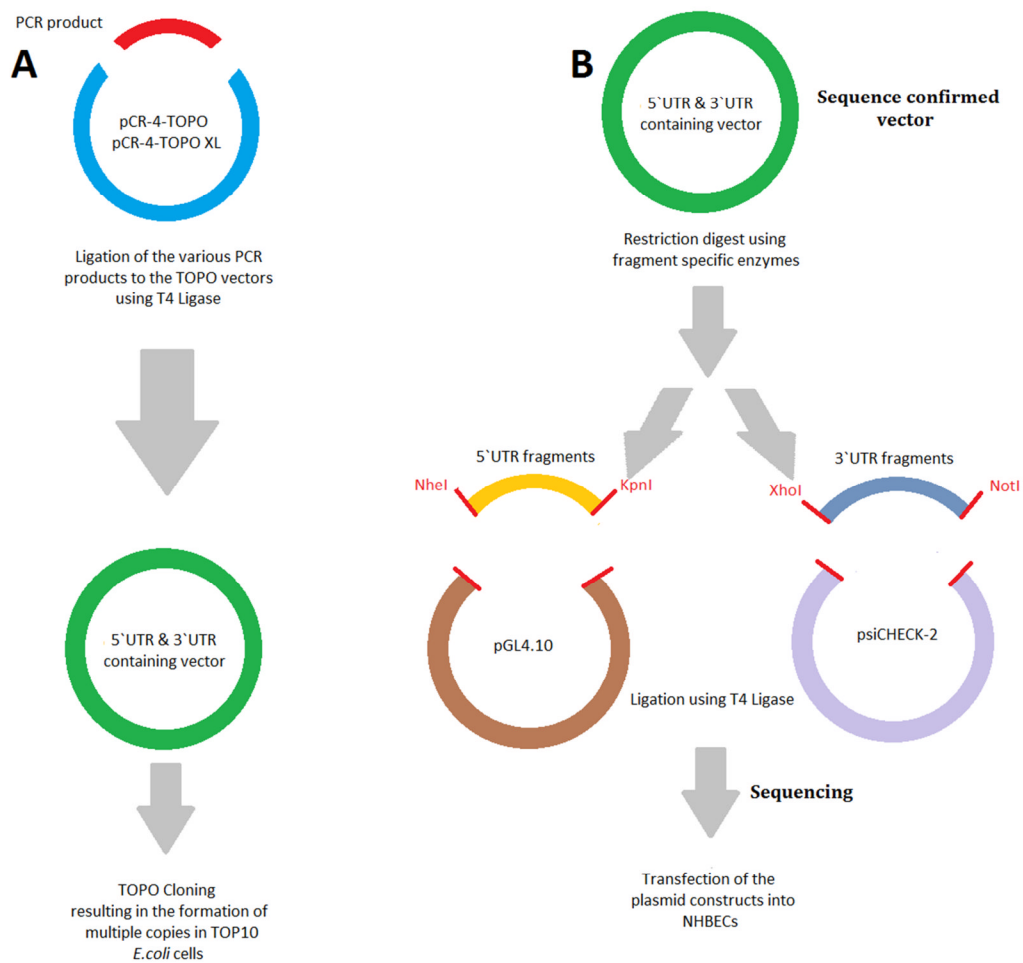
Figure 5.1: Process of plasmid construction. PCR constructs (5`UTR and 3`UTR) were ligated to the pCR®4-TOPOXL®/pCR®4-TOPO® vector (A). Following bulking up in Top10 *E.coli* cells inserts were removed via restriction digest and ligated into the pGL4.10 (5`UTR) and psiCHECK-2 (3`UTR) vectors (B).

In brief, constructs of increasing length from the *PLAUR* TSS (Fig. 5.2) and relating to the two 3`UTR isoforms (mPLAUR and ssPLAUR) were created using PCR (see Section 2.2.1) using the primers outlined in Table 5.1.
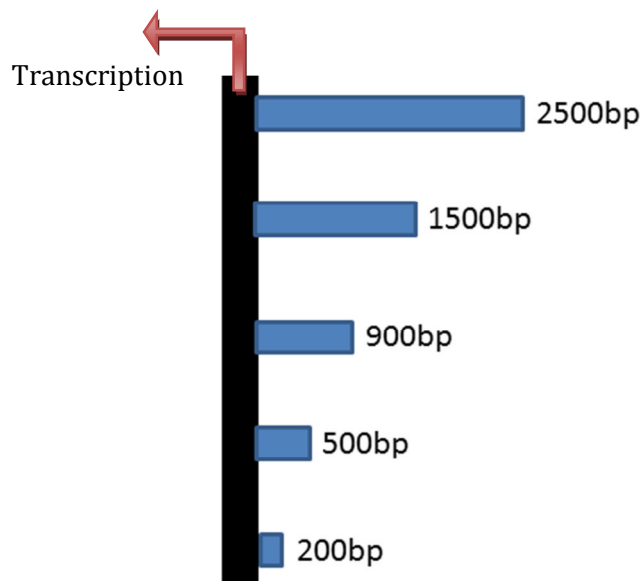
Figure 5.2: *PLAUR* 5`UTR fragments cloned into the luciferase expressing vectors. All fragments originate from the gene's transcriptional start site and so should drive *PLAUR* transcription.

Variant	Product Length	Primer Pair	
5`UTR	Forward	CTGAGCTAGCGGGTCCCTGCAGTCTT	
(200)	199	CTGAGGTACCCGAGCCAGCCCCTTCAC	
(500)	490	CTGAGGTACCGAAGCAAAGCAAGGGTTAAGT	
(900)	887	CTGAGGTACCTCCCACCTAAGCATACAGCC	
(1500)	1484	CTGAGGTACCCCCACAGAAAAGGAGACAGAATGGCA	
(2500)	2584	CTGAGGTACCCAGGCATGCATGAGAATC	
3`UTR (Exon 7a)	Forward	ATAGTCGAGACCTGAAATCCCCCTCTCT	
	419bp	ATAGCGGCCGCGCAGGGGCCTCAAACATGACCC	
3`UTR (Exon 7b)	Forward	ATAGTCGAGAGAGCCCCAGATGTTTCAGCCA	
	314bp	ATAGCGGCCGCGAGGTCTCACTGTGTTGCCCAGG	

Table 5.1: Primers used for the construction of plasmid vectors used in this chapter. Restriction enzyme sites were introduced to the primers (red characters; 5`UTR FWD: Nhe1; 5`UTR REV: Kpn1; 3`UTR FWD: Xho1; 3`UTR REV: Not1). 4 nonsense base pairs were added to the end to prevent loss of required sequence through cloning. Primers for fragments larger than 2586bp are for reference only as their resulting product failed to form a usable vector construct. **FWD**=Forward Primers; **REV**=Reverse Primers.

The gel-purified PCR constructs were then inserted into the Invitrogen vector pCR®4-TOPO XL® (1.5bp and 2.5kp constructs)/pCR®4TOPO® (200bp – 900bp constructs) for sequence verification (see Section 2.2.4 for details), generating the required pCR®4-TOPOXL®/pCR®4-TOPO® constructs (Figure 5.1A). The required sequence was then extracted by restriction digestion and inserted into either the pGL4.10 (5`UTR) or psiCHECK2 (3`UTR) vector (Fig.5.3), so as to produce the respective luciferase expressing constructs (Fig.5.1B). Presence of the correct sequence/insert was confirmed by dideoxynucleotide triphosphate chain terminator sequencing (see Section 2.2.7). Multiple attempts to construct an Isoform 2 psiCHECK-2 construct were unsuccessful and therefore a commercial firefly luciferase expression vector (PLAUR 3UTR_01) was purchased (PLAUR 3UTR_01).

A   **B**
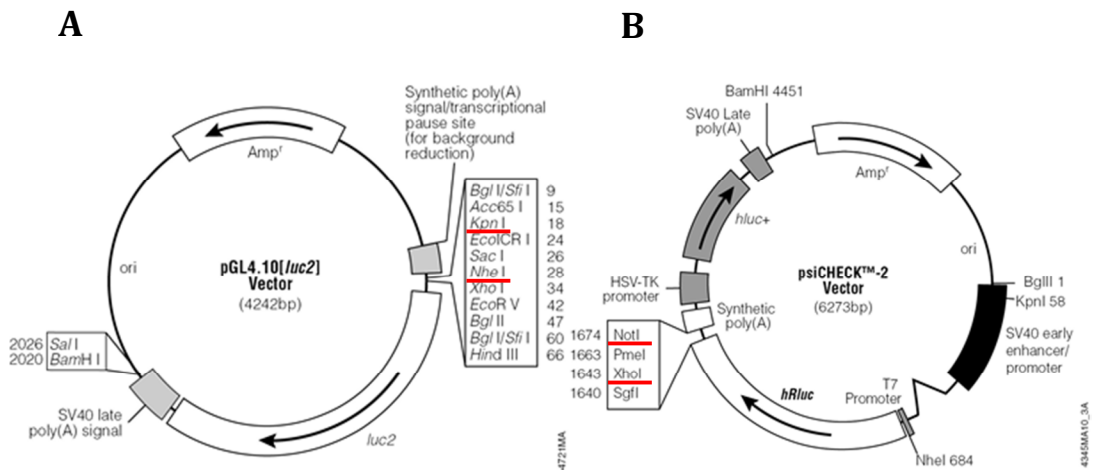
Figure 5.3: Plasmid vector backbones used in this chapter. The pGL4.10 vector is used for 5`UTR promoter studies, with 5`UTR constructs driving the expression of Firefly Luciferase. The psiCHECK-2 vector is used for 3`UTR analyses, where the influence of 3`UTR constructs on *Renilla* Luciferase expression driven by the T7 promoter was investigated. Firefly luciferase is transiently expressed by the psiCHECK-2 vector and acts as a transfection control. Restriction enzymes used in each vector are highlighted in red.

5.5 METHODS – CELL BASED

5.5.1 CULTURING OF BRONCHIAL EPITHELIAL CELLS AND FIBROBLASTS

For the purpose of this chapter the bronchial epithelial cell line Beas2BR1, the fibroblast cell line MRC-5 and primary normal human bronchial epithelial cells (Donors 7F3158 and 7F3206) were cultured. For a detailed description of the culturing procedures see Sections 2.4.1 & 2.4.2.

5.5.2 TRANSIENT TRANSFECTION OF PLASMID CONSTRUCTS

Plasmids were transfected into NHBECs using the FuGENE® 6 transfection reagent as described in Section 2.4.5. In this chapter a transfection ratio of FuGENE® 6 to DNA of 3:2 was used. Vectors expressing only Firefly Luciferase (pGL4.10; PLAUR 3UTR_01) were co-transfected with the *Renilla* Luciferase expressing control vector pRL-TK at a ratio of Firefly:*Renilla* of 1:5. The SV40 promoter driven pGL4 vector pGL4.13, was also transfected as a positive control in each experiment. For a detailed description of the transfection procedure refer to Section 2.4.5.

5.5.3 IMMUNOFLUORESCENCE

Methods detailed below deal with this specific chapter, for a detailed description of the immunofluorescence technique refer to Section 2.5.4.

5.5.3.1 CONFIRMATION OF THE EPITHELIAL CELL PHENOTYPE

In order to confirm the phenotype of the commercially obtained (Lonza) NHBECs used in this chapter, cell populations from donors 7F3158 and 7F3206 were cultured in 4 well chamber well slides and stained both for epithelial cell markers as well as

contamination by fibroblasts. A control fibroblast cell line (Normal Human Foetal Lung Fibroblast: MRC-5) was also stained for the same proteins in parallel. To this aim the following primary antibodies were used:

a) Mouse Anti-Cytokeratin 14 IgG monoclonal Antibody (Millipore MAB3232)

b) Mouse Fibroblast Surface Protein IgM monoclonal Antibody 1B10 (Abcam AB11333)

Anti-cytokeratin 14 (CK-14) was used based on the knowledge that cytokeratins are proteins of keratin-containing intermediate filaments found in the intracytoplasmic cytoskeleton of epithelial tissue, specific to basal epithelial cells, which has previously been used before to identify NHBECs (Wetzels et al., 1992). Anti-1B10 was used to determine whether any fibroblast contamination was present in any of the NHBEC populations.

Fluorescence was driven by the use of the following secondary antibody visualised on the Improvision spinning disk confocal microscope:

a) Fluorescein isothiocyanate (FITC) anti-mouse monoclonal secondary antibody (Sigma F0257) visualised using green filters.

While the following isotype controls were used as controls:

a) Mouse IgG1 from MOPC-21 isotype control (Sigma M7894).

b) Mouse IgM from MM-30 isotype control (Abcam AB18400).

Primary antibodies originating from different species were mixed together to allow for dual staining of the population, while controls were set for the non-specificity of secondary antibodies, all isotypes and cell auto fluorescence, using a layout as outlined in Fig. 5.4A&B.

A

Chamber Well Slide A			

CK-14 + CC26	CK-14 + 1B10	TRITC 2º Cont.	FITC 2º Control
1:200 + 1:500	1:200 + 1:500	1:100	1:100

B

Chamber Well Slide B			

Cells Only	Mouse IgM Iso	Mouse IgG Iso	Rabbit IgG Iso
	1:2500	1:1250	1:1 *(Pre-dilute Add Neat)*

Figure 5.4: Layout of the 8-well chamber slide used to confirm the epithelial cell phenotype by immunofluorescence. This layout includes secondary (2º) antibody controls, isotype controls as well as a 'cells only' well to identify autofluoresence. This layout was replicated for both NHBEC donors and the MRC-5 population.

5.5.3.2 IDENTIFYING CELLULAR TRANSFECTION EFFICIENCY

In order to determine the rate of transfection of DNA into Beas2BR1 cells and NHBECs, immunostaining was carried out on cells cultured in 4 well chamber well slides and transiently transfected with either the pGL4.10+500bp truncation, pisCHECK-2+Isoform 1 or the commercial PLAUR 3UTR_01. Cells were stained with the pAb anti-firefly luciferase antibody (Abcam AB21176) with secondary staining carried out using the Goat anti Rabbit IgG Rhodamine TRITC (Stratech 111-025-0003) with Rabbit polyclonal IgG (Abcam AB27472) used as the isotype control. Total number of cells and number of stained cells were counted in five fields of a Neubauer Haemocytometer. Transfection efficiency was calculated by dividing total number of fluorescent cells by total number of cells.

5.5.4 DUAL LUCIFERASE ASSAY

Dual Luciferase assays (DL) (Promega UK - E1960) make use of plasmid vectors that express Firefly or/and *Renilla* luciferase to infer the role of 5` or 3` untranslated region determined effects on gene expression. As Firefly and *Renilla* luciferase proteins are not expressed by mammalian cells, it is possible to specifically determine the effect of the fragment of interest on gene expression independently of baseline cell expression by measuring luciferase activity. Corrections for differences in cell density and transfection efficiency are tackled by measuring and normalising to alternate luciferase gene expression driven by an independent promoter. In this thesis, the Firefly luciferase expressing pGL4 vector constructs and the commercial Isoform 2 vector were normalised using the *Renilla* expressing pRL-TK vector (Fig. 5.5). In the psiCHECK™-2 vector, *Renilla* luciferase levels were normalised using HSV-TK promoter driven Firefly luciferase expressed by the same plasmid vector (Fig. 5.3B).
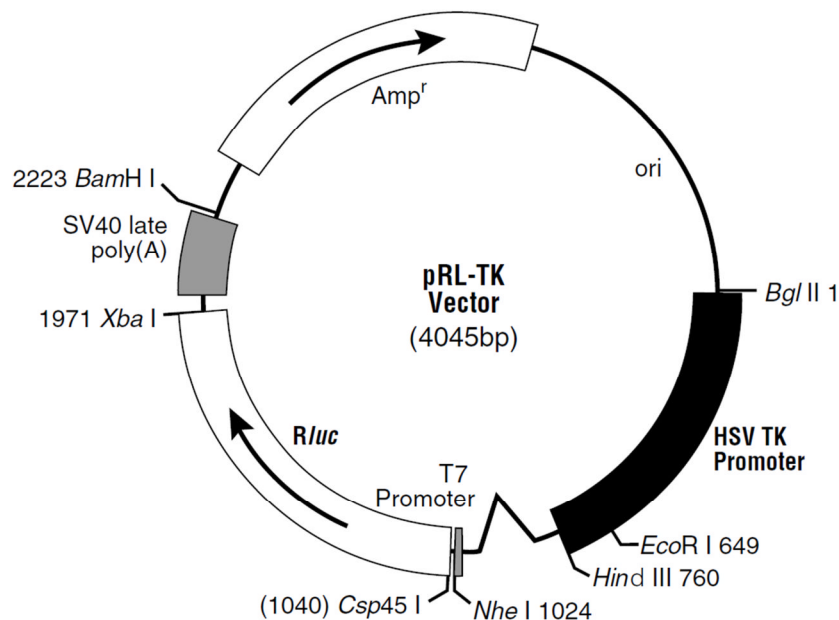
Figure 5.5: The pRL-TK vector. This vector was used as the control vector for the pGL4 and PLAUR 3UTR_01vectors through its expression of *Renilla* luciferase driven by the HSV TK promoter. This control vector was chosen as it had a different promoter to the positive control vector and therefore would have minimal interaction in the control plates.

Briefly, at 24 hours post transfection, the DLR assay was carried out as follows:

1. Cells were lysed by the addition of 1X Passive Lysis Buffer (96 well plate: 20µl per well; 48 well plate: 65µl per well) and freezing overnight at -80°C.

2. 20µl of the lysate was added to a black 96-well plate.

3. To measure Firefly Luciferase activity, 75µl of Luciferase Assay Reagent (LAR; Luciferase Assay Substrate + Luciferase Assay Buffer II) was added to each well

4. Luminescence was read for 10 seconds following a 2 second delay.

5. To measure *Renilla* Luciferase activity, 75µl of Stop and Glo® were then added to the same wells and luminescence read again for 10 seconds following a 2 second delay.

All readings were taken using a Luminoskan Ascent Microplate Luminometer. Data were then corrected to the pRL-TK *Renilla* readings (pGL4.10; PLAUR 3UTR_01) or Firefly readings (psiCHECK™-2) so as to normalise for variation in transfection efficiency and differences in cell number using the following equation:

$$x = Gene\ Regulated\ Luciferase\ \div Control\ Luciferase$$

Expression values were not normalised to the empty pGL4.10 vector (internal control) as transfection of the internal control into Beas2BR1 and NHBECs resulted in negligible luciferase activity values (~0.1-0.2) when compared to those expressed by the experimental constructs. Therefore correcting the large experimental value to the minute control value resulted in artificially variable results. Successful transient transfection was confirmed in each experiment by the internal positive control pGL4.13 (pGL4- SV40).

5.5.5 SCRATCH-WOUND ASSAY

In order to identify the role of mechanical injury on modifying PLAUR expression through 5`UTR and 3`UTR mechanisms, NHBECs were wounded with 4 wounds in a cross-hatch pattern (Fig. 5.6) 16 hours post-transfection in bronchial epithelial wounding media (BEWM) (see Section 2.5.1). Changes in gene expression were investigated using a Dual Luciferase assay at 8 and 24 hours post-wounding (Section 5.5.4).

In order to investigate the role of ssPLAUR on the rate of scratch wound healing, NHBECs recombinantly over-expressing mPLAUR and ssPLAUR were investigated using the scratch wound assay as outlined in Section 2.5.1.
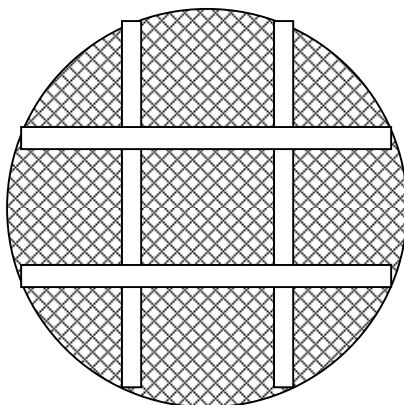
Figure 5.6: Example of a well layout used in the DLR scratch wound assay. Wounds were formed using a sterile P200 tip on a confluent well of a 6 well plate in a cross hatch pattern.

5.5.6 IDENTIFYING HOW EXPOSURE TO CIGARETTE SMOKE EXTRACT EFFECTS 5`UTR AND 3`UTR DRIVEN CHANGES IN PLAUR EXPRESSION

In order to identify the role of cigarette smoke extract on modifying PLAUR expression through 5`UTR and 3`UTR regulation, NHBECs were treated with freshly made 5% v/v Cigarette Smoke Extract (CSE) (see Section 2.4.6) at 24 hours post transfection. BEBM was used for the control wells. Changes in gene expression were investigated using a Dual Luciferase assay at 8 and 24 hours post-wounding (see Section 5.5.4).

5.5.7 WESTERN BLOTTING

In this chapter, western blotting was utilised to confirm qPCR results on changes in *PLAUR* mRNA expression on the addition of 5% v/v CSE to NHBECs. Following culture, protein was harvested by mechanical scraping (see Section 2.3.2.1) and protein levels of total, soluble spliced and membrane PLAUR were determined using the mAB IIIF10 (0.25µg/ml) and normalised using anti β-actin (0.1µg/ml) (see Section 2.3.2.3).

5.5.8 MTT ASSAY

In order to identify a role for ssPLAUR in NHBECs, the effect of ssPLAUR on the rate of epithelial proliferation was investigated through the determination of the rate of cellular respiration. NHBECs, recombinantly over-expressing ssPLAUR and mPLAUR were allowed to reach 50% confluence before the rate of cellular respiration was investigated using the MTT assay as described in Section 2.5.2. Data from the MTT assay was normalised to the rate of cells transfected with the empty vector (pcDNA3) in order to remove donor dependant variation.

5.5.9 APO-ONE® HOMOGENEOUS CASPASE-3/7 ASSAY

In order to further identify a role for ssPLAUR in NHBECs, the effect of ssPLAUR on the rate of epithelial apoptosis was investigated. NHBECs recombinantly over-expressing ssPLAUR and mPLAUR were investigated using an Apo-ONE® Homogeneous Caspase-3/7 Assay as described in Section 2.5.3. Data from the apoptosis assay was normalised to the rate of apoptosis in cells transfected with just the empty vector (pcDNA3) in order to remove donor dependant variation.

5.6 RESULTS - BIOINFORMATICS

5.6.1 GENERATING *PLAUR* 5`UTR AND 3`UTR FRAGMENTS BY PCR

In order to form the required fragments for plasmid construction (see Section 5.4.2) a series of PCRs were carried out using genomic DNA from subject A073. PCR successfully generated fragments up to 2584bp upstream of the gene's TSS and form both 3`UTR isoforms (Fig. 5.7).
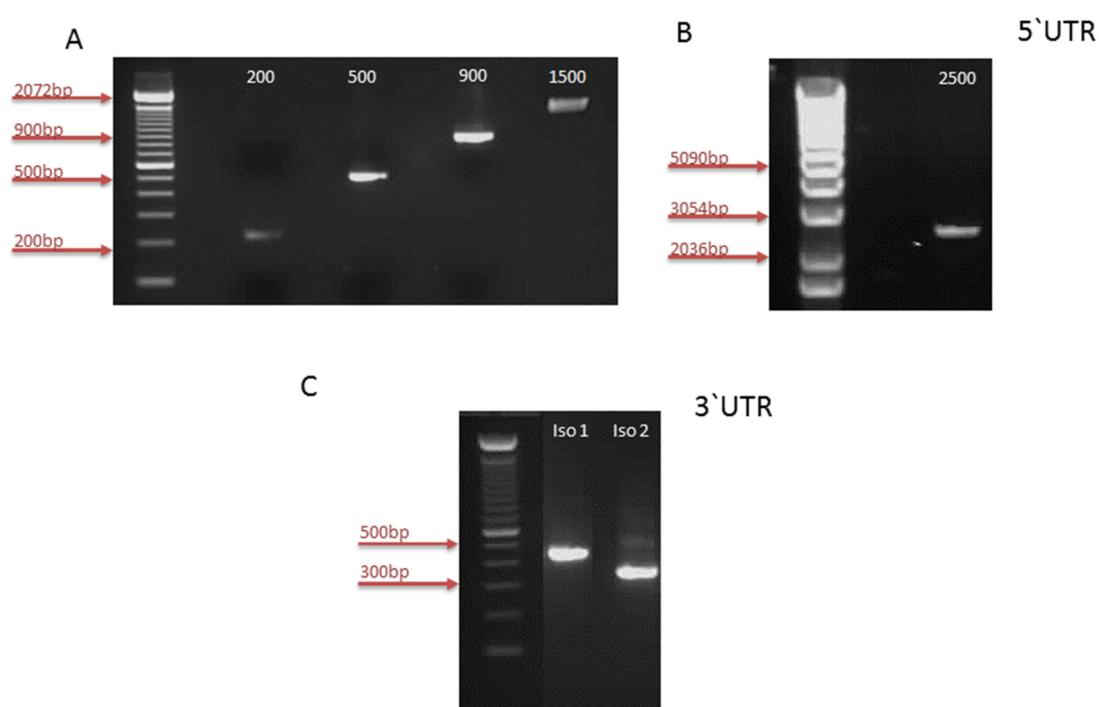
Figure 5.7: 5`UTR Products (A&B) and 3`UTR products (C) formed via PCR using Invitrogen Platinum *Taq* and compared to the Invitrogen 1kB (A&B) and 100bp (C) DNA ladders. Products from these gels were gel purified and ligated to their respective plasmid vectors. 200 – 2500: Base Pair fragment size; Iso1: mPLAUR 3`UTR (419bp); iso2: ssPLAUR 3`UTR (314bp).

5.6.2 THE *PLAUR* GENE, 5`UTR AND 3`UTR SHOW A HIGH DEGREE OF INTER-SPECIES HOMOLOGY.

Alignment plots generated by VISTA (Fig. 5.8) and the USCS genome browser (Fig. 5.9) identify that the *PLAUR* gene, its 5`UTR and 3`UTR are highly conserved between humans and the higher primates (Orang-utan, Chimp, Rhesus and Gorilla), with conservation generally reaching values of >90%. However, significantly less conservation is present in the lower mammals, as defined by the mouse genome. Here conservation was sparse and mainly limited to the gene exon regions, where conservation at maximum reached 54%. The data replicates well between the both databases. The untranslated regions are especially well conserved in the higher primates achieving close to 100% conservation in Chimps and Rhesus monkeys.

At the amino acid level, the human PLAUR protein shows 99% homology with the Chimpanzee protein but only 43% homology when compared to both the mouse and the rat protein sequence. This homology was also highly fragmented and did not show any preference for domain coding regions (Fig. 5.10). This mirrors well with the data generated by the gene homology report.

The H3K27AC track available on the USCS genome browser utilises ENCODE data and identifies regulatory elements within the genome. This identifies that active regulatory elements are present in the intronic regions between exons 1 and 2, between exons 3 and 4 and in exon 6. Interestingly, active regulatory elements are identified within the first 500bp upstream of the TSS, with the peak present at around 250bp upstream of the TSS. This identifies that the regions present within the reporter vector constructs, may be important in gene transcriptional regulation. However, the presence of a strong regulatory region at ~5000bp upstream of the TSS identifies that certain important regulatory elements may be missed in the dual luciferase assay experimental setup (maximum fragment length analysed: 2584bp).
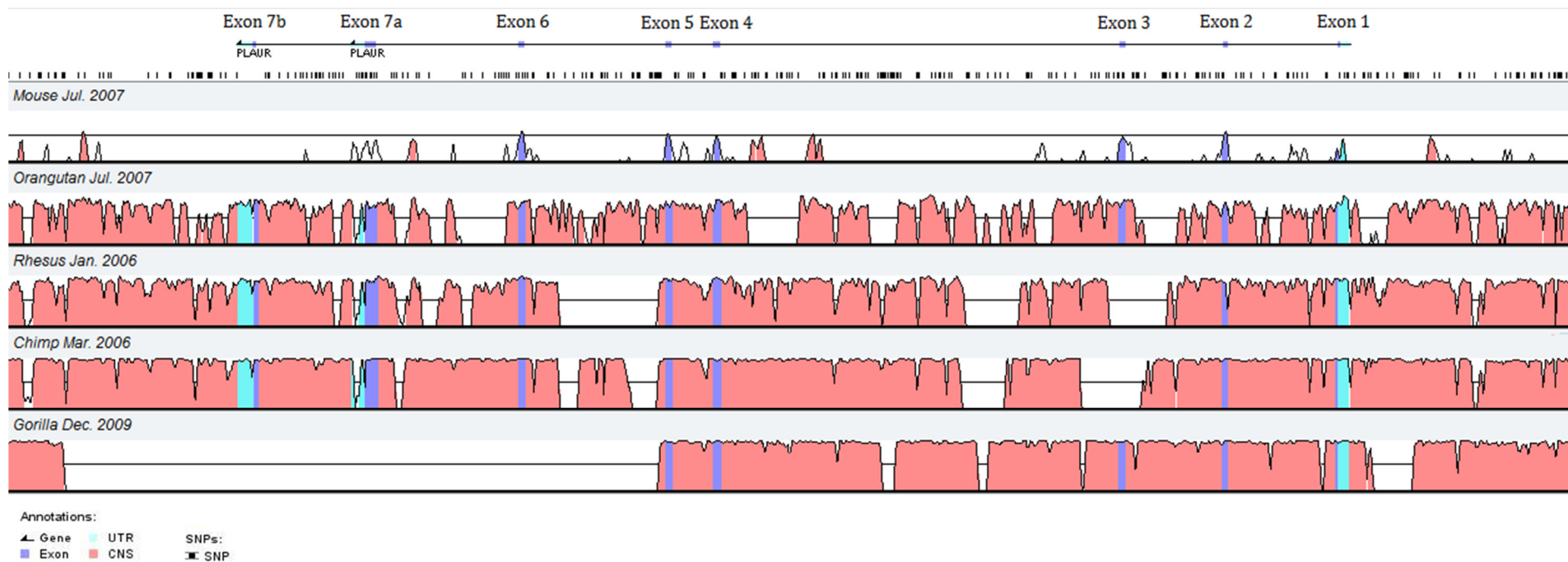
Figure 5.8: VISTA alignment plot demonstrating peaks of conservation in the pairwise sequence alignment of the PLAUR gene and its 5`UTR and 3`UTR. Conserved sequences are shown on the VISTA plot relative to their position on the human genome (Horizontal Axis) with the percentage identities shown on the vertical axis. The horizontal line identifies the 50% conservation line. Exons are identified by dark blue bands while UTRs are identified with turquoise bands. The location of validated SNPs across the region is identified by small black boxes. The gene runs from the 3`UTR on the left to the 5`UTR on the right.
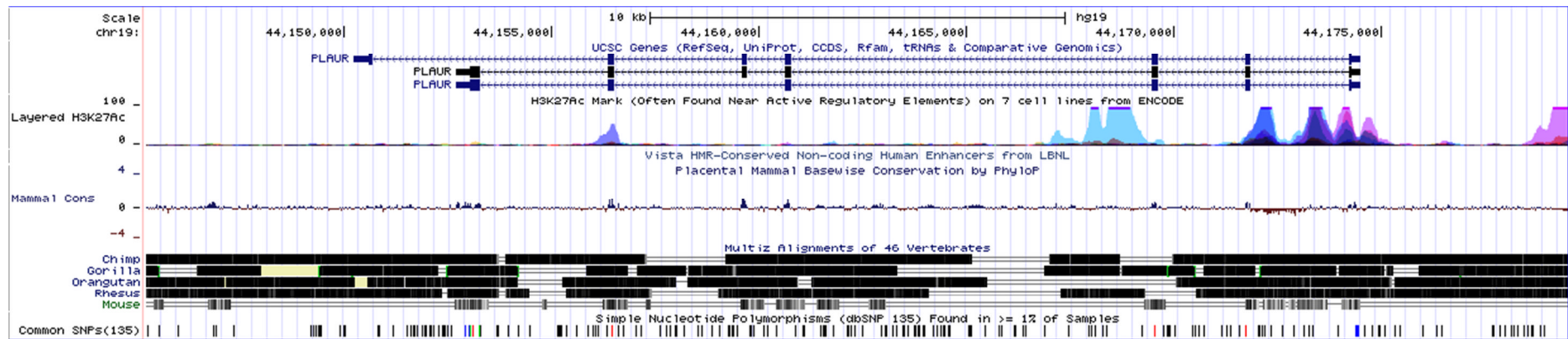
Figure 5.9: USCS alignment plot demonstrating areas of conservation in the pairwise sequence alignment of the Human *PLAUR* gene and its 5`UTR and 3`UTR. Conserved sequences are shown on the USCS plot relative to their position on the human genome (Horizontal Axis). The location of validated SNPs across the region is identified by small black boxes at the bottom of the plot. Layered H3K27AC values identify that probable regulatory elements are restricted within the gene and partially in the 3`UTR. The gene runs from the 3`UTR on the left to the 5`UTR on the right.

```
1    MG--HPPLLPLLLLLHTCVPASWGLRCMQCKTNGDCRVEECALGQDLCRTTIVRLWEEGE    58   Q03405   UPAR_HUMAN
1    MG--HPPLLPLLLLLHTCVPASWGLRCMQCKTNGDCRVEECALGQDLCRTTIVRMWEEGE    58   Q9GK80   UPAR_PANTR
1    MGLP-RRLLLLLLLATTCVPASQGLQCMQCESNQSCLVEECALGQDLCRTTVLREWQDDR    59   P35456   UPAR_MOUSE
1    MGLLRRRLLLLVVVVTTCVPASQGLRCIQCESNQDCLVEECALGQDLCRTTVLREWEDAE    60   P49616   UPAR_RAT
     **       **  *:::    ****** **:*:**::* .*  *************::* *:: .

59   ELELVEKSCTHSEKTNRTLSYRTGLKITSLTEVVCGLDLCNQGNSG-RAVTYSRSRYLEC   117   Q03405   UPAR_HUMAN
59   ELELVEKSCTHSEKTNRTLSYRTGLKITSLTEVVCGLDLCNQGNSG-RAVTYSRSRYLEC   117   Q9GK80   UPAR_PANTR
60   ELEVVTRGCAHSEKTNRTMSYRMGSMIISLTETVCATNLCNRPRPGARGRAFPQGRYLEC   119   P35456   UPAR_MOUSE
61   ELEVVTRGCAHKEKTNRTMSYRMGSVIVSLTETVCATNLCNRPRPGARGRPFPRGRYLEC   120   P49616   UPAR_RAT
     ***:*  :.*:*.****** :****  *  *  ****.**.  :***:  . * *.   :  :.****

118  ISCGSSDMSCERGRHQSLQCRSPEEQCLDVVTHWIQEGEEGRPKDDRHLRGCGYLPGCPG   177   Q03405   UPAR_HUMAN
118  ISCGSSNMSCERGRHQSLQCRNPEEQCLDVVTHWIQEGEEGRPKDDRHLRGCGYLPGCPG   177   Q9GK80   UPAR_PANTR
120  ASCTSLDQSCERGREQSLQCRYPTEHCIEVVTLQS---TERSLKDEDYTRGCGSLPGCPG   176   P35456   UPAR_MOUSE
121  ASCTSLDQSCERGREQSLQCRYPTEHCIEVVTLQS---TERSVKDEPYTKGCGSLPGCPG   177   P49616   UPAR_RAT
     ** * :  ******.****** * *:*::***       *    **: :  :*** ******

178  SNGFHNNDTFHFLKCCNTTKCNEGPILELENLPQNGRQCYSCKGNSTHGCSSEETFLIDC   237   Q03405   UPAR_HUMAN
178  SNGFHNNDTFHFLKCCNTTKCNEGPILELENLPQNGRQCYSCKGNSTHGCSSEETFLIDC   237   Q9GK80   UPAR_PANTR
177  TAGFHSNQTFHFLKCCNYTHCNGGPVLDLQSFPPNGFQCYSCEGNNTLGCSSEEASLINC   236   P35456   UPAR_MOUSE
178  TAGFHSNQTFHFLKCCNFTQCNGGPVLDLQSLPPNGFQCYSCEGNSTFGCSYEETSLIDC   237   P49616   UPAR_RAT
     :  ***.*:********** *:** **:*:*::.:* **  *****:**.* *** **:  **:*

238  RGPMNQCLVATGTHEPKNQSYMVRGCATASMCQHAHLGDAFSMN-HIDVSCCTKSGCNHP   296   Q03405   UPAR_HUMAN
238  RGPMNQCLVATGTHEPKNQSYMVRGCATASMCQHAHLGDAFSMN-HIDVSCCTKSGCNHP   296   Q9GK80   UPAR_PANTR
237  RGPMNQCLVATGLDVLGNRSYTVRGCATASWCQGSHVADSFPTHLNVSVSCCHGSGCNSP   296   P35456   UPAR_MOUSE
238  RGPMNQCLEATGLDVLGNRSYTVRGCATASWCQGSHVADSFQTHVNLSISCCNGSGCNRP   297   P49616   UPAR_RAT
     ******* ***  .    *:** ******** **  :*:.*:*   .  .::.:***   **** *

297  DLDVQYRSGAAPQPGPAHLSLTITLLMTARLWGGTLLWT   335   Q03405   UPAR_HUMAN
297  DLDVQYRSGAAPQPGPAHLSLTITLLMTARLWGGTLLWT   335   Q9GK80   UPAR_PANTR
297  -------TGGAPRPGPAQLSLIASLLLTLGLWGV-LLWT   327   P35456   UPAR_MOUSE
298  -------TGGAPGPGPAHLILIASLLLTLRLWGI-PLWT   328   P49616   UPAR_RAT
             :*.** ****:* *  :**:*  ***   ***
```

Figure 5.10: UniProt alignment of Human PLAUR with Chimpanzee (PANTR), mouse and rat protein. Alignment identifies that near complete homology (99%) occurs between the Human and Chimpanzee protein. However, dissimilarities are present within receptor domain 1 (Green Line) and Domain II (Red Line), suggesting that these may have important functional implications. Homology between the human and rodent proteins identifies a much lower degree of homology (43%) which is fragmented across the entire protein structure. Domain I is highlighted by a green line, Domain II a red line and Domain III a blue one.

5.6.3 THE *PLAUR* 5`UTR IS POTENTIALLY REGULATED BY A NUMBER OF TRANSCRIPTION FACTORS.

Bioinformatics were used to identify potential transcription factors that interact with the region upstream of the *PLAUR* TSS up to a maximum of 2500 base pairs from the TSS. A total of 23 individual transcription factors (TFs) were identified, with 7 TFs (Ets-1, AP-1, CEBP-α, c-Jun, GATA-1, NF-1 and YY1) present for more than 4 distinct occasions in the upstream region (Table 5.2). This suggests that the gene's 5`UTR has a strong potential for regulation by a number of these TFs.

Transcription Factor	Location (Base Pairs from TSS)
Ets-1	37
Elk-1	38
AP-1	94
c-Jun	95
Sp-1	123
Ets-1	163
E2F-1	175
c-Jun	208
AP-1	211
C/EBP-α	244
c-Jun	388
GATA-1	427
PEA3	438
Ets-2	554
YY1	572
C/EBP-β	600
YY1	622
NF-1	839
GATA-1	854
GR	970
TF11D	1047
NF-1	1110
IRF-2	1126
NF-1	1133
C/EBP-β	1182
MEF-2A	1197
NF-1	1258
C/EBP-α	1313
POU3F2	1368
NF-1	1408
YY1	1412
C/EBP-β	1589
C/EBP-α	1628

AP-1	1653
c-Myb	1656
RXR-α	1684
YY1	1713
YY1	1725
ER-α	1732
ER-α	1754
c-Jun	1757
NF-1	1784
NF-1	1823
GATA-1	1864
C/EBP-α	1909
C/EBP-α	1925
YY1	1951
RBP-Jκ	2056
Mzf-1	2076
GATA-1	2086
GATA-1	2096
c-Ets-2	2142
c-Ets-1	2153
GATA-1	2159
GR-α	2236
YY1	2271
NF-1	2287
c-Ets-1	2388
AP-1	2410
C/EBP-α	2520

Table 5.2: The upstream region of the PLAUR gene has a potential of being regulated by a maximum of 23 transcription factors. Bioinformatic analysis of the 2.5kb region upstream of the gene's TSS identified 23 individual TFs that survived quality control. Of these 7 TFs (Ets-1, AP-1, CEBP-α, c-Jun, GATA-1, NF-1 and YY1) could be defined as common TFs (≥4 identifications). Each coloured section identifies transcription factors located in different truncations of the vector constructs (see section 5.4.2).

5.6.4 BIOINFORMATICS IDENTIFIES ISOFORM SPECIFIC miRNAs, THAT MAY REGULATE THE *PLAUR* 3`UTR AND MRNA STABILITY

Bioinformatics have allowed us to identify a number of potential regulators of 3`UTR activity, i.e. miRNAs, that are specific to the two different 3` UTR isoforms of the *PLAUR* gene (Table 5.3). Six miRNAs are specific to the 3`UTR of the membrane bound receptor (Isoform 1) while 3 were specific to the 3`UTR of the soluble spliced receptor (Isoform 2). The identified miRNAs all had negative mirSVR scores, which is a relatively novel regression method for predicting the likelihood of target mRNA down-regulation from sequence and structure features in microRNA/mRNA predicted target sites (Betel

et al., 2010). This identifies that all miRNAs contribute to down regulation of the target gene with miR-135 potentially having the strongest effect.

miRNA	mirSVR value	Isoform Present
Let-7a	-0.295	Isoform 1
Let-7b	-0.295	Isoform 1
Let-7c	-0.295	Isoform 1
mIR-133a	-0.145	Isoform 1
mIR-320	-0.305	Isoform 1
mIR-146b	-0.124	Isoform 1
mIR-222	-0.105	Isoform 2
mIR-135	-0.716	Isoform 2
mIR-23b	-0.295	Isoform 2

**Table 5.3: Putative miRNAs which selectively target different isoforms of the *PLAUR* 3`UTR.** Using the online database available at http://www.microrna.org/microrna/home.do selected for all miRNAs with good miRSRV values, 6 miRNAs selective to the membrane bound receptor's 3`UTR and 3 to the 3`UTR of the soluble spliced receptors were identified. All miRNAs present with a negative mirSVR values and therefore are predicted to contribute towards the down-regulation of *PLAUR* with varying degrees of magnitude.

5.7 RESULTS – MOLECULAR BIOLOGY

5.7.1 NHBEC POPULATIONS SHOW EPITHELIAL CELL MORPHOLOGY

NHBECs from both epithelial cell populations (donors 7F3158 and 7F3206) stained positive for the epithelial cell marker CK-14 (Fig. 5.11). This identified that the cell used experimentally throughout this thesis presented with epithelial cell morphology. Importantly, both populations did not stain against the 1B10 fibroblast specific antibody (Fig.5.11). This identified that there was no contamination of either cell populations with fibroblast cells, which can occur during isolation.

The 1B10 antibody was validated through positive staining in a Fibroblast cell line (MRC-5), while the specificity of the anti-CK14 antibody was confirmed through lack of staining in the MRC-5 population (Fig.5.11). Isotype controls for the IgG Mouse and IgM Mouse antibodies gave no visible background staining, indicating specific antibody binding to its antigen (Fig.5.12). This therefore identifies that the staining observed above is largely due to the primary antibodies binding to the protein of interest and the secondary antibody binding to their primary antibody rather than due to non-specific staining. All experiments were replicated 3 times.

For basic morphology of MRC-5 cells and NHBECs refer to Sections 2.4.1 and 2.4.2.
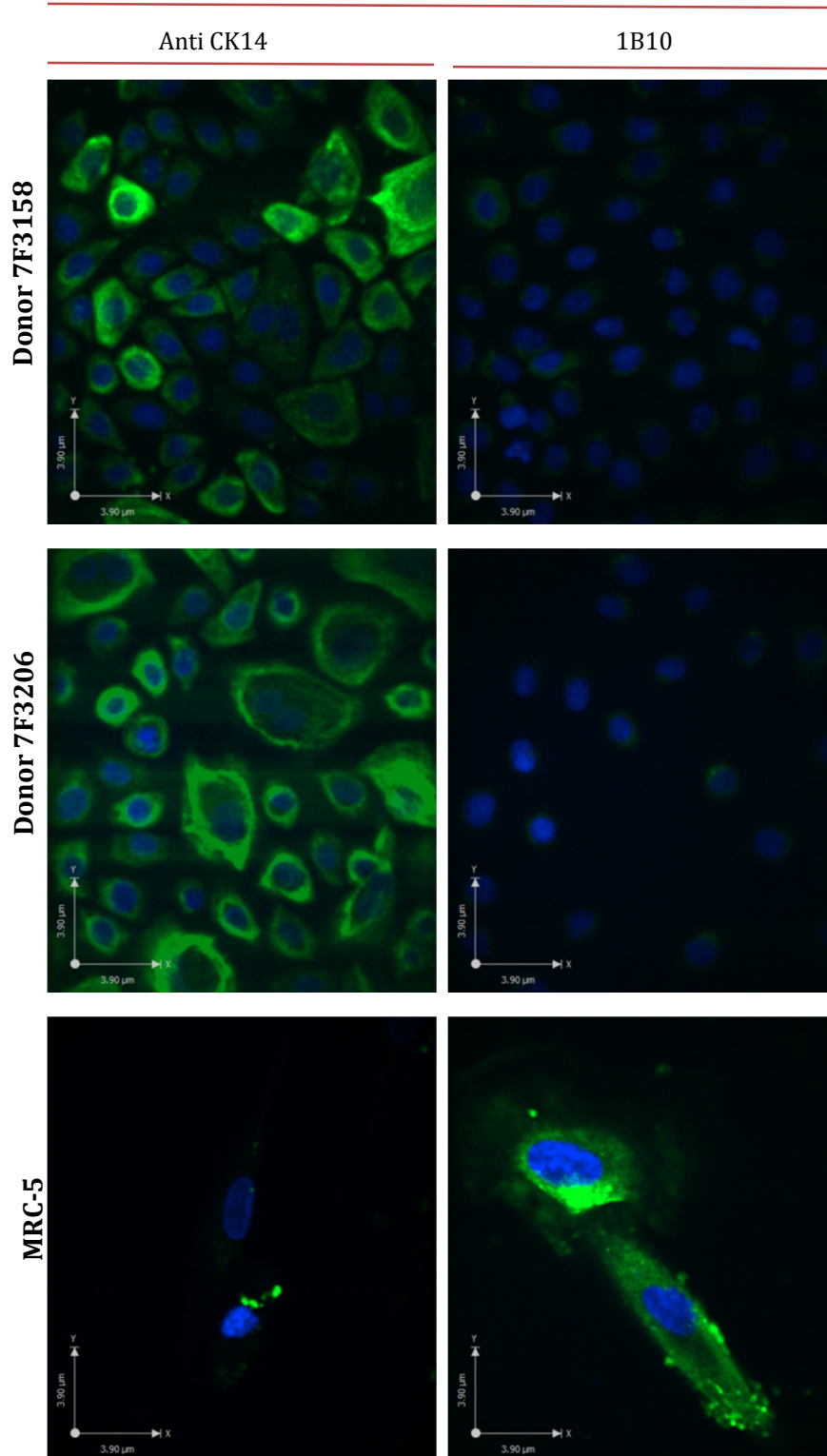
Figure 5.11: Immunofluorescence images of undifferentiated NHBECs and MRC-5 fibroblast cells using basal (CK14-green), non-ciliated (CC26-red) and fibroblast (1B10-Green) cell markers. Cell cultures from donors 7F3158 and 7F3206 showed positive staining for CK14 and CC26, but not 1B10. Fibroblast cells show positive staining for 1B10 (Green), with no staining for the epithelial cell markers. Nuclei were counterstained with DAPI (blue). Images are representative of *n*=3 experiments with random fields digitally captured.

	FITC Secondary Control	IgM Mouse Isotype	IgG Mouse Isotype

Donor 7F3158

Donor 7F3206
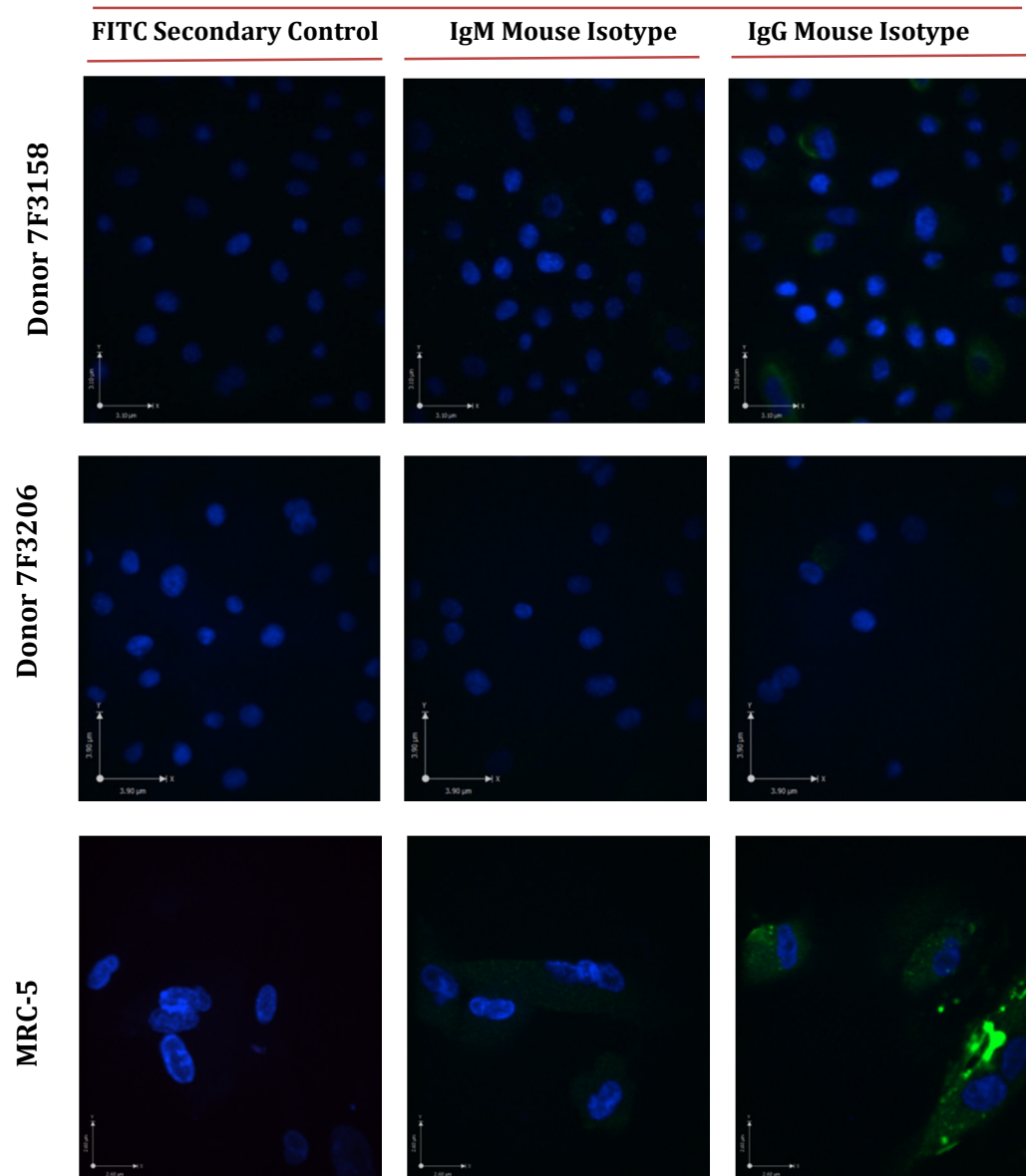
MRC-5

Figure 5.12: Immunofluorescence of undifferentiated NHBECs and MRC-5 cells treated with isotype and secondary antibody controls. Negligible staining occurs for the isotype (CK14: IgG Mouse CC26: IgG Rabbit; 1B10: IgM Mouse) or secondary antibody controls. Nuclei were counterstained with DAPI (blue). Images are random fields representative of *n=3* experiments.

5.7.2 PLAUR LEVELS ARE ALTERED IN NHBECS ABOVE PASSAGE 4.

Experiments were performed in order to determine the cell passage number at which *PLAUR* expression changes from baseline and so identifies how *PLAUR* levels drift in cell culture. This is important as cells must be used experimentally at a passage where the cell phenotype is similar to that when it is freshly extracted from tissue (Passage 0 & 1). To determine this, *PLAUR* mRNA levels were quantified from each NHBEC donor that were cultured from passage 2 up to a passage where cells were no longer viable, commonly passage 6, (*n*=6). Donor 7F3158 HBECs failed to proliferate beyond passage 6, with cells failing to achieve confluence above 60% after 20 days in culture as opposed to normally achieving 90% confluence five days after seeding. Donor 7F3206 NHBECs were successfully cultured up to passage 10 at which time the experiment was stopped. Determination of *PLAUR* mRNA expression was successful, with donor 7F3158 expressing half the amount of *PLAUR* mRNA as donor 7F3206 NHBECs ($P<1\text{x}10^{-4}$). PLAUR expression, dropped significantly at passage 5 ($P<1\text{x}10^{-4}$), followed by an elevation at passage 6 ($P<1\text{x}10^{-4}$) (Fig. 5.13) identifying passage 4 as the maximal passage at which cell gene expression follows that of cells at earlier passages.
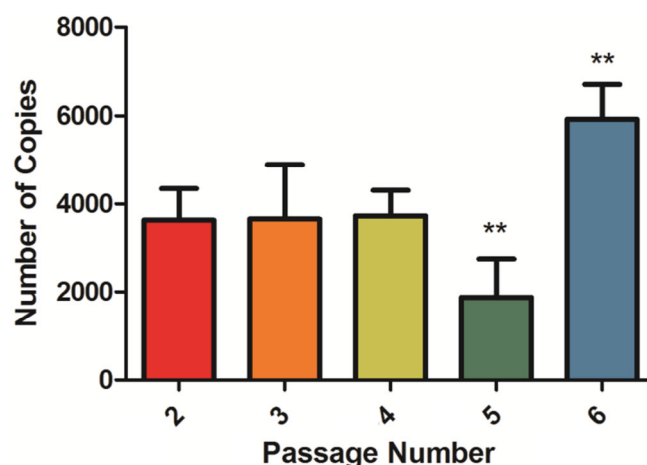
Figure 5.13: PLAUR mRNA levels are altered from baseline above passage 4. PLAUR mRNA levels remain constant from passage 2 up to and including passage 4. At passage 5 mRNA levels drop by ~50% ($P<0.01$) while at passage 6 the mRNA levels increase by ~50% ($P<0.01$); One-way ANOVA $P:<1\text{x}10^{-4}$. Therefore passage 4 was the maximal passage at which cells were used experimentally (*n*=3 over two donors).

5.7.3 IDENTIFYING THE OPTIMAL TRANSFECTION PARAMETERS FOR THE LUCIFERASE EXPRESSING VECTORS

In order to obtain optimal results from the DL assay, the best transfection ratio for the luciferase expressing vectors with FuGENE® 6 in NHBECs had to be determined. Also, since DL assays may be affected by the *trans* effects that occur between promoters on co-transfected plasmids (Farr and Roman, 1992), it is important to determine the maximal Firefly:*Renilla* ratio that can be used in NHBECs when co-transfecting the pRL-TK control vector and the Firefly luciferase expressing experimental vectors. Selection of the correct ratio will ensure independent expression analyses between the experimental and control reporter genes.

Using DL, the optimal FuGENE® 6 to DNA ratio was determined to be 3:2 when the control vector pGL4.13 and the largest pGL4.10 construct were transfected into both NHBECs (n=6 over two donors) and Beas2BR1 cells (n=3) (Fig. 5.14). Using 3 *Renilla*:Firefly ratios of 1:5, 1:8 and 1:10, the ratio of 1 part pRL-TK to 5 parts of Firefly expressing vector was determined to be the only viable ratio in NHBECs, with the 1:8 and 1:10 ratios resulting in no measurable *Renilla* Luciferase. All ratios presented with measurable *Renilla* values in Beas2BR1 cells. Therefore throughout this chapter all transfections were carried out with a FuGENE® 6 to DNA ratio of 3:2 and a *Renilla*:Firefly ratios of 1:5.

NHBECs and Beas2BR1 cells transfected with the pGL4.10 vector, with the 2.5kb construct or pRL-TK control vector alone, and NHBECs and Beas2BR1 cells co-transfected with the pRL-TK vector and the pGL4.10 vector with the 2.5kb construct did not show any variation in the Firefly luciferase readings (Fig. 5.15). Therefore no *trans* effects can be said to be present when transfecting the pRL-TK promoter with the experimental promoters when transfecting these vectors at a ratio of 1:5.
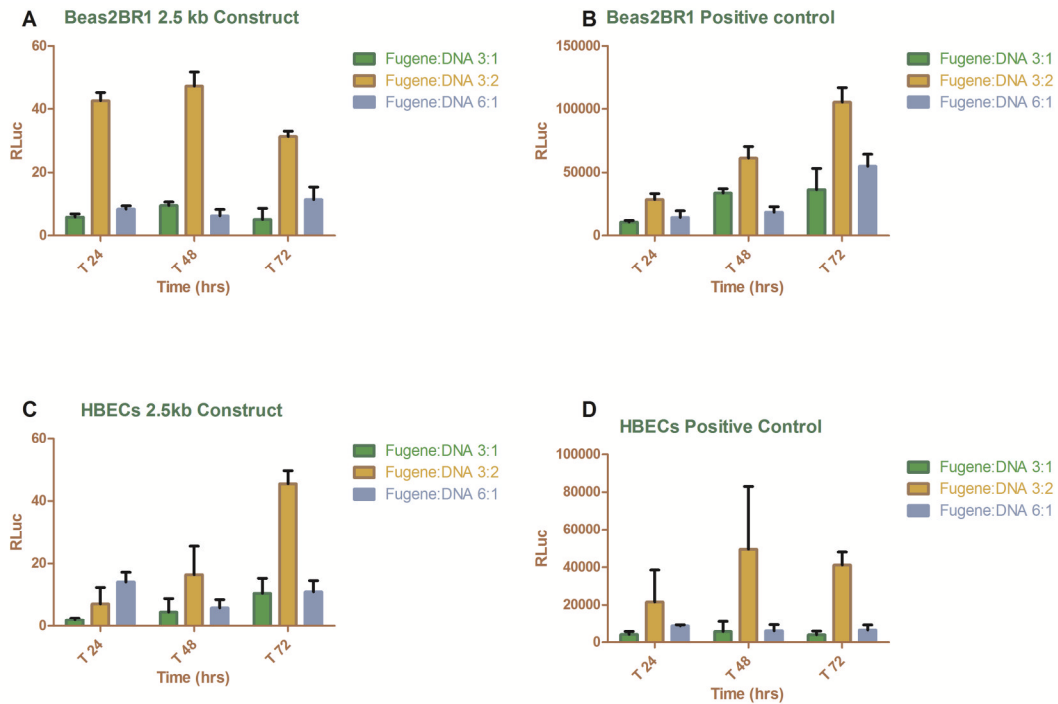
Figure 5.14: Transfection optimisation experiments identify a FuGENE® 6:DNA ratio of 3:2 as optimal for transfection of the plasmid constructs. Readings were taken at 24, 48 and 72 hours using the largest pGL4.10 construct (A&C) and the positive control vector pGL4.13 [pGL4SV40] (B&D) in Beas2BR1 (A&B) and NHBECs (C&D). Based on results showing overall significantly pronounced results by 48 hours a ratio of 3:2 and readings at 24 and 48 hours were chosen.
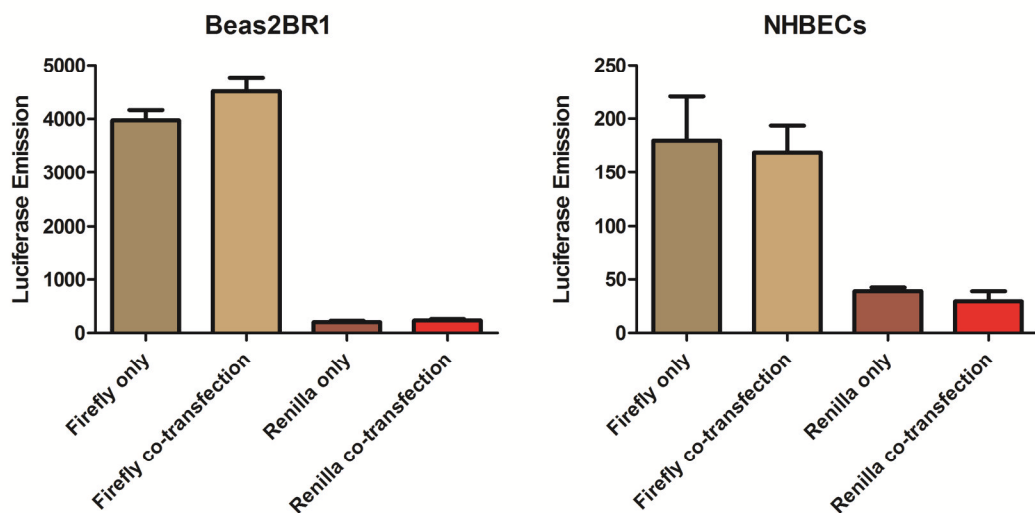
Figure 5.15: No *trans* effect is discernible on co-transfecting pRL-TK and vectors containing experimental promoters. Using the pGL4.10 vector containing the largest (2.5kb) construct, no change in either Firefly or *Renilla* luciferase values could be identified when vectors were transfected into Beas2BR1 and NHBECs on their own or when co-transfected at a ratio of 1:5.

235

5.7.4 IDENTIFYING TRANSFECTION EFFICIENCY OF PLASMID CONSTRUCTS

Immunostaining carried out on both NHBEC donors and Beas2BR1 cells identify that a high degree (>75%) of transfection exists ($P>0.05$) following transient transfection with either the pGL4.10+500bp truncation vector, the pisCHECK-2+Isoform 1 vector or the commercial PLAUR 3UTR_01 vector (Fig. 5.16A).

Lack of immunofluorescence in all isotype controls (Fig. 5.16B) identifies that immunofluorescent readings taken in the transiently transfected cells are due to specific binding of the antibodies to their target proteins rather than being due to non-specific binding. This adds credibility to the results identified above (Fig.5.16A).

All experiments were replicated 3 times, with 5 counting fields taken per experiment.
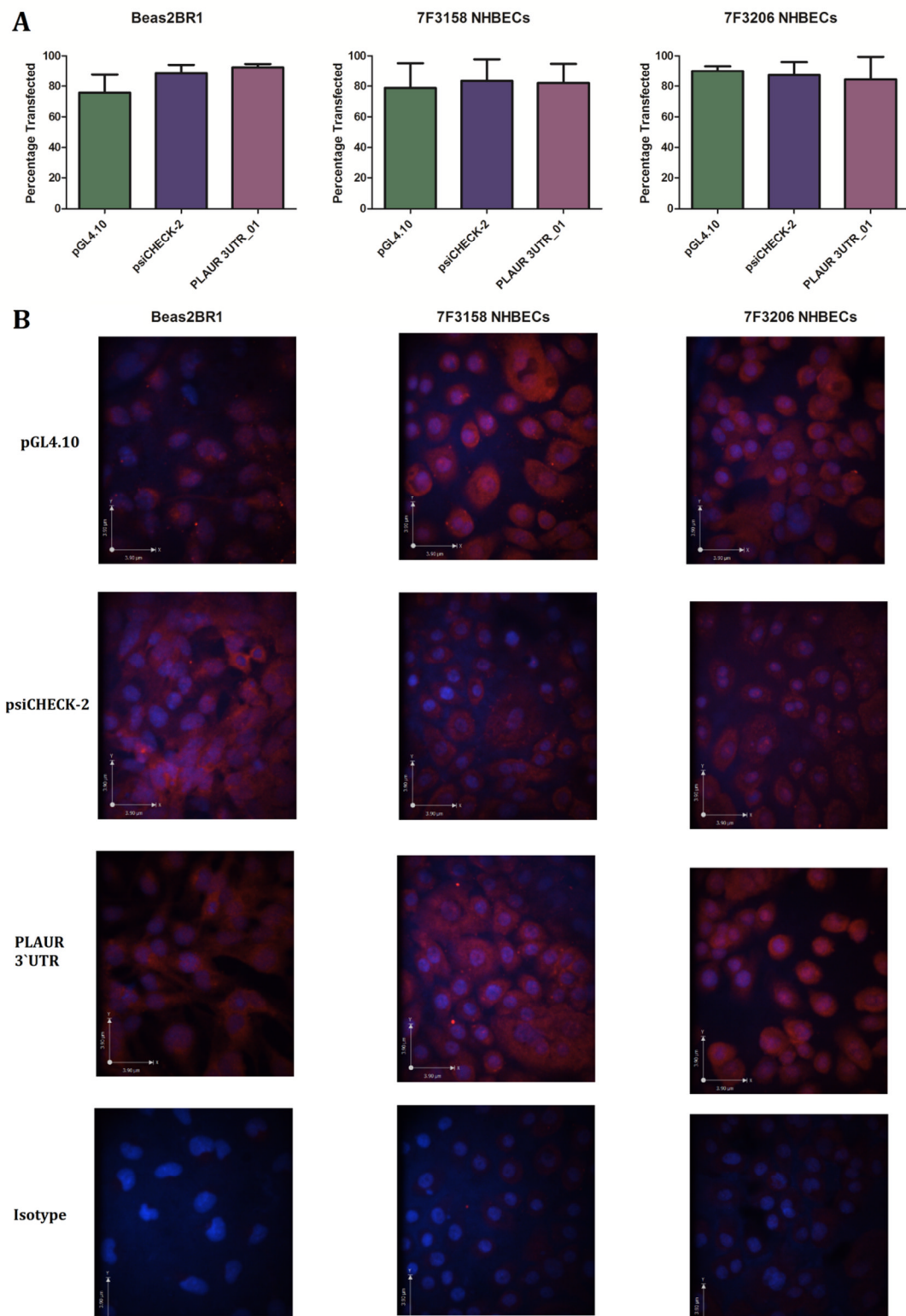
Figure 5.16: A high rate of transfection efficiency can be detected in Beas2BR1 cells and NHBECs. Using the primary polyclonal anti-firefly luciferase antibody with secondary staining carried out using the Goat anti Rabbit IgG Rhodamine TRITC and a Rabbit polyclonal IgG isotype control, one can visually identify a high degree of transfected cells for all plasmids in all cell types. Percentage transfection was determined by taking the number of transfected cells from 5 randomly selected images per well per experiment. Images are representative of *n*=3 independent experiments.

A robust promoter element was observed within the first construct, which includes the first 199bp upstream of the gene's TSS (Fig. 5.17). This result was first identified in the Beas2BR1 cells line and then replicated in both NHBEC donors. Although the same effect can be identified in both NHBEC donors, the magnitude of effect of the promoter in donor 7F3206 is double that identified in donor 7F3158, identifying donor specific variation in *PLAUR* expression. This however follows well from qPCR data on donor specific total PLAUR expression (see Section 5.7.2) adding credibility to the data and suggesting that the relevant site has been cloned into the reporter vector.

While no change in gene transcription is identified in the 490bp construct, when compared to the 199bp construct, the 397bp region between 490bp and 887bp resulted in a near doubling of gene transcription in the Beas2BR1 cell line ($P < 1 \times 10^{-3}$) and in donor 7F3158 NHBECs ($P = 0.037$) (Fig.5.17). Although this result was not fully replicated in donor 7F3206 NHBECs ($P = 0.07$), a trend in the data where the presence of the 887bp construct results in the doubling of gene transcription can still be identified. This suggests that a transcription regulatory element may be present in this region which enhances the effect of the gene's core promoter. Interestingly, increasing the construct size beyond 887bp resulted in a decrease in gene expression. This is most likely due to effects resulting from plasmid size rather than by the presence of a transcriptional regulatory element although the possibility of reduction in transcriptional activity by the larger fragments cannot be fully excluded.

At the 48 hour time point a similar pattern can be observed as at the 24 hour time point for the first 4 truncations in Beas2BR1 cells and the 2 NHBEC donors. The increased PLAUR transcription driven by the 397bp region between 490bp and 887bp

upstream of the TSS and was found to be statistically significant by paired testing in Beas2BR1 (P=0.03) and donor 7F3158 NHBECs ($P<1$x10^{-3}). Although it appears that the larger fragments (1.5kb and 2.5kb) achieve the same effect on the rate of transcription as the 900bp fragment at 48 hours, this does not replicate in both NHBEC donors and therefore no conclusions can be reached about these fragments.
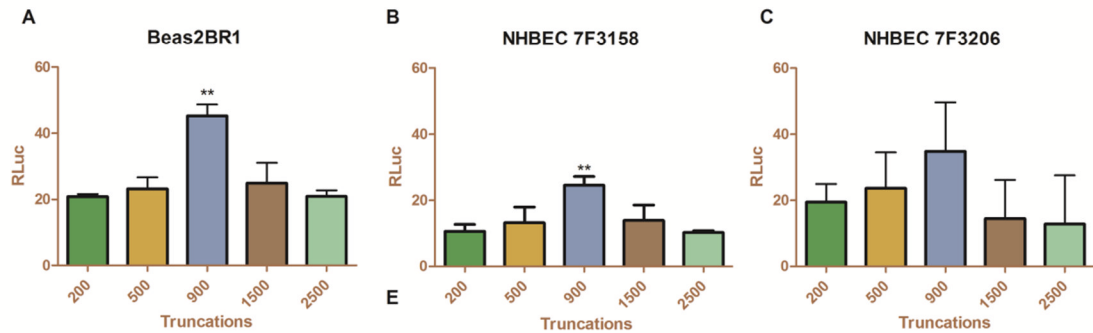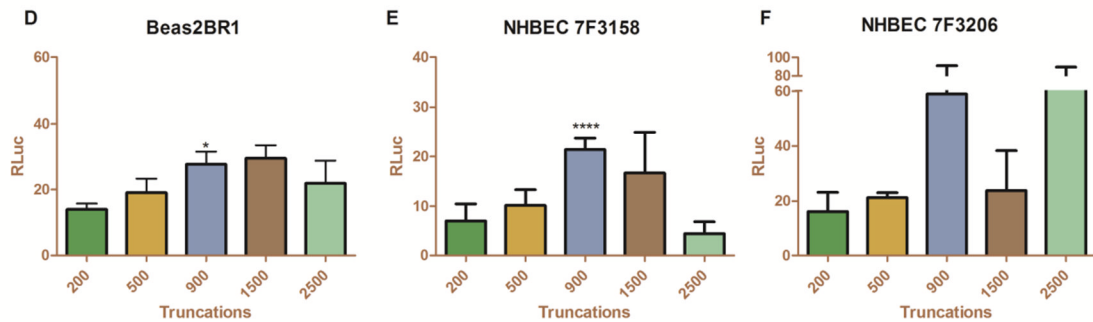
Figure 5.17: The minimal *PLAUR* promoter lies within the first 199bp upstream from the receptor's TSS and is doubled by addition of the 397bp region between 490bp and 887bp upstream of the TSS. A Dual Luciferase assay identified that *PLAUR* expression is strongly induced by a region within the first 199bp (200) upstream of the TSS in Beas2BR1 cells (A) and in two NHBEC donors (B&C) (Beas2BR1: $P<1$X10^{-3}; 7F3158: P=0.037; 7F3206: P=0.07), The region present in the 887bp construct (900) results in doubling of transcriptional activity in all the populations, which is lost on subsequent enlarging of the promoter fragment to include the 1500bp and 2500bp fragments. At 48 hours the same pattern of results can be seen for the Beas2BR1 (D) and 2 NHBEC donors (E&F), with the elevation in the 900bp fragment significant in Beas2BR1 (P=0.03) and NHBECs ($P<1$x10^{-3}). Although the larger 1.5kb and 2.5kb fragments appear to achieve the same effect as the 900bp fragment on transcription rate in Beas2BR1 cells, this was not replicated in NHBECs. Each graph represents Firefly luciferase values normalised to pRL-TK for differences in transfection and cell density (n=3).

5.7.6 THE 3`UTR REGULATES PLAUR GENE LEVELS

Multiple attempts to construct a psiCHECK-2 vector for the Isoform 2 3`UTR were unsuccessful. Therefore a commercial Firefly luciferase expressing vector containing the Isoform 3`UTR (PLAUR 3UTR_01; Switchgear Genomics; S202937) and its corresponding empty vector (EMPTY_3UTR; Switchgear Genomics; S290005) were purchased and sequence verified (data not shown).

In the case of the 3`UTR vectors, DL data was first normalised to the vector-specific control luciferase, i.e. Firefly for psiCHECK-2 and *Renilla* for the SWG_Vectors, followed by normalisation to the empty vector. This was possible as the readings presented by the empty vector controls were of values that did not introduce artificial variation to the results as was experienced with the empty pGL4.10 vector (Section 5.7.5). As all transfections were carried out in tandem with the pGL4 vectors, the internal positive control (pGL4 SV40) was taken as a universal control to confirm successful transient transfection.

The 3`UTR in both the membrane bound (Isoform 1) and soluble spliced (Isoform 2) receptor were found to suppress luciferase gene expression (Fig. 5.18). In the membrane bound receptor presence of the 3`UTR led to a decrease in detectable luciferase of ~75% at 24 hours, which was replicated at 48 hours (Fig. 5.18a-c), this was first detected in Beas2BR1 cells ($P<0.001$) (Fig.5.18A) and then replicated in donor 7F3158 ($P<0.001$) and 7F3206 ($P<0.001$) NHBECs (Fig.5.18B&C). In the soluble spiced receptor, 3`UTR led to a decrease in detectable luciferase of ~30% at 24 hours in Beas2BR1 ($P=0.011$) (Fig. 5.18D) and donor 7F3206 NHBECs ($P<0.001$) (Fig. 5.18F), which remained at 48 hours. In donor 7F3158 NHBECs however, a significant decrease in detectable luciferase levels was only detectable at 48 hours ($P=7\times10^{-4}$), with a slight and non-significant decrease detected at 24 hours (Fig. 5.18E).
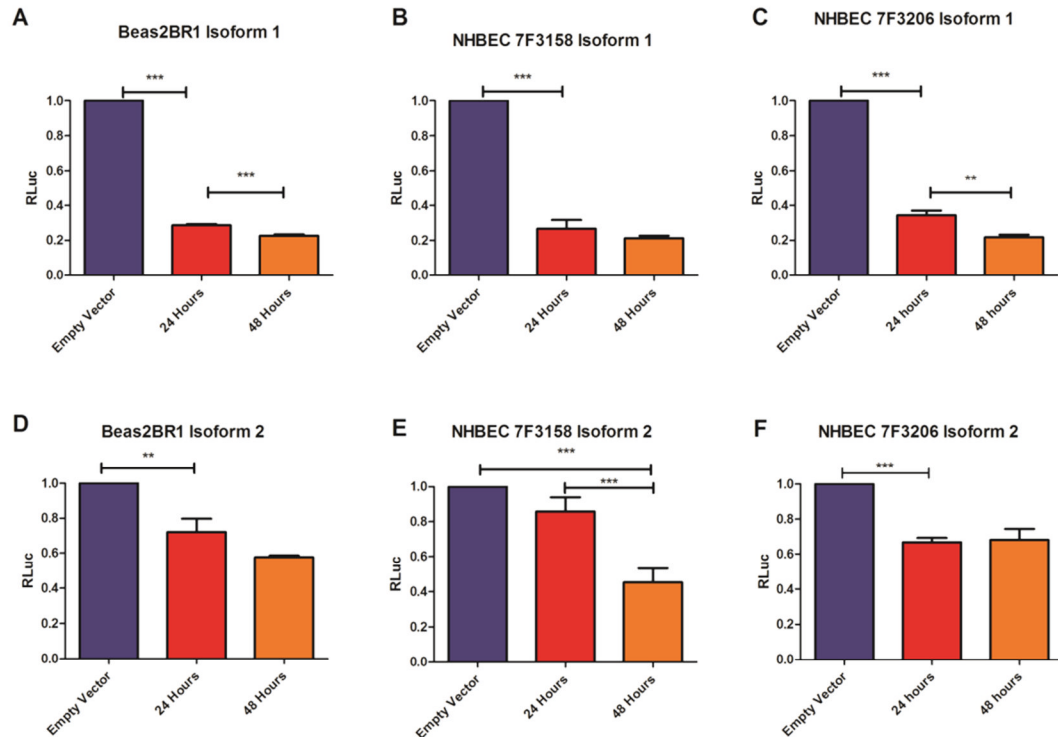
**Figure 5.18: Both of the PLAUR 3`UTR isoforms supress luciferase expression.** Dual-Luciferase analyses identified ~75% inhibition of gene expression at the 24 hour time point for the membrane bound receptor in Beas2BR1 (A) and NHBECs (B&C) ($P<0.001$). In the soluble spliced receptor the 3`UTR causes a ~30% reduction in gene expression at 24 hours in Beas2B (D) ($P<0.011$) and one NHBEC donor (F) ($P<0.001$). Although a reduction in gene expression was not evident at 24 hours in NHBEC donor 7F3158, this became evident at the 48 hour time point (E) ($P=7X10^{-4}$). Each graph represents Firefly luciferase values normalised to pRL-TK for differences in transfection and cell density (fold) which in turn was normalised to the relevant empty vector ($n=3$).

5.7.7 THE 5`UTR OR 3`UTR ARE NOT MAJOR REGULATORS OF SCRATCH-WOUND DRIVEN CHANGES IN *PLAUR* EXPRESSION

5.7.7.1 OPTIMISATION OF THE WOUND ASSAY

It was first necessary to determine the optimal time point post-wounding for determining changes in gene expression using the luciferase vector system. Therefore a time course was carried out on NHBECs transfected with the pGL4.10+887bp construct with levels of expressed luciferase expression determined in wounded and unwounded NHBECs at 0, 2, 4, 8, 12 and 24 hours post wounding.

Differences could be determined between wounded and unwounded cells at 8 hours, with the difference becoming statistically significant at 24 hours (mean RLuc unwounded: 19.55, wounded: 31.03; *P*=0.041; *n*=3) (Fig.5.19A). Evidence previously published by Dr Ceri Stewart (Stewart et al., 2012) confirmed the results of the DL assay. In this study total PLAUR mRNA was up regulated in NHBECs at both the 8 and 24 hour time-point post-wounding (*n*=3) (Fig. 5.19B). Therefore for the purpose of this thesis the 8 and 24 hour time points post NHBEC wounding were selected as the optimal periods in which to investigate 5`UTR and 3` distal region regulation of gene expression via a DL assay.
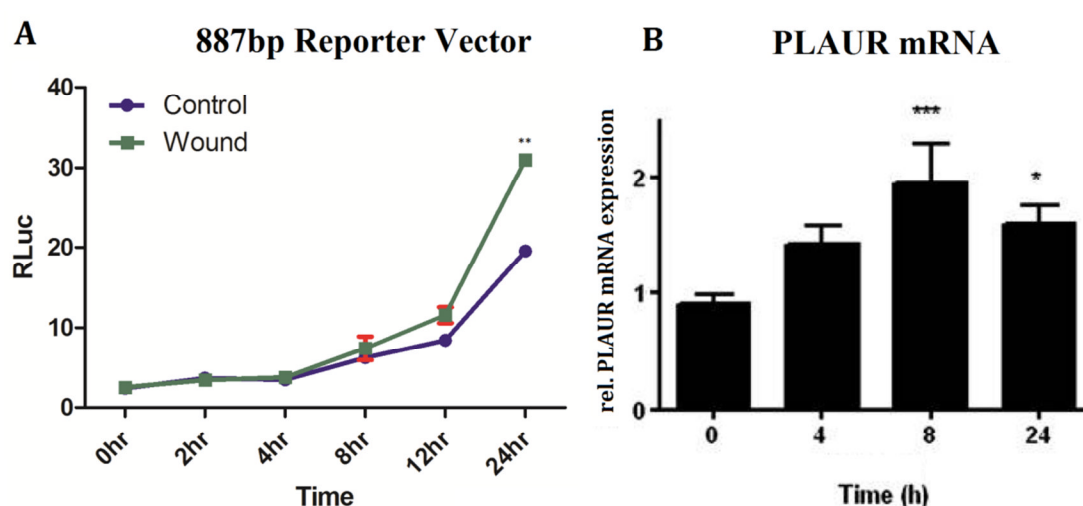
Figure 5.19: 8 and 24 hours post wounding in NHBECs are the optimal time-points to investigate 5`UTR and 3` distal region regulation of gene expression. Differences in gene expression as defined by the luciferase expression of the pGL4 vector with the 887bp 5`UTR fragment ($P=4\times10^{-3}$) between wounded and unwounded NHBECs is evident from 8 hours post-wounding but is only significant at the 24 hour time-point (A). *PLAUR* mRNA experiments confirm dual luciferase experimental results identifying elevations in *PLAUR* mRNA at the 8 and 24 hour time point. The wound healing experiment was carried out in donor 7F3158 NHBECs (*n*=3) while mRNA levels data was provided from previously published data by Dr Ceri Stewart (Stewart et al., 2012). Graphs represent means and standard error of the mean. RLuc = Relative luciferase; *=$P<0.05$; **=$P<0.01$; ***=$P<0.001$.

5.7.7.2 DETERMINING THE EFFECT OF MECHANICAL DAMAGE ON *PLAUR* 5`UTR AND 3`UTR DRIVEN GENE REGULATION

Results from the unwounded NHBECs confirm the results described in sections 5.7.5 and 5.7.6. For the 5`UTR, the basal promoter was once again determined to lie within the first 199bp upstream of the *PLAUR* TSS and to be enhanced by a region between 490 to 887bp upstream of the TSS ($P$=0.0126 at 8 hours; $P$=0.025 at 24 hours) leading to a doubling in the expression level. With regards to the 3`UTR, in mPLAUR the 3`UTR drove a 75% decrease in gene expression ($P$=2x10$^{-4}$ at 8 hours; $P$=1x10$^{-4}$ at 24 hours) while in ssPLAUR the 3`UTR drove a 30% decrease in gene expression (P=9x10^{-3} at 8 hours; P=9.3x10^{-3} at 24 hours). This therefore adds weight to the conclusions derived in sections 5.7.5 and 5.7.6.

When investigating the role of scratch-wounding on *PLAUR* gene regulation, results in this section identify that overall, mechanical damage caused by scratch-wounding did not significantly regulate *PLAUR* expression as driven by the gene's 5`UTR and 3`UTR (Fig.5.20). Although a number of differences can be identified for the 5`UTR and the soluble spliced receptor's 3`UTR at both time-points, the only statistically significant difference was identified for the 500bp fragment, which contains the region between 199bp and 490bp upstream from the TSS, at 24 hours (P=0.04). However, the change in effect is small with wounding causing just a 25% decrease in gene expression when compared to baseline. Therefore it is unlikely that this change is translated into significant changes in the PLAUR protein levels.

Bearing in mind the positive association reported for the 887bp reporter construct in section 5.7.7.1, it is worth noting that while donor 7F3158 NHBECs did once again present with this finding, this was not replicated in donor 7F3206. Therefore this was not considered a true effect.

Although not significant (P=0.06), differences identified at 8 hours between wounded and unwounded NHBECs containing the 500bp truncation and at 24 hours in cells transfected with the soluble spliced receptor's 3`UTR remain interesting due to the

presence of the same direction of effect in each separate experiment over 2 individual donors (*n*=6). Failure of these changes to reach significance is probably due to changes in gene expression being very slight, with replication in 4 experiments not being enough to achieve statistical significance.
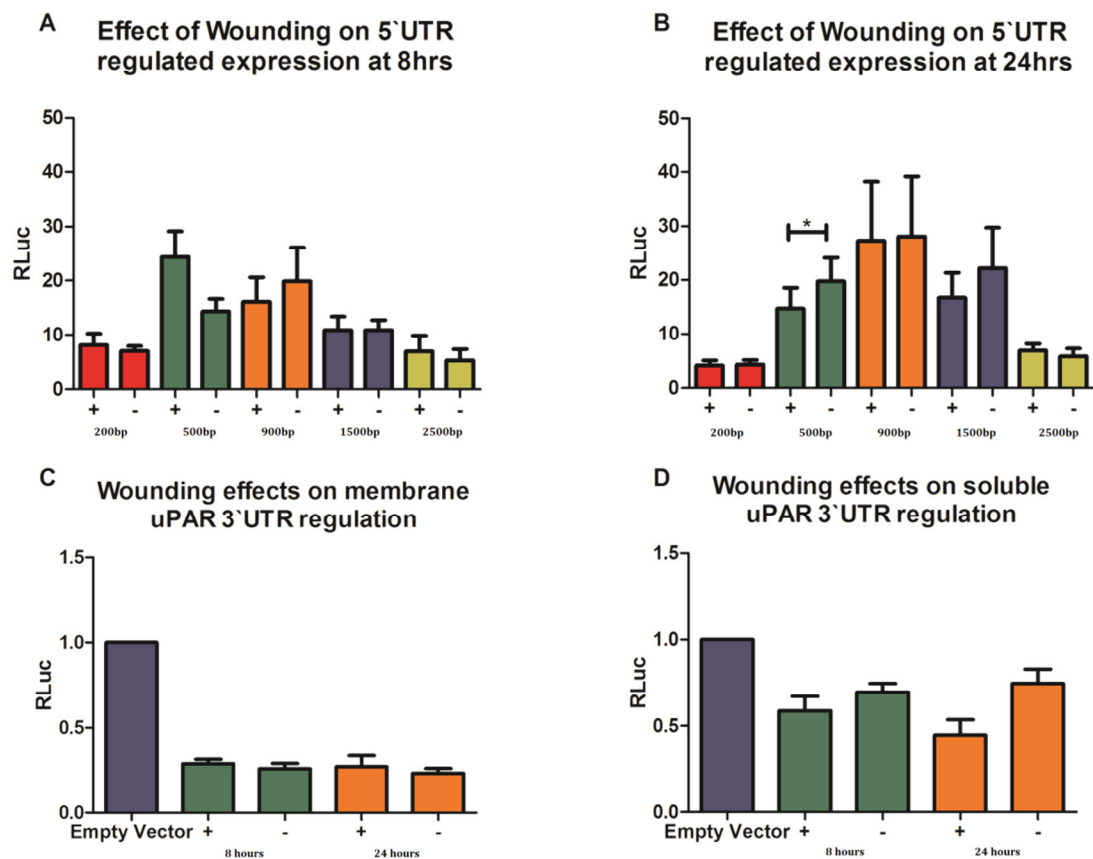
Figure 5.20: Mechanical injury caused by a scratch-wound assay does not play a major role in altering 5`UTR (A&B) and 3`UTR (C&D) regulated gene expression. Significant changes in gene expression can only be identified in cells containing the 500bp truncation after an incubation of 24 hours post-wounding (B). Here, gene expression in wounded cells is reduced by a factor of 0.25 when compared to cells at the baseline (*P*=0.04). Each graph represents 4 independent experiments carried out in 2 NHBEC donors (*n*=4 over two donors). RLuc = Relative luciferase, +=Wounded, -=Unwounded; *=*P*=0.04.

5.7.8 CIGARETTE SMOKE EXTRACT REGULATES SSPLAUR THROUGH THE 3`UTR BUT DOES NOT MODIFY 5`UTR DRIVEN TRANSCRIPTION.

Since cigarette smoke is a known causative factor for both asthma and COPD, while the smoking pack/year phenotype has been strongly correlated with scPLAUR levels in human serum (see Section 3.4.3), it was of interest to investigate whether cigarette smoke has a direct effect on PLAUR expression.

As in section 5.7.7.2, results from the basal NHBECs confirm the results described in sections 5.7.5 and 5.7.6. with regards to basal 5`UTR and 3`UTR driven regulation of gene expression.

In this assay, data was collected at the 8 and 24 hour time points in order to be comparable to the scratch wound assay. Interestingly, exposure of NHBECs to 5% v/v CSE did not alter the level of gene expression driven by the 5`UTR. However, exposure to 5% v/v CSE did selectively affect 3`UTR driven regulation of gene expression for the soluble spliced receptor. Here, gene expression doubled back to baseline, identifying a CSE dependant loss of 3`UTR driven inhibitory effects on gene expression (P=0.039) (Fig. 5.21).
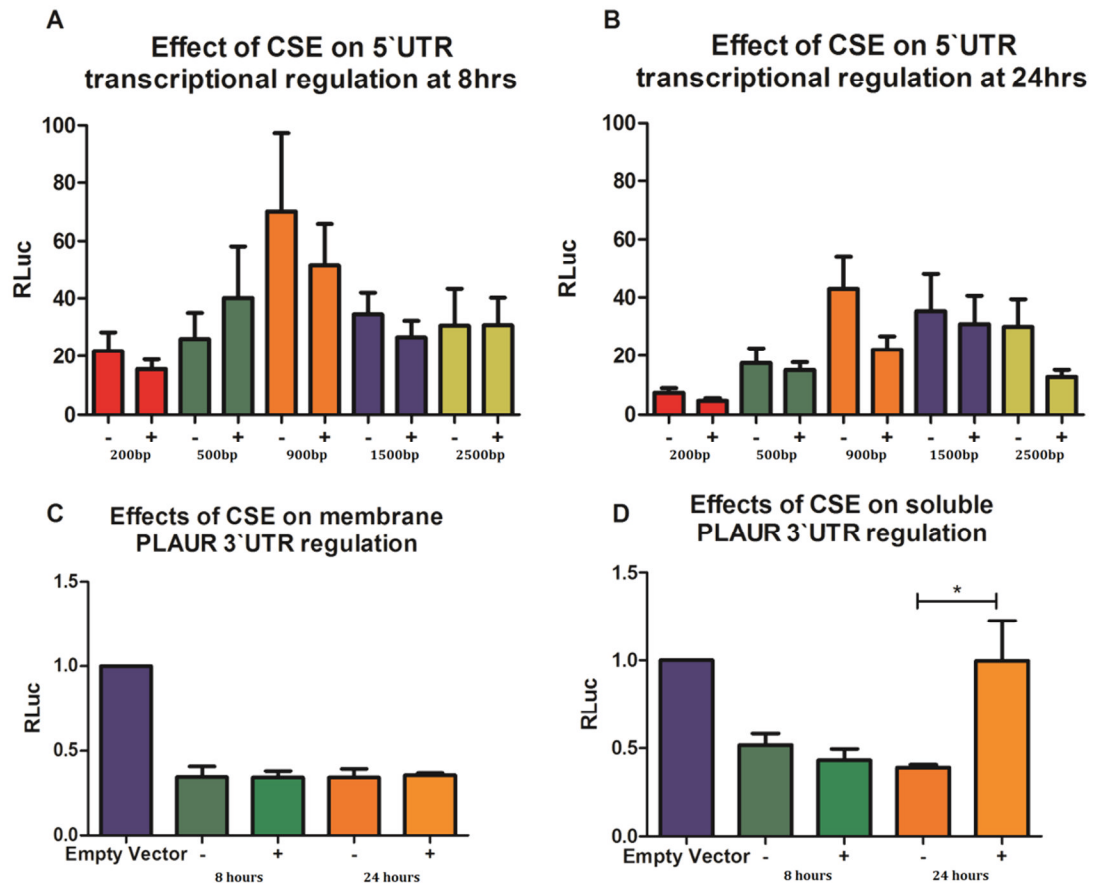
**Figure 5.21: 5%v/v cigarette smoke extract exclusively modifies effects on gene expression in the soluble spliced receptor 3`UTR.** NHBECs cultured in the presence of 5%v/v cigarette smoke extract do not have altered 5`UTR driven transcription when compared to basal NHBECs (A&B). Similarly exposure to 5%v/v cigarette smoke extract did not modify 3`UTR regulation of gene expression for the membrane bound receptor (C). However, expression levels of the gene for the soluble spliced receptor were modified, where the expression suppressing effect of the 3`UTR appears to be completely reversed (P=0.039) (D) (n=4 over two donors). RLuc = Relative luciferase; *=P=0.039.

5.7.9 NHBEC SSPLAUR MRNA LEVELS ARE ELEVATED ON ADDITION OF 5%V/V CSE

Expression of specific forms of PLAUR, as defined by mRNA expression, was shown to follow the same pattern as suggested by 3 prime reporter work on exposure to 5%v/v CSE (Section 5.7.8) (Fig. 5.22). PLAUR mRNA levels were found to increase from 4 to 24 hours for the total, membrane bound and soluble spliced PLAUR mRNAs. At 4 hours post exposure to 5%v/v CSE no marked change in mRNA levels were identified for any of the qPCR assays, while total PLAUR also had no identifiable change in mRNA levels

from the baseline at 24 hours. Although a slight decrease in mRNA for membrane PLAUR was observed at 24 hours and was replicated in all 6 experiments over 2 donors, this did not achieve statistical significance by paired testing (P=0.384; n=6 over 2 donors). However, soluble spliced PLAUR mRNA levels were increased by 76.4% compared to baseline, following a 24 hour stimulation with 5% v/v CSE ($P<1x10^{-4}$). This confirms that mRNA levels are regulated by CSE as suggested by the 3`UTR model system described in Section 5.7.8).
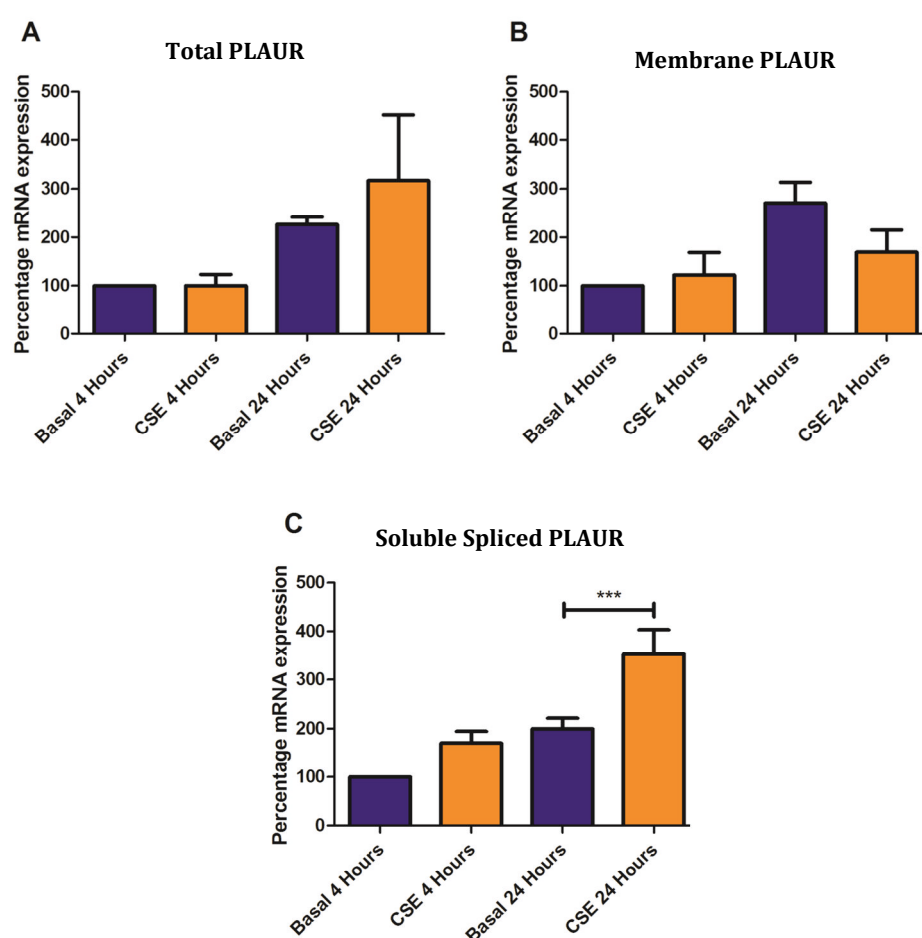
Figure 5.22: 5%v/v cigarette smoke extract selectively elevates intracellular soluble spliced mRNA levels. While total (A) and membrane (B) *PLAUR* mRNA levels are not significantly affected by the addition of cigarette smoke extract, ssPLAUR mRNA levels are elevated by ~1.5 fold when compared to cells grown at baseline ($P<1x10^{-4}$)at the 24 hour time point (C) (n=6 over 2 donors).

5.7.10 5%V/V CSE ELEVATES SSPLAUR PROTEIN LEVELS

The protein expression pattern of soluble spliced PLAUR on exposure to 5%v/v CSE emulated the qPCR results described in Section 5.7.9, where it was shown that exposure to 5%v/v CSE did not alter total and mPLAUR mRNA levels (Fig. 5.23A&B) but selectively elevated intracellular ssPLAUR mRNA levels (Fig. 5.24A).

When stained with the monoclonal antibody for PLAUR D_I (IIIF10), the soluble spliced form of the receptor forms a band at *circa* 45kDa which is separate and distinct from the band for membrane bound and soluble cleaved PLAUR (*circa* 55kDa) (Fig. 5.24B). This allows for the specific probing of the ssPLAUR form of the receptor. While at 4 hours post CSE stimulation no significant difference in expressed ssPLAUR protein can be identified between basal and stimulated cells (Fig. 5.24A&B), at 24 hours post-stimulation, ssPLAUR protein levels increase by 35% when compared to baseline protein levels (Fig. 5.24A). This was determined to be statistically significant (P=3.2x10^{-3}). This data therefore confirms that data obtained from i) the DLR assay and ii) mRNA, are translated to protein levels.
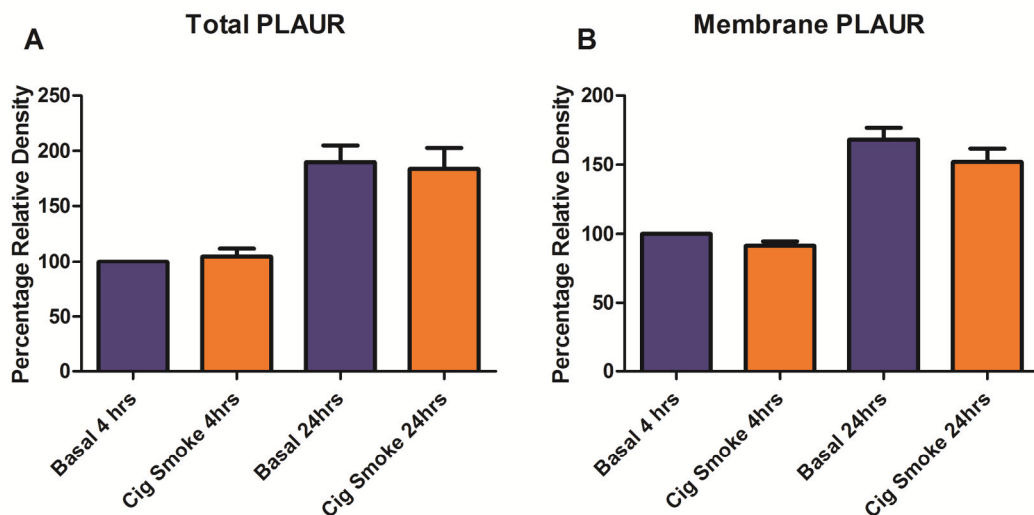
Figure 5.23: 5%v/v cigarette smoke extract does not affect intracellular levels of total and membrane bound PLAUR. When probed with the D_I specific antibody IIIF10, no difference can be seen between basal and stimulated NHBECs. Data from *n=4* experiments.
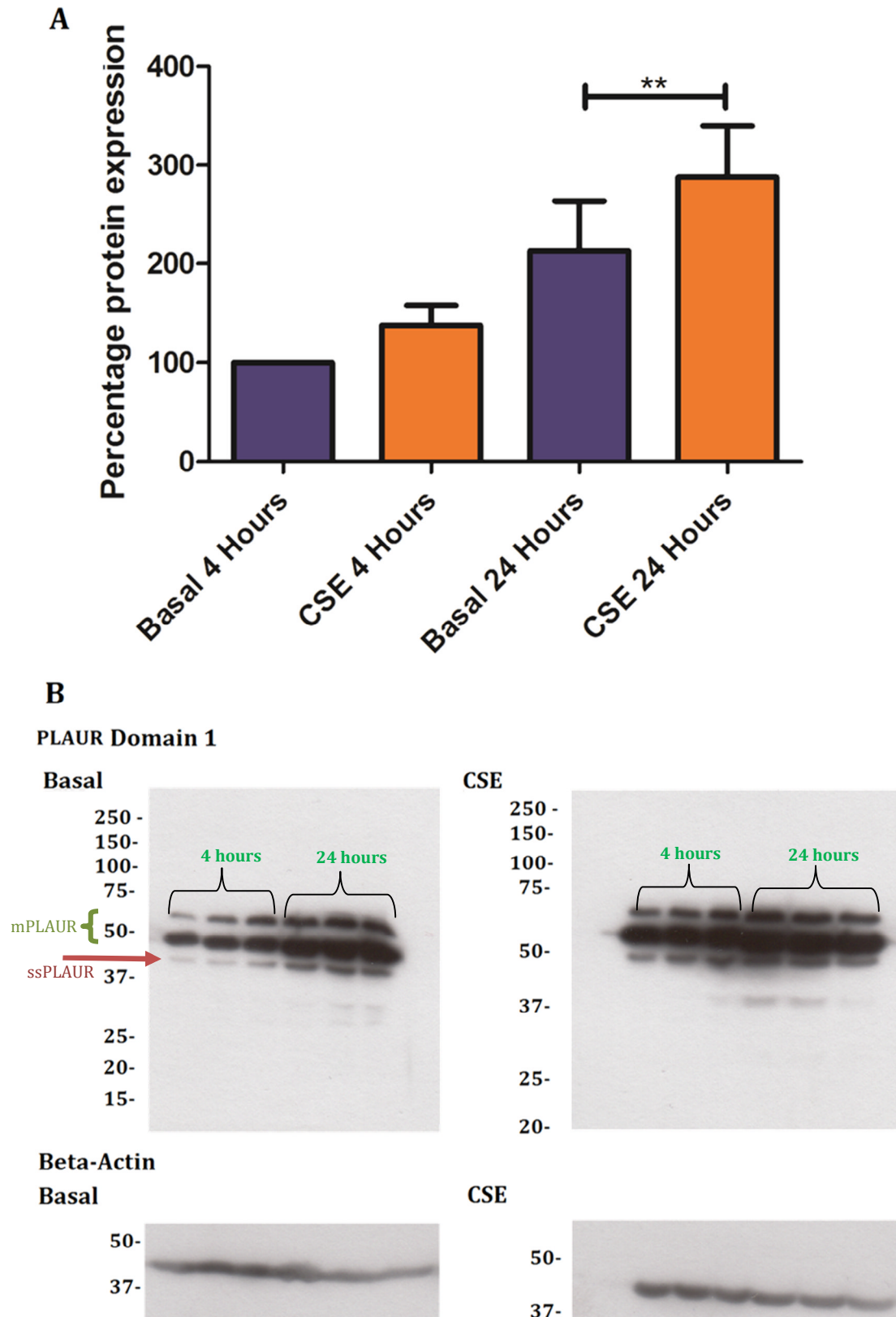
Figure 5.24: 5%v/v cigarette smoke extract elevates intracellular soluble spliced PLAUR protein levels. When probed with the D_I specific antibody IIIF10, soluble spliced PLAUR protein levels were shown to increase by 35% after a 24 hour stimulation with 5%v/v CSE (A) (P=3.2x10^{-3}). Western Blots (B) identify the band representative of ssPLAUR within the blot for total PLAUR. The 2 larger distinct bands are known to represent mPLAUR (Stewart et al., 2012). Blots are representative of 2 separate blots, each displaying data of n=3 cell-based experiments. Probing for β-actin was included as a 'housekeeping' protein for normalisation.

5.7.11 THE EFFECT OF SELECTIVE OVER-EXPRESSION OF MPLAUR OR SSPLAUR ON NHBEC FUNCTION

5.7.11.1 QUALITY CONTROL OF NHBECS RECOMBINANTLY EXPRESSING VARIOUS FORMS OF PLAUR

In order to determine whether the cells were successfully transfected with the pcDNA3 vectors for the recombinant over-expression of mPLAUR and ssPLAUR, levels of total intracellular PLAUR protein were investigated. Elevated levels of PLAUR protein in NHBECs transiently transfected to over-express either mPLAUR or ssPLAUR were identified when compared to cells transiently transfected with the empty pcDNA3 vector (P=2x10^{-4}) (Fig. 5.25). This identifies successful transfection of the cell populations and successful over-expression of the protein of interest in these populations.
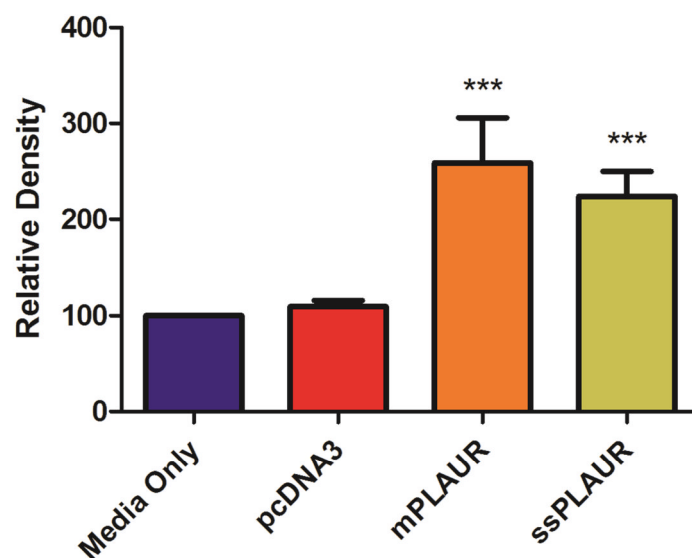
Figure 5.25: Intracellular PLAUR protein expression is elevated in NHBECs transiently transfected with pcDNA3 vectors for mPLAUR and ssPLAUR. Using the D$_I$ specific antibody IIIF10, levels of intracellular PLAUR protein are found to be ~2.5 fold higher in NHBECs recombinantly expressing either mPLAUR or ssPLAUR when compared to cells transiently transfected with the empty pcDNA3 vector. Protein levels were normalised to β-actin and then normalised to cells cultured in media only. This corrected for inter-experimental variation (n=4 over 2 donors). ***=P:2x10^{-4}.

5.7.11.2 SSPLAUR INDUCES MITOCHONDRIAL ACTIVITY IN NHBECS

The rate of mitochondrial activity was not altered in NHBECs recombinantly over-expressing mPLAUR, identifying that mPLAUR does not alter the rate of NHBEC cellular respiration. However, recombinant over-expression of ssPLAUR by NHBECs resulted in an 88% increase in the rate of NHBEC respiration, which was identified to be statistically significant when analysed using a paired t-test ($P=2x10^{-4}$) (Fig. 5.26).
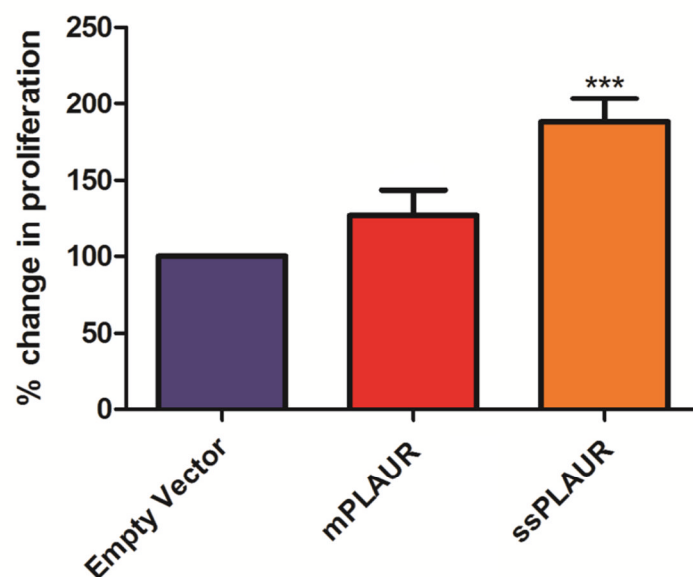
Figure 5.26: Soluble spliced PLAUR increases NHBEC mitochondrial activity independently of mPLAUR. Analysis identifies that over expression of the soluble spliced form of PLAUR increases cellular respiration by 88% when compared to NHBECs recombinantly over-expressing both the empty vector and the membrane form of the receptor ($P=2x10^{-4}$)($n=4$ over 2 donors).

5.7.11.3 SSPLAUR DOES NOT ALTER THE RATE OF APOPTISIS OR THE RATE OF WOUND REPAIR IN NHBECS

Recombinant over-expression of mPLAUR in NHBECs was found to attenuate wound healing at 4, 8 and 24 hours post-wounding ($P<0.01$), replicating data previously published by researchers from the same group (Stewart et al., 2012). However, over-expression of the ssPLAUR variant was found to not significantly alter the rate of wound healing from the baseline ($P=0.17$) (Fig. 5.27).

Over-expression of ssPLAUR also did not alter the rate of apoptosis of NHBECs either under basal conditions (P=0.75) (Fig. 5.28A) or when stimulated using a 300μM solution of H_2O_2 (P=0.49) (Fig.5.28B) previously shown to stimulate NHBEC apoptosis (Bucchieri et al., 2002). Membrane PLAUR also had no effect on apoptosis in basal cells and while showing a trend for a decrease in the rate of apoptosis in H_2O_2 stimulated cells, this was not statistically significant to the rate expressed by NHBECs transfected with just the empty vector (pcDNA3) (P=0.77).
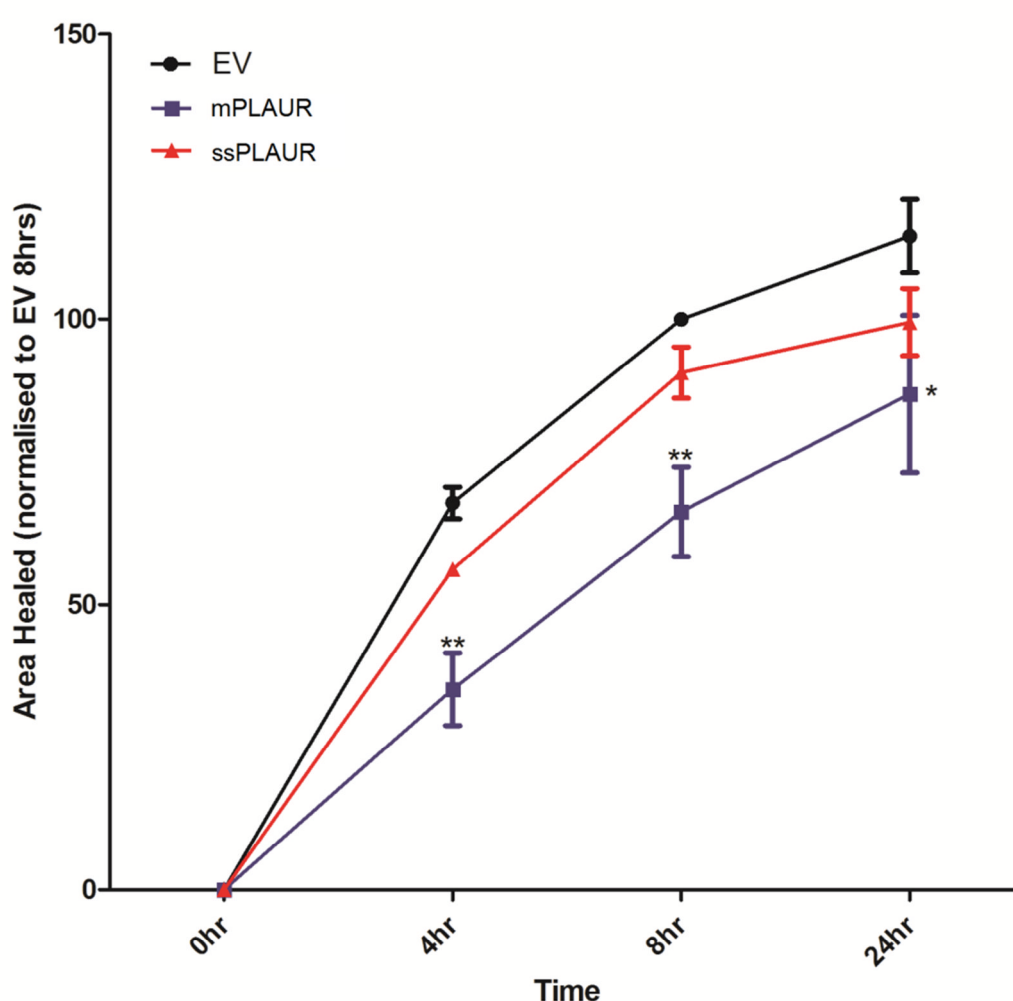
Figure 5.27: Investigating the effect of soluble spliced PLAUR (ssPLAUR) on the rate of cell migration. The rate of wound repair as defined by the rate of wound-healing of NHBECs over expressing the soluble spliced form of the receptor does not vary significantly from cells transfected with the empty vector (EV) (P=0.17). NHBECs over expressing membrane PLAUR (mPLAUR) were used as a positive control, attenuating the rate of wound-repair at the 4, 8 and 24 hour time point (P<0.01). The graph represents data from 4 individual experiments carried out over 2 individual donors, with data normalised to the wound area of cells transfected with the empty vector at 8 hours.
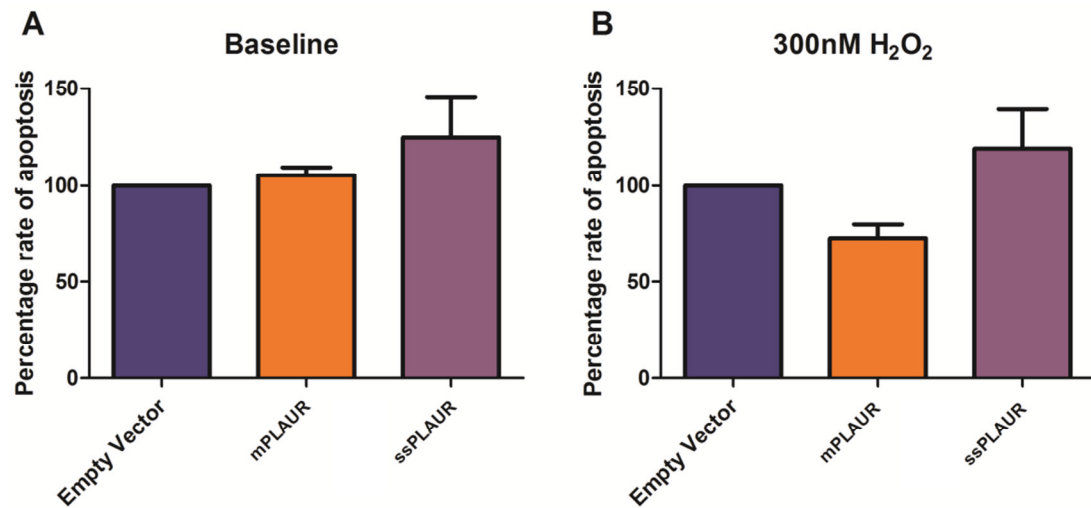
Figure 5.28: Investigating the effect of ssPLAUR on the rate of epithelial apoptosis. When compared to baseline cells transfected with the empty pcDNA3 vector, both mPLAUR and ssPLAUR over-expressing cells do not appear to alter the rate of epithelial cell apoptosis. The rate was unaltered both when cells were cultured at baseline and when cultured in the presence of 300μM of H_2O_2 ($P>0.05$; $n=4$ over 2 individual donors).

5.8 DISCUSSION

The aims of this chapter were to characterise the *PLAUR* 3`UTR and 'core' 5`UTR through bioinformatics followed by experimentally determining these regions' role in regulating *PLAUR* expression under both basal and stimulated (scratch wound & CSE) conditions, which are both relevant to airway disease. This work subsequently developed these aims further and characterised a role for the CSE elevated ssPLAUR in NHBEC functions.

In silico investigations identified the degree of gene interspecies homology as well as the location of putative transcription factor binding sites and putative miRNA binding sites. A high degree of conservation between higher primates (including *Homo sapiens*) for all UTRs identifies a high probability for the presence of gene regulatory elements. Indeed, this chapter predicts a large number of 5`UTR transcription factors, of which 7 were present at a frequency of ≥4. Interestingly, 4 of these have a pre-defined role in the asthmatic and/or COPD airway; namely ETs-1 (McKinlay et al., 1998, Nakamura et al., 2004), YY1 (Natanek et al., 2011), CEPBα (Roth et al., 2004, Borger et al., 2009) and AP-1 (Desmet et al., 2005), while elevated levels of AP-1 have also been reported in mice lungs following cigarette smoke exposure (Li et al., 2009b). Moreover, AP-1 (Park et al., 2011, Bhattacharya et al., 2001), SP-1 (Bhattacharya et al., 2001) and Ets-1 (Mylona et al., 2006) have previously been shown to regulate *PLAUR*, while c/EBP, SP-1, AP-1 and GATA have also been previously predicted *in silico* to regulate PLAUR expression (Stewart and Sayers, 2009). This highlights that regions regulated by these transcription factors are potentially important in regulating 5`UTR driven regulation of gene transcription. Interestingly the 199bp construct is rich in AP-1, Sp-1 and Ets-1 sites, highlighting a potential reason for the recorded strong gene regulatory function of this 5`UTR construct.

At the 3`UTR a number of isotype specific miRNAs were detected, of which a number have been previously associated with airway disease. Expression levels of the Isoform 1 specific miRNA miR-133a, were found to be supressed in the bronchial smooth muscle in a mouse model of allergic bronchial asthma when compared to healthy controls (Chiba and Misawa, 2010). Other Isoform 1 unique miRNAs were also associated with the airway; mir-320 was found to be significantly down regulated in human airway smooth muscle cells by a pro-inflammatory stimulus of IL-1beta, TNF-alpha, and IFN-gamma (Kuhn et al., 2010) and miR-146b was determined to be a regulatory component in the negative feedback loop for TGFβ regulated induction of epithelial cell differentiation. Let-7b has been found to be highly over expressed in human airway tissue, with levels 70 fold higher than the average miRNA (Williams et al., 2009). The Isoform 2 specific miRNA miR-222 has been implicated in the regulation of non-small cell lung cancer (Acunzo et al., 2012) and general lung cancer (Zhang et al., 2011). Therefore bioinformatics identifies a strong regulatory potential for the *PLAUR* 3`UTR, for the mPLAUR and ssPLAUR forms, as well as the 5`UTR in respiratory disease. This confirms that investigating both the 5`UTR and 3`UTR is pertinent to this work.

This provided a platform for further experimental studies to study the role of the 5`UTR and 3`UTR *in vitro*. Although previous studies on the putative *PLAUR* promoter have been published, these are limited by their use of cancerous cell lines, namely the colon cancer cell lines HCT116 and DEO (Dang et al., 1999) and the cervical epithelial tumour cell line HeLa (Soravia et al., 1995). Therefore, prior to this investigation, *PLAUR* 5`UTR driven regulation had not been investigated in primary cells *per se* or in airway cells, which are pertinent based on elevations of PLAUR detected in NHBECs in asthma (Stewart et al., 2012). In this chapter, experimental studies have located the minimal *PLAUR* promoter within the first 199bp upstream from the TSS, confirming previously published results in colon cancer and U937 lymphoma cells (Dang et al.,

1999, Soravia et al., 1995). This minimal promoter was determined to be robust, based on luciferase reading well above those normally published for similar promoters (~ 1to 5 fold elevation) (Bonello and Khachigian, 2004, Takeuchi et al., 2002) confirming a high level of regulation by the baseline promoter. The importance of this region is further emphasised by the gene regulation associated transcription factors AP-1 and Sp-1. Increased gene transcription driven by the region between 490 and 887 base pairs upstream of the TSS suggests that transcriptional regulatory elements that are relevant to the modulation of PLAUR regulation are also present in this region, a finding that has not been previously reported. Potential gene regulatory elements within this truncation include YY1 and C/EBPβ, transcription factors which are known to be deregulated in COPD (Natanek et al., 2011) and asthma (Roth et al., 2004). Interestingly this region also contains the lung function and asthma associated SNP rs2356338, which has been previously associated with changes in circulating PLAUR levels and so provides further evidence that this region is important in regulating gene expression. Therefore, although the effect of this region is modest (it does not cause a doubling of the rate of gene expression), it is still relevant to gene regulation and it may be of increased importance in obstructive lung disease through possible disease driven effects by these gene regulatory elements. A decrease in transcriptional activity by the 1.5kb and 2.5kb fragments is unexpected and is likely to be due to changes in the conformation of the plasmid brought about by large inserts which could affect plasmid driven promoter activity. Therefore, effects driven by these large fragments were difficult to interpret.

Identification that gene expression is strongly suppressed by alternate gene regulatory elements within the individual 3`UTRs of the membrane bound and soluble splice variant of the receptor (see Fig. 1.8 Chapter 1) highlights that these regions also play an important role in modulating *PLAUR* expression by probable post-translational mechanisms. The membrane bound receptor 3` distal region has already been shown

to effect *PLAUR* expression through the interaction of phosphoglycerate kinase (PGK) with *PLAUR* mRNA *in vivo* and in cell free systems. Stability of *PLAUR* mRNA was reported to occur through mRNA phosphorylation (Shetty et al., 2004), mediated by PGK binding to a 37 mRNA nucleotide sequence (nucleotides 1051 to 1088) (Shetty et al., 2004). Other investigations identified that heterogeneous nuclear ribonucleic protein C1 (hnRNPC), binds to a 110 mRNA nucleotide sequence (Shetty, 2005) preventing mRNA degradation, an effect increased by the presence of PLAU (Velusamy et al., 2008). Therefore the 3`UTR directed work described in this chapter builds on this data, focusing on the mRNA coding 3`UTR. Results confirm previously published inferences that the mPLAUR 3`UTR is an important gene regulatory element under basal conditions and have identified that the 3`UTR is also an important regulatory region for the soluble spliced receptor, limiting gene expression of both receptor forms via a repressive mechanism as yet undefined in NHBECs.

Interestingly, recent publication by the Encyclopaedia of DNA Elements (ENCODE) Consortium (Rosenbloom et al., 2012) of a now completed ENCODE dataset identifying markers for promoter and enhancer elements, has provided supporting evidence for the conclusions arrived at in this chapter (Fig. 5.29).
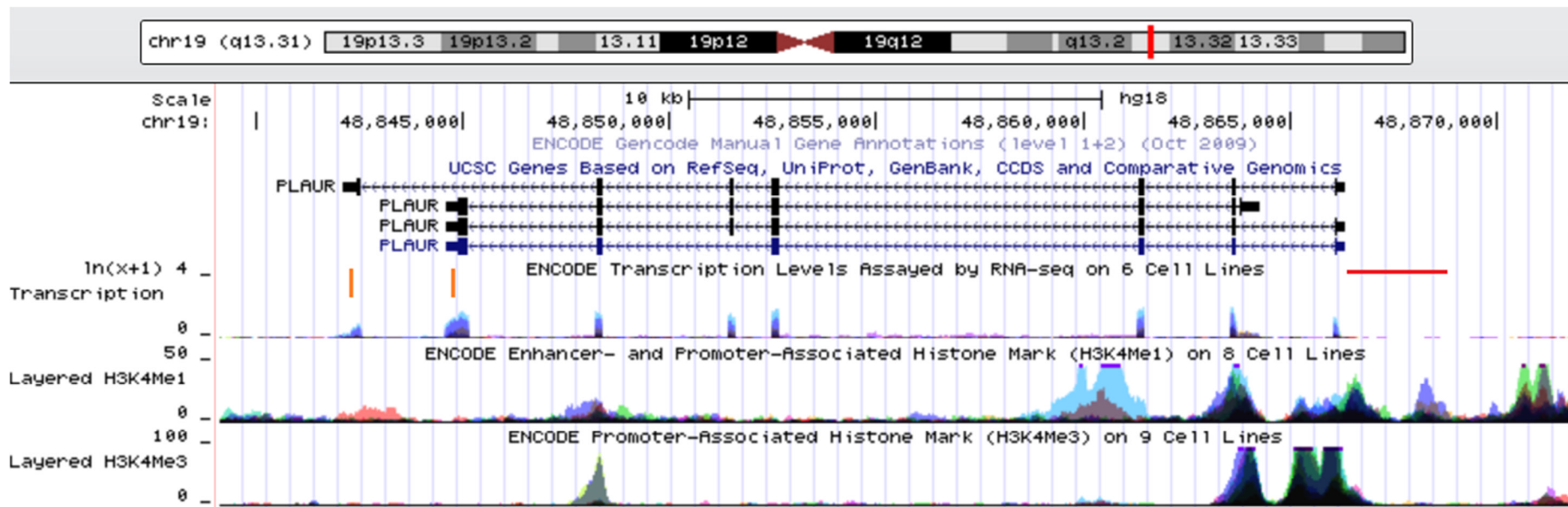
Figure 5.29: ENCODE identifies important gene regulatory elements within the *PLAUR* gene and its 5`UTR. Strong gene regulatory elements present in the gene 5'UTR and replicated in both the H3K4Me1 and H3K4Me3 tracks identifies important regions of gene transcriptional regulation. A particularly strong association in the region that corresponds to the 199bp fragment supports the finding presented in this thesis that the *PLAUR* gene is strongly regulated by its minimal promoter present in this region. A region associated with promoter/enhancer activity towards the end of the 2.5kb fragment studied in this thesis is only present in the H3K4Me1 track and does not reflect dual luciferase assay results presented. This adds weight to the conclusion derived in this chapter that dual luciferase assay results for the larger 1.5kb and 2.5kb are difficult to interpret. A strong tag for a promoter/enhancer region in the region ~5kb upstream of the gene suggests that further regulatory regions exist for *PLAUR* which have not been tackled by this thesis. Low degrees of tagging for promoter/enhancer elements at the 3`UTR for mPLAUR (top fragment) and ssPLAUR (second fragment from the bottom), suggests that the changes in gene expression that were experimentally discovered in this chapter are more likely to be driven by post-translational effects.

Markers identify important regulatory elements within the 2.5kb fragments analysed, especially within the first 300bp upstream from the TSS, supporting previously published results, confirmed by this work, that the region corresponding to the first 200bp upstream of the TSS are important in gene transcriptional regulation. The presence of another peak towards the end of the 2.5kb fragment however does not match with results presented in this thesis. This may suggest that, as previously concluded, results obtained by the larger fragments may not be skewed due to vector size dependant effects and are therefore difficult to interpret. However this promoter/enhancer marker is absent in ENCODE's H3K4Me3 track, making a correct interpretation of the data difficult. The appearance of another strong promoter/enhancer region further upstream of the region investigated in this thesis, present in both the H3K4Me1 and H3K4Me3 ENCODE tracks, identifies that an important regulatory region may exist ~5kb upstream of the gene. This therefore suggests that further gene regulatory mechanisms remain uninvestigated, which may be important in basal gene regulation or in altering gene expression on epithelial cell stimulation. This is of importance when considering that the mechanism of alteration of *PLAUR* expression on scratch-wounding has still not been conclusively determined (see below). The low degrees of tagging for promoter/enhancer elements present in the 3`UTR for mPLAUR and ssPLAUR suggests that the changes in gene expression described in this chapter are more likely to be driven by post-translational effects, as expected.

Once regulation of gene expression in NHBECs had been investigated, it was pertinent to investigate changes in gene expression following cellular stimulation by scratch-wounding and CSE exposure. These outcomes were selected based on previous evidence from the same research group identifying an elevation of PLAUR at the wound edge of a scratch wound (Stewart et al., 2012), the association of *PLAUR* SNPs with lung

function in smokers (Stewart et al., 2009) and the correlation between ssPLAUR and smoking pack/years described in Section 3.4.3.

Scratch-wounding stimulation of NHBECs appears to only effect gene expression through the 5`UTR region between 490 and 887 base pairs upstream of the TSS. While this is of interest due to the presence of SNP rs344781 within this fragment (466bp), which has previously shown borderline significant association with baseline lung function as defined by the FEV_1/VC ratio in smokers (Stewart, Hall et al. 2009), the increase is not large enough (0.25 fold) to translate to a significant change in gene expression. Therefore, overall epithelial cell damage can be said not to alter expression driven by the investigated 5`UTR regions or the either isoform specific 3`UTR, suggesting that neither the 3`UTR nor the studied 2.5kb region of the 5`UTR are key regulatory regions for PLAUR regulation on mechanical damage. Therefore the causative mechanism for the reported increase in PLAUR levels at the NHBEC wound edge (Stewart et al., 2012) has not been identified with the gene regulatory elements likely present further upstream of the gene or within the *PLAUR* gene.

As above, the regulatory region for changes in *PLAUR* expression driven by 5%v/v CSE is independent of the 2.5kb 5`UTR as well as the 3`UTR of the membrane bound receptor. Therefore, as in the scratch wound model, no causative mechanism has been identified for CSE modulation of mPLAUR and its associated soluble form (scPLAUR). Again however, one must take into consideration that lack of regulation simply identifies that no regulatory region is present in the studied areas and that regulatory elements may be present further upstream of the gene or within the *PLAUR* gene structure itself. However with regards to ssPLAUR, inhibition by CSE of the 3`UTR driven suppression of gene expression suggests that CSE selectively elevates ssPLAUR, a finding confirmed at the mRNA and protein level. This is of special interest as

investigations into the soluble spliced form of the receptor are severely lacking in the field, with a role for ssPLAUR not yet defined.

Cell migration, MTT and apoptosis assays identified that the role of ssPLAUR in NHBECs is limited to the modulation of cellular respiration, similar to that identified for scPLAUR (see Section 4.7.12/3). Similarity in effect between scPLAUR and ssPLAUR independent of mPLAUR allows for the hypothesis that the presence of a free-floating intact domain 1 (the only domain which is identical between the two forms) is the essential structure that regulates PLAUR activity on epithelial cell respiration. As previously discussed, changes in cellular respiration can be due to changes n the rate of cellular proliferation. As increased cell proliferation is a known constituent of airway remodelling (Wilson, 1998, Busse et al., 1999), it is natural to suppose that elevated ssPLAUR may play a detrimental effect in the process of airway remodelling, leading to changes in obstructive airway disease. This ties in well with the known role of cigarette smoke in affecting airway remodelling (Niewoehner et al., 1974, Floreani and Rennard, 1999, Churg et al., 2006) and may potentially be one of the factors driving this effect. Interestingly, ssPLAUR does not mimic scPLAUR's role in modifying epithelial wound repair in a scratch wound model (see Section 4.7.12), suggesting that a mechanism involving the full length receptor's D_{III} is involved.

In conclusion, this chapter identifies, through bioinformatics, that the gene's 5`UTR and 3`UTR do have regulatory potential that is conserved through different species. Experimental investigations in a bronchial epithelial cell line (Beas2BR1) and in primary bronchial epithelial cells (NHBECs) identify a role for the 5`UTR and 3`UTR under basal and stimulated (scratch wound & CSE) conditions. *PLAUR* transcription was found to be strongly influenced by the minimal promoter region present in the first 199bp upstream of the TSS as previously reported. Transcription was found to be augmented by a region between 490bp and 887bp upstream of the TSS. This chapter

also confirms a role for the 3`UTR in the regulation of mPLAUR and ssPLAUR expression via gene suppression. While the regulatory mechanism for changes in *PLAUR* expression on mechanical damage as defined by a scratch-wound model still remain to be identified, CSE was found to selectively elevate ssPLAUR through inhibition of 3`UTR driven gene suppression. This led to an increase in the rate of NHBEC respiration, indicating a possible effect on cellular proliferation and so identifying a possible role for ssPLAUR in airway remodelling. Therefore this thesis, for the first time, identifies a biological effect for this specific gene isoform.

CHAPTER 6:

IDENTIFYING COMMON AND RARE VARIANTS ACROSS THE PLAUR GENE USING NEXT-GENERATION SEQUENCING

CHAPTER 6: IDENTIFYING COMMON AND RARE VARIANTS ACROSS THE PLAUR GENE USING NEXT-GENERATION SEQUENCING

6.1 INTRODUCTION

Significant evidence is present in the literature which highlights the importance of the urokinase plasminogen activator receptor in the progression and modulation of a variety of disease states (Eugen-Olsen et al., 2010b, Haupt et al., 2012, Langkilde et al., 2011, Sidenius et al., 2000, Barton et al., 2009), while work in this thesis has identified a link between *PLAUR* and the obstructive lung diseases, asthma and COPD (Section 3.4.4) as well as smoking (Sections 3.4.3 & 5.7.8). At the cellular level, work in this thesis suggests a role for the different forms of the receptor in airway remodelling (Sections 4.7.12 & 5.7.11), an important process in obstructive airway disease (O'Donnell et al., 2002). Therefore, variation in receptor expression or function may play an important role in the modulation of disease.

Variation in the genetic code in the form of SNPs or insertion/deletions (indels) can result in changes in the rate of gene expression or, in the case of non-synonymous SNPs, changes in the amino acid sequence that may affect protein structure and any role the protein may have on disease risk and/or progression. Indeed work by colleagues in the same group has identified variants within the gene to either have a regulatory effect on PLAUR expression, elevating the levels of scPLAUR in serum (Barton et al., 2009), to be associated with an increase in the decline of lung function in asthma and smokers (Barton et al., 2009, Stewart et al., 2009) or the development of a

number of disease states (Tee et al., 2012, Manetti et al., 2011, Shih et al., 2011, Turkmen et al., 1997).

Work on the effect of variance within the *PLAUR* gene and its untranslated regions through the tagging of SNPs spanning the *PLAUR* gene (Barton et al., 2009), has been limited to work on common variants, defined as SNPs with a MAF >1% (Lemire, 2011). The importance of discovering novel variants is highlighted by previous work on *PLAUR* where the gene was identified as an asthma susceptibility gene, yet the causative polymorphism(s) behind the association remained as yet undetermined (Barton et al., 2009).

Further scope to identify novel rare variants that may be involved in the regulation of *PLAUR* gene expression and/or asthma is based on the long-standing idea that rare variants, over common variants, could be the driving force behind a number of common diseases such as asthma (Schork et al., 2009, Pritchard, 2001, Bodmer and Bonilla, 2008). This idea was expanded upon by a recent study by Cirulli and Goldstein where the authors hypothesised that much of the genetic control of common diseases occurs via rare variants, which are usually deleterious in nature (Cirulli and Goldstein, 2010). The authors go on to describe the effect of rare variants on the risk of common diseases such as autism, mental retardation, epilepsy and schizophrenia as being strong in individual patients (Cirulli and Goldstein, 2010).

The 1000 genome project (1000_Genome_Project, 2010) identified over eight million novel variants (SNPs and insertion/deletions) by 2010, a large percentage of which were rare genome variants. The presence of so many novel variants highlights that many may still remain to be discovered genome wide, including a large number of *PLAUR* variants, which may regulate PLAUR expression and activity.

Therefore, detection of rare variants will increase understanding of the *PLAUR* gene structure with regards to polymorphisms spanning the gene and its untranslated

regions. Stratification of results based on asthma disease status will help identify which of the novel and other detected variants have an impact on disease risk and/or susceptibility. Recent advances in next-generation sequencing (NGS) has improved sequence 'coverage' for most genes as well as the onset of more cost-efficient processes, providing the opportunity to be able to identify rare variants within the total pool of identified variants.

6.2 AIMS

1. To carry out next-generation sequencing on the chromosome 19q13 locus relating to the *PLAUR* gene and its untranslated regions (8317bp at the 3`UTR and 34971bp at the 5`UTR) in order to identify novel variants using 200 severe asthma cases and 200 non-wheeze, non-atopic controls.

2. To identify whether these novel variants are unique to either the asthma or control populations.

6.3 METHODS

The experimental processes described in this chapter were carried out for the PLAUR gene in conjunction with next generation sequencing for the IL1RL1 and IL18R1 genes.

6.3.1 STUDY POPULATIONS

Next-generation sequencing was carried out on DNA from 200 severe asthma cases and 200 non-asthmatic, non-atopic, non-wheeze controls. Case subjects were obtained from the Genome-Wide Association Study To Identify Genetic Determinants Of Severe Asthma (AUGOSA) study cohort (Wan et al., 2012), while a subset of general population controls from the Nottingham Gedling cohort (McKeever et al., 2001), were selected to be the non-asthmatic, non-wheeze and non-atopic controls (Table 6.1). Attempts were made to sex match the cases and controls, but controls were chosen to be slightly older than the asthmatics in order to provide further assurance of their non-asthmatic status. Therefore the resulting samples were made of cases with a population of 69.4% female with an average age of 48 years (±15) and controls with a population of 73.0% female with an average age of 57 years (±13).

	AUGOSA Cohort	Gedling Cohort
Age (Yrs)	48 ±14.88	57 ±12.64
Percentage Male	30.6	27.0
Height (M)	1.64 ±0.08	1.66 ±9.06
FEV$_1$ (L)	2.17 ±0.84	2.77 ±0.79
Smoking pack/years	11.82 ±20.25	8.40 ±18.61
Percentage Never Smokers	52.0	53.5

Table 6.1: Demographics comparing the case (AUGOSA) and control subjects (Gedling) sequenced in this chapter.

6.3.2 REGION SELECTION

The untranslated regions, included in the experimental design due to their potential in regulating gene expression as suggested by previously published work (Barton et al., 2009), and the gene region of *PLAUR* (chromosome 19q13) were selected for sequencing. This gave a total selected region of Chr19: 44,141,930-44,209,469 (Fig. 6.1). This included the region 8317 base pairs downstream of the 3`UTR and 34971 base pairs upstream of the TSS. The length of the 3`UTR investigated was limited by the location of the cell adhesion molecule 4 (CADM4) gene (Chr19:44126522-44143991). The region encompassing the 5`UTR was selected to capture SNP rs346054, previously associated with bronchial hyper-responsiveness, located at 30147 base pairs downstream of the gene's transcriptional start site (Barton et al., 2009). All co-ordinates are reported in the Genome Reference Consortium GRCh37.p9 Primary Assembly.
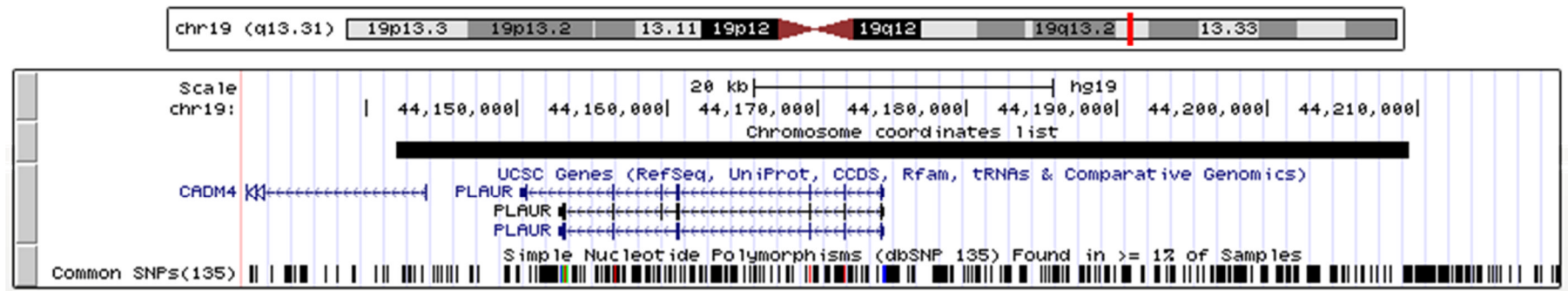
Figure 6.1: Region selected for next-generation sequencing. The region selected for next generation sequencing, located within chromosome 19(q13.31), is highlighted by the black band within the above diagram that represents the region of Chr19:44131930-44219469 (Feb 2009 build). This includes the 3` untranslated region up to and including part of the cell adhesion molecule 4 (CADM4) gene and the 5` untranslated region up to ~35kb upstream of the transcriptional start site.

6.3.3 BAIT DESIGN

Baits are 120bp oligonucleotides used to carry out sample target enrichment. Bait design was carried out *in silico* using the SureSelect™ e-array design software[11]. In this software, the following protocol was used:

- The Illumina Chip was selected from the Sequencing Technology bar
- From the Design option tab 'Paired-End long read' was selected. This allows for the design of a library targeted towards paired-end sequencing (shotgun sequencing), where long DNA fragments are broken down into shorter fragments and sequenced from both ends before being re-arranged together to form a sequence of the original DNA strand
- The default parameters were then modified as follows:
  - The amount of bait tiling was increased to 'X5'; this results in each nucleotide being selected by five individual baits, increasing coverage
  - A justified design was selected; this allowed design of baits with a good degree of overlap allowing for repeated sequencing of the DNA regions
  - An overlap of '40' was selected for inclusion into avoided regions; this allows for optimised anchoring of the baits to the required regions
- Both of the 'avoid standard repeat masked regions' tabs was selected. This selected the 'repeat' and the 'windows' masker algorithms. This minimises the degree of masking of the sequencing areas and so increases the number of baits designed for the region of interest

---

[11] available at https://earray.chem.agilent.com/earray

Following the submission of the design and the online generation of the bait library, the following files were formed:

1. A .zip file containing a .summary file describing both the design and the results
2. A .fate file listing the number of baits generated in the target region
3. A .bed file that mapped the location of each individual bait and
4. A .tdt file which provided the sequence and target position of each of the baits

The .bed files were then loaded as custom tracks on the USCS genome browser on which the custom MAP readability track[12], designed by Mr Richard Capper (Agilent UK), had been activated to allow visualisation of the baits mapped onto the region of interest.

---

[12] Available at http://genome.ucsc.edu/cgi-bin/hgTracks?hgS_doOtherUser=submit&hgS_otherUserName=Richard%20Capper&hgS_otherUserSessionName=Ian%20Sayers

6.3.4 NEXT-GENERATION SEQUENCING

The experimental process of re-sequencing in terms of library preparation, target enrichment (Fig. 6.2), cluster generation, cluster sequencing and base calling (Fig. 6.3) were carried out by SourceBioscience (Nottingham, UK). Next-generation sequencing was carried out on two separate lanes, one for cases and the other for controls, using the Illumina HiSeq2000™ systems pipeline (San Diego, USA). Sequencing used a paired-end design using 100bp reads.

Since generation of data on an individual level can be costly, multiplexing was carried out on the sample pool, with the case and control subjects split into 3 randomly indexed pools of 66, 66 and 68 individuals (Cases=Pools 1, 2, 3; Controls=Pools 4, 5, 6). To ensure that relatively identical DNA concentrations were present for each sample prior to pooling, DNA concentrations were determined using an Agilent BioAnalyzer. DNA samples in each pool were then sheared and target sequence enrichment carried out using the Agilent SureSelect Custom Capture kit, built with the bait library designed in Section 6.3.3; this had a capture size range of 500Kb to 1.5Mb. These biotinylated RNA baits hybridise to the regions of interest in the now fragmented DNA allowing Streptavidin coated beads to select out the regions of interest in order to focus the area for amplification prior to the cluster generation and sequencing steps (Mamanova et al., 2010, Leproust, 2012). Prior to sample library preparation each of the 6 sample pools were indexed by bar-coding with unique adaptor sequences (Harismendy and Frazer, 2009, Meldrum et al., 2011, Kenny et al., 2011).
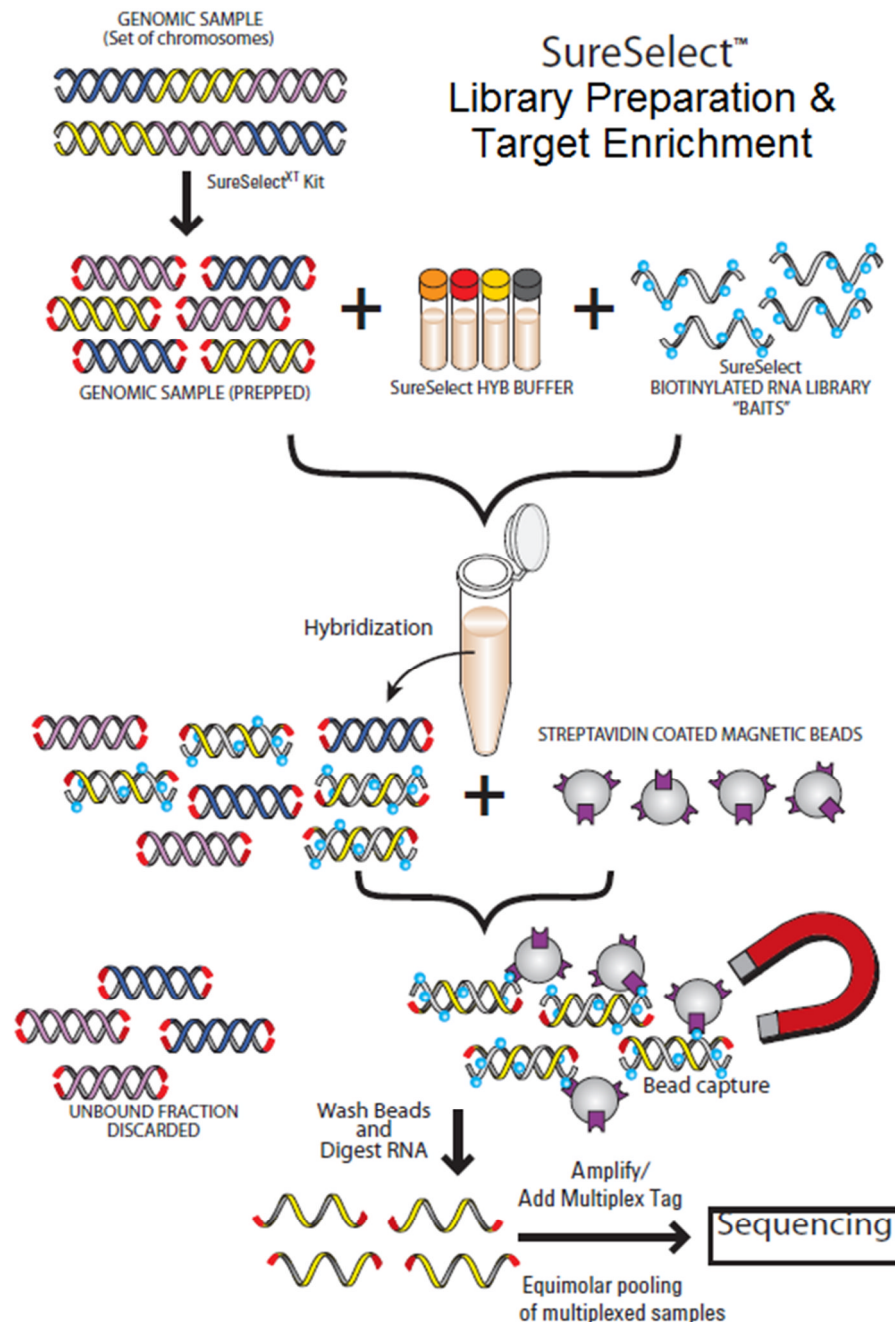
Figure 6.2: Sureselect™ library preparation and target enrichment. Genomic DNA samples are prepped using the Sureselect™ Kit, where the DNA is sheared, repaired, indexed and selected via PCR using SureSelect™ Primer and SureSelect™ Pre-capture Reverse PCR primers. Following hybridisation with the SureSelect™ capture library, regions of interest are captured using streptavidin magnetic beads. DNA sequences are then washed off the magnetic beads and RNA contamination removed. The samples are then ready for sequencing. Diagram adapted from (Agilent, 2012).

Illumina sequencing utilises cBot for automated cluster generation, followed by a sequencing by synthesis (SBS) reversible terminator technology, to generate data for the region of interest (Shendure and Ji, 2008, Metzker, 2010, Ansorge, 2009). Fragmented genomic DNA is bound to two unique adapter oligonucleotides at both

ends resulting in fragments between 150 and 200bp in size. These fragments are then immobilised on a flow-cell surface that facilitates the access to DNA polymerase enzymes, reducing the degree of fluorescently labelled dNTP non-specific binding and therefore resulting in a highly stable surface template. This immobilization occurs through the hybridisation of the adapter oligonucleotides to a lawn of corresponding oligonucleotides present on the surface of the flow-cell. As the free distal end of the DNA fragments is complimentary to nearby surface bound oligonuceotides, a dense cluster of fragments (*circa.* 2000 per cluster) of the original DNA template is able to form via 3 prime replication using solid phase bridge amplification (Fig. 6.3a). Sequencing is then carried out by the addition of a single fluorescently labelled dNTP to the DNA chain followed by the capture of fluorescence following laser excitation. The dNTP is enzymatically cleaved and the next dNTP incorporated. In this way bases are identified sequentially (Fig. 6.3b).
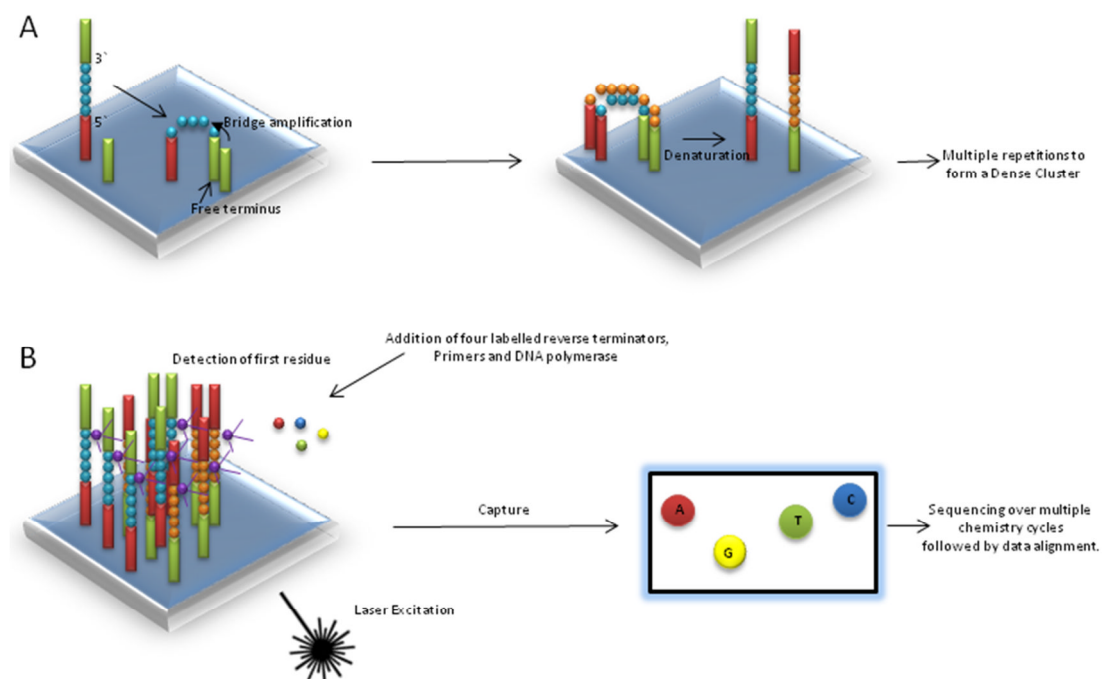
Figure 6.3: Solid phase bridge amplification, cluster formation (A) followed by Illumina sequencing (B). Adaptor sequences bound to fragmented genomic DNA are immobilised on a flow-cell. Binding to adjacent free adaptors allow for 3 prime directed bridge amplification, forming a dense cluster of the same sequence. Fluorescent based sequencing is then carried out followed by data alignment.

As the total region sequenced was 67539bp (Chr19:44,141,930-44,209,469) the total region size sequenced in a single lane was 4.5Mb (67539bp x 66) for each indexed sample. The Illumina product specifications identify that approximately 10GB of data is generated for each lane of sequencing with 60% on target efficiency expected using the HiSeq2000 systems pipeline. Therefore, considering that sequencing for *PLAUR* was carried out in tandem with sequencing for *IL33* and *IL1RL1/IL18R1* locus to a total sequence of 54MB, the estimated average coverage per individual was 37-fold calculated from: 10GB data/3 pools/54MB region x 0.60 efficiency.

6.3.5 DATA ANALYSIS

6.3.5.1 QUALITY CONTROL

All data analysis was carried out in collaboration with Mr Nick Shrine (University of Leicester) using the UNIX operating system. Data was converted into a Sequence Alignment/Map (SAM) Output format using the Burroughs-Wheeler transform construction algorithm (Burroughs and Wheeler, 1994). SAM files are TAB-delimited text files consisting of an optional header section and an alignment section. Each alignment line has 11 mandatory fields for essential alignment information such as mapping position, and variable number of optional fields for flexible or aligner specific information. Data was then run using the software package SAM Tools (Li et al., 2009a) which provides various utilities for manipulating alignments in the SAM format, including sorting, merging, indexing and generating alignments in a per-position format. Briefly, using SAM Tools, any unmapped reads and duplicate reads were removed and mapped reads sorted. Base quality was then re-calibrated, which assigned a score to each read reflecting the degree of confidence of the base-calling algorithm. This score operates within an effective dynamic range of 2-40, where 40

indicates that there is a 1 in 10,000 chance that the called base is incorrect (99.99% accurate) and is currently the highest effective score that a single base can receive under normal conditions.

6.3.5.2 VARIANT CALLING AND MAPPING

Data was then transformed in a Variant Call Format (VCF) output. VCF files are a text files format that contains meta-information lines, a header line, and data lines, each containing information about a position in the human genome. Conversion to VCF format allowed mapping of the reads to the NCBI GRCh37 genome template using the command: /human_glk_v37.fasta/ and alignment of called variations to the NCBI's SNP database (dbSNP) in order to identify already known variants, using the command dbSNP_132_b37.vcf. Realignment around insertion deletions and recalibration of quality scores was carried out using the freeware software programme GATK (DePristo et al., 2011), while variant detection was carried out using the freeware software program Syzgy® (Rivas et al., 2011), both run on the UNIX platform, forming tables identifying total and novel variations. Variants were called using a cut-off quality score of 10 which corresponds to a P-value of $P{\leq}0.1$, below which the accuracy of the called SNPs cannot be confidently established. Using this cut off point reduced the number of false calls in this analysis.

Novel variants were differentiated from the total number of variants called using data from the 1000 Genomes Project. The 1000 Genomes Project is a continuously updating sequencing and genotyping project with data being freely deposited online. The latest data releases, which contains calls based on 629 individuals, for the full project genotype release (16 December 2010) and indel release (16 February 2011) were

analysed using VCF version 4.0 files. These were extracted from the EBI FTP site[13] using the following commands in UNIX via tabix (Li, 2011):

tabix -h

ftp://ftp.1000genomes.ebi.ac.uk/vol1/ftp/release/20100804/ALL.2of4intersectoin.20100804.genotypes.vcf.gz

19:44,141,930-44,209,469

6.3.6 IDENTIFYING WHETHER IDENTIFIED NON-SYNONYMOUS SNPS ALTER *PLAUR* STRUCTURE

In order to identify whether any identified novel non-synonymous SNPs caused a change in PLAUR structure and therefore whether these SNPs had potential biological reference, SNPs were analysed *in silico*, using PolyPhen-2[14].

Briefly, the protein FASTA sequence for full length PLAUR was pasted into the required field, the position within the protein sequence of the amino acid altered by the identified non-synonymous SNP was entered into the required field and the type of amino-acid change selected before the query was submitted.

---

[13] Available at - ftp://ftp.1000genomes.ebi.ac.uk/vol1/ftp/
[14] Available at - http://genetics.bwh.harvard.edu/pph2/index.shtml

6.4 RESULTS

6.4.1 BAIT DESIGN

Sureselect™ run statistics identified that 39270 base pairs of the total selected target length of 67540 base pairs were covered by the bait design, i.e. a total of 58.14% of the targeted base pairs being covered. Visualisation of the bait design on the USCS genome browser (Fig. 6.4) highlights that the areas not targeted by baits have been strongly masked by both the windows and repeat maskers identifying that these regions (>40% of the selected region) were unreadable using current technology. This is due to the presence of a large number of repeats and runs in the genetic sequence in these regions. Therefore these regions were not integrated into the analyses. Unreadable regions were present throughout the whole region of interest in both the untranslated ends and in the gene intron structure. The largest unreadable region is present in the intronic region between exons 6 and 7 with other large unreadable regions present in the regions between exons 2 and 3 and 3 and 4 as well as in the 5`UTR. The 3`UTR is relatively well covered by the baits. However, gene exon regions were fully covered by the designed baits and therefore have the potential to be completely sequenced.
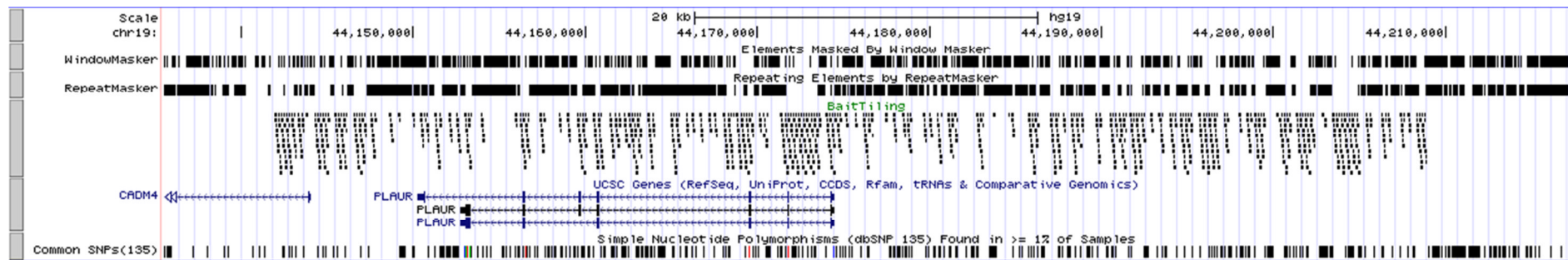
Figure 6.4: A screenshot from the USCS genome browser identifying regions on chromosome 19 covered by the designed baits. Loading of .bed files into the UCSC browser along with the custom track designed by Mr Richard Capper (see Section 6.3.3) displays tracks identifying areas masked by the windows and repeat masker, locations of known SNPs and the location of the *PLAUR* gene. This identifies that a large section of the gene and its untranslated regions are unreadable using current technology and therefore will not be integrated into the current analyses. Baits at the 3 prime end overlap with the gene for cell adhesion molecule 4 (*CADM4*) which is in close proximity to the *PLAUR* gene. Although present within an alternate gene these baits were included in the final library used for sequencing as they may still affect *PLAUR* expression through their close proximity to *PLAUR*.

6.4.2 DETERMINING SEQUENCING DATA ENRICHMENT EFFICIENCY

Bait mapping quality was significantly low, with data generated for the region of interest being only marginally elevated when compared to non-targeted sequencing throughout the human genome (Fig. 6.5). The percentage mapped reads for the individual pools for the region of interest averaged at 3.49% compared to a non-specific mapping of ∼1.5% on other non-specific chromosomes.
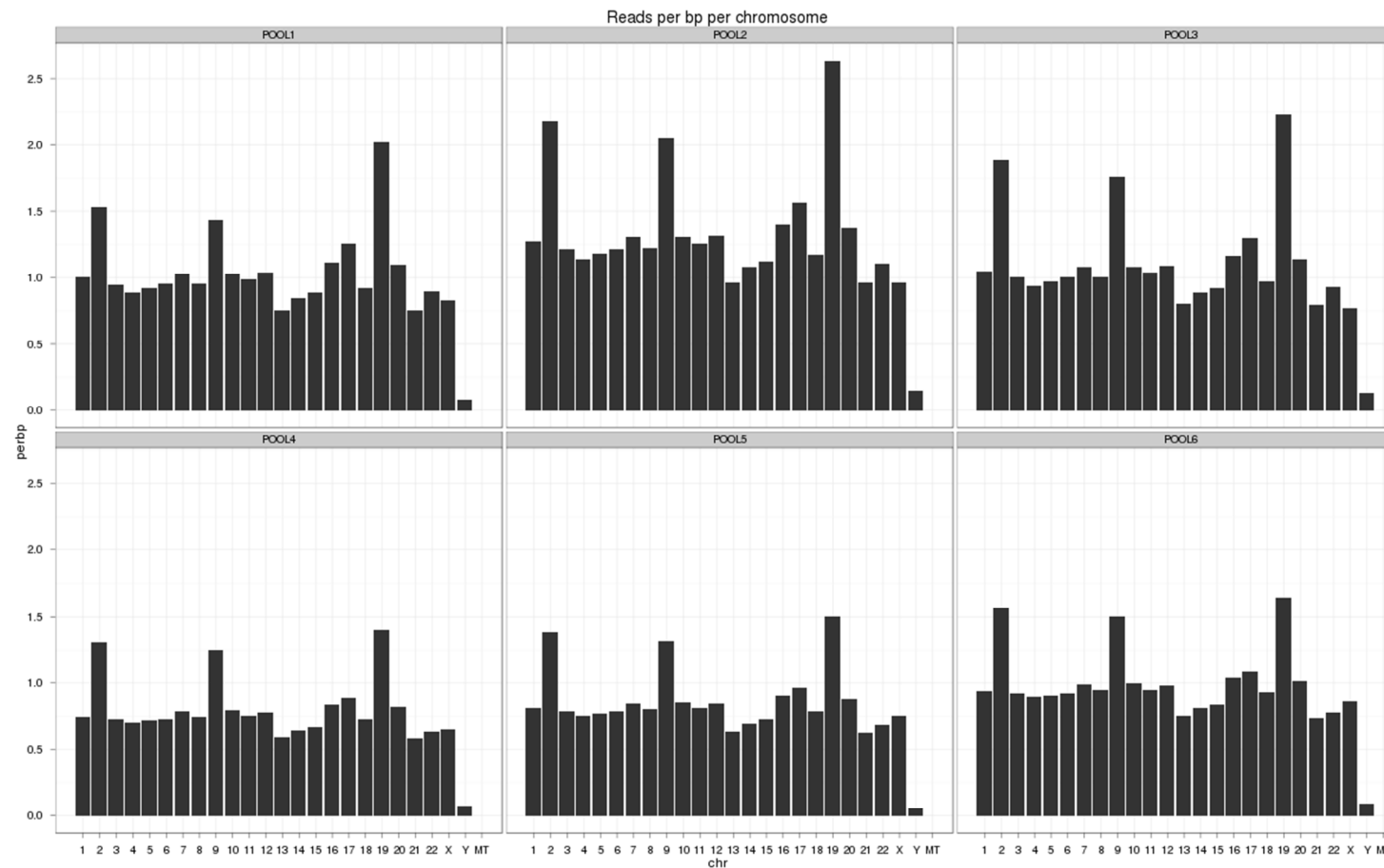
Figure 6.5: Mapping distribution of reads across the human genome. Reads obtained from the next generation sequencing targeted to PLAUR (Chromosome 19), which was run in conjunction with targets in Chromosomes 2 and 9, identify that mapping to targeted areas was only modestly enriched for Chromosomes 2, 9 and 19 using SureSelect® enrichment. This identifies that the sequencing procedure is not optimal and may therefore not produce accurate variant calling results.

Overall percentage mapped reads for individual pools for all 3 regions sequenced averaged at just 9.15% (Table 6.2).

Pool	Percentage Mapped (*PLAUR* only)
Pool 1	7.5%
Pool 2	9.7%
Pool 3	10.5%
Pool 4	9.5%
Pool 5	9.1%
Pool 6	8.6%

Table 6.2: Percentage mapped reads per sample pool. A uniform degree of low mappability for the *PLAUR* gene is present across all pools.

This therefore affected coverage of the targeted region, limiting the overall and specific (*PLAUR*) gene coverage as identified in Table 6.3.

	Min.	1st Qu.	Median	Mean	3rd Qu.	Max
POOL1	0	3.39	5.38	4.93	6.5	11.36
POOL2	0	4.74	8.41	7.82	10.77	17.42
POOL3	0	4.09	7.29	6.83	9.4	14.74
POOL4	0	2.5	4.38	4.03	5.52	9.53
POOL5	0	2.62	4.55	4.17	5.67	8.88
POOL6	0.01	2.82	4.71	4.41	5.88	9.59

Table 6.3: Coverage statistics for the PLAUR region (67.5Kb) based on sample coverage. As indicated by the low mapping specificity of the sequencing reaction, coverage for the targeted area is low. Values define fold coverage per sample in the *PLAUR* targeted region. Min = Minimal coverage detected; 1st Qu. = First Quartile (25% of values are below this value); 3rd Qu. = Third Quartile (75% of values are below this value); Max = Maximal coverage detected.

Importantly 75% of all subjects had a coverage of <11% with the control population (Pools 4-6) having the lowest coverage (<6%). This highlights the limitation of this study in that poor coverage has reduced overall quantity of sequencing data as well as its quality as there is a) around 50% less coverage and therefore data in the control population and b) there are a number of samples with no coverage, reducing pool numbers. This results in the next-generation sequencing being unable to reliably call

rare variants. However, despite this limitation, some analyses could be performed and these are summarised in the next section.

6.4.3 IDENTIFICATION OF VARIANTS PRESENT IN THE COMBINED POPULATION

Variant detection was carried out through the alignment of the genomic position of each identified variant (SNPs or insertion/deletions) to the reference genome in order to identify positions at which differences between read and reference occur in a significant degree. Using a number of criteria including read depth and mapping quality, a quality threshold (indicating the probability of error in the variant call) was determined for the data. This helps identify false calls within the dataset and therefore allows for subsequent removal of the false call data from the dataset. Standard quality score thresholds for next-generation sequencing, such as that carried out in the 1000 Genomes Project, is <30 which corresponds to $P \leq 0.001$ error, i.e. a 1 in 1000 probability that the base call is wrong (99.9% accuracy of base calling). However, this was not utilised in this dataset due to the high level of false negatives called at this level, with a quality threshold for exclusion set to <10 instead. This corresponds to a $P \leq 0.100$ error, i.e. a 1 in 10 probability that the base call is wrong (90% accuracy of base calling). Using a quality threshold of <10, 398 variants including 15 SNPs validated by the 1000 Genomes Project that would have been excluded at a quality threshold level of <30 were included in list of variants called. This was equivalent to 42.66% of all called variants.

Called variants mapped to data from the 1000 genome project identified a total of 933 variants of which 597 were defined as novel, present in the combined population but not in the 1000 Genome Project mapped to the GRCh37/hg19 build of the human

assembly. Of the novel variants, 62 (10%) had a frequency of less than 1% (Table 6.4)

and can therefore be defined as rare variants (Lemire, 2011).

Variants Called	Number of variants	Variants called by the 1000 Genomes Project
Total	933	1498 (total) 329 (common [>5%])
Novel and Quality Controlled	597	n/a
Novel, Quality Controlled and Rare (<1%)	62	n/a

Table 6.4: Variant calling results for the *PLAUR* gene and its surrounding areas. Variant calling identified a total of 933 variants that satisfied quality control criteria of which the majority (64%) were novel variants. Of these novel SNPs, 62 (10% of total) were identified as rare variants. Although only ~23% of the total number of called variants by the 1000 genomes project in the same region have been identified in this analysis, when only common variants were selected in both datasets ~81% (267 variants) of the total common variants defined by the 1000 genome project were identified .

Of the 597 novel variants identified, 7 novel SNPs were identified within *PLAUR* exons

regions (Table 6.5), specifically within exons 1, 5, 6 and the terminal exon (7a), which

is unique to the membrane bound receptor. All of these exon SNPs were, at the time of

detection, novel variants; however by the time of writing all variants except that at

position 44156419 were reported by the 1000 Genome Project.

Position (Chr 19)	Exon	Type	A.A	Major/Minor Alleles	Frequency (Cases)	Frequency (Controls)
44174249	1	Synonymous SNP		C|T	0.0033	0.0149
44159722	5	Non-synonymous SNP Change from [R] to [H]	159	C|T	0.0056	2.00E-04
44156419	6	Synonymous SNP		G|A	0.005	1.00E-04
44156472	6	Non-synonymous SNP Change from [K] to [R]	191	T|C	0.1926	0.1751
44153100	7a	Non-Synonymous SNP Change from [L] to [P]	274	A|G	0.1528	0.1415
44153248	7a	Non-synonymous SNP Change from [M] to [V]	268	T|C	0.0014	0.0054
44153255	7a	Synonymous SNP		G|A	0.0154	0.0246

Table 6.5: Identification of novel variants located in the *PLAUR* exons. Through re-sequencing 7 SNPs located in the gene's exon regions were identified 4 of which cause a change in the gene's amino acid backbone. These changes are located at amino acid positions 159 and 175 (Domain II) and at positions 268 and 272 (Domain III). 4 of these SNPs are rare variants occurring in <1% of the population. A.A. = Amino acid.

However this analysis, as suggested by the quality control results, was highly limited. In the first instance a total of 24 SNPs documented in database SNP and the 1000 Genomes Project were excluded in the final dataset as they did not achieve a quality score of >10. Secondly, only 336 previously known variants for the entire region analysed were identified (for full list of called variants see Appendices). Considering that as of writing the 1000 Genomes Project has identified 1498 variants with the same region, it would suggest that a large number of variants have not been called in this analysis. However, when only common variants were selected in both datasets ~81% (267 variants) of the total common variants defined by the 1000 genome project (329 variants) were identified. This therefore suggests, as indicated by the low coverage generated for this analyses (see Table 6.3) that this analysis while being able to pick up most common variants, is unable to reliably call rare variation. Therefore a number of false negative calls have, especially with regards to rare variants, likely been made and subsequently a large number of variants have been missed by this experimental procedure.

6.4.4 ONE NON-SYNONYMOUS SNP ALTERS PLAUR STRUCTURE

Using PolyPhen-2, the polymorphism at position chr19:44153100, produced a high PolPhen-2 score and was therefore deduced to be damaging to the PLAUR protein structure (Table 6.6) and therefore potentially results in a biologically relevant role. All other non-synonymous polymorphisms were identified as benign, causing no change to PLAUR protein structure.

SNP Position	Amino Acid	Amino Acid change	Score	Result
44159722	159	[R] to [H]	0.002	Benign
44156472	191	[K] to [R]	0.000	Benign
44153100	274	[L] to [P]	0.999	Probably Damaging
44153248	268	[M] to [V]	0.346	Benign

Table 6.6: Only one of the novel non-synonymous SNPs causes an amino acid change that is potentially damaging to PLAUR structure. This identifies that this SNP has a potential biological role through alteration of PLAUR function. All other non-synonymous SNPs cause amino acid changes that do not significantly alter the PLAUR protein structure.

6.4.5 IDENTIFICATION OF ASTHMA SPECIFIC VARIANTS

Variant calling was split based on pools, with data from pools 1, 2 and 3, (pools containing samples from the asthma population) compared to data from pools 4,5 and 6, (pools containing data for the control population). Analyses of the split data identified that a total of 4 novel variants were exclusive to Pools 1, 2 and 3 and therefore exclusive to the asthma population (Table 6.7). No unique SNPs were identified for pools 4, 5 and 6, i.e. the control population. All of these identified asthma specific SNPs were novel and rare variants.

Mapping of the asthma specific variants to the human genome identified that the SNP at position 44167227 is located within the gene region for *PLAUR* (chr19:44,150,271-44,174,502; Build 37). Closer investigation identified that this SNP lies in intron 3. The remaining variants (one insertion and two SNPs) were respectively located in the gene's 5'UTR at 9206bp, 20634bp and 30138bp upstream from the gene's TSS.

Position (Chr19)	Type	Major/Minor Alleles	Frequency (Cases)	Frequency (Controls)
44167227	SNP	C|T	0.0085	0
44183708	Insertion	G|GAT	0.0034	0
44195136	SNP	C|T	0.0056	0
44204640	SNP	G|T	0.0058	0

Table 6.7: Identification of rare variants unique to the disease population. An analysis has identified 4 variants unique to asthmatics of which one lies in the gene's intronic region between exons 3 and 4. The remaining variants were found to lie in the gene's 5`UTR up to a maximum of 30138 base pairs upstream of the transcriptional start site.

6.5 DISCUSSION

The aim of this chapter was to identify novel variants, including both SNPs and insertion-deletions, present within the *PLAUR* gene and its 3`UTR and 5`UTRs, with a special interest in the detection of rare variants. Secondary to that any novel variants that were unique to either 200 severe asthma patients or the control population of 200 non-asthmatic, non-atopic and non-wheeze individuals would also be identified.

Although attempts to tackle these aims can be considered to be successful based on the calling of a number of variants, one must take into consideration that limitations in the dataset exist. Firstly, the bait design protocol has, due to restraints of current technology, been unable to map more than 58.14% of the targeted base pairs, meaning that potential variation in >40% of the targeted region has been missed. Secondly, results were obtained from an experimental dataset with poor mapping and limited target enrichment/coverage. Poor target enrichment and coverage suggests that the resulting sequencing would be unreliable in the calling of rare variants within the region. This was confirmed by the identification that while ~81% of the common variants known to be present within the region were successfully identified by this analysis, only 69 of the 1169 rare variants called by the 1000 Genomes Project (~6%) were called. Therefore although this work has confidently presented novel variants and meaningful data on variant distribution in a combined and separated asthma and control cohort, it is not a complete picture of *PLAUR* variation as it has been identified that the analyses were severely underpowered in the detection of rare variants. However, due to the high degree of detection for common variants one is able to confidently exclude the existence of any common novel variants present just in the asthma population.

Using pooled data, a number of novel variants have been detected to be present in the combined case and control population and a number of SNPs (*n*=4) unique to the diseased population have been identified. These identified variants included a number of rare variants, which the re-sequencing was able to detect due to the high depth of coverage that results from process of next-generation sequencing (37 fold expected).

Although only a small number of SNPs (n=4) were identified as unique to the disease cohort, these were all classified as rare variants, i.e. present in less than 1% of the studied population. Rare variants have been hypothesised to play an important role in both common and complex disease (Pritchard, 2001, Iyengar and Elston, 2007) where, unlike common associated variants which usually generate small effect sizes, rare variants have been hypothesised to be the primary drivers of common disease (Cirulli and Goldstein, 2010). With reference to respiratory disease and in keeping with the common disease/rare variant hypothesis, where it is supposed that rare allelic variation has an impact on clinical applications such as the design of prognostic assays and the planning of therapeutic investigations (Iyengar and Elston, 2007), rare variants have been associated with asthma susceptibility (Torgerson et al., 2012, Haller et al., 2009). This adds significance to the identification of *PLAUR* rare variants in the asthma population, where presence of the risk alleles of these rare variants may be contributing significantly to the development and/or modulation of asthma.

Of the 4 rare variants unique to the asthma cohort, one was also present within the gene itself. Although one may at first dismiss this variant due to its presence in one of the gene's intronic regions, meaning that this SNP does not alter the PLAUR protein structure, there is still potential that it may play a role in the modulation of asthma. This argument is based on recent work by Torgerson *et al.* that have identified non-coding rare variants in gene intronic regions to be significant contributing factors towards asthma susceptibility (Torgerson et al., 2012).

Detection of 7 novel variants within several exon regions of the *PLAUR* gene has identified novel regions that may cause potential structural changes in the receptor. This was confirmed by the identification of 4 of these variants as non-synonymous, causing a change in the amino acid backbone of the protein within the receptor's Domains II and III. *In silico* analysis identified that one of these variants, which is present in the region coding for Domain III, has the potential to alter receptor domain structure and therefore domain driven receptor effects, such as binding to integrins, marking this variant as of possible biological importance. The location of this SNP within domain III is of special importance considering the conclusions derived in Chapter 5, that Domain III is the essential region driving PLAUR effects on scratch-wound healing.

All the 7 novel variants within several exon regions of the *PLAUR* gene were classified as SNPs, with half defined as rare variants. Therefore when one considers the rare variant hypothesis, it can be supposed that these SNPs might play a greater role in *PLAUR* regulation, an important observation when considering their potential in affecting receptor structure. By the time of writing, 7 of these identified variants had been validated by the 1000 genome study, with the synonymous SNP at position 44156419 being the only one currently unreported.

Therefore, in conclusion, this work has added to the knowledge of *PLAUR* gene and untranslated region variation, identifying a number of novel common and rare variants. Identification of novel disease specific rare variants provide possible new targets for further study of disease specific gene regulation, while identification of novel rare variants within the gene's exon structure relating to Domains II and III identifies variants that have a potential effect on *PLAUR* driven biological functions and *PLAUR* associated diseases.

Overall, these results add weight to the hypothesis that rare variation explains some of the genetic heritability that still needs to be identified in asthma. Further work will need to be conducted to determine the functional implications of both the disease specific variants and the exon region variants. Also it would be interesting to investigate the relationship between common *PLAUR* SNPs previously associated with asthma, lung function and gene expression (Barton et al., 2009, Stewart et al., 2009) and the newly identified rare variants.

CHAPTER 7:

GENERAL DISCUSSION

CHAPTER 7: GENERAL DISCUSSION

7.1 HYPOTHESIS AND AIMS

The basis of this work is the hypothesis that the urokinase plasminogen activator receptor plays an important role as a marker and modulator of disease in asthma and COPD. This hypothesis is based on two observations. Firstly there has been ample evidence that the coagulation/fibrinolytic pathways, in which PLAUR plays an important role, are important in the development and progression of both asthma and COPD (Polosa et al., 2011, de Boer et al., 2012). Here increased deposition of fibrin in the airways significantly contributed to airway hyper-responsiveness (Wagers et al., 2004) while elevated levels of plasmin had a direct role in modulating the degree of airway remodelling (Kucharewicz et al., 2003). Secondly, at the genetic level, studies carried out by colleagues in the same research group have identified an association between *PLAUR* SNPs and asthma susceptibility, lung function decline and serum PLAUR levels (Barton et al., 2009). In addition, *PLAUR* SNPs were found to determine baseline lung function in smokers (Stewart et al., 2009), while PLAUR protein levels were found to be elevated in the airways of asthma patient particularly in the epithelium. Similar findings were also described by others in COPD (Wang et al., 2008). Therefore, it was hypothesised that differential regulation of the expression of different forms of the receptor (full length membrane, soluble cleaved and soluble spliced), which potentially have their own specialised functions, would play an important role in the development of PLAUR mediated airway disease through the alteration of lung-expressed and circulating PLAUR levels.

Although there have been multiple publications tackling the transcriptional regulation and post-transcriptional modification of PLAUR mRNA (Allgayer et al., 1999, Buchler et al., 2009, Dang et al., 1999, Soravia et al., 1995, Bhandary et al., 2009, Shetty and Idell,

1999, Velusamy et al., 2008), these have been limited to cancer cell lines which, by their very definition, are different from the cells normally present in the body. Also a lack of studies investigating how the regulation of PLAUR differs under stimulus pertinent to respiratory disease made the study of *PLAUR* regulation an important aim. Interestingly, there has also been no attempt to discern the regulation of the soluble spliced form of the receptor or whether this structurally different molecule has a role similar to that of full-length PLAUR, a question this thesis has also undertaken to answer.

The aims of this thesis were:

1. To investigate the relationship between scPLAUR and obstructive lung disease (asthma & COPD) diagnosis and clinical parameters

2. To identify novel genetic mechanisms regulating scPLAUR levels

3. To define the relative contribution of proximal PLAUR regulatory regions in determining gene expression

4. To determine the functional role of different PLAUR forms in primary bronchial epithelial cells

5. To identify both rare and common genetic variants spanning PLAUR and to identify which of these are relevant to asthma

7.2 MAIN FINDINGS

Levels of scPLAUR in serum were found to be elevated in COPD subjects in relation to asthmatics and controls and in asthmatics when compared to controls. The elevation identified in the asthmatic phenotype was particularly driven by the non-atopic sub-population, which presents with a different clinical picture to atopic asthma in the study population. In general non-atopic asthmatics have a greater degree of macrophage dysfunction with inflammatory processes having a less significant role in the pathophysiology of the disease (Humbert et al., 1999, Rackemann, 1947). Non-atopics also tend to be older and develop a more severe form of the disease (Rackemann, 1947, Humbert et al., 1999). Indeed recent data (unpublished) suggests an association between PLAUR SNPs and age of onset of asthma. In the studied cohort, non-atopic asthmatics had a lower degree of fixed airway obstruction than atopic asthmatics, to a degree approaching that of COPD. Further evidence linking PLAUR to changes occurring in the airway is provided by the identified strong correlation between smoking and PLAUR expression, which indicates that cigarette smoke, which is an important causative factor for the airway changes occurring in both asthma and COPD (Wang et al., 2005), has a role in modulating PLAUR driven effects.

As serum scPLAUR levels did not change when subjects were stratified based on the GOLD defined score of COPD severity or asthma severity as defined by nocturnal awakenings, it suggests that while scPLAUR may be associated with the disease *per se*, it is not involved in disease progression leading to a more severe disease state in the analysed datasets. However, previous association of scPLAUR with COPD severity in induced sputum (Jiang et al., 2010) suggests that the soluble receptor is in fact associated with disease progression, but only locally at the airways with the changes not translated to changes in scPLAUR levels in the periphery. Association with disease severity would correspond to the later deduction that PLAUR has an active role in

modulating changes in the airway (see below). Association with disease follows from previously published literature, where in general elevated scPLAUR levels have been associated with other inflammatory diseases as a marker of disease-related mortality, while specifically elevated scPLAUR has been identified in the asthmatic and COPD lungs and in the induced sputum of asthmatics and COPD patients (Stewart et al., 2012, Wang et al., 2008, Xiao et al., 2005, Jiang et al., 2010). Strong associations with non-atopic asthma and COPD potentially suggest that scPLAUR may be related to the more severe changes occurring in these airways (lower degree of airway reversibility/greater degree of airway obstruction), supported by the reported association between PLAUR SNPs and FEV_1/VC in smokers (Stewart et al., 2009). Therefore it is likely that scPLAUR is involved in airway remodelling, even though this process can vary significantly between asthma and COPD (Dournes and Laurent, 2012).

The hypothesis that scPLAUR plays a role in the process of airway remodelling follows on well from published work that suggests that PLAUR and the plasminogen activator system have active roles in airway remodelling (Stewart et al., 2012, Kucharewicz et al., 2003, Stewart and Sayers, 2013), with the effects of full-length PLAUR potentially explained by the soluble cleaved form of the receptor (Stewart et al., 2012). A recent study by Zhang *et al.* has also associated changes in PLAUR and its related molecules (PLAU and PAI-1) to airway remodelling (Zhang et al., 2012). An *in vitro* study using NHBECs where mechanical stimulation of cells in order to mimic the process that occurs in the lung during bronchoconstriction resulted in a 16.2 fold increase in the expression of PLAUR (Chu et al., 2006), added further weight to this hypothesis. This is of importance when considering that this repeated contraction of the airways has been shown to be a driving force of airway remodelling in the absence of inflammation through progressive extracellular matrix deposition (Holgate et al., 2010). More direct evidence of a role for PLAUR in airway remodelling has been recently made available by colleagues from the same group (unpublished work). Here *PLAUR* SNPs have been

associated with a number of pro-airway remodelling outcomes such as thickening of the basement membrane, increased collagen III deposition and airway epithelial proliferation, all hallmarks of remodelling in asthma, while other PLAUR SNPs have been associated with lung function decline (Barton et al., 2009, Koppelman and Sayers, 2011).

Over-expression studies involving mPLAUR and scPLAUR, confirmed a role for the receptor in bronchial epithelial cells with PLAUR and scPLAUR attenuating wound repair and scPLAUR independently doubling the rate of cellular respiration. This therefore identified a role for scPLAUR in the bronchial epithelium independently of the membrane-bound receptor such as that recently described by Wei *et al.* in the kidney disease, focal segmental glomerulosclerosis (FSGS) (Wei et al., 2011, Wei et al., 2008). Here the authors describe how circulating levels of scPLAUR independently activate podocyte β_3 integrin, resulting in the modulation of the disease and therefore suggesting that scPLAUR is essential for disease development and not simply a by-product of disease. The migration and cellular respiration results obtained on cultured NHBECs presented in this thesis, combined with data identifying an elevation of scPLAUR in disease with pronounced airway remodelling, allows one to hypothesise that scPLAUR may act in a similar way in asthma and COPD. Here scPLAUR may directly modulate the changes occurring in the airway, such as dysregulation of the rate of wound repair and the rate of proliferation, which are reflective of airway remodelling, independently of other forms of PLAUR. This in turn is at least in part driven by effects of specific PLAUR SNPs on expression levels.

Failure, in the same dataset, to associate lung function and bronchial hyper-responsiveness to circulating levels of scPLAUR may seem surprising in light of the originating studies that identified the *PLAUR* gene as a gene involved in BHR and lung function (Barton et al., 2009, Stewart et al., 2009). However, this may be explained if

one considers that SNPs may regulate any of the different forms of PLAUR and ergo, the reported gene-based effect on lung function decline may not be due to scPLAUR. Also, there are fundamental differences between the analysed datasets. Firstly, while the original analysis identified the main genetic evidence in children with asthma, the dataset analysed in this thesis dealt with a general population. Secondly, this work has looked at a cross-sectional measurement of lung function, which differs from the measurements originally reported both by Barton *et al* and Stewart *et al.,* which were longitudinal in nature. Therefore, if the effects of PLAUR on lung function are exclusive to changes in decline of lung function over a period of time, it would be unsurprising that an association would not be detected by investigating scPLAUR levels at only one time point.

In order to identify novel regulatory networks, a genome-wide association approach was used. This method allows for the examination of genetic variants over multiple individuals identifying, in a hypothesis-free environment, novel variants associated with a trait. Using this method, potential obscure regulatory pathways for scPLAUR expression could be identified, that would otherwise not be identified by traditional methods of detection for novel regulatory pathways, such as familial inheritance studies using genetic linkage. In this thesis, GWAS identified a novel scPLAUR regulatory protein, Human Plasma Kallikrein (KLKB1). KLKB1 was found to regulate scPLAUR through a novel mechanism, that is, proteolytic cleavage in the D_I region of PLAUR and lateral to the D_{III} region. Although this novel regulatory mechanism was present in the general population, KLKB1 activity was significantly attenuated in both asthmatics and COPD subjects. Alteration in KLKB1 function may therefore go some way in explaining the elevations of scPLAUR identified in the asthmatic and COPD populations and therefore may also be an important part of the cellular dysfunction process regulated by PLAUR. Importantly, the process of determining this novel regulatory mechanism was, at the time of writing, the first procedure by which a hit

from a GWAS was followed on and confirmed at the protein level. This has highlighted the limitations of attempting to define regulatory procedures solely through changes in mRNA levels. Indeed, attempts to replicate the protein-based association on an mRNA-based bioinformatics platform and on total cellular mRNA both failed to highlight association. Also, recent investigations to determine genetic variants affecting gene expression in human lung tissue did not highlight the *KLKB1* locus as a expression quantitative trait locus (eQTL)(Hao et al., 2012).

Transcription regulation studies have confirmed that in primary normal human bronchial epithelial cells, the minimal promoter region lies in the first 199bp downstream of the TSS, as previously reported (Dang et al., 1999, Soravia et al., 1995). However, this work is the first to report a region between 490bp and 887bp downstream of the TSS as being an additional PLAUR 5`UTR regulatory region. Also the 3`UTRs of the *PLAUR* gene for both full length and soluble spliced were determined to have an overall suppressor role on PLAUR mRNA expression, which is also novel, being the first description of 3`UTR directed gene suppression for *PLAUR*. This therefore confirms the general outlook on *PLAUR* expression in that it is a balance between 5`UTR (transcriptional) and 3`UTR (post-transcriptional) events. Investigations into how stimulations relevant to the asthmatic and COPD lung affected *PLAUR* gene expression identified that changes in PLAUR expression driven by scratch wounding (Stewart et al., 2012) were not driven by either 5`UTR (corresponding to the limited 5`UTR investigated) or 3`UTR driven regulatory effects. This suggests that changes in PLAUR expression levels in NHBECs, driven by wounding of the bronchial epithelium, probably occur distally to those includeg in the reporter constructs (see Section 7.3). These could include intragenic regions, as well as lateral regions to the 5`UTR and 3`UTR constructs used. Stimulation by cigarette smoke extract similarly has no effect on expression of the *PLAUR* gene driven by the investigated 5`UTR. However, it does appear to fully negate the 3`UTR driven suppression of the *PLAUR* gene that encodes

the soluble spliced form of the receptor. Protein and mRNA-based experiments confirmed that cigarette smoke extract specifically elevates ssPLAUR but does not affect the expression of full length PLAUR. This is of special interest when considering that ssPLAUR over-expression experiments identified a substantial increase in the rate of NHBEC cellular respiration driven by ssPLAUR independently of the full length membrane bound receptor. Using the hypothesis that the rate of cellular respiration indicates a change in the rate of cellular proliferation, one is able to putatively link ssPLAUR to one of the mechanisms by which cigarette smoke affects the airways. This suggests that ssPLAUR may also have a role in airway remodelling and more importantly it could be the significantly contributing molecule behind PLAUR driven changes in the airways caused through smoke inhalation, i.e. changes occurring in COPD. This work is the first to identify a role for ssPLAUR and is also the first to identify the way by which this form of the receptor is transcriptionally regulated under both basal and stimulated conditions.

PLAUR is known to be an extensively polymorphic gene with 1315 polymorphisms identified by the 1000 genomes project within the gene region (Chr 19:44150247-44174498). The highly polymorphic nature of the gene makes it likely that further undefined variation is present within the gene and its untranslated regions that could affect general and disease-specific gene expression. Next generation sequencing of the *PLAUR* gene and its lateral regions has identified a number of novel variants and novel rare variants, substantially increasing the knowledge on variation for this gene and its regulatory regions. A number of variants were determined to lie within the gene's coding region and result in changes to the amino acid structure of the receptor, which makes these variants likely to have a role in affecting receptor gene structure and function. This analysis has also identified a number of variants that are exclusively present in the pool of severe asthma subjects. These may therefore contain gene regulatory elements that drive altered gene expression in disease.

7.3 LIMITATIONS

The work in this thesis however has not been without its limitations. In the first results chapter experimentation was carried out in a cohort of unrelated asthmatic individuals. However, the study by Barton *et al.*, from which this study has progressed, consisted of a study in a family cohort of two disease affected sibling pairs. Therefore, results of *PLAUR* SNP association studies must be considered in the light of:

a) The use of a different population in the original study, in which it is likely that the disease phenotype is altered (children tend to express atopic asthma with higher reversibility and are expected to be non-smokers) and

b) Analyses carried out in a cross sectional format (FEV_1 and FEV_1/VC at one time-point) as opposed to the longitudinal study (decline in FEV_1) carried out in the original study.

This may therefore in part explain the lack of replication for the association between lung function and *PLAUR* SNPs/scPLAUR levels occurring in this thesis.

In the second chapter a GWAS was undertaken; generally GWA studies require large populations in order to have the power to detect positive associations. The populations used in this chapter however were relatively small, with a control population of 104 and an asthma population of 480. Therefore it is highly probable that a number of regions that are in actual fact associated with scPLAUR serum levels did not achieve genome-wide significance in this study due to a low power of detection driven by small population sizes. This is highlighted by the detection of a number of other associated regions when using less stringent criteria that made biological sense such as Factor XII and NRG1, which are either known to directly interact with PLAUR or the PLAUR associated pathways. A true replication of the GWAS in an alternate population, which could have confirmed the association, was also not available at the time. The only

attempt at duplication was carried out in the COPD population, however this was also limited through small population numbers and by not being a true GWAS replication. Finally, further limitations in this experimental design are that GWAS itself is only powered to detect common variants (>5%), thereby missing potentially important regulatory rare variants, and that the investigation was carried out using a first generation platform containing ~300,000 SNPs, which gives significantly less coverage than the platforms currently on the market (e.g. the Illumina Infinium Human OmniExpress Exome BeadChip Kit that has over 700,000 genome-wide markers). Therefore, it is highly probable that other serum scPLAUR regulatory regions, describing other novel regulatory pathways, have been missed by this work.

In the third results chapter, successful introduction of a maximal length of 2584bp of the 5`UTR meant that known polymorphisms in the 5`UTR that had been associated with lung function and asthma (Table 7.1) were not investigated and therefore their effect on PLAUR expression was not quantifiable.

SNP	Location upstream of TSS
rs344779	3666bp
rs7259340	12331bp
rs11668247	20040bp
rs346043	20459bp
rs740587	22346bp
rs346043	20459bp
rs346054	30147bp

Table 7.1: Disease and lung function associated *PLAUR* SNPs not included in the Dual Luciferase reporter assay. As these SNPs have been shown to be associated with disease and changes in lung function it is likely that they may have an effect on PLAUR expression. Inability to include these SNPs into the dual reporter assay serves as a limitation when investigating 5`UTR driven changes in *PLAUR* expression.

Recent developments by ENCODE have confirmed this limitation in the approach utilised in this thesis to determine 5`UTR driven transcriptional regulation. Visualisation of the untranslated regions in the UCSC genome browser (Rosenbloom et

al., 2012) (see Section 5.5, Figure 5.29) identifies a transcriptionally relevant region, as defined by the ENCODE dataset, ~5kb upstream of the transcriptional start site confirming that experimentally an important regulatory region has been missed in the dual-luciferase assay. Also, ENCODE has determined that gene promoters are strongly regulated by long-range distal elements interacting with the promoter via a looping mechanism, most of which (>93%) do not interact with their closest gene (Sanyal et al., 2012). This suggests that gene promoter regulation is more complex than the model assumed in a dual-luciferase assay, i.e. a linear promoter region distal to the gene it regulates which extends to a certain distance upstream of the TSS and independently regulates gene expression.

Finally in the fourth results chapter, next-generation sequencing analysis has been limited through low capture due to bait design and lack of enrichment, especially with regards to rare variants. Therefore, while it is unlikely that the dataset has generated a set of false positive results, it is highly probable that a large number of false negatives have been generated and so a large number of PLAUR variants have not been detected by this analysis, especially when considering rare variants.

However, although it is appreciated that the work presented in this thesis has its limitations, these limitations are concerned with the generation of false negatives, and so do not detract from any of the findings presented.

7.4 PROPOSED FURTHER WORK

While this work has attempted to investigate the regulation of *PLAUR* gene expression, further work is still necessary to fully define the regulatory mechanisms involved in determining both mRNA and protein levels in health and respiratory disease. Full understanding of the regulatory process of *PLAUR* would require the inclusion of techniques such as the Chromosome Conformation Capture technique, DNase footprinting assay and the ChIP-on-chip method. These methods allow for determination of the structural properties and spatial organization of chromosomes important to the regulation of gene expression and the determination of interactions between proteins such as histones and transcription factors with DNA *in vivo*, respectively.

Suggested future work more closely related to the presented work would include investigation into the effect of PLAUR 5`UTR SNPs on gene regulation. Using the plasmid constructs built in this thesis, site-directed mutagenesis could be used to introduce mutations translating to SNPs rs4251805 and rs2356338. These are located at the 119bp and 649bp regions downstream of the TSS respectively, regions determined to be important to basal gene transcription. Other work involving the 5`UTR SNPs could be carried out by introducing small fragments containing asthma and lung function SNPs up to 10kb downstream of the TSS, to investigate whether gene folding, which may bring the SNPs in close proximity to the core promoter region, has any effect on basal *PLAUR* transcription. Although this work has successfully identified regulatory effect of the 3`UTR in mPLAUR and ssPLAUR expression, the mechanism is still not fully understood. *In silico* based analysis has identified a number of potential miRNA regulators and therefore experiments using these miRNA mimics and inhibitors would be useful in determining whether these molecules play a role in 3`UTR driven PLAUR regulation. Recent publications have also identified a number of miRNAs whose

expression in the airways is driven by the exposure of cigarette smoke (Pottelberge et al., 2011, Schembri et al., 2009, Izzotti et al., 2009), which putatively bind to the ssPLAUR 3`UTR. Inclusion of these miRNAs into a future study would also be of interest in light of the cigarette smoke extract driven changes in ssPLAUR 3`UTR regulation.

Results presented in this thesis also present scope for further work by presenting new questions about the role and regulation of PLAUR. The identification of KLKB1 as a novel regulator of scPLAUR expression raises the question whether this novel mechanism is relevant in scPLAUR associated disease such as focal segmental glomerulosclerosis and obstructive lung disease. This is especially relevant when considering the statistically significant difference in KLKB1 activity determined between control and asthma/COPD populations (see Chapter 4). This could be addressed through quantification of KLKB1 expression in the plasma of disease populations. Identification of a role for scPLAUR and ssPLAUR raises the question of what further processes these molecules are involved in. In order to obtain a complete understanding of the potential role of PLAUR it would be pertinent to use animal models. Animal studies using knockout and overexpressing mouse models would allow investigation of either scPLAUR or ssPLAUR driven effects in a complex living model rather than in simple single cell *in vitro* models.

Finally, although a number of novel variants have been determined through next generation sequencing for the PLAUR gene and its untranslated regions, the experimental set-up used in this thesis has not allowed for the direct identification of common and rare variants that drive the expression levels of PLAUR. Identification of such variants can achieved through the design of a novel next generation sequencing experiment where the frequency of detected variants across pools of subjects stratified according to plasma scPLAUR expression levels are compared.

7.5 CONCLUSIONS

In conclusion, this work has identified an association between scPLAUR levels in serum and the obstructive lung diseases asthma and COPD. Regulation of serum scPLAUR has been determined to involve proteolytic cleavage by KLKB1 at the PLAUR's D_I region and adjacent to the D_{III} region and scPLAUR having a probable role in modifying epithelial functions independently of the membrane bound receptor. Transcriptional regulatory studies have confirmed that the PLAUR minimal promoter in bronchial epithelial cells lies in the first 199bp downstream of the TSS and identified that PLAUR regulation is additionally driven by a region between 490 and 887bp downstream of the TSS as well as the 3`UTR (both membrane and soluble spliced forms). While scratch wounding did not alter PLAUR regulation, exposure to cigarette smoke extract nullified the suppressor role of the soluble spliced receptor's 3`UTR, resulting in an elevation of ssPLAUR, which this work has identified, has a probable role in modulating changes in the airway through a possible effect on epithelial cell proliferation rates. Various novel variants have been detected for PLAUR, including a number of rare variants and coding region SNPs as well as disease specific variants that substantially add to knowledge about variation in the PLAUR gene and its untranslated regions.

Apart from furthering the general understanding of the urokinase plasminogen activator receptor, these data have also confirmed a role for the receptor as a marker and modulator of asthma and COPD. In this way, these data have also addressed the originating hypothesis for this work, increasing the volume of evidence identifying that the various forms of PLAUR are important molecules that drive and maintain the asthma and COPD phenotype.

APPENDICES

APPENDIX I - BUFFERS AND SOLUTIONS

1. **50x TAE buffer:** Add 57.1ml glacial acetic acid to 242g Tris base and 100ml 0.5M EDTA at pH 8. Make up to 1l with deionised WATER. Dilute 1 in 50 to make 1x TAE buffer when required.

2. **6x Orange G loading dye:** Make up 30% glycerol (v/v) in deionised water. Add Orange G dye to make a solution of 0.25% w/v.

3. **1Kb and 100bp DNA ladders (ready to use):** Add 250μl 1Kb DNA ladder, or 50μl 100bp DNA ladder, to 500μl 10x BlueJuice™ or 100μl 6x Orange G gel loading buffer respectively. Make up to 2500μl or 500μl respectively using sterile water. Store in aliquots at -20°C.

4. **LB (Lysogeny Broth) Agar**: Add 400ml sterile water to 16g Miller LB agar. Autoclave immediately and store at room temperature.

5. **LB agar plates with antibiotics:** Melt the LB agar (see above) slowly until melted and starting to boil. Allow to cool to approximately 32°C. Add ampicillin or kanamycin as required to final concentration of 100μg/ml or 50μg/ml respectively, and mix quickly. Pour 25ml agar per plate and allow to set for 30 minutes. Store upside down, to prevent condensation dripping onto the agar, at 4°C.

6. **LB broth:** Add 500ml sterile water to 12.5g Miller LB broth powder. Autoclave immediately and store at room temperature.

7. **5x Reducing gel loading buffer:** Add 5.2ml 1M Tris (pH 6.8) to 1g DTT and swirl to dissolve. Add 1.3g SDS and mix. Add 6.5ml glycerol and 130μl 10% bromophenol blue. Mix by linear oscillation for at least 30 minutes. Divide into 500μl aliquots and store at -20oC.

8. **10x Tris-Glycine-SDS running buffer (250mM Tris base, 1.92M glycine, 1% SDS):** Add 800ml sterile water to 30.3g Tris base, 144g Glycine and 100ml 10%

SDS. Stir to dissolve. Add sterile water to a final volume of 1l. Do not adjust pH and store at room temperature. Dilute 1:10 to make 1x Tris-Glycine-SDS running buffer when required.

9. **10x Tris-Glycine transfer buffer (250mM Tris base, 1.92M glycine):** Add 800ml sterile water to 30.3g Tris base and 144g Glycine. Stir to dissolve. Add sterile water to a final volume of 1l. Do not adjust pH and store at room temperature. Dilute 1:10 to make 1x Tris-Glycine transfer buffer when required. Do not adjust pH and store at 4°C.

Donor	7F3158	7F3206
Age	56	50
Sex	Male	Male
Race	Caucasian	Caucasian
Seeding Efficiency	31%	45%
Viability Blue Exclusion	70	75
Doubling Time	24	21
Drinks Alcohol	Yes	Yes
Smoker	Yes	Yes

Cigarette Design Criteria

Cigarette Length	84 mm
Tobacco Rod Circumference	24.8 mm
Tobacco rod Length	57 mm
Filter Length	27 mm
Total Resistance to Draw (RTD)	128 mm H_2O
"Tar"	9.5 mg/cigarette

Cigarette Rod		Cigarette Filter	
Filter	3R4F Blend	Tow	Cellulose Acetate 2.9/41,000
Cuts per Inch	30	Plasticizer	9% Triacetin
Paper Permeability	24 CORESTA units	4-up Resistance to Draw	115 mm H_2O
Paper Citrate	0.60 %	Circumference	24.45 mm
Tobacco Weight (13% OV)	0.783 mg	Length	27 mm
Length	57 mm		

Target Total Cigarette

Tipping Paper Length	32 mm, white
Dilution	30 +/- 5%
Circumference	24.8 mm
Length	84 mm
Resistance to Draw	128 mm H_2O
Weight	1.06 g
Pack Moisture	13% Oven Volatiles

Final Total Cigarette Measurements (n = 11)

Dilution	29 (4.2) %
Circumference	24.9 (0.07) mm
Total Resistance to Draw	133.5 (4.45) mm H_2O
Cigarette Weight	1.05 (0.002) g
Tobacco Weight	0.775 (0.001) g
Pack Moisture	12.9 (0.33)% Oven Volatiles
Firmness	2.43 (0.113) mm

Preliminary FTC Smoking Results Average

Butt Length	35 mm
Puff Count	9.0 (0.112)
Total Particulate Matter, TPM	10.9 (0.168) mg/cigarette
"Tar"	9.4 (0.142) mg/cigarette
Nicotine	0.726 (0.009) mg/cigarette
Carbon Monoxide	11.9 (0.208) mg/cigarette

Final FTC Smoking Results Average (n=12)

Puff Count	9.0 (0.15)
Total Particulate Matter, TPM	11.0 (0.33) mg/cigarette
"Tar"	9.4 (0.30) mg/cigarette
Nicotine	0.73 (0.013) mg/cigarette
Carbon Monoxide	12.0 (0.48) mg/cigarette

Preliminary Filler Analysis

Total Alkaloids	1.98 % (.04) at 13% Oven Volatiles
Reducing Sugars	8.4 % (0.4) at 13% Oven Volatiles
Glycerin	2.7 % (0.1) at 13% Oven Volatiles

Final Filler Analysis (n=23)

Total Alkaloids (as-is)	2.05 % (0.04) at 11.6% Oven Volatiles
Reducing Sugars (as-is)	8.7% (0.3) at 11.6% Oven Volatiles
Glycerin (as-is)	2.36 % (0.05) at 11.6% Oven Volatiles

Blend Summary	**2R4F**	**3RF4**
Flue Cured	32.51 %	35.41%
Burley	19.94 %	21.62%
Maryland	1.24 %	1.35%
Oriental	11.08 %	12.07%
Reconstituted (Schweitzer Process)	27.13 %	29.55%
Glycerin (dry-weight basis @ 11.6% OV)	2.80 %	2.67%
Isosweet (Sugar)	5.30 %	6.41%

Position	Type	Major/Minor Alleles	Frequency (Cases)	Frequency (Controls)
44196927	SNP	C|A	0.0041	1.00E-04
44156419	SNP	G|A	0.005	1.00E-04
44188641	SNP	A|T	0.0061	1.00E-04
44200795	SNP	G|A	0.0087	1.00E-04
44167224	SNP	T|A	0.0091	1.00E-04
44202308	SNP	T|C	0.0111	1.00E-04
44177686	Insertion	C|CT	0.004	2.00E-04
44177685	SNP	G|T	0.0041	2.00E-04
44159722	SNP	C|T	0.0056	2.00E-04
44184816	SNP	G|A	0.0065	2.00E-04
44204928	SNP	G|T	0.0045	3.00E-04
44173484	SNP	G|T	0.0055	3.00E-04
44149992	SNP	G|A	0.0067	5.00E-04
44148884	SNP	G|C	0.0061	8.00E-04
44149557	SNP	C|G	0.0064	0.0012
44195188	SNP	C|T	0.0069	0.0021
44186622	SNP	G|A	0.0055	0.0024
44157254	Deletion	TG|T	0.0058	0.0029
44159198	SNP	C|G	0.0088	0.0031
44150085	SNP	G|T	2.00E-04	0.0033
44155605	SNP	G|T	0.0106	0.0036
44180769	SNP	T|G	0.0023	0.0038
44191490	Insertion	G|GCC	0.0064	0.0039
44206434	SNP	C|G	1.00E-04	0.0041
44163558	SNP	G|A	0.0017	0.0041
44168210	SNP	T|C	0.0159	0.0042
44145481	SNP	C|T	2.00E-04	0.0043
44196517	SNP	G|A	1.00E-04	0.0047
44166621	SNP	G|T	0.0013	0.0047
44184671	SNP	G|A	0.004	0.0047
44208803	SNP	G|T	1.00E-04	0.0048
44159200	SNP	G|T	0.0147	0.0048
44159201	SNP	A|C	0.0149	0.0049
44168870	SNP	G|A	1.00E-04	0.005
44187178	SNP	C|T	0.0099	0.005
44197509	SNP	G|C	4.00E-04	0.0053
44153248	SNP	T|C	0.0014	0.0054

44192726	SNP	G|A	0.0181	0.0059
44182729	SNP	A|C	0.004	0.006
44207022	SNP	G|A	0.0124	0.006
44145626	SNP	G|A	0.0172	0.006
44204952	SNP	T|C	0.0043	0.0063
44148866	Insertion	A|AC	0.0117	0.0066
44180322	SNP	T|G	0.0018	0.0068
44173227	SNP	G|A	0.0073	0.0068
44159202	SNP	C|T	0.0148	0.0074
44202687	SNP	C|T	0.0139	0.0077
44165924	SNP	C|T	0.0031	0.008
44191724	SNP	G|T	0.0106	0.008
44193332	SNP	C|T	0.0017	0.0082
44189517	Insertion	A|AC	0.0153	0.0082
44194305	SNP	G|A	0.0084	0.0083
44202100	SNP	C|T	0.0106	0.0086
44149651	SNP	G|T	0.0182	0.0089
44172130	SNP	T|C	0.0101	0.009
44191545	SNP	G|A	0.0086	0.0091
44191726	SNP	C|T	0.0057	0.0092
44180328	Deletion	GCC|G	0.0071	0.0093
44180424	SNP	G|A	0.0092	0.0093
44184981	SNP	A|T	0.0132	0.0093
44179442	SNP	C|G	0.0173	0.0095
44149326	SNP	G|A	0.0073	0.0096
44193668	Deletion	AT|A	0.0149	0.0097
44143205	Deletion	CAG|C	0.0017	0.0099
44199474	Deletion	AG|A	0.0144	0.01
44186061	SNP	G|A	0.0138	0.0101
44197488	Deletion	GTA|G	0.0107	0.0106
44196433	SNP	G|A	0.0142	0.0109
44167962	SNP	C|A	0.0068	0.0114
44160393	SNP	C|A	0.005	0.0116
44149289	SNP	T|A	0.0033	0.0119
44190172	Deletion	GT|G	0.0082	0.012
44202978	SNP	A|G	0.0147	0.0121
44158630	SNP	C|G	0.006	0.0123
44197478	SNP	G|T	0.0142	0.0124
44202840	SNP	A|T	0.0093	0.0125
44191629	SNP	T|C	0.0034	0.0128
44186575	SNP	C|A	0.0151	0.0129
44166075	SNP	G|A	0.0013	0.0132
44190034	Insertion	C|CA	0.019	0.0133
44182396	SNP	T|C	0.0191	0.0135
44188204	Insertion	C|CA	0.0195	0.0136
44170629	SNP	C|T	0.0043	0.0137

44205241	Insertion	T|TG	0.0096	0.0137
44201075	SNP	G|T	0.0183	0.0137
44153799	SNP	G|A	0.0121	0.0139
44175090	SNP	C|G	0.0133	0.0139
44190252	Insertion	G|GC	0.0153	0.014
44202146	Deletion	ATG|A	0.0185	0.0145
44191681	SNP	T|G	0.0193	0.0145
44176880	Insertion	T|TC	0.0162	0.0148
44190237	Deletion	CA|C	0.029	0.0148
44174249	SNP	C|T	0.0033	0.0149
44144997	SNP	SNP G|A	0.02	0.015
44186619	SNP	A|T	0.022	0.0152
44187496	SNP	T|C	0.008	0.0154
44206930	SNP	T|C	0.0267	0.0154
44149281	Insertion	T|TA	0.0182	0.0156
44153794	SNP	A|G	0.0163	0.0157
44192091	SNP	C|T	0.0136	0.0159
44142740	SNP	C|T	0.0044	0.0166
44160401	SNP	T|C	0.0125	0.0166
44205257	SNP	G|C	0.0146	0.0166
44160412	Deletion	AT|A	0.0145	0.0167
44206242	SNP	A|G	0.0135	0.0169
44160383	SNP	T|C	0.013	0.017
44166565	Insertion	A|AC	0.0107	0.0173
44147348	SNP	T|A	0.0137	0.0175
44180267	SNP	T|C	0.0112	0.0176
44205063	Deletion	CT|C	0.016	0.018
44184984	SNP	T|A	0.023	0.018
44189749	SNP	C|T	0.0133	0.0182
44200549	SNP	T|C	0.0137	0.0182
44155607	SNP	G|A	0.0087	0.0183
44159456	Deletion	TG|T	0.0177	0.0184
44177861	SNP	C|T	0.0039	0.0186
44206036	SNP	C|T	0.0411	0.0192
44169465	SNP	C|T	0.0189	0.0196
44202833	Deletion	GA|G	0.0189	0.0196
44197479	Deletion	TG|T	0.0263	0.0197
44186263	SNP	C|A	0.0184	0.0198
44161111	SNP	C|T	0.0241	0.0199
44164336	Insertion	G|GTTTTGTTTTA	0.0195	0.02
44146296	Deletion	CCA|C	0.0171	0.0202
44160421	SNP	T|A	0.0191	0.0205
44161618	SNP	G|A	0.0358	0.0205
44165566	SNP	T|G	0.0282	0.021
44182160	SNP	G|C	0.0197	0.0212
44164338	SNP	G|T	0.0205	0.0212

44154319	SNP	T|C	0.0157	0.0213
44187802	SNP	G|A	0.0192	0.0213
44195183	SNP	A|G	0.0083	0.0214
44185006	SNP	T|G	0.0198	0.0214
44197477	Deletion	TG|T	0.0286	0.0215
44197460	SNP	G|C	0.0128	0.0218
44154950	Insertion	G|GC	0.0204	0.0219
44191720	SNP	C|G	0.0208	0.0223
44170973	SNP	A|G	0.0173	0.0224
44154324	SNP	A|G	0.0181	0.0229
44197430	Insertion	T|TA	0.0228	0.0229
44152286	SNP	T|A	0.0373	0.0232
44194459	SNP	T|C	0.0244	0.0236
44184987	SNP	T|C	0.0289	0.0237
44197657	Deletion	AT|A	0.0179	0.0239
44152426	SNP	G|C	0.0138	0.0241
44153255	SNP	G|A	0.0154	0.0246
44190229	Insertion	C|CA	0.0287	0.0246
44150963	SNP	T|G	0.0214	0.0248
44202643	SNP	T|C	0.008	0.0256
44203307	SNP	G|A	0.0209	0.0257
44153824	Deletion	AGAAG|A	0.0208	0.026
44144598	Insertion	A|AG	0.0186	0.0261
44176882	Insertion	G|GC	0.0283	0.0262
44190191	Deletion	GC|G	0.0256	0.0267
44168134	SNP	C|G	0.0319	0.0273
44173987	Deletion	CA|C	0.0258	0.0274
44192552	Deletion	CTCTG|C	0.0182	0.0276
44151687	SNP	G|A	0.0143	0.028
44152151	SNP	C|T	0.0226	0.0285
44161149	SNP	G|A	0.0237	0.0286
44190241	Insertion	A|AC	0.0337	0.029
44180333	SNP	T|C	0.0378	0.029
44164483	SNP	A|G	0.027	0.0291
44179027	Deletion	TTTG|T	0.0283	0.0295
44209414	Insertion	G|GA	0.032	0.0298
44179646	Deletion	GAC|G	0.0326	0.0298
44175982	SNP	C|T	0.0298	0.0303
44207790	SNP	C|T	0.0222	0.0305
44151987	SNP	G|A	0.0253	0.0306
44209364	Insertion	T|TCC	0.033	0.0307
44153785	SNP	A|G	0.0247	0.031
44152495	SNP	A|G	0.0184	0.0313
44190582	SNP	G|A	0.0349	0.0319
44152414	SNP	A|G	0.0194	0.0321
44185010	SNP	T|G	0.0329	0.0323

44190230	Insertion	A|AGG	0.0419	0.0324
44151183	SNP	C|T	0.0221	0.0326
44184216	SNP	T|A	0.0386	0.0326
44180290	SNP	A|G	0.0374	0.0327
44152367	SNP	A|G	0.0157	0.0331
44185005	SNP	A|T	0.033	0.0331
44173984	Deletion	AAG|A	0.0285	0.0333
44202979	SNP	G|A	0.0403	0.0337
44154341	SNP	C|T	0.0266	0.0341
44164533	SNP	G|A	0.057	0.0343
44152091	SNP	T|C	0.042	0.0346
44179910	Deletion	CAG|C	0.04	0.0347
44176884	Deletion	TA|T	0.0316	0.0351
44174441	SNP	C|T	0.0291	0.0352
44150095	Deletion	GT|G	0.033	0.0353
44152585	SNP	A|T	0.0228	0.0357
44183623	Insertion	C|CTCAAAAA	0.0388	0.0364
44191719	SNP	T|G	0.0425	0.0365
44180334	SNP	G|C	0.0506	0.0365
44166187	SNP	A|C	0.0542	0.0366
44146462	SNP	T|A	0.0394	0.037
44176871	Insertion	A|ATGCATCAGCT	0.0423	0.0374
44162297	SNP	A|G	0.0371	0.038
44153003	SNP	C|T	0.0187	0.0392
44151770	SNP	A|C	0.0218	0.0392
44149900	SNP	C|T	0.0318	0.0398
44153898	Deletions	GA|G	0.0366	0.041
44157857	SNP	T|C	0.0473	0.0412
44200203	Insertion	T|TA	0.0335	0.0414
44206074	Insertion	C|CA	0.0483	0.0416
44170593	SNP	C|T	0.0265	0.0422
44167949	SNP	C|A	0.0563	0.0427
44202961	SNP	G|A	0.0297	0.0431
44209334	SNP	C|A	0.0398	0.0442
44186618	Deletion	A|AT	0.0446	0.0453
44198172	SNP	G|T	0.0489	0.0459
44193729	SNP	C|T	0.053	0.0476
44146459	SNP	G|A	0.043	0.0479
44157612	SNP	C|G	0.0532	0.048
44150864	SNP	G|T	0.0502	0.0485
44162194	Deletion	TA|T	0.0453	0.0486
44160133	SNP	G|A	0.0464	0.0502
44206291	SNP	T|C	0.041	0.0506
44189348	Insertion	A|AC	0.053	0.0506
44164337	SNP	A|T	0.0455	0.051
44185009	SNP	A|T	0.0556	0.0514

44160868	SNP	A|G	0.0374	0.0515
44202660	SNP	A|G	0.048	0.0516
44155868	SNP	G|A	0.0539	0.0521
44201206	Deletion	AATTT|A	0.0338	0.0524
44159377	SNP	G|A	0.0537	0.0529
44159365	SNP	T|G	0.0553	0.0535
44187494	SNP	C|T	0.0482	0.054
44176935	Deletion	AG|A	0.0668	0.0542
44161498	SNP	C|G	0.0428	0.0549
44159280	SNP	T|C	0.0543	0.0554
44176883	Deletion	C|CTAT	0.0637	0.0557
44189286	SNP	A|T	0.0471	0.0558
44158528	SNP	G|T	0.0575	0.0558
44206278	SNP	A|C	0.041	0.0559
44161573	SNP	G|C	0.0467	0.0559
44154218	SNP	C|T	0.0506	0.0561
44157776	SNP	C|A	0.064	0.0563
44143612	SNP	T|C	0.0586	0.0564
44189160	SNP	C|T	0.0397	0.0567
44147349	SNP	A|T	0.06	0.0567
44161486	SNP	T|A	0.0427	0.0569
44162115	SNP	G|T	0.0618	0.0569
44197788	Deletion	AG|A	0.0395	0.057
44161081	SNP	A|T	0.0467	0.0573
44184997	Deletion	A|AC	0.0613	0.0574
44158016	SNP	G|A	0.0561	0.0578
44156600	SNP	G|A	0.0559	0.058
44151698	SNP	C|T	0.0657	0.058
44180332	SNP	G|C	0.0627	0.0586
44156741	SNP	C|T	0.0561	0.0591
44201920	SNP	T|C	0.057	0.0593
44162199	Insertion	A|AC	0.0492	0.0596
44196889	SNP	G|T	0.0416	0.0601
44162144	SNP	T|C	0.0714	0.0603
44159489	SNP	G|A	0.0733	0.0608
44156118	SNP	C|T	0.0813	0.0609
44200667	SNP	C|A	0.0561	0.061
44186820	Insertion	C|CA	0.0616	0.0618
44206883	SNP	C|T	0.0423	0.0619
44162145	SNP	G|A	0.0708	0.0625
44201167	SNP	C|T	0.0481	0.0626
44161781	SNP	T|C	0.0464	0.0634
44209348	SNP	T|G	0.0476	0.0641
44162233	SNP	A|G	0.0762	0.0641
44184990	SNP	T|A	0.0702	0.0643
44158004	SNP	G|A	0.0619	0.0651

44159876	SNP	G|A	0.0414	0.0654
44202704	SNP	T|C	0.0701	0.0655
44198947	Deletion	AAC|A	0.0424	0.0658
44198884	SNP	G|A	0.0457	0.0664
44186617	SNP	G|A	0.0752	0.0673
44202701	SNP	A|G	0.0716	0.068
44198377	SNP	G|A	0.0758	0.0683
44153775	Deletion	AAAAG|A	0.0791	0.0688
44161050	SNP	C|A	0.0576	0.0698
44157156	SNP	A|G	0.0648	0.0698
44187577	SNP	A|G	0.0484	0.0709
44151525	SNP	C|T	0.0567	0.0709
44159819	SNP	T|C	0.0626	0.0709
44186577	Insertion	A|AGTC	0.0508	0.0724
44200928	SNP	G|C	0.0556	0.0726
44206375	SNP	G|A	0.0415	0.0727
44202920	SNP	A|C	0.0618	0.0732
44205852	SNP	G|A	0.0555	0.0739
44199523	SNP	C|T	0.0512	0.0745
44177700	SNP	C|T	0.1073	0.075
44198376	SNP	C|G	0.0638	0.0757
44206922	Insertion	C|CTT	0.0644	0.0757
44198020	Insertion	AG|A	0.0753	0.0757
44184996	SNP	T|A	0.0822	0.0761
44184993	Insertion	A|AC	0.0746	0.0765
44209093	Deletion	AT|A	0.0859	0.0766
44163471	SNP	G|A	0.0794	0.077
44197098	Insertion	C|CA	0.0727	0.0773
44155355	SNP	C|T	0.082	0.079
44180292	SNP	G|T	0.0873	0.0791
44163594	SNP	G|A	0.1172	0.0792
44200246	Insertion	C|CA	0.0522	0.0795
44167978	Deletion	CA|C	0.0889	0.0804
44197490	SNP	A|G	0.0863	0.0824
44188104	SNP	C|T	0.0854	0.0826
44200812	SNP	C|T	0.0522	0.0839
44188002	SNP	C|G	0.0552	0.0843
44182486	SNP	G|A	0.0798	0.0854
44188485	SNP	C|T	0.0768	0.0864
44202855	SNP	A|T	0.0519	0.0868
44201312	SNP	C|T	0.0564	0.0877
44176124	Deletion	GT|G	0.0909	0.0897
44164271	Insertion	T|TGCG	0.0883	0.09
44199926	SNP	G|A	0.0611	0.0908
44149661	SNP	G|T	0.1071	0.0919
44164305	Insertion	C|CGTTTT	0.0879	0.0936

44183635	SNP	G|A	0.0883	0.0942
44149322	SNP	G|A	0.0902	0.0948
44149283	SNP	T|A	0.0969	0.0965
44160417	SNP	T|A	0.0937	0.0973
44186616	Deletion	TGA|T	0.1117	0.0979
44197458	SNP	G|C	0.0958	0.0981
44176869	SNP	T|A	0.1075	0.0986
44197440	Deletion	CTGTGTGTG|C	0.0926	0.0992
44207318	SNP	C|T	0.0786	0.1011
44158277	Deletion	GA|G	0.1099	0.1042
44149275	Deletion	AGT|A	0.0983	0.1067
44184986	SNP	T|A	0.1002	0.1072
44209257	Insertion	T|TGGTC	0.1249	0.1082
44176867	Deletion	TC|T	0.1255	0.1089
44167953	SNP	A|C	0.1089	0.1098
44202101	Insertion	A|AAC	0.1134	0.1098
44176872	SNP	T|G	0.1087	0.1105
44176946	SNP	A|G	0.1305	0.1123
44165783	SNP	G|A	0.115	0.1127
44177028	Deletion	GCATTCTCCAC|G	0.105	0.1129
44149660	Deletion	TG|T	0.1207	0.1134
44151621	SNP	T|C	0.1306	0.115
44154472	SNP	T|G	0.1295	0.1165
44197452	SNP	G|C	0.1117	0.1176
44197454	SNP	G|C	0.1122	0.1182
44206241	Deletion	GA|G	0.1131	0.1194
44149324	SNP	A|G	0.1161	0.12
44197456	SNP	G|C	0.1147	0.1207
44164478	SNP	C|T	0.1236	0.1216
44184992	SNP	T|A	0.118	0.1225
44176947	SNP	C|T	0.1435	0.1242
44202965	Deletion	CA|C	0.1171	0.1255
44154170	Deletion	GT|G	0.1133	0.1257
44159252	Insertion	A|AC	0.1517	0.1259
44154473	SNP	G|T	0.1418	0.1294
44201064	Deletion	CTGT|C	0.1421	0.1325
44205337	SNP	T|A	0.1632	0.1329
44142882	SNP	T|C	0.144	0.1333
44205082	SNP	G|A	0.1415	0.1339
44147333	Insertion	C|CCTT	0.1478	0.1339
44164437	SNP	T|C	0.176	0.1356
44164609	SNP	G|A	0.1511	0.1368
44207803	SNP	C|T	0.1717	0.1381
44177666	SNP	A|T	0.1828	0.1393
44186621	SNP	A|T	0.1514	0.1401
44164386	SNP	C|T	0.156	0.1405

44153100	SNP	A|G	0.1528	0.1415
44163954	SNP	C|T	0.1335	0.1433
44177049	SNP	G|T	0.1417	0.144
44163994	SNP	A|C	0.1354	0.1461
44155589	Deletion	GT|G	0.1457	0.1486
44184977	Deletion	TTTTATTTATTTATTTA|T	0.1519	0.1487
44183618	SNP	C|T	0.1719	0.1502
44183619	SNP	A|G	0.1711	0.1525
44165454	SNP	G|A	0.1578	0.1527
44177057		TGCA|T	0.1521	0.1557
44165091	SNP	G|A	0.1458	0.1558
44209418	SNP	A|G	0.1603	0.1561
44178928	SNP	C|T	0.1888	0.1576
44191717	SNP	G|T	0.1559	0.1582
44163033	SNP	T|G	0.1719	0.159
44183464	SNP	A|C	0.1744	0.1598
44165065	SNP	T|C	0.1427	0.1599
44178272	SNP	A|G	0.1618	0.1606
44167452	Deletion	TACACACAC|T	0.1569	0.1613
44183469	Insertion	C|CA	0.1681	0.1613
44197450	SNP	G|C	0.1496	0.1635
44163314	SNP	C|T	0.1403	0.164
44163061	SNP	T|C	0.1699	0.1659
44209319	SNP	C|T	0.1756	0.1664
44146930	SNP	C|A	0.1766	0.1665
44198146	Insertion	A|ACTT	0.1597	0.1687
44191682	Insertion	C|CATCGTG	0.1673	0.1692
44183605	SNP	C|T	0.1836	0.1733
44156472	SNP	T|C	0.1926	0.1751
44183603	SNP	G|A	0.1893	0.1784
44205026	SNP	A|G	0.185	0.1793
44209388	Deletion	CT|C	0.185	0.184
44183642	SNP	G|A	0.2233	0.1901
44205851	SNP	T|C	0.2125	0.1904
44145282	SNP	A|G	0.2111	0.1913
44202983	Insertion	A|AACC	0.208	0.1925
44209323	SNP	G|C	0.1992	0.1932
44183602	SNP	T|C	0.2042	0.1938
44150940	Deletion	CT|C	0.1715	0.1941
44197448	SNP	G|C	0.2041	0.195
44176885	Insertion	A|AC	0.2108	0.196
44164627	Deletion	GT|G	0.1878	0.1963
44150012	SNP	T|A	0.2027	0.1981
44204339	Deletion	GTTC|G	0.2244	0.1991
44190195	Deletion	ATT|A	0.1853	0.1992
44161093	Deletion	CT|C	0.2049	0.1994

44176971	SNP	G|A	0.2179	0.2011
44174971	SNP	G|T	0.2305	0.2015
44145543	SNP	T|A	0.1891	0.2021
44173267	Insertion	T|TA	0.2267	0.2026
44183594	SNP	G|A	0.2249	0.2034
44153729	SNP	G|A	0.168	0.2059
44183577	SNP	C|T	0.2249	0.2061
44142771	SNP	A|G	0.204	0.2075
44197480	SNP	G|T	0.2286	0.2086
44175100	Insertion	G|GA	0.2144	0.2091
44186627	SNP	A|G	0.2253	0.2091
44198771	Deletion	CAT|C	0.2093	0.2114
44183556	Deletion	A|G	0.2119	0.2148
44149479	Deletion	AT|A	0.2397	0.2156
44152090	Deletion	CT|C	0.2205	0.2171
44149449	SNP	A|G	0.2318	0.2173
44160202	SNP	T|C	0.2361	0.2177
44186628	SNP	G|A	0.236	0.2194
44209246	SNP	G|A	0.2262	0.2209
44189107	SNP	G|A	0.2409	0.223
44160413	SNP	T|A	0.2501	0.2242
44202748	SNP	C|T	0.2248	0.2243
44196531	SNP	C|T	0.258	0.2272
44209019	SNP	C|T	0.2464	0.228
44168281	SNP	C|T	0.2201	0.2292
44146463	Insertion	A|AAATAATAGT	0.2526	0.2301
44197446	SNP	G|C	0.2347	0.2317
44184856	SNP	C|T	0.2382	0.2319
44180595	SNP	G|A	0.2531	0.2374
44148315	Deletion	GT|G	0.2424	0.2375
44178815	SNP	C|T	0.2036	0.2376
44176970	SNP	T|C	0.2583	0.2401
44183541	SNP	T|C	0.2396	0.2409
44202819	SNP	G|A	0.2591	0.2409
44180254	SNP	G|A	0.3195	0.2427
44173961	Deletion	CAAAA|C	0.2457	0.2445
44179004	Deletion	CTT|C	0.2323	0.2455
44192580	SNP	T|C	0.2463	0.2459
44163781	SNP	A|T	0.2598	0.2459
44171283	SNP	C|T	0.2686	0.2473
44209457	SNP	A|G	0.2713	0.2501
44159428	Deletion	CA|C	0.2482	0.255
44191505	Deletion	CT|C	0.2333	0.2573
44181125	SNP	T|C	0.2628	0.2585
44183651	SNP	C|T	0.2963	0.2586
44190834	SNP	C|T	0.2426	0.2614

44181952	Insertion	T|TAGAG	0.2701	0.2622
44172025	SNP	C|T	0.2748	0.264
44183538	SNP	C|T	0.2714	0.2674
44186623	Deletion	AAAAAG|A	0.2637	0.2713
44164484	Deletion	AT|A	0.2963	0.2782
44201669	SNP	G|A	0.2665	0.2788
44184068	SNP	T|C	0.2622	0.2801
44207848	Deletion	CA|C	0.2839	0.2805
44176995	SNP	C|A	0.3007	0.2847
44148867	Deletion	CT|C	0.2799	0.2905
44163319	Insertion	C|CTTTTGTT	0.31	0.2914
44176989	SNP	G|A	0.303	0.2918
44204384	SNP	A|G	0.2845	0.2922
44180539	SNP	T|A	0.3374	0.2928
44176999	SNP	C|A	0.3106	0.2951
44209232	SNP	T|A	0.2902	0.2973
44177005	SNP	C|T	0.3138	0.2983
44176987	SNP	A|G	0.3201	0.3002
44183632	SNP	G|A	0.3281	0.3003
44195633	Deletion	CAA|C	0.3146	0.3085
44177016	SNP	C|T	0.3245	0.3091
44165552	Deletion	CTTTTTTT|C	0.3191	0.3139
44183518	SNP	G|T	0.2979	0.314
44200052	Insertion	C|CA	0.3194	0.318
44197444	SNP	G|C	0.3074	0.3181
44177019	SNP	A|G	0.3503	0.3227
44146297		CA|C	0.3049	0.3245
44180282	Deletion	TTGTGTGCATG|T	0.3515	0.3267
44201512	SNP	C|G	0.3013	0.3278
44187506	SNP	C|T	0.2999	0.3282
44184051	SNP	A|C	0.3339	0.3332
44166872	Deletion	GT|G	0.3489	0.3332
44204519	SNP	G|A	0.3125	0.3358
44188073	SNP	C|T	0.354	0.3369
44183481	SNP	A|G	0.3664	0.339
44189244	SNP	T|C	0.3405	0.3469
44203408	SNP	T|A	0.3477	0.3474
44190626	SNP	C|A	0.3205	0.3482
44185753	SNP	G|A	0.3514	0.3485
44203256	SNP	G|C	0.329	0.3506
44180407	Deletion	CGT|C	0.354	0.3521
44186592	SNP	T|C	0.3528	0.3546
44203093	SNP	G|A	0.3296	0.3551
44183699	SNP	T|C	0.3724	0.3555
44184046	SNP	C|T	0.3573	0.3626
44186653	SNP	C|A	0.3758	0.3718

44188128	SNP	C|T	0.4016	0.3724
44183505	SNP	A|T	0.3583	0.3732
44189349	Insertion	C|CA	0.3619	0.3749
44191567	SNP	C|G	0.3598	0.3799
44197442	SNP	G|C	0.3659	0.3888
44194362	SNP	C|T	0.4075	0.3905
44192556	SNP	G|C	0.3988	0.394
44192554	Deletion	CTG|C	0.3879	0.3947
44190371	SNP	C|T	0.4367	0.3971
44180330	Deleltion	CTG|C	0.4113	0.3989
44183485	SNP	G|A	0.4318	0.4017
44177874	Deletion	GA|G	0.431	0.4048
44184031	SNP	A|G	0.4008	0.406
44169854	SNP	T|C	0.415	0.4075
44198021	SNP	G|A	0.4262	0.4183
44183728	SNP	G|A	0.4386	0.4187
44184213	Deletion	AAATAATAATAAT|A	0.4271	0.4207
44183771	SNP	T|A	0.4188	0.4208
44190662	SNP	G|A	0.4451	0.424
44183776	SNP	G|T	0.419	0.4251
44163746	SNP	G|A	0.389	0.4287
44169855	SNP	G|A	0.4421	0.4302
44183494	SNP	C|T	0.4039	0.4349
44193731	SNP	C|T	0.4444	0.4351
44192475	SNP	G|A	0.4593	0.4352
44197805	SNP	G|A	0.465	0.445
44199977	SNP	C|T	0.492	0.4513
44196668	SNP	T|C	0.4381	0.4515
44183800	SNP	A|C	0.4448	0.4559
44199905	SNP	T|C	0.4865	0.4643
44184007	SNP	T|A	0.4752	0.4647
44198241	SNP	C|T	0.5054	0.4681
44162954	SNP	A|G	0.481	0.4686
44182301	Insertion	T|TGGGG	0.4747	0.4704
44183838	SNP	A|G	0.4501	0.4737
44172890	SNP	A|C	0.4898	0.4852
44172188	SNP	T|C	0.4948	0.5042
44166375	SNP	C|T	0.4877	0.5062
44197545	SNP	C|T	0.4773	0.508
44196994	SNP	A|G	0.5094	0.5102
44170586	SNP	A|T	0.492	0.5117
44180550	SNP	A|C	0.4832	0.5126
44171349	SNP	C|T	0.5346	0.5135
44198526	SNP	G|T	0.5756	0.5174
44182142	SNP	C|T	0.515	0.5212
44204469	SNP	G|C	0.5315	0.5308

44183886	SNP	T|A	0.5481	0.5331
44164560	SNP	T|C	0.5275	0.5399
44208102	SNP	T|C	0.5449	0.542
44171582	SNP	T|A	0.5321	0.5449
44198242	SNP	A|G	0.5783	0.5476
44198577	SNP	G|A	0.5714	0.5493
44169865	SNP	C|T	0.5693	0.5666
44202776	SNP	G|A	0.5762	0.5745
44179956	SNP	C|T	0.6156	0.5875
44177988	SNP	T|G	0.6251	0.616
44166424	SNP	T|C	0.6534	0.6648
44166888	SNP	G|A	0.6614	0.6652
44177867	SNP	T|C	0.7674	0.7361
44197840	SNP	A|G	0.751	0.7395
44169738	SNP	G|C	0.7502	0.7415
44178649	SNP	A|G	0.7936	0.7436
44178630	SNP	G|C	0.7988	0.7438
44178137	SNP	T|C	0.7731	0.7457
44176333	SNP	C|A	0.7943	0.7667
44174788	SNP	C|T	0.7977	0.7724
44194781	SNP	C|T	0.7517	0.7744
44178437	SNP	T|C	0.82	0.7861
44171142	SNP	T|C	0.8109	0.7906
44179760	SNP	G|A	0.8125	0.7908
44181195	SNP	C|T	0.8245	0.7954
44181531	SNP	C|T	0.8208	0.7988
44193244	SNP	A|C	0.7791	0.7998
44193644	SNP	T|C	0.7856	0.8035
44182554	SNP	T|A	0.8883	0.879
44182291	SNP	T|C	0.8841	0.8875
44185202	SNP	A|T	0.8988	0.8899
44185926	SNP	G|A	0.9227	0.8986
44185752	SNP	T|C	0.8991	0.9028
44186073	SNP	A|G	0.9177	0.9061
44185724	SNP	G|A	0.9051	0.9087
44186072	SNP	T|C	0.9058	0.9092
44185352	SNP	T|A	0.9124	0.9098
44182695	SNP	A|G	0.9228	0.9121
44182805	SNP	T|C	0.9174	0.9151
44184962	SNP	A|T	0.932	0.9173
44185710	SNP	C|A	0.9102	0.919
44186501	SNP	G|A	0.9196	0.9246
44183698	SNP	G|C	0.9518	0.9452
44169897	SNP	G|C	0.9714	0.9678

BIBLIOGRAPHY

1000_GENOME_PROJECT 2010. A map of human genome variation from population-scale sequencing. *Nature,* 467**,** 1061-73.

ACUNZO, M., VISONE, R., ROMANO, G., VERONESE, A., LOVAT, F., PALMIERI, D., BOTTONI, A., GAROFALO, M., GASPARINI, P., CONDORELLI, G., CHIARIELLO, M. & CROCE, C. M. 2012. miR-130a targets MET and induces TRAIL-sensitivity in NSCLC by downregulating miR-221 and 222. *Oncogene,* 31**,** 634-42.

AGILENT 2012. Illumina HiSeq and MiSeq Multiplexed Sequencing Platforms Protocol.

AGUIRRE-GHISO, J. A., LIU, D., MIGNATTI, A., KOVALSKI, K. & OSSOWSKI, L. 2001. Urokinase receptor and fibronectin regulate the ERK(MAPK) to p38(MAPK) activity ratios that determine carcinoma cell proliferation or dormancy in vivo. *Mol Biol Cell,* 12**,** 863-79.

AGUIRRE GHISO, J. A., KOVALSKI, K. & OSSOWSKI, L. 1999. Tumor dormancy induced by downregulation of urokinase receptor in human carcinoma involves integrin and MAPK signaling. *J Cell Biol,* 147**,** 89-104.

ALLGAYER, H., WANG, H., WANG, Y., HEISS, M. M., BAUER, R., NYORMOI, O. & BOYD, D. 1999. Transactivation of the urokinase-type plasminogen activator receptor gene through a novel promoter motif bound with an activator protein-2alpha-related factor. *J Biol Chem,* 274**,** 4702-14.

ALMASI, C. E., BRASSO, K., IVERSEN, P., PAPPOT, H., HOYER-HANSEN, G., DANO, K. & CHRISTENSEN, I. J. 2011. Prognostic and predictive value of intact and cleaved forms of the urokinase plasminogen activator receptor in metastatic prostate cancer. *Prostate,* 71**,** 899-907.

ANDERSEN, O., EUGEN-OLSEN, J., KOFOED, K., IVERSEN, J. & HAUGAARD, S. 2008. Soluble urokinase plasminogen activator receptor is a marker of dysmetabolism in HIV-infected patients receiving highly active antiretroviral therapy. *Journal of medical virology,* 80**,** 209-225.

ANDOLFO, A., ENGLISH, W. R., RESNATI, M., MURPHY, G., BLASI, F. & SIDENIUS, N. 2002. Metalloproteases cleave the urokinase-type plasminogen activator receptor in the D1-D2 linker region and expose epitopes not present in the intact soluble receptor. *Thromb Haemost,* 88**,** 298-306.

ANDREASEN, P. A., EGELUND, R. & PETERSEN, H. H. 2000. The plasminogen activation system in tumor growth, invasion, and metastasis. *Cell Mol Life Sci,* 57**,** 25-40.

ANDRES, S. A., EDWARDS, A. B. & WITTLIFF, J. L. 2012. Expression of urokinase-type plasminogen activator (uPA), its receptor (uPAR), and inhibitor (PAI-1) in human breast carcinomas and their clinical relevance. *J Clin Lab Anal,* 26**,** 93-103.

ANSORGE, W. J. 2009. Next-generation DNA sequencing techniques. *N Biotechnol,* 25**,** 195-203.

ASTHMAUK. 2012. *Key facts on asthma* [Online]. Available: http://www.asthma.org.uk/news-centre/facts-for-journalists/ [Accessed 06.09.2012 2012].

BAEK, M. K., KIM, M. H., JANG, H. J., PARK, J. S., CHUNG, I. J., SHIN, B. A., AHN, B. W. & JUNG, Y. D. 2008. EGF stimulates uPAR expression and cell invasiveness through ERK, AP-1, and NF-kappaB signaling in human gastric carcinoma cells. *Oncol Rep,* 20**,** 1569-75.

BAEK, M. K., PARK, J. S., PARK, J. H., KIM, M. H., KIM, H. D., BAE, W. K., CHUNG, I. J., SHIN, B. A. & JUNG, Y. D. 2010. Lithocholic acid upregulates uPAR and cell invasiveness via MAPK and AP-1 signaling in colon cancer cells. *Cancer Lett,* 290**,** 123-8.

BAI, T. R., COOPER, J., KOELMEYER, T., PARE, P. D. & WEIR, T. D. 2000. The effect of age and duration of disease on airway structure in fatal asthma. *Am J Respir Crit Care Med,* 162**,** 663-9.

BARNES, P. J. 1995. Is asthma a nervous disease? The Parker B. Francis Lectureship. *Chest,* 107**,** 119S-125S.

BARNES, P. J. 2000. Mechanisms in COPD: differences from asthma. *Chest,* 117**,** 10S-4S.

BARNES PJ, D. J., RENNARD S, THOMSON N (ed.) 2002. *Asthma and COPD,* London: Academic Press.

BARNES, P. J., SHAPIRO, S. D. & PAUWELS, R. A. 2003. Chronic obstructive pulmonary disease: molecular and cellular mechanisms. *Eur Respir J,* 22**,** 672-88.

BARRETT, J. C., FRY, B., MALLER, J. & DALY, M. J. 2005. Haploview: analysis and visualization of LD and haplotype maps. *Bioinformatics,* 21**,** 263-5.

BARTEL, D. P. 2009. MicroRNAs: target recognition and regulatory functions. *Cell,* 136**,** 215-33.

BARTON, S. J., KOPPELMAN, G. H., VONK, J. M., BROWNING, C. A., NOLTE, I. M., STEWART, C. E., BAINBRIDGE, S., MUTCH, S., ROSE-ZERILLI, M. J., POSTMA, D. S., MANIATIS, N., HENRY, A. P., HALL, I. P., HOLGATE, S. T., TIGHE, P., HOLLOWAY, J. W. & SAYERS, I. 2009. PLAUR polymorphisms are associated with asthma, PLAUR levels, and lung function decline. *J Allergy Clin Immunol,* 123**,** 1391-400 e17.

BAUMGARTEN, C. R., NICHOLS, R. C., NACLERIO, R. M., LICHTENSTEIN, L. M., NORMAN, P. S. & PROUD, D. 1986. Plasma kallikrein during experimentally induced allergic rhinitis: role in kinin formation and contribution to TAME-esterase activity in nasal secretions. *J Immunol,* 137**,** 977-82.

BEAUFORT, N., DEBELA, M., CREUTZBURG, S., KELLERMANN, J., BODE, W., SCHMITT, M., PIDARD, D. & MAGDOLEN, V. 2006. Interplay of human tissue kallikrein 4 (hK4) with the plasminogen activation system: hK4 regulates the structure and functions of the urokinase-type plasminogen activator receptor (uPAR). *Biol Chem,* 387**,** 217-22.

BEAUFORT, N., LEDUC, D., EGUCHI, H., MENGELE, K., HELLMANN, D., MASEGI, T., KAMIMURA, T., YASUOKA, S., FEND, F., CHIGNARD, M. & PIDARD, D. 2007. The human airway trypsin-like protease modulates the urokinase receptor (uPAR, CD87) structure and functions. *Am J Physiol Lung Cell Mol Physiol,* 292**,** L1263-72.

BEAUFORT, N., LEDUC, D., ROUSSELLE, J. C., MAGDOLEN, V., LUTHER, T., NAMANE, A., CHIGNARD, M. & PIDARD, D. 2004. Proteolytic regulation of the urokinase receptor/CD87 on monocytic cells by neutrophil elastase and cathepsin G. *J Immunol,* 172**,** 540-9.

BEHRENDT, N. 2004. The urokinase receptor (uPAR) and the uPAR-associated protein (uPARAP/Endo180): membrane proteins engaged in matrix turnover during tissue remodeling. *Biol Chem,* 385**,** 103-36.

BEHRENDT, N. & DANO, K. 1996. Effect of purified, soluble urokinase receptor on the plasminogen-prourokinase activation system. *FEBS Lett,* 393**,** 31-6.

BEHRENDT, N., PLOUG, M., PATTHY, L., HOUEN, G., BLASI, F. & DANO, K. 1991. The ligand-binding domain of the cell surface receptor for urokinase-type plasminogen activator. *J Biol Chem,* 266**,** 7842-7.

BERNSTEIN, A. M., TWINING, S. S., WAREJCKA, D. J., TALL, E. & MASUR, S. K. 2007. Urokinase receptor cleavage: a crucial step in fibroblast-to-myofibroblast differentiation. *Mol Biol Cell,* 18**,** 2716-27.

BETEL, D., KOPPAL, A., AGIUS, P., SANDER, C. & LESLIE, C. 2010. Comprehensive modeling of microRNA targets predicts functional non-conserved and non-canonical sites. *Genome Biol,* 11**,** R90.

BETEL, D., WILSON, M., GABOW, A., MARKS, D. S. & SANDER, C. 2008. The microRNA.org resource: targets and expression. *Nucleic Acids Res,* 36**,** D149-53.

BHANDARY, Y. P., SHETTY, S. K., MARUDAMUTHU, A. S., GYETKO, M. R., IDELL, S., GHARAEE-KERMANI, M., SHETTY, R. S., STARCHER, B. C. & SHETTY, S. 2012. Regulation of alveolar epithelial cell apoptosis and pulmonary fibrosis by coordinate expression of components of the fibrinolytic system. *Am J Physiol Lung Cell Mol Physiol,* 302**,** L463-73.

BHANDARY, Y. P., VELUSAMY, T., SHETTY, P., SHETTY, R. S., IDELL, S., CINES, D. B., JAIN, D., BDEIR, K., ABRAHAM, E., TSURUTA, Y. & SHETTY, S. 2009. Post-transcriptional regulation of urokinase-type plasminogen activator receptor expression in lipopolysaccharide-induced acute lung injury. *Am J Respir Crit Care Med,* 179**,** 288-98.

BHATTACHARYA, A., LAKKA, S. S., MOHANAM, S., BOYD, D. & RAO, J. S. 2001. Regulation of the urokinase-type plasminogen activator receptor gene in different grades of human glioma cell lines. *Clin Cancer Res,* 7**,** 267-76.

BIFULCO, K., LONGANESI-CATTANI, I., MASUCCI, M. T., DE CHIARA, A., FAZIOLI, F., DI CARLUCCIO, G., PIROZZI, G., GALLO, M., LA ROCCA, A., APICE, G., ROCCO, G. & CARRIERO, M. V. 2011. Involvement of the soluble urokinase receptor in chondrosarcoma cell mobilization. *Sarcoma,* 2011**,** 842842.

BLASI, F. & CARMELIET, P. 2002. uPAR: a versatile signalling orchestrator. *Nat Rev Mol Cell Biol,* 3**,** 932-43.

BLASI, F. & VERDE, P. 1990. Urokinase-dependent cell surface proteolysis and cancer. *Semin Cancer Biol,* 1**,** 117-26.

BLF 2008. Invisible Lives: Chronic Obstructive Pulmonary Disease (COPD) finding the missing millions.

BMA., R. 2012. *British National Formulary*, BMJ Publishing Group.

BODMER, W. & BONILLA, C. 2008. Common and rare variants in multifactorial susceptibility to common diseases. *Nat Genet,* 40**,** 695-701.

BONELLO, M. R. & KHACHIGIAN, L. M. 2004. Fibroblast growth factor-2 represses platelet-derived growth factor receptor-alpha (PDGFR-alpha) transcription via ERK1/2-dependent Sp1 phosphorylation and an atypical cis-acting element in the proximal PDGFR-alpha promoter. *J Biol Chem,* 279**,** 2377-82.

BORGER, P., MIGLINO, N., BARAKET, M., BLACK, J. L., TAMM, M. & ROTH, M. 2009. Impaired translation of CCAAT/enhancer binding protein alpha mRNA in bronchial smooth muscle cells of asthmatic patients. *J Allergy Clin Immunol,* 123**,** 639-45.

BOUSQUET, J., MANTZOURANIS, E., CRUZ, A. A., AIT-KHALED, N., BAENA-CAGNANI, C. E., BLEECKER, E. R., BRIGHTLING, C. E., BURNEY, P., BUSH, A., BUSSE, W. W., CASALE, T. B., CHAN-YEUNG, M., CHEN, R., CHOWDHURY, B., CHUNG, K. F., DAHL, R., DRAZEN, J. M., FABBRI, L. M., HOLGATE, S. T., KAUFFMANN, F., HAAHTELA, T., KHALTAEV, N., KILEY, J. P., MASJEDI, M. R., MOHAMMAD, Y., O'BYRNE, P., PARTRIDGE, M. R., RABE, K. F., TOGIAS, A., VAN WEEL, C., WENZEL, S., ZHONG, N. & ZUBERBIER, T. 2010. Uniform definition of asthma severity, control, and exacerbations: document presented for the World Health Organization Consultation on Severe Asthma. *J Allergy Clin Immunol,* 126**,** 926-38.

BOVE, P. F., HRISTOVA, M., WESLEY, U. V., OLSON, N., LOUNSBURY, K. M. & VAN DER VLIET, A. 2008. Inflammatory levels of nitric oxide inhibit airway epithelial cell migration by inhibition of the kinase ERK1/2 and activation of hypoxia-inducible factor-1 alpha. *J Biol Chem,* 283**,** 17919-28.

BRADFORD, M. M. 1976. A rapid and sensitive method for the quantitation of microgram quantities of protein utilizing the principle of protein-dye binding. *Anal Biochem,* 72**,** 248-54.

BRIMS, F. J., CHAUHAN, A. J., HIGGINS, B. & SHUTE, J. K. 2009. Coagulation factors in the airways in moderate and severe asthma and the effect of inhaled steroids. *Thorax,* 64**,** 1037-43.

BROOKS, A. M., BATES, M. E., VRTIS, R. F., JARJOUR, N. N., BERTICS, P. J. & SEDGWICK, J. B. 2006. Urokinase-type plasminogen activator modulates airway eosinophil adhesion in asthma. *Am J Respir Cell Mol Biol,* 35**,** 503-11.

BRUSASCO, V., CRIMI, E. & PELLEGRINO, R. 1998. Airway hyperresponsiveness in asthma: not just a matter of airway inflammation. *Thorax,* 53**,** 992-8.

BTS 2011. British Guideline on the Managment of Asthma.

BUCCHIERI, F., PUDDICOMBE, S. M., LORDAN, J. L., RICHTER, A., BUCHANAN, D., WILSON, S. J., WARD, J., ZUMMO, G., HOWARTH, P. H., DJUKANOVIC, R., HOLGATE, S. T. & DAVIES, D. E. 2002. Asthmatic bronchial epithelium is more susceptible to oxidant-induced apoptosis. *Am J Respir Cell Mol Biol,* 27**,** 179-85.

BUCHLER, P., REBER, H. A., TOMLINSON, J. S., HANKINSON, O., KALLIFATIDIS, G., FRIESS, H., HERR, I. & HINES, O. J. 2009. Transcriptional regulation of urokinase-type plasminogen activator receptor by hypoxia-inducible factor 1 is crucial for invasion of pancreatic and liver cancer. *Neoplasia,* 11**,** 196-206.

BURROUGHS, M. & WHEELER, D. 1994. A block sorting lossless data compression algorithm. *Digital Equipment Corporation.*

BUSSE, W., ELIAS, J., SHEPPARD, D. & BANKS-SCHLEGEL, S. 1999. Airway remodeling and repair. *Am J Respir Crit Care Med,* 160**,** 1035-42.

CARAMORI, G., GRONEBERG, D., ITO, K., CASOLARI, P., ADCOCK, I. M. & PAPI, A. 2008. New drugs targeting Th2 lymphocytes in asthma. *J Occup Med Toxicol,* 3 Suppl 1**,** S6.

CARAMORI, G., PANDIT, A. & PAPI, A. 2005. Is there a difference between chronic airway inflammation in chronic severe asthma and chronic obstructive pulmonary disease? *Curr Opin Allergy Clin Immunol,* 5**,** 77-83.

CARP, H. & JANOFF, A. 1978. Possible mechanisms of emphysema in smokers. In vitro suppression of serum elastase-inhibitory capacity by fresh cigarette smoke and its prevention by antioxidants. *Am Rev Respir Dis,* 118**,** 617-21.

CARTHARIUS, K., FRECH, K., GROTE, K., KLOCKE, B., HALTMEIER, M., KLINGENHOFF, A., FRISCH, M., BAYERLEIN, M. & WERNER, T. 2005. MatInspector and beyond: promoter analysis based on transcription factor binding sites. *Bioinformatics,* 21**,** 2933-42.

CASEY, J. R., PETRANKA, J. G., KOTTRA, J., FLEENOR, D. E. & ROSSE, W. F. 1994. The structure of the urokinase-type plasminogen activator receptor gene. *Blood,* 84**,** 1151-6.

CELLI, B. R., PAUWELS, R. & SNIDER, G. L. 2004. Standards for the diagnosis and managment of patients with COPD.

CHAVAKIS, T., KANSE, S. M., LUPU, F., HAMMES, H. P., MULLER-ESTERL, W., PIXLEY, R. A., COLMAN, R. W. & PREISSNER, K. T. 2000. Different mechanisms define the antiadhesive function of high molecular weight kininogen in integrin- and urokinase receptor-dependent interactions. *Blood,* 96**,** 514-22.

CHAVAKIS, T., MAY, A. E., PREISSNER, K. T. & KANSE, S. M. 1999. Molecular mechanisms of zinc-dependent leukocyte adhesion involving the urokinase receptor and beta2-integrins. *Blood,* 93**,** 2976-83.

CHEN, W., JIN, W. Q., CHEN, L. F., WILLIAMS, T., ZHU, W. L. & FANG, Q. 2012. Urokinase receptor surface expression regulates monocyte migration and is associated with accelerated atherosclerosis. *Int J Cardiol*.

CHETTA, A., FORESI, A., DEL DONNO, M., BERTORELLI, G., PESCI, A. & OLIVIERI, D. 1997. Airways remodeling is a distinctive feature of asthma and is related to severity of disease. *Chest,* 111**,** 852-7.

CHETTY, C., LAKKA, S. S., BHOOPATHI, P., GONDI, C. S., VEERAVALLI, K. K., FASSETT, D., KLOPFENSTEIN, J. D., DINH, D. H., GUJRATI, M. & RAO, J. S. 2010. Urokinase plasminogen activator receptor and/or matrix metalloproteinase-9 inhibition induces apoptosis signaling through lipid rafts in glioblastoma xenograft cells. *Mol Cancer Ther,* 9**,** 2605-17.

CHEVALIER, F., LOPEZ-PRADOS, J., GROVES, P., PEREZ, S., MARTIN-LOMAS, M. & NIETO, P. M. 2006. Structure and dynamics of the conserved protein GPI anchor core inserted into detergent micelles. *Glycobiology,* 16**,** 969-80.

CHEVALIER, F., LOPEZ-PRADOS, J., PEREZ, S., MARTIN-LOMAS, M. & NIETO, P. M. 2005. Conformational Study of GPI Anchors: the Common Oligosaccharide GPI Anchor Backbone. *European Journal of Organic Chemistry***,** 3489-3498.

CHIBA, Y. & MISAWA, M. 2010. MicroRNAs and their therapeutic potential for human diseases: MiR-133a and bronchial smooth muscle hyperresponsiveness in asthma. *J Pharmacol Sci,* 114**,** 264-8.

CHO, M. H., CASTALDI, P. J., WAN, E. S., SIEDLINSKI, M., HERSH, C. P., DEMEO, D. L., HIMES, B. E., SYLVIA, J. S., KLANDERMAN, B. J., ZINITI, J. P., LANGE, C., LITONJUA, A. A., SPARROW, D., REGAN, E. A., MAKE, B. J., HOKANSON, J. E., MURRAY, T., HETMANSKI, J. B., PILLAI, S. G., KONG, X., ANDERSON, W. H., TAL-SINGER, R., LOMAS, D. A., COXSON, H. O., EDWARDS, L. D., MACNEE, W., VESTBO, J., YATES, J. C., AGUSTI, A., CALVERLEY, P. M., CELLI, B., CRIM, C., RENNARD, S., WOUTERS, E., BAKKE, P., GULSVIK, A., CRAPO, J. D., BEATY, T. H. & SILVERMAN, E. K. 2012. A genome-wide association study of COPD identifies a susceptibility locus on chromosome 19q13. *Hum Mol Genet,* 21**,** 947-57.

CHO, S. H., RYU, C. H. & OH, C. K. 2004. Plasminogen activator inhibitor-1 in the pathogenesis of asthma. *Exp Biol Med (Maywood),* 229**,** 138-46.

CHO, S. H., TAM, S. W., DEMISSIE-SANDERS, S., FILLER, S. A. & OH, C. K. 2000. Production of plasminogen activator inhibitor-1 by human mast cells and its possible role in asthma. *J Immunol,* 165**,** 3154-61.

CHU, E. K., CHENG, J., FOLEY, J. S., MECHAM, B. H., OWEN, C. A., HALEY, K. J., MARIANI, T. J., KOHANE, I. S., TSCHUMPERLIN, D. J. & DRAZEN, J. M. 2006. Induction of the plasminogen activator system by mechanical stimulation of human bronchial epithelial cells. *Am J Respir Cell Mol Biol,* 35**,** 628-38.

CHUNG, K. F. 2005. The role of airway smooth muscle in the pathogenesis of airway wall remodeling in chronic obstructive pulmonary disease. *Proc Am Thorac Soc,* 2**,** 347-54; discussion 371-2.

CHURG, A., TAI, H., COULTHARD, T., WANG, R. & WRIGHT, J. L. 2006. Cigarette smoke drives small airway remodeling by induction of growth factors in the airway wall. *Am J Respir Crit Care Med,* 174**,** 1327-34.

CIRULLI, E. T. & GOLDSTEIN, D. B. 2010. Uncovering the roles of rare variants in common disease through whole-genome sequencing. *Nat Rev Genet,* 11**,** 415-25.

COLMAN, R. W., PIXLEY, R. A., NAJAMUNNISA, S., YAN, W., WANG, J., MAZAR, A. & MCCRAE, K. R. 1997. Binding of high molecular weight kininogen to human endothelial cells is mediated via a site within domains 2 and 3 of the urokinase receptor. *J Clin Invest,* 100**,** 1481-7.

CONNOLLY, B. M., CHOI, E. Y., GARDSVOLL, H., BEY, A. L., CURRIE, B. M., CHAVAKIS, T., LIU, S., MOLINOLO, A., PLOUG, M., LEPPLA, S. H. & BUGGE, T. H. 2010. Selective abrogation of the uPA-uPAR interaction in vivo reveals a novel role in suppression of fibrin-associated inflammation. *Blood,* 116**,** 1593-603.

COONS, A. H., CREECH, H. J. & JONES, R. N. 1941. Immunological Properties of an Antibody Containing a Fluorescent Group. *Proc Soc Exp Biol Med,* 47**,** 200-202.

COONS, A. H. & KAPLAN, M. H. 1950. Localization of antigen in tissue cells; improvements in a method for the detection of antigen by means of fluorescent antibody. *J Exp Med,* 91**,** 1-13.

COX, D. G. & KRAFT, P. 2006. Quantification of the power of Hardy-Weinberg equilibrium testing to detect genotyping error. *Hum Hered,* 61**,** 10-4.

CRIPPA, M. P. 2007. Urokinase-type plasminogen activator. *Int J Biochem Cell Biol,* 39**,** 690-4.

CSGA 1997. A genome-wide search for asthma susceptibility loci in ethnically diverse populations. The Collaborative Study on the Genetics of Asthma (CSGA). *Nat Genet,* 15**,** 389-92.

CURKENDALL, S. M., DELUISE, C., JONES, J. K., LANES, S., STANG, M. R., GOEHRING, E., JR. & SHE, D. 2006. Cardiovascular disease in patients with chronic obstructive pulmonary disease, Saskatchewan Canada cardiovascular disease in COPD patients. *Ann Epidemiol,* 16**,** 63-70.

CURRIE, G. P. 2007. *ABC of COPD,* Oxford, Blackwell Publisihing Ltd.

CZEKAY, R. P., KUEMMEL, T. A., ORLANDO, R. A. & FARQUHAR, M. G. 2001. Direct binding of occupied urokinase receptor (uPAR) to LDL receptor-related protein is required for endocytosis of uPAR and regulation of cell surface urokinase activity. *Mol Biol Cell,* 12**,** 1467-79.

D'MELLO, V., SINGH, S., WU, Y. & BIRGE, R. B. 2009. The urokinase plasminogen activator receptor promotes efferocytosis of apoptotic cells. *J Biol Chem,* 284**,** 17030-8.

DANG, J., BOYD, D., WANG, H., ALLGAYER, H., DOE, W. F. & WANG, Y. 1999. A region between -141 and -61 bp containing a proximal AP-1 is essential for constitutive expression of urokinase-type plasminogen activator receptor. *Eur J Biochem,* 264**,** 92-9.

DE BOER, J. D., MAJOOR, C. J., VAN 'T VEER, C., BEL, E. H. & VAN DER POLL, T. 2012. Asthma and coagulation. *Blood,* 119**,** 3236-44.

DE PAULIS, A., MONTUORI, N., PREVETE, N., FIORENTINO, I., ROSSI, F. W., VISCONTE, V., ROSSI, G., MARONE, G. & RAGNO, P. 2004. Urokinase induces basophil chemotaxis through a urokinase receptor epitope that is an endogenous ligand for formyl peptide receptor-like 1 and -like 2. *J Immunol,* 173**,** 5739-48.

DEMEO, D. L., CELEDON, J. C., LANGE, C., REILLY, J. J., CHAPMAN, H. A., SYLVIA, J. S., SPEIZER, F. E., WEISS, S. T. & SILVERMAN, E. K. 2004. Genome-wide linkage of forced mid-expiratory flow in chronic obstructive pulmonary disease. *Am J Respir Crit Care Med,* 170**,** 1294-301.

DEMEO, D. L. & SILVERMAN, E. K. 2004. Alpha1-antitrypsin deficiency. 2: genetic aspects of alpha(1)-antitrypsin deficiency: phenotypes and genetic modifiers of emphysema risk. *Thorax,* 59**,** 259-64.

DEPRISTO, M. A., BANKS, E., POPLIN, R., GARIMELLA, K. V., MAGUIRE, J. R., HARTL, C., PHILIPPAKIS, A. A., DEL ANGEL, G., RIVAS, M. A., HANNA, M., MCKENNA, A., FENNELL, T. J., KERNYTSKY, A. M., SIVACHENKO, A. Y., CIBULSKIS, K., GABRIEL, S. B., ALTSHULER, D. & DALY, M. J. 2011. A framework for variation discovery and genotyping using next-generation DNA sequencing data. *Nat Genet,* 43**,** 491-8.

DESMET, C., GOSSET, P., HENRY, E., GARZE, V., FAISCA, P., VOS, N., JASPAR, F., MELOTTE, D., LAMBRECHT, B., DESMECHT, D., PAJAK, B., MOSER, M., LEKEUX, P. & BUREAU, F. 2005. Treatment of experimental asthma by decoy-mediated local inhibition of activator protein-1. *Am J Respir Crit Care Med,* 172**,** 671-8.

DICKINSON, J. L., BATES, E. J., FERRANTE, A. & ANTALIS, T. M. 1995. Plasminogen activator inhibitor type 2 inhibits tumor necrosis factor alpha-induced apoptosis. Evidence for an alternate biological function. *J Biol Chem,* 270**,** 27894-904.

DIEFFENBACH, C. W., LOWE, T. M. & DVEKSLER, G. S. 1993. General concepts for PCR primer design. *PCR Methods Appl,* 3**,** S30-7.

DIXON, A. L., LIANG, L., MOFFATT, M. F., CHEN, W., HEATH, S., WONG, K. C., TAYLOR, J., BURNETT, E., GUT, I., FARRALL, M., LATHROP, G. M., ABECASIS, G. R. & COOKSON, W. O. 2007. A genome-wide association study of global gene expression. *Nat Genet,* 39**,** 1202-7.

DOUGLAS, G. & ELWARD, K. 2011. *Asthma: Clinician's Desk Reference*, Manson Publishing.

DOURNES, G. & LAURENT, F. 2012. Airway Remodelling in Asthma and COPD: Findings, Similarities, and Differences Using Quantitative CT. *Pulm Med,* 2012**,** 670414.

DRAPKIN, P. T., O'RIORDAN, C. R., YI, S. M., CHIORINI, J. A., CARDELLA, J., ZABNER, J. & WELSH, M. J. 2000. Targeting the urokinase plasminogen activator receptor enhances gene transfer to human airway epithelia. *J Clin Invest,* 105**,** 589-96.

DRAZEN, J. 1998. Clinical pharmacology of leukotriene receptor antagonists and 5-lipoxygenase inhibitors. *Am J Respir Crit Care Med,* 157**,** S233-7; discussion S247-8.

DUFFY, D. L., MARTIN, N. G., BATTISTUTTA, D., HOPPER, J. L. & MATHEWS, J. D. 1990. Genetics of asthma and hay fever in Australian twins. *Am Rev Respir Dis,* 142**,** 1351-8.

DWEIK, R. A., BOGGS, P. B., ERZURUM, S. C., IRVIN, C. G., LEIGH, M. W., LUNDBERG, J. O., OLIN, A. C., PLUMMER, A. L. & TAYLOR, D. R. 2011. An official ATS clinical practice guideline: interpretation of exhaled nitric oxide levels (FENO) for clinical applications. *Am J Respir Crit Care Med,* 184**,** 602-15.

EDFORS-LUBS, M. L. 1971. Allergy in 7000 twin pairs. *Acta Allergol,* 26**,** 249-85.

EDMAN, P. 1949. A method for the determination of amino acid sequence in peptides. *Arch Biochem,* 22**,** 475.

ELIAS, J. A., ZHU, Z., CHUPP, G. & HOMER, R. J. 1999. Airway remodeling in asthma. *J Clin Invest,* 104**,** 1001-6.

ELLIS, V., PYKE, C., ERIKSEN, J., SOLBERG, H. & DANO, K. 1992. The urokinase receptor: involvement in cell surface proteolysis and cancer invasion. *Ann N Y Acad Sci,* 667**,** 13-31.

EUGEN-OLSEN, J., ANDERSEN, O., LINNEBERG, A., LADELUND, S., HANSEN, T., LANGKILDE, A., PETERSEN, J., PIELAK, T., MØLLER, L., JEPPESEN, J., LYNGBAEK, S., FENGER, M., OLSEN, M., HILDEBRANDT, P., BORCH-JOHNSEN, K., JØRGENSEN, T. & HAUGAARD, S. 2010a. Circulating soluble urokinase plasminogen activator receptor predicts cancer, cardiovascular disease, diabetes and mortality in the general population. *Journal of internal medicine,* 268**,** 296-604.

EUGEN-OLSEN, J., ANDERSEN, O., LINNEBERG, A., LADELUND, S., HANSEN, T. W., LANGKILDE, A., PETERSEN, J., PIELAK, T., MOLLER, L. N., JEPPESEN, J., LYNGBAEK, S., FENGER, M., OLSEN, M. H., HILDEBRANDT, P. R., BORCH-JOHNSEN, K., JORGENSEN, T. & HAUGAARD, S. B. 2010b. Circulating soluble urokinase plasminogen activator receptor predicts cancer, cardiovascular disease, diabetes and mortality in the general population. *J Intern Med,* 268**,** 296-308.

FARR, A. & ROMAN, A. 1992. A pitfall of using a second plasmid to determine transfection efficiency. *Nucleic Acids Res,* 20**,** 920.

FAZIOLI, F., RESNATI, M., SIDENIUS, N., HIGASHIMOTO, Y., APPELLA, E. & BLASI, F. 1997. A urokinase-sensitive region of the human urokinase receptor is responsible for its chemotactic activity. *EMBO J,* 16**,** 7279-86.

FINK, E., BHOOLA, K. D., SNYMAN, C., NETH, P. & FIGUEROA, C. D. 2007. Cellular expression of plasma prekallikrein in human tissues. *Biol Chem,* 388**,** 957-63.

FISH, R. J. & KRUITHOF, E. K. 2006. Evidence for serpinB2-independent protection from TNF-alpha-induced apoptosis. *Exp Cell Res,* 312**,** 350-61.

FLOREANI, A. A. & RENNARD, S. I. 1999. The role of cigarette smoke in the pathogenesis of asthma and as a trigger for acute symptoms. *Curr Opin Pulm Med,* 5**,** 38-46.

FONTE, V., KAPULKIN, V., TAFT, A., FLUET, A., FRIEDMAN, D. & LINK, C. D. 2002. Interaction of intracellular beta amyloid peptide with chaperone proteins. *Proc Natl Acad Sci U S A,* 99**,** 9439-44.

FRAZER, K. A., BALLINGER, D. G., COX, D. R., HINDS, D. A., STUVE, L. L., GIBBS, R. A., BELMONT, J. W., BOUDREAU, A., HARDENBOL, P., LEAL, S. M., PASTERNAK, S.,

WHEELER, D. A., WILLIS, T. D., YU, F., YANG, H., ZENG, C., GAO, Y., HU, H., HU, W., LI, C., LIN, W., LIU, S., PAN, H., TANG, X., WANG, J., WANG, W., YU, J., ZHANG, B., ZHANG, Q., ZHAO, H., ZHOU, J., GABRIEL, S. B., BARRY, R., BLUMENSTIEL, B., CAMARGO, A., DEFELICE, M., FAGGART, M., GOYETTE, M., GUPTA, S., MOORE, J., NGUYEN, H., ONOFRIO, R. C., PARKIN, M., ROY, J., STAHL, E., WINCHESTER, E., ZIAUGRA, L., ALTSHULER, D., SHEN, Y., YAO, Z., HUANG, W., CHU, X., HE, Y., JIN, L., LIU, Y., SUN, W., WANG, H., WANG, Y., XIONG, X., XU, L., WAYE, M. M., TSUI, S. K., XUE, H., WONG, J. T., GALVER, L. M., FAN, J. B., GUNDERSON, K., MURRAY, S. S., OLIPHANT, A. R., CHEE, M. S., MONTPETIT, A., CHAGNON, F., FERRETTI, V., LEBOEUF, M., OLIVIER, J. F., PHILLIPS, M. S., ROUMY, S., SALLEE, C., VERNER, A., HUDSON, T. J., KWOK, P. Y., CAI, D., KOBOLDT, D. C., MILLER, R. D., PAWLIKOWSKA, L., TAILLON-MILLER, P., XIAO, M., TSUI, L. C., MAK, W., SONG, Y. Q., TAM, P. K., NAKAMURA, Y., KAWAGUCHI, T., KITAMOTO, T., MORIZONO, T., NAGASHIMA, A., OHNISHI, Y., SEKINE, A., TANAKA, T., TSUNODA, T., et al. 2007. A second generation human haplotype map of over 3.1 million SNPs. *Nature,* 449**,** 851-61.

FUJIWARA, A., TAGUCHI, O., TAKAGI, T., D'ALESSANDRO-GABAZZA, C. N., BOVEDA-RUIZ, D., TODA, M., YASUKAWA, A., MATSUSHIMA, Y., MIYAKE, Y., KOBAYASHI, H., KOBAYASHI, T., GIL-BERNABE, P., NAITO, M., YOSHIDA, M., MORSER, J., TAKEI, Y. & GABAZZA, E. C. 2012. Role of thrombin-activatable fibrinolysis inhibitor in allergic bronchial asthma. *Lung,* 190**,** 189-98.

GABRIEL, S. B., SCHAFFNER, S. F., NGUYEN, H., MOORE, J. M., ROY, J., BLUMENSTIEL, B., HIGGINS, J., DEFELICE, M., LOCHNER, A., FAGGART, M., LIU-CORDERO, S. N., ROTIMI, C., ADEYEMO, A., COOPER, R., WARD, R., LANDER, E. S., DALY, M. J. & ALTSHULER, D. 2002. The structure of haplotype blocks in the human genome. *Science,* 296**,** 2225-9.

GANNE, F., VASSE, M., BEAUDEUX, J. L., PEYNET, J., FRANCOIS, A., PAYSANT, J., LENORMAND, B., COLLET, J. P., VANNIER, J. P., SORIA, J. & SORIA, C. 1999. Increased expression of u-PA and u-PAR on monocytes by LDL and Lp(a) lipoproteins--consequences for plasmin generation and monocyte adhesion. *Thromb Haemost,* 81**,** 594-600.

GAO, X. & HUANG, L. 1995. Cationic liposome-mediated gene transfer. *Gene Ther,* 2**,** 710-22.

GHAVAMI, S., HASHEMI, M., ANDE, S. R., YEGANEH, B., XIAO, W., ESHRAGHI, M., BUS, C. J., KADKHODA, K., WIECHEC, E., HALAYKO, A. J. & LOS, M. 2009. Apoptosis and cancer: mutations within caspase genes. *J Med Genet,* 46**,** 497-510.

GINA 2011. Global Strategy for Asthma Managment and Prevention. Global Initiative for Asthma.

GOLD 2011. Global Strategy for the diagnosis, managment and prevention of chronic obstructive pulmonary disease.

GONDI, C. S., DINH, D. H., GUJRATI, M. & RAO, J. S. 2008. Simultaneous downregulation of uPAR and MMP-9 induces overexpression of the FADD-associated protein RIP and activates caspase 9-mediated apoptosis in gliomas. *Int J Oncol,* 33**,** 783-90.

GRAHAM, C. H., FITZPATRICK, T. E. & MCCRAE, K. R. 1998. Hypoxia stimulates urokinase receptor expression through a heme protein-dependent pathway. *Blood,* 91**,** 3300-7.

GRAINGE, C. L., LAU, L. C., WARD, J. A., DULAY, V., LAHIFF, G., WILSON, S., HOLGATE, S., DAVIES, D. E. & HOWARTH, P. H. 2011. Effect of bronchoconstriction on airway remodeling in asthma. *N Engl J Med,* 364**,** 2006-15.

GUM, R., JUAREZ, J., ALLGAYER, H., MAZAR, A., WANG, Y. & BOYD, D. 1998. Stimulation of urokinase-type plasminogen activator receptor expression by PMA requires JNK1-dependent and -independent signaling modules. *Oncogene,* 17**,** 213-25.

HALAMKOVA, J., KISS, I., PAVLOVSKY, Z., JARKOVSKY, J., TOMASEK, J., TUCEK, S., HANAKOVA, L., MOULIS, M., CECH, Z., ZAVRELOVA, J. & PENKA, M. 2011. Clinical relevance of uPA, uPAR, PAI 1 and PAI 2 tissue expression and plasma PAI 1 level in colorectal carcinoma patients. *Hepatogastroenterology,* 58**,** 1918-25.

HALLER, G., TORGERSON, D. G., OBER, C. & THOMPSON, E. E. 2009. Sequencing the IL4 locus in African Americans implicates rare noncoding variants in asthma susceptibility. *J Allergy Clin Immunol,* 124**,** 1204-9 e9.

HANSEN, L. V., GARDSVOLL, H., NIELSEN, B. S., LUND, L. R., DANO, K., JENSEN, O. N. & PLOUG, M. 2004. Structural analysis and tissue localization of human C4.4A: a protein homologue of the urokinase receptor. *Biochem J,* 380**,** 845-57.

HAO, K., BOSSE, Y., NICKLE, D. C., PARE, P. D., POSTMA, D. S., LAVIOLETTE, M., SANDFORD, A., HACKETT, T. L., DALEY, D., HOGG, J. C., ELLIOTT, W. M., COUTURE, C., LAMONTAGNE, M., BRANDSMA, C. A., VAN DEN BERGE, M., KOPPELMAN, G., REICIN, A. S., NICHOLSON, D. W., MALKOV, V., DERRY, J. M., SUVER, C., TSOU, J. A., KULKARNI, A., ZHANG, C., VESSEY, R., OPITECK, G. J., CURTIS, S. P., TIMENS, W. & SIN, D. D. 2012. Lung eQTLs to Help Reveal the Molecular Underpinnings of Asthma. *PLoS Genet,* 8**,** e1003029.

HAPKE, S., GAWAZ, M., DEHNE, K., KOHLER, J., MARSHALL, J. F., GRAEFF, H., SCHMITT, M., REUNING, U. & LENGYEL, E. 2001. beta(3)A-integrin downregulates the urokinase-type plasminogen activator receptor (u-PAR) through a PEA3/ets transcriptional silencing element in the u-PAR promoter. *Mol Cell Biol,* 21**,** 2118-32.

HARISMENDY, O. & FRAZER, K. 2009. Method for improving sequence coverage uniformity of targeted genomic intervals amplified by LR-PCR using Illumina GA sequencing-by-synthesis technology. *Biotechniques,* 46**,** 229-31.

HAUPT, T. H., PETERSEN, J., ELLEKILDE, G., KLAUSEN, H. H., THORBALL, C. W., EUGEN-OLSEN, J. & ANDERSEN, O. 2012. Plasma suPAR levels are associated with mortality, admission time, and Charlson Comorbidity Index in the acutely admitted medical patient: a prospective observational study. *Crit Care,* 16**,** R130.

HEGUY, A., HARVEY, B. G., LEOPOLD, P. L., DOLGALEV, I., RAMAN, T. & CRYSTAL, R. G. 2007. Responses of the human airway epithelium transcriptome to in vivo injury. *Physiol Genomics,* 29**,** 139-48.

HEID, C. A., STEVENS, J., LIVAK, K. J. & WILLIAMS, P. M. 1996. Real time quantitative PCR. *Genome Res,* 6**,** 986-94.

HIGGINS, M. & KELLER, J. 1975. Familial occurrence of chronic respiratory disease and familial resemblance in ventilatory capacity. *J Chronic Dis,* 28**,** 239-51.

HIMES, B. E., SHEPPARD, K., BERNDT, A., LEME, A. S., MYERS, R. A., GIGNOUX, C. R., LEVIN, A. M., GAUDERMAN, W. J., YANG, J. J., MATHIAS, R. A., ROMIEU, I., TORGERSON, D. G., ROTH, L. A., HUNTSMAN, S., ENG, C., KLANDERMAN, B., ZINITI, J., SENTER-SYLVIA, J., SZEFLER, S. J., LEMANSKE, R. F., JR., ZEIGER, R. S., STRUNK, R. C., MARTINEZ, F. D., BOUSHEY, H., CHINCHILLI, V. M., ISRAEL, E., MAUGER, D., KOPPELMAN, G. H., POSTMA, D. S., NIEUWENHUIS, M. A., VONK, J. M., LIMA, J. J., IRVIN, C. G., PETERS, S. P., KUBO, M., TAMARI, M., NAKAMURA, Y., LITONJUA, A. A., TANTISIRA, K. G., RABY, B. A., BLEECKER, E. R., MEYERS, D. A., LONDON, S. J., BARNES, K. C., GILLILAND, F. D., WILLIAMS, L. K., BURCHARD, E. G., NICOLAE, D. L., OBER, C., DEMEO, D. L., SILVERMAN, E. K., PAIGEN, B., CHURCHILL, G., SHAPIRO, S. D. & WEISS, S. T. 2013. Integration of mouse and human genome-wide association data identifies KCNIP4 as an asthma gene. *PLoS One,* 8**,** e56179.

HOLGATE, S. T., ARSHAD, H. S., ROBERTS, G. C., HOWARTH, P. H., THURNER, P. & DAVIES, D. E. 2010. A new look at the pathogenesis of asthma. *Clin Sci (Lond),* 118**,** 439-50.

HOLLAND, P. M., ABRAMSON, R. D., WATSON, R. & GELFAND, D. H. 1991. Detection of specific polymerase chain reaction product by utilizing the 5'----3' exonuclease activity of Thermus aquaticus DNA polymerase. *Proc Natl Acad Sci U S A,* 88**,** 7276-80.

HOSKING, L., LUMSDEN, S., LEWIS, K., YEO, A., MCCARTHY, L., BANSAL, A., RILEY, J., PURVIS, I. & XU, C. F. 2004. Detection of genotyping errors by Hardy-Weinberg equilibrium testing. *Eur J Hum Genet,* 12**,** 395-9.

HOYER-HANSEN, G., BEHRENDT, N., PLOUG, M., DANO, K. & PREISSNER, K. T. 1997a. The intact urokinase receptor is required for efficient vitronectin binding: receptor cleavage prevents ligand interaction. *FEBS Lett,* 420**,** 79-85.

HOYER-HANSEN, G. & LUND, I. K. 2007. Urokinase receptor variants in tissue and body fluids. *Adv Clin Chem,* 44**,** 65-102.

HOYER-HANSEN, G., PLOUG, M., BEHRENDT, N., RONNE, E. & DANO, K. 1997b. Cell-surface acceleration of urokinase-catalyzed receptor cleavage. *Eur J Biochem,* 243**,** 21-6.

HOYER-HANSEN, G., RONNE, E., SOLBERG, H., BEHRENDT, N., PLOUG, M., LUND, L. R., ELLIS, V. & DANO, K. 1992. Urokinase plasminogen activator cleaves its cell surface receptor releasing the ligand-binding domain. *J Biol Chem,* 267**,** 18224-9.

HSE 2011. Chronic Obstructive Pulmonary Disease.

HUAI, Q., MAZAR, A. P., KUO, A., PARRY, G. C., SHAW, D. E., CALLAHAN, J., LI, Y., YUAN, C., BIAN, C., CHEN, L., FURIE, B., FURIE, B. C., CINES, D. B. & HUANG, M. 2006. Structure of human urokinase plasminogen activator in complex with its receptor. *Science,* 311**,** 656-9.

HUANG, J., LIU, X. J., BAO, H. R., ZHANG, Y., TAN, E. L. & LIAO, J. M. 2011. [The relationship between coagulation/anticoagulation imbalance and oxidative stress in patients with chronic obstructive pulmonary disease]. *Zhonghua Nei Ke Za Zhi,* 50**,** 664-7.

HUIART, L., ERNST, P. & SUISSA, S. 2005. Cardiovascular morbidity and mortality in COPD. *Chest,* 128**,** 2640-6.

HUMBERT, M., MENZ, G., YING, S., CORRIGAN, C. J., ROBINSON, D. S., DURHAM, S. R. & KAY, A. B. 1999. The immunopathology of extrinsic (atopic) and intrinsic (non-atopic) asthma: more similarities than differences. *Immunol Today,* 20**,** 528-33.

ICHINOSE, A., FUJIKAWA, K. & SUYAMA, T. 1986. The activation of pro-urokinase by plasma kallikrein and its inactivation by thrombin. *J Biol Chem,* 261**,** 3486-9.

IDELL, S. 2002. Endothelium and disordered fibrin turnover in the injured lung: newly recognized pathways. *Crit Care Med,* 30**,** S274-80.

IRIGOYEN, J. P. & NAGAMINE, Y. 1999. Cytoskeletal reorganization leads to induction of the urokinase-type plasminogen activator gene by activating FAK and Src and subsequently the Ras/Erk signaling pathway. *Biochem Biophys Res Commun,* 262**,** 666-70.

IYENGAR, S. K. & ELSTON, R. C. 2007. The genetic basis of complex traits: rare variants or "common gene, common disease"? *Methods Mol Biol,* 376**,** 71-84.

IZZOTTI, A., CALIN, G. A., ARRIGO, P., STEELE, V. E., CROCE, C. M. & DE FLORA, S. 2009. Downregulation of microRNA expression in the lungs of rats exposed to cigarette smoke. *FASEB J,* 23**,** 806-12.

JACOBS, J. P., JONES, C. M. & BAILLE, J. P. 1970. Characteristics of a human diploid cell designated MRC-5. *Nature,* 227**,** 168-70.

JANCIAUSKIENE, S. M., BALS, R., KOCZULLA, R., VOGELMEIER, C., KOHNLEIN, T. & WELTE, T. 2011. The discovery of alpha1-antitrypsin and its role in health and disease. *Respir Med,* 105**,** 1129-39.

JATAKANON, A., UASUF, C., MAZIAK, W., LIM, S., CHUNG, K. F. & BARNES, P. J. 1999. Neutrophilic inflammation in severe persistent asthma. *Am J Respir Crit Care Med,* 160**,** 1532-9.

JEFFERY, P. K. 1998. Structural and inflammatory changes in COPD: a comparison with asthma. *Thorax,* 53**,** 129-36.

JIANG, Y., XIAO, W., ZHANG, Y. & XING, Y. 2010. Urokinase-type plasminogen activator system and human cationic antimicrobial protein 18 in serum and induced sputum of patients with chronic obstructive pulmonary disease. *Respirology,* 15**,** 939-46.

JO, M., THOMAS, K. S., MAROZKINA, N., AMIN, T. J., SILVA, C. M., PARSONS, S. J. & GONIAS, S. L. 2005. Dynamic assembly of the urokinase-type plasminogen activator signaling receptor complex determines the mitogenic activity of urokinase-type plasminogen activator. *J Biol Chem,* 280**,** 17449-57.

JOOS, L., HE, J. Q., SHEPHERDSON, M. B., CONNETT, J. E., ANTHONISEN, N. R., PARE, P. D. & SANDFORD, A. J. 2002. The role of matrix metalloproteinase polymorphisms in the rate of decline in lung function. *Hum Mol Genet,* 11**,** 569-76.

KAMENTSKY, L., JONES, T. R., FRASER, A., BRAY, M. A., LOGAN, D. J., MADDEN, K. L., LJOSA, V., RUEDEN, C., ELICEIRI, K. W. & CARPENTER, A. E. 2011. Improved structure, function and compatibility for CellProfiler: modular high-throughput image analysis software. *Bioinformatics,* 27**,** 1179-80.

KANSE, S. M., KOST, C., WILHELM, O. G., ANDREASEN, P. A. & PREISSNER, K. T. 1996. The urokinase receptor is a major vitronectin-binding protein on endothelial cells. *Exp Cell Res,* 224**,** 344-53.

KATSUDA, I., MARUYAMA, F., EZAKI, K., SAWAMURA, T. & ICHIHARA, Y. 2007. A new type of plasma prekallikrein deficiency associated with homozygosity for Gly104Arg and Asn124Ser in apple domain 2 of the heavy-chain region. *Eur J Haematol,* 79**,** 59-68.

KENNY, E. M., CORMICAN, P., GILKS, W. P., GATES, A. S., O'DUSHLAINE, C. T., PINTO, C., CORVIN, A. P., GILL, M. & MORRIS, D. W. 2011. Multiplex target enrichment using DNA indexing for ultra-high throughput SNP detection. *DNA Res,* 18**,** 31-8.

KENT, W. J., SUGNET, C. W., FUREY, T. S., ROSKIN, K. M., PRINGLE, T. H., ZAHLER, A. M. & HAUSSLER, D. 2002. The human genome browser at UCSC. *Genome Res,* 12**,** 996-1006.

KERMODE, J. A., BROWN, N. J., HARDAKER, K. M., FARAH, C. S., BEREND, N., KING, G. G. & SALOME, C. M. 2011. The effect of airway remodelling on airway hyper-responsiveness in asthma. *Respir Med,* 105**,** 1798-804.

KIM, C. D., SOHN, K. C., LEE, S. S., LEE, J. H., KIM, S., LEE, Y. H., RYU, E. K. & PARK, Y. S. 2011. Plasminogen activator inhibitor-2 (PAI-2) secreted from activated mast cells induces alpha-smooth muscle actin (alpha-SMA) expression in dermal fibroblasts. *J Dermatol Sci,* 62**,** 204-6.

KIYAN, Y., LIMBOURG, A., KIYAN, R., TKACHUK, S., LIMBOURG, F. P., OVSIANIKOV, A., CHICHKOV, B. N., HALLER, H. & DUMLER, I. 2012. Urokinase receptor associates with myocardin to control vascular smooth muscle cells phenotype in vascular disease. *Arterioscler Thromb Vasc Biol,* 32**,** 110-22.

KJAERGAARD, M., HANSEN, L. V., JACOBSEN, B., GARDSVOLL, H. & PLOUG, M. 2008. Structure and ligand interactions of the urokinase receptor (uPAR). *Front Biosci,* 13**,** 5441-61.

KJOLLER, L. & HALL, A. 2001. Rac mediates cytoskeletal rearrangements and increased cell motility induced by urokinase-type plasminogen activator receptor binding to vitronectin. *J Cell Biol,* 152**,** 1145-57.

KOOLWIJK, P., SIDENIUS, N., PETERS, E., SIER, C. F., HANEMAAIJER, R., BLASI, F. & VAN HINSBERGH, V. W. 2001. Proteolysis of the urokinase-type plasminogen activator receptor by metalloproteinase-12: implication for angiogenesis in fibrin matrices. *Blood,* 97**,** 3123-31.

KOPPELMAN, G. H., MEYERS, D. A., HOWARD, T. D., ZHENG, S. L., HAWKINS, G. A., AMPLEFORD, E. J., XU, J., KONING, H., BRUINENBERG, M., NOLTE, I. M., VAN DIEMEN, C. C., BOEZEN, H. M., TIMENS, W., WHITTAKER, P. A., STINE, O. C.,

BARTON, S. J., HOLLOWAY, J. W., HOLGATE, S. T., GRAVES, P. E., MARTINEZ, F. D., VAN OOSTERHOUT, A. J., BLEECKER, E. R. & POSTMA, D. S. 2009. Identification of PCDH1 as a novel susceptibility gene for bronchial hyperresponsiveness. *Am J Respir Crit Care Med,* 180**,** 929-35.

KOPPELMAN, G. H. & SAYERS, I. 2011. Evidence of a genetic contribution to lung function decline in asthma. *J Allergy Clin Immunol,* 128**,** 479-84.

KOSHELNICK, Y., EHART, M., HUFNAGL, P., HEINRICH, P. C. & BINDER, B. R. 1997. Urokinase receptor is associated with the components of the JAK1/STAT1 signaling pathway and leads to activation of this pathway upon receptor clustering in the human kidney epithelial tumor cell line TCL-598. *J Biol Chem,* 272**,** 28563-7.

KOTIPATRUNI, R. R., NALLA, A. K., ASUTHKAR, S., GONDI, C. S., DINH, D. H. & RAO, J. S. 2012. Apoptosis Induced by Knockdown of uPAR and MMP-9 is Mediated by Inactivation of EGFR/STAT3 Signaling in Medulloblastoma. *PLoS One,* 7**,** e44798.

KOTZSCH, M., FARTHMANN, J., MEYE, A., FUESSEL, S., BARETTON, G., TJAN-HEIJNEN, V. C., SCHMITT, M., LUTHER, T., SWEEP, F. C., MAGDOLEN, V. & SPAN, P. N. 2005. Prognostic relevance of uPAR-del4/5 and TIMP-3 mRNA expression levels in breast cancer. *Eur J Cancer,* 41**,** 2760-8.

KOTZSCH, M., MAGDOLEN, V., GREITHER, T., KAPPLER, M., BACHE, M., LAUTENSCHLAGER, C., FUSSEL, S., ECKERT, A. W., LUTHER, T., BARETTON, G., WURL, P. & TAUBERT, H. 2011. Combined mRNA expression levels of members of the urokinase plasminogen activator (uPA) system correlate with disease-associated survival of soft-tissue sarcoma patients. *BMC Cancer,* 11**,** 273.

KRUITHOF, E. K. 1988. Plasminogen activator inhibitors--a review. *Enzyme,* 40**,** 113-21.

KRUITHOF, E. K., VASSALLI, J. D., SCHLEUNING, W. D., MATTALIANO, R. J. & BACHMANN, F. 1986. Purification and characterization of a plasminogen activator inhibitor from the histiocytic lymphoma cell line U-937. *J Biol Chem,* 261**,** 11207-13.

KUCHAREWICZ, I., KOWAL, K., BUCZKO, W. & BODZENTA-LUKASZYK, A. 2003. The plasmin system in airway remodeling. *Thromb Res,* 112**,** 1-7.

KUHN, A. R., SCHLAUCH, K., LAO, R., HALAYKO, A. J., GERTHOFFER, W. T. & SINGER, C. A. 2010. MicroRNA Expression in Human Airway Smooth Muscle Cells Role of miR-25 in Regulation of Airway Smooth Muscle Phenotype. *American Journal of Respiratory Cell and Molecular Biology,* 42**,** 506-513.

KUMAR, S. & BAGLIONI, C. 1991. Protection from tumor necrosis factor-mediated cytolysis by overexpression of plasminogen activator inhibitor type-2. *J Biol Chem,* 266**,** 20960-4.

KUMAR, S. D., EMERY, M. J., ATKINS, N. D., DANTA, I. & WANNER, A. 1998. Airway mucosal blood flow in bronchial asthma. *Am J Respir Crit Care Med,* 158**,** 153-6.

KURAMOTO, E., NISHIUMA, T., KOBAYASHI, K., YAMAMOTO, M., KONO, Y., FUNADA, Y., KOTANI, Y., SISSON, T. H., SIMON, R. H. & NISHIMURA, Y. 2009. Inhalation of urokinase-type plasminogen activator reduces airway remodeling in a murine asthma model. *Am J Physiol Lung Cell Mol Physiol,* 296**,** L337-46.

KUSENDA, B., MRAZ, M., MAYER, J. & POSPISILOVA, S. 2006. MicroRNA biogenesis, functionality and cancer relevance. *Biomed Pap Med Fac Univ Palacky Olomouc Czech Repub,* 150**,** 205-15.

LACOSTE, J. Y., BOUSQUET, J., CHANEZ, P., VAN VYVE, T., SIMONY-LAFONTAINE, J., LEQUEU, N., VIC, P., ENANDER, I., GODARD, P. & MICHEL, F. B. 1993. Eosinophilic and neutrophilic inflammation in asthma, chronic bronchitis, and chronic obstructive pulmonary disease. *J Allergy Clin Immunol,* 92**,** 537-48.

LAITINEN, L. A., LAITINEN, A. & HAAHTELA, T. 1993. Airway mucosal inflammation even in patients with newly diagnosed asthma. *Am Rev Respir Dis,* 147**,** 697-704.

LANGKILDE, A., HANSEN, T. W., LADELUND, S., LINNEBERG, A., ANDERSEN, O., HAUGAARD, S. B., JEPPESEN, J. & EUGEN-OLSEN, J. 2011. Increased plasma soluble uPAR level is a risk marker of respiratory cancer in initially cancer-free individuals. *Cancer Epidemiol Biomarkers Prev,* 20**,** 609-18.

LATCHMAN, D. S. 1997. Transcription factors: an overview. *Int J Biochem Cell Biol,* 29**,** 1305-12.

LAUFS, S., SCHUMACHER, J. & ALLGAYER, H. 2006. Urokinase-receptor (u-PAR): an essential player in multiple games of cancer: a review on its role in tumor progression, invasion, metastasis, proliferation/dormancy, clinical outcome and minimal residual disease. *Cell Cycle,* 5**,** 1760-71.

LEE, J. A., COCHRAN, B. J., LOBOV, S. & RANSON, M. 2011. Forty years later and the role of plasminogen activator inhibitor type 2/SERPINB2 is still an enigma. *Semin Thromb Hemost,* 37**,** 395-407.

LEE, T. I. & YOUNG, R. A. 2000. Transcription of eukaryotic protein-coding genes. *Annu Rev Genet,* 34**,** 77-137.

LEMIRE, M. 2011. Defining rare variants by their frequencies in controls may increase type I error. *Nat Genet,* 43**,** 391-2; author reply 394-5.

LENGYEL, E., WANG, H., GUM, R., SIMON, C., WANG, Y. & BOYD, D. 1997. Elevated urokinase-type plasminogen activator receptor expression in a colon cancer cell line is due to a constitutively activated extracellular signal-regulated kinase-1-dependent signaling cascade. *Oncogene,* 14**,** 2563-73.

LENGYEL, E., WANG, H., STEPP, E., JUAREZ, J., WANG, Y., DOE, W., PFARR, C. M. & BOYD, D. 1996. Requirement of an upstream AP-1 motif for the constitutive and phorbol ester-inducible expression of the urokinase-type plasminogen activator receptor gene. *J Biol Chem,* 271**,** 23176-84.

LEPROUST, E. 2012. Target enrichment strategies for next generation sequencing. *MLO Med Lab Obs,* 44**,** 26-7.

LEVY, B. D., VACHIER, I. & SERHAN, C. N. 2012. Resolution of inflammation in asthma. *Clin Chest Med,* 33**,** 559-70.

LEWIN, B. 2004. *Genes VIII*, Pearson Prentice Hall.

LI, C., CAO, S., LIU, Z., YE, X., CHEN, L. & MENG, S. 2010. RNAi-mediated downregulation of uPAR synergizes with targeting of HER2 through the ERK pathway in breast cancer cells. *Int J Cancer,* 127**,** 1507-16.

LI, H. 2011. Tabix: fast retrieval of sequence features from generic TAB-delimited files. *Bioinformatics,* 27**,** 718-9.

LI, H., HANDSAKER, B., WYSOKER, A., FENNELL, T., RUAN, J., HOMER, N., MARTH, G., ABECASIS, G. & DURBIN, R. 2009a. The Sequence Alignment/Map format and SAMtools. *Bioinformatics,* 25**,** 2078-9.

LI, Y. T., HE, B. & WANG, Y. Z. 2009b. Exposure to cigarette smoke upregulates AP-1 activity and induces TNF-alpha overexpression in mouse lungs. *Inhal Toxicol,* 21**,** 641-7.

LIANG, O. D., CHAVAKIS, T., KANSE, S. M. & PREISSNER, K. T. 2001. Ligand binding regions in the receptor for urokinase-type plasminogen activator. *J Biol Chem,* 276**,** 28946-53.

LIJNEN, H. R. 2001. Elements of the fibrinolytic system. *Ann N Y Acad Sci,* 936**,** 226-36.

LILLA, J. N., JOSHI, R. V., CRAIK, C. S. & WERB, Z. 2009. Active plasma kallikrein localizes to mast cells and regulates epithelial cell apoptosis, adipocyte differentiation, and stromal remodeling during mammary gland involution. *J Biol Chem,* 284**,** 13792-803.

LIMA, A. R., ALVES, F. M., ANGELO, P. F., ANDRADE, D., BLABER, S. I., BLABER, M., JULIANO, L. & JULIANO, M. A. 2008. S(1)' and S(2)' subsite specificities of human plasma kallikrein and tissue kallikrein 1 for the hydrolysis of peptides derived from the bradykinin domain of human kininogen. *Biol Chem,* 389**,** 1487-94.

LIU, D., AGUIRRE GHISO, J., ESTRADA, Y. & OSSOWSKI, L. 2002a. EGFR is a transducer of the urokinase receptor initiated signal that is required for in vivo growth of a human carcinoma. *Cancer Cell,* 1**,** 445-57.

LIU, W., JIAO, H., MURRAY, N. C., O'CONNOR, M. & ROELOFS, W. L. 2002b. Gene characterized for membrane desaturase that produces (E)-11 isomers of mono- and diunsaturated fatty acids. *Proc Natl Acad Sci U S A,* 99**,** 620-4.

LIU, X., TOGO, S., AL-MUGOTIR, M., KIM, H., FANG, Q., KOBAYASHI, T., WANG, X., MAO, L., BITTERMAN, P. & RENNARD, S. 2008. NF-kappaB mediates the survival of human bronchial epithelial cells exposed to cigarette smoke extract. *Respir Res,* 9**,** 66.

LIVAK, K. J. & SCHMITTGEN, T. D. 2001. Analysis of relative gene expression data using real-time quantitative PCR and the 2(-Delta Delta C(T)) Method. *Methods,* 25**,** 402-8.

LLINAS, P., LE DU, M. H., GARDSVOLL, H., DANO, K., PLOUG, M., GILQUIN, B., STURA, E. A. & MENEZ, A. 2005. Crystal structure of the human urokinase plasminogen activator receptor bound to an antagonist peptide. *EMBO J,* 24**,** 1655-63.

LOO, A. E., HO, R. & HALLIWELL, B. 2011. Mechanism of hydrogen peroxide-induced keratinocyte migration in a scratch-wound model. *Free Radic Biol Med,* 51**,** 884-92.

LOSKUTOFF, D. J., CURRIDEN, S. A., HU, G. & DENG, G. 1999. Regulation of cell adhesion by PAI-1. *APMIS,* 107**,** 54-61.

LOTVALL, J., AKDIS, C. A., BACHARIER, L. B., BJERMER, L., CASALE, T. B., CUSTOVIC, A., LEMANSKE, R. F., JR., WARDLAW, A. J., WENZEL, S. E. & GREENBERGER, P. A. 2011. Asthma endotypes: a new approach to classification of disease entities within the asthma syndrome. *J Allergy Clin Immunol,* 127**,** 355-60.

LOUIS, R., LAU, L. C., BRON, A. O., ROLDAAN, A. C., RADERMECKER, M. & DJUKANOVIC, R. 2000. The relationship between airways inflammation and asthma severity. *Am J Respir Crit Care Med,* 161**,** 9-16.

LOWHAGEN, O. 2012. Diagnosis of asthma - a new approach. *Allergy,* 67**,** 713-7.

LUDVIKSDOTTIR, D., DIAMANT, Z., ALVING, K., BJERMER, L. & MALINOVSCHI, A. 2012. Clinical aspects of using exhaled NO in asthma diagnosis and management. *Clin Respir J,* 6**,** 193-207.

LUND, L. R., ELLIS, V., RONNE, E., PYKE, C. & DANO, K. 1995. Transcriptional and post-transcriptional regulation of the receptor for urokinase-type plasminogen activator by cytokines and tumour promoters in the human lung carcinoma cell line A549. *Biochem J,* 310 (Pt 1)**,** 345-52.

LUTHER, T., KOTZSCH, M., MEYE, A., LANGERHOLC, T., FUSSEL, S., OLBRICHT, N., ALBRECHT, S., OCKERT, D., MUEHLENWEG, B., FRIEDRICH, K., GROSSER, M., SCHMITT, M., BARETTON, G. & MAGDOLEN, V. 2003. Identification of a novel urokinase receptor splice variant and its prognostic relevance in breast cancer. *Thromb Haemost,* 89**,** 705-17.

MADSEN, C. D., FERRARIS, G. M., ANDOLFO, A., CUNNINGHAM, O. & SIDENIUS, N. 2007. uPAR-induced cell adhesion and migration: vitronectin provides the key. *J Cell Biol,* 177**,** 927-39.

MAHUT, B., TRINQUART, L., BOKOV, P., PEIFFER, C. & DELCLAUX, C. 2010. Lung function impairment evidenced by sequential specific airway resistance in childhood persistent asthma: a longitudinal study. *J Asthma,* 47**,** 655-9.

MAMANOVA, L., COFFEY, A. J., SCOTT, C. E., KOZAREWA, I., TURNER, E. H., KUMAR, A., HOWARD, E., SHENDURE, J. & TURNER, D. J. 2010. Target-enrichment strategies for next-generation sequencing. *Nat Methods,* 7**,** 111-8.

MANETTI, M., ALLANORE, Y., REVILLOD, L., FATINI, C., GUIDUCCI, S., CUOMO, G., BONINO, C., RICCIERI, V., BAZZICHI, L., LIAKOULI, V., CIPRIANI, P., GIACOMELLI, R., ABBATE, R., BOMBARDIERI, S., VALESINI, G., MONTECUCCO, C., VALENTINI, G., IBBA-MANNESCHI, L. & MATUCCI-CERINIC, M. 2011. A genetic variation

located in the promoter region of the UPAR (CD87) gene is associated with the vascular complications of systemic sclerosis. *Arthritis Rheum,* 63**,** 247-56.

MANNINO, D. M. 2002. COPD: epidemiology, prevalence, morbidity and mortality, and disease heterogeneity. *Chest,* 121**,** 121S-126S.

MARCH, M. E., SLEIMAN, P. M. & HAKONARSON, H. 2013. Genetic polymorphisms and associated susceptibility to asthma. *Int J Gen Med,* 6**,** 253-65.

MARTINEZ, F. D. & HOLBERG, C. J. 1995. Segregation analysis of physician-diagnosed asthma in Hispanic and non-Hispanic white families. *Clin Exp Allergy,* 25 Suppl 2**,** 68-70; discussion 95-6.

MARTINS, C. J., GENELHU, V., SANJULIANI, A. F., CABELLO, P. H. & FRANCISCHETTI, E. A. 2012. Association between leptin and its soluble receptor with cardiometabolic risk factors in a Brazilian population. *Eur J Intern Med,* 23**,** e131-5.

MAY, A. E., KANSE, S. M., LUND, L. R., GISLER, R. H., IMHOF, B. A. & PREISSNER, K. T. 1998. Urokinase receptor (CD87) regulates leukocyte recruitment via beta 2 integrins in vivo. *J Exp Med,* 188**,** 1029-37.

MAYOR, C., BRUDNO, M., SCHWARTZ, J. R., POLIAKOV, A., RUBIN, E. M., FRAZER, K. A., PACHTER, L. S. & DUBCHAK, I. 2000. VISTA : visualizing global DNA sequence alignments of arbitrary length. *Bioinformatics,* 16**,** 1046-7.

MAZAR, A. P., HENKIN, J. & GOLDFARB, R. H. 1999. The urokinase plasminogen activator system in cancer: implications for tumor angiogenesis and metastasis. *Angiogenesis,* 3**,** 15-32.

MAZUMDAR, A., ADAM, L., BOYD, D. & KUMAR, R. 2001. Heregulin regulation of urokinase plasminogen activator and its receptor: human breast epithelial cell invasion. *Cancer Res,* 61**,** 400-5.

MAZZIERI, R. & BLASI, F. 2005. The urokinase receptor and the regulation of cell proliferation. *Thromb Haemost,* 93**,** 641-6.

MAZZIERI, R., D'ALESSIO, S., KENMOE, R. K., OSSOWSKI, L. & BLASI, F. 2006. An uncleavable uPAR mutant allows dissection of signaling pathways in uPA-dependent cell migration. *Mol Biol Cell,* 17**,** 367-78.

MCCLOSKEY, S. C., PATEL, B. D., HINCHLIFFE, S. J., REID, E. D., WAREHAM, N. J. & LOMAS, D. A. 2001. Siblings of patients with severe chronic obstructive pulmonary disease have a significant risk of airflow obstruction. *Am J Respir Crit Care Med,* 164**,** 1419-24.

MCKEEVER, T. M., LEWIS, S. A., SMITH, C., COLLINS, J., HEATLIE, H., FRISCHER, M. & HUBBARD, R. 2001. Siblings, multiple births, and the incidence of allergic disease: a birth cohort study using the West Midlands general practice research database. *Thorax,* 56**,** 758-62.

MCKINLAY, L. H., TYMMS, M. J., THOMAS, R. S., SETH, A., HASTHORPE, S., HERTZOG, P. J. & KOLA, I. 1998. The role of Ets-1 in mast cell granulocyte-macrophage colony-stimulating factor expression and activation. *J Immunol,* 161**,** 4098-105.

MEDCALF, R. L. 2011. Plasminogen activator inhibitor type 2: still an enigmatic serpin but a model for gene regulation. *Methods Enzymol,* 499**,** 105-34.

MEKKAWY, A. H., MORRIS, D. L. & POURGHOLAMI, M. H. 2012. HAX1 Augments Cell Proliferation, Migration, Adhesion, and Invasion Induced by Urokinase-Type Plasminogen Activator Receptor. *J Oncol,* 2012**,** 950749.

MELDRUM, C., DOYLE, M. A. & TOTHILL, R. W. 2011. Next-generation sequencing for cancer diagnostics: a practical perspective. *Clin Biochem Rev,* 32**,** 177-95.

MERRETT, J. & MERRETT, T. G. 1987. Phadiatop--a novel IgE antibody screening test. *Clin Allergy,* 17**,** 409-16.

MESSEGUER, X., ESCUDERO, R., FARRE, D., NUNEZ, O., MARTINEZ, J. & ALBA, M. M. 2002. PROMO: detection of known transcription regulatory elements using species-tailored searches. *Bioinformatics,* 18**,** 333-4.

METZKER, M. L. 2010. Sequencing technologies - the next generation. *Nat Rev Genet,* 11**,** 31-46.

MILES, L. A., GREENGARD, J. S. & GRIFFIN, J. H. 1983. A comparison of the abilities of plasma kallikrein, beta-Factor XIIa, Factor XIa and urokinase to activate plasminogen. *Thromb Res,* 29**,** 407-17.

MIZUKAMI, I. F. & TODD, R. F., 3RD 1998. A soluble form of the urokinase plasminogen activator receptor (suPAR) can bind to hematopoietic cells. *J Leukoc Biol,* 64**,** 203-13.

MOFFATT, M. F., GUT, I. G., DEMENAIS, F., STRACHAN, D. P., BOUZIGON, E., HEATH, S., VON MUTIUS, E., FARRALL, M., LATHROP, M. & COOKSON, W. O. 2010. A large-scale, consortium-based genomewide association study of asthma. *N Engl J Med,* 363**,** 1211-21.

MONTEMURRO, P., BARBUTI, G., CONESE, M., GABRIELE, S., PETIO, M., COLUCCI, M. & SEMERARO, N. 1999. Retinoic acid stimulates plasminogen activator inhibitor 2 production by blood mononuclear cells and inhibits urokinase-induced extracellular proteolysis. *Br J Haematol,* 107**,** 294-9.

MONTUORI, N., CARRIERO, M. V., SALZANO, S., ROSSI, G. & RAGNO, P. 2002. The cleavage of the urokinase receptor regulates its multiple functions. *J Biol Chem,* 277**,** 46932-9.

MONTUORI, N., VISCONTE, V., ROSSI, G. & RAGNO, P. 2005. Soluble and cleaved forms of the urokinase-receptor: degradation products or active molecules? *Thromb Haemost,* 93**,** 192-8.

MOSMANN, T. 1983. Rapid colorimetric assay for cellular growth and survival: application to proliferation and cytotoxicity assays. *J Immunol Methods,* 65**,** 55-63.

MOTTA, G., ROJKJAER, R., HASAN, A. A., CINES, D. B. & SCHMAIER, A. H. 1998. High molecular weight kininogen regulates prekallikrein assembly and activation on endothelial cells: a novel mechanism for contact activation. *Blood,* 91**,** 516-28.

MUSTJOKI, S., SIDENIUS, N. & VAHERI, A. 2000. Enhanced release of soluble urokinase receptor by endothelial cells in contact with peripheral blood cells. *FEBS Lett,* 486**,** 237-42.

MYLONA, E. E., ALEXANDROU, P. T., GIANNOPOULOU, I. A., RAFAILIDIS, P. I., MARKAKI, S., KERAMOPOULOS, A. & NAKOPOULOU, L. L. 2006. Study of the topographic distribution of ets-1 protein expression in invasive breast carcinomas in relation to tumor phenotype. *Cancer Detect Prev,* 30**,** 111-7.

NAGARAJU, G. P., NALLA, A. K., GUPTA, R., MOHANAM, S., GUJRATI, M., DINH, D. H. & RAO, J. S. 2011. siRNA-mediated downregulation of MMP-9 and uPAR in combination with radiation induces G2/M cell-cycle arrest in Medulloblastoma. *Mol Cancer Res,* 9**,** 51-66.

NAKAMURA, Y., ESNAULT, S., MAEDA, T., KELLY, E. A., MALTER, J. S. & JARJOUR, N. N. 2004. Ets-1 regulates TNF-alpha-induced matrix metalloproteinase-9 and tenascin expression in primary bronchial fibroblasts. *J Immunol,* 172**,** 1945-52.

NALDINI, L., VIGNA, E., BARDELLI, A., FOLLENZI, A., GALIMI, F. & COMOGLIO, P. M. 1995. Biological activation of pro-HGF (hepatocyte growth factor) by urokinase is controlled by a stoichiometric reaction. *J Biol Chem,* 270**,** 603-11.

NALLA, A. K., GORANTLA, B., GONDI, C. S., LAKKA, S. S. & RAO, J. S. 2010. Targeting MMP-9, uPAR, and cathepsin B inhibits invasion, migration and activates apoptosis in prostate cancer cells. *Cancer Gene Ther,* 17**,** 599-613.

NATANEK, S. A., RIDDOCH-CONTRERAS, J., MARSH, G. S., HOPKINSON, N. S., MAN, W. D., MOXHAM, J., POLKEY, M. I. & KEMP, P. R. 2011. Yin Yang 1 expression and localisation in quadriceps muscle in COPD. *Arch Bronconeumol,* 47**,** 296-302.

NHLBI. 2007. *Expert Panel Report 3 (EPR-3): Guidelines for the Diagnosis and Management of Asthma* [Online]. National Heart Lung and Blood Institute. Available: http://www.nhlbi.nih.gov/guidelines/asthma/asthsumm.htm 2007].

NHS. 2010. *NHS choices - COPD* [Online]. Available:
http://www.nhs.uk/conditions/chronic-obstructive-pulmonary-disease/Pages/Introduction.aspx [Accessed 06.09.2012.

NICE 2010. CG101 Chronic obstructive pulmonary disease (update): full guideline.

NIEWOEHNER, D. E., KLEINERMAN, J. & RICE, D. B. 1974. Pathologic changes in the peripheral airways of young cigarette smokers. *N Engl J Med,* 291**,** 755-8.

NIKOLOV, D. B. & BURLEY, S. K. 1997. RNA polymerase II transcription initiation: a structural view. *Proc Natl Acad Sci U S A,* 94**,** 15-22.

NOLAN, T., HANDS, R. E. & BUSTIN, S. A. 2006. Quantification of mRNA using real-time RT-PCR. *Nat Protoc,* 1**,** 1559-82.

NOWICKI, T. S., ZHAO, H., DARZYNKIEWICZ, Z., MOSCATELLO, A., SHIN, E., SCHANTZ, S., TIWARI, R. K. & GELIEBTER, J. 2011. Downregulation of uPAR inhibits migration, invasion, proliferation, FAK/PI3K/Akt signaling and induces senescence in papillary thyroid carcinoma cells. *Cell Cycle,* 10**,** 100-7.

O'DONNELL, R. A., DAVIES, D. E. & HOLGATE, S. T. 2002. Airway Remodelling. *In:* BARNES, P., DRAZEN, J., RENNARD, S. & THOMSON, N. (eds.) *Asthma and COPD.* London: Academic Press.

ODEKON, L. E., BLASI, F. & RIFKIN, D. B. 1994. Requirement for receptor-bound urokinase in plasmin-dependent cellular conversion of latent TGF-beta to TGF-beta. *J Cell Physiol,* 158**,** 398-407.

OHNUKI, Y., REDDEL, R. R., BATES, S. E., LEHMAN, T. A., LECHNER, J. F. & HARRIS, C. C. 1996. Chromosomal changes and progressive tumorigenesis of human bronchial epithelial cell lines. *Cancer Genet Cytogenet,* 92**,** 99-110.

OKAN, E., DREWETT, V., SHAW, P. E. & JONES, P. 2001. The small-GTPase RalA activates transcription of the urokinase plasminogen activator receptor (uPAR) gene via an AP1-dependent mechanism. *Oncogene,* 20**,** 1816-24.

OSSOWSKI, L., CLUNIE, G., MASUCCI, M. T. & BLASI, F. 1991. In vivo paracrine interaction between urokinase and its receptor: effect on tumor cell invasion. *J Cell Biol,* 115**,** 1107-12.

PALMER, L. J., CELEDON, J. C., CHAPMAN, H. A., SPEIZER, F. E., WEISS, S. T. & SILVERMAN, E. K. 2003. Genome-wide linkage analysis of bronchodilator responsiveness and post-bronchodilator spirometric phenotypes in chronic obstructive pulmonary disease. *Hum Mol Genet,* 12**,** 1199-210.

PANHUYSEN, C. I., BLEECKER, E. R., KOETER, G. H., MEYERS, D. A. & POSTMA, D. S. 1998. Characterization of obstructive airway disease in family members of probands with asthma. An algorithm for the diagnosis of asthma. *Am J Respir Crit Care Med,* 157**,** 1734-42.

PARK, J. S., PARK, J. H., KHOI, P. N., JOO, Y. E. & JUNG, Y. D. 2011. MSP-induced RON activation upregulates uPAR expression and cell invasiveness via MAPK, AP-1 and NF-kappaB signals in gastric cancer cells. *Carcinogenesis,* 32**,** 175-81.

PARK, Y. J., LIU, G., TSURUTA, Y., LORNE, E. & ABRAHAM, E. 2009. Participation of the urokinase receptor in neutrophil efferocytosis. *Blood,* 114**,** 860-70.

PERSSON, C. G. 1986. Role of plasma exudation in asthmatic airways. *Lancet,* 2**,** 1126-9.

PERSSON, M., ENGSTROM, G., BJORKBACKA, H. & HEDBLAD, B. 2012. Soluble urokinase plasminogen activator receptor in plasma is associated with incidence of CVD. Results from the Malmo Diet and Cancer Study. *Atherosclerosis,* 220**,** 502-5.

PLESNER, T., PLOUG, M., ELLIS, V., RONNE, E., HOYER-HANSEN, G., WITTRUP, M., PEDERSEN, T. L., TSCHERNING, T., DANO, K. & HANSEN, N. E. 1994a. The receptor for urokinase-type plasminogen activator and urokinase is translocated from two distinct intracellular compartments to the plasma membrane on stimulation of human neutrophils. *Blood,* 83**,** 808-15.

PLESNER, T., RALFKIAER, E., WITTRUP, M., JOHNSEN, H., PYKE, C., PEDERSEN, T. L., HANSEN, N. E. & DANO, K. 1994b. Expression of the receptor for urokinase-type

plasminogen activator in normal and neoplastic blood cells and hematopoietic tissue. *Am J Clin Pathol,* 102**,** 835-41.

PLOUG, M. 2003. Structure-function relationships in the interaction between the urokinase-type plasminogen activator and its receptor. *Curr Pharm Des,* 9**,** 1499-528.

PLOUG, M., BEHRENDT, N., LOBER, D. & DANO, K. 1991a. Protein structure and membrane anchorage of the cellular receptor for urokinase-type plasminogen activator. *Semin Thromb Hemost,* 17**,** 183-93.

PLOUG, M., ELLIS, V. & DANO, K. 1994. Ligand interaction between urokinase-type plasminogen activator and its receptor probed with 8-anilino-1-naphthalenesulfonate. Evidence for a hydrophobic binding site exposed only on the intact receptor. *Biochemistry,* 33**,** 8991-7.

PLOUG, M., RONNE, E., BEHRENDT, N., JENSEN, A. L., BLASI, F. & DANO, K. 1991b. Cellular receptor for urokinase plasminogen activator. Carboxyl-terminal processing and membrane anchoring by glycosyl-phosphatidylinositol. *J Biol Chem,* 266**,** 1926-33.

POLOSA, R., MALERBA, M., CACCIOLA, R. R., MORJARIA, J. B., MAUGERI, C., PROSPERINI, G., GULLO, R., SPICUZZA, L., RADAELI, A. & DI MARIA, G. U. 2011. Effect of acute exacerbations on circulating endothelial, clotting and fibrinolytic markers in COPD patients. *Intern Emerg Med*.

POSTMA, D. S. & TIMENS, W. 2006. Remodeling in asthma and chronic obstructive pulmonary disease. *Proc Am Thorac Soc,* 3**,** 434-9.

POTTELBERGE, G. R., MESTDAGH, P., BRACKE, K. R., THAS, O., DURME, Y. M., JOOS, G. F., VANDESOMPELE, J. & BRUSSELLE, G. G. 2011. MicroRNA expression in induced sputum of smokers and patients with chronic obstructive pulmonary disease. *Am J Respir Crit Care Med,* 183**,** 898-906.

PREISSNER, K. T., KANSE, S. M. & MAY, A. E. 2000. Urokinase receptor: a molecular organizer in cellular communication. *Curr Opin Cell Biol,* 12**,** 621-8.

PRITCHARD, J. K. 2001. Are rare variants responsible for susceptibility to complex diseases? *Am J Hum Genet,* 69**,** 124-37.

PROFITA, M., BONANNO, A., MONTALBANO, A. M., FERRARO, M., SIENA, L., BRUNO, A., GIRBINO, S., ALBANO, G. D., CASAROSA, P., PIEPER, M. P. & GJOMARKAJ, M. 2011. Cigarette smoke extract activates human bronchial epithelial cells affecting non-neuronal cholinergic system signalling in vitro. *Life Sci,* 89**,** 36-43.

PURCELL, S., NEALE, B., TODD-BROWN, K., THOMAS, L., FERREIRA, M. A., BENDER, D., MALLER, J., SKLAR, P., DE BAKKER, P. I., DALY, M. J. & SHAM, P. C. 2007. PLINK: a tool set for whole-genome association and population-based linkage analyses. *Am J Hum Genet,* 81**,** 559-75.

PURICELLI, L., PROIETTI, C. J., LABRIOLA, L., SALATINO, M., BALANA, M. E., AGUIRRE GHISO, J., LUPU, R., PIGNATARO, O. P., CHARREAU, E. H., BAL DE KIER JOFFE, E. & ELIZALDE, P. V. 2002. Heregulin inhibits proliferation via ERKs and phosphatidyl-inositol 3-kinase activation but regulates urokinase plasminogen activator independently of these pathways in metastatic mammary tumor cells. *Int J Cancer,* 100**,** 642-53.

PYKE, C., ERIKSEN, J., SOLBERG, H., NIELSEN, B. S., KRISTENSEN, P., LUND, L. R. & DANO, K. 1993. An alternatively spliced variant of mRNA for the human receptor for urokinase plasminogen activator. *FEBS Lett,* 326**,** 69-74.

QIAGEN 2010. RNeasy® Mini Handbook.

QUIGLEY, J. P., GOLD, L. I., SCHWIMMER, R. & SULLIVAN, L. M. 1987. Limited cleavage of cellular fibronectin by plasminogen activator purified from transformed cells. *Proc Natl Acad Sci U S A,* 84**,** 2776-80.

RABBANI, S. A. & MAZAR, A. P. 2001. The role of the plasminogen activation system in angiogenesis and metastasis. *Surg Oncol Clin N Am,* 10**,** 393-415, x.

RACKEMANN, F. M. 1947. Intrinsic asthma. *J Nerv Ment Dis,* 106**,** 497.

RASMUSSEN, F., TAYLOR, D. R., FLANNERY, E. M., COWAN, J. O., GREENE, J. M., HERBISON, G. P. & SEARS, M. R. 2002. Risk factors for airway remodeling in asthma manifested by a low postbronchodilator FEV1/vital capacity ratio: a longitudinal population study from childhood to adulthood. *Am J Respir Crit Care Med,* 165**,** 1480-8.

REDDEL, R. R., KE, Y., GERWIN, B. I., MCMENAMIN, M. G., LECHNER, J. F., SU, R. T., BRASH, D. E., PARK, J. B., RHIM, J. S. & HARRIS, C. C. 1988. Transformation of human bronchial epithelial cells by infection with SV40 or adenovirus-12 SV40 hybrid virus, or transfection via strontium phosphate coprecipitation with a plasmid containing SV40 early region genes. *Cancer Res,* 48**,** 1904-9.

REIHSAUS, E., INNIS, M., MACINTYRE, N. & LIGGETT, S. B. 1993. Mutations in the gene encoding for the beta 2-adrenergic receptor in normal and asthmatic subjects. *Am J Respir Cell Mol Biol,* 8**,** 334-9.

REPAPI, E., SAYERS, I., WAIN, L. V., BURTON, P. R., JOHNSON, T., OBEIDAT, M., ZHAO, J. H., RAMASAMY, A., ZHAI, G., VITART, V., HUFFMAN, J. E., IGL, W., ALBRECHT, E., DELOUKAS, P., HENDERSON, J., GRANELL, R., MCARDLE, W. L., RUDNICKA, A. R., BARROSO, I., LOOS, R. J., WAREHAM, N. J., MUSTELIN, L., RANTANEN, T., SURAKKA, I., IMBODEN, M., WICHMANN, H. E., GRKOVIC, I., JANKOVIC, S., ZGAGA, L., HARTIKAINEN, A. L., PELTONEN, L., GYLLENSTEN, U., JOHANSSON, A., ZABOLI, G., CAMPBELL, H., WILD, S. H., WILSON, J. F., GLASER, S., HOMUTH, G., VOLZKE, H., MANGINO, M., SORANZO, N., SPECTOR, T. D., POLASEK, O., RUDAN, I., WRIGHT, A. F., HELIOVAARA, M., RIPATTI, S., POUTA, A., NALUAI, A. T., OLIN, A. C., TOREN, K., COOPER, M. N., JAMES, A. L., PALMER, L. J., HINGORANI, A. D., WANNAMETHEE, S. G., WHINCUP, P. H., SMITH, G. D., EBRAHIM, S., MCKEEVER, T. M., PAVORD, I. D., MACLEOD, A. K., MORRIS, A. D., PORTEOUS, D. J., COOPER, C., DENNISON, E., SHAHEEN, S., KARRASCH, S., SCHNABEL, E., SCHULZ, H., GRALLERT, H., BOUATIA-NAJI, N., DELPLANQUE, J., FROGUEL, P., BLAKEY, J. D., BRITTON, J. R., MORRIS, R. W., HOLLOWAY, J. W., LAWLOR, D. A., HUI, J., NYBERG, F., JARVELIN, M. R., JACKSON, C., KAHONEN, M., KAPRIO, J., PROBST-HENSCH, N. M., KOCH, B., HAYWARD, C., EVANS, D. M., ELLIOTT, P., STRACHAN, D. P., HALL, I. P. & TOBIN, M. D. 2010. Genome-wide association study identifies five loci associated with lung function. *Nat Genet,* 42**,** 36-44.

RESNATI, M., GUTTINGER, M., VALCAMONICA, S., SIDENIUS, N., BLASI, F. & FAZIOLI, F. 1996. Proteolytic cleavage of the urokinase receptor substitutes for the agonist-induced chemotactic effect. *EMBO J,* 15**,** 1572-82.

RESNATI, M., PALLAVICINI, I., WANG, J. M., OPPENHEIM, J., SERHAN, C. N., ROMANO, M. & BLASI, F. 2002. The fibrinolytic receptor for urokinase activates the G protein-coupled chemotactic receptor FPRL1/LXA4R. *Proc Natl Acad Sci U S A,* 99**,** 1359-64.

RIJNEVELD, A. W., LEVI, M., FLORQUIN, S., SPEELMAN, P., CARMELIET, P. & VAN DER POLL, T. 2002. Urokinase receptor is necessary for adequate host defense against pneumococcal pneumonia. *J Immunol,* 168**,** 3507-11.

RIVAS, M. A., BEAUDOIN, M., GARDET, A., STEVENS, C., SHARMA, Y., ZHANG, C. K., BOUCHER, G., RIPKE, S., ELLINGHAUS, D., BURTT, N., FENNELL, T., KIRBY, A., LATIANO, A., GOYETTE, P., GREEN, T., HALFVARSON, J., HARITUNIANS, T., KORN, J. M., KURUVILLA, F., LAGACE, C., NEALE, B., LO, K. S., SCHUMM, P., TORKVIST, L., DUBINSKY, M. C., BRANT, S. R., SILVERBERG, M. S., DUERR, R. H., ALTSHULER, D., GABRIEL, S., LETTRE, G., FRANKE, A., D'AMATO, M., MCGOVERN, D. P., CHO, J. H., RIOUX, J. D., XAVIER, R. J. & DALY, M. J. 2011. Deep resequencing of GWAS loci identifies independent rare variants associated with inflammatory bowel disease. *Nat Genet,* 43**,** 1066-73.

ROCHAT, T. 2005. [Is intrinsic or non-atopic asthma a particular disease?]. *Rev Med Suisse,* 1**,** 2640-3.

ROEMER E, SCHRAMKE H, WEILER H, BUETTNER A, KAUSCHE S, WEBER S, BERGES A, STUEBER M, MUENCH M, TRELLES-STICKEN E, PYPE J, KOHLGRUEBER K, VOELKEL H & S, W. 2012. Mainstream Smoke Chemistry and In Vitro and In Vivo Toxicity of the Reference Cigarettes 3R4F and 2R4F. *Contributions to Tobacco Research,* 25**,** 316-335.

ROGERS, D. F. & EVANS, T. W. 1992. Plasma exudation and oedema in asthma. *Br Med Bull,* 48**,** 120-34.

ROJKJAER, R. & SCHMAIER, A. H. 1999. Activation of the plasma kallikrein/kinin system on endothelial cell membranes. *Immunopharmacology,* 43**,** 109-14.

ROLDAN, A. L., CUBELLIS, M. V., MASUCCI, M. T., BEHRENDT, N., LUND, L. R., DANO, K., APPELLA, E. & BLASI, F. 1990. Cloning and expression of the receptor for human urokinase plasminogen activator, a central molecule in cell surface, plasmin dependent proteolysis. *EMBO J,* 9**,** 467-74.

ROMER, J., LUND, L. R., ERIKSEN, J., PYKE, C., KRISTENSEN, P. & DANO, K. 1994. The receptor for urokinase-type plasminogen activator is expressed by keratinocytes at the leading edge during re-epithelialization of mouse skin wounds. *J Invest Dermatol,* 102**,** 519-22.

ROSENBLOOM, K. R., DRESZER, T. R., LONG, J. C., MALLADI, V. S., SLOAN, C. A., RANEY, B. J., CLINE, M. S., KAROLCHIK, D., BARBER, G. P., CLAWSON, H., DIEKHANS, M., FUJITA, P. A., GOLDMAN, M., GRAVELL, R. C., HARTE, R. A., HINRICHS, A. S., KIRKUP, V. M., KUHN, R. M., LEARNED, K., MADDREN, M., MEYER, L. R., POHL, A., RHEAD, B., WONG, M. C., ZWEIG, A. S., HAUSSLER, D. & KENT, W. J. 2012. ENCODE whole-genome data in the UCSC Genome Browser: update 2012. *Nucleic Acids Res,* 40**,** D912-7.

ROTH, M., JOHNSON, P. R., BORGER, P., BIHL, M. P., RUDIGER, J. J., KING, G. G., GE, Q., HOSTETTLER, K., BURGESS, J. K., BLACK, J. L. & TAMM, M. 2004. Dysfunctional interaction of C/EBPalpha and the glucocorticoid receptor in asthmatic bronchial smooth-muscle cells. *N Engl J Med,* 351**,** 560-74.

RYAN 2004. General Guide for Cryogenically Storing Animal Cell Cultures: Technical Bulletin. Corning, Inc.

RYBAKOWSKI, J. K., REMLINGER-MOLENDA, A., CZECH-KUCHARSKA, A., WOJCICKA, M., MICHALAK, M. & LOSY, J. 2012. Increased serum matrix metalloproteinase-9 (MMP-9) levels in young patients during bipolar depression. *J Affect Disord*.

SALANTI, G., AMOUNTZA, G., NTZANI, E. E. & IOANNIDIS, J. P. 2005. Hardy-Weinberg equilibrium in genetic association studies: an empirical evaluation of reporting, deviations, and power. *Eur J Hum Genet,* 13**,** 840-8.

SALVESEN, G. S. 2002. Caspases: opening the boxes and interpreting the arrows. *Cell Death Differ,* 9**,** 3-5.

SANYAL, A., LAJOIE, B. R., JAIN, G. & DEKKER, J. 2012. The long-range interaction landscape of gene promoters. *Nature,* 489**,** 109-13.

SAVVA, A., RAFTOGIANNIS, M., BAZIAKA, F., ROUTSI, C., ANTONOPOULOU, A., KOUTOUKAS, P., TSAGANOS, T., KOTANIDOU, A., APOSTOLIDOU, E., GIAMARELLOS-BOURBOULIS, E. J. & DIMOPOULOS, G. 2011. Soluble urokinase plasminogen activator receptor (suPAR) for assessment of disease severity in ventilator-associated pneumonia and sepsis. *J Infect,* 63**,** 344-50.

SAYERS, I., BEGHÉ, B., HOLLOWAY, J. & HOLGATE, S. T. 2008. Genetics of Asthma: What's New?

SCHEMBRI, F., SRIDHAR, S., PERDOMO, C., GUSTAFSON, A. M., ZHANG, X., ERGUN, A., LU, J., LIU, G., BOWERS, J., VAZIRI, C., OTT, K., SENSINGER, K., COLLINS, J. J., BRODY, J. S., GETTS, R., LENBURG, M. E. & SPIRA, A. 2009. MicroRNAs as modulators of smoking-induced gene expression changes in human airway epithelium. *Proc Natl Acad Sci U S A,* 106**,** 2319-24.

SCHEWE, D. M., BILLER, T., MAURER, G., ASANGANI, I. A., LEUPOLD, J. H., LENGYEL, E. R., POST, S. & ALLGAYER, H. 2005. Combination analysis of activator protein-1

family members, Sp1 and an activator protein-2alpha-related factor binding to different regions of the urokinase receptor gene in resected colorectal cancers. *Clin Cancer Res,* 11**,** 8538-48.

SCHEWE, D. M., LEUPOLD, J. H., BOYD, D. D., LENGYEL, E. R., WANG, H., GRUETZNER, K. U., SCHILDBERG, F. W., JAUCH, K. W. & ALLGAYER, H. 2003. Tumor-specific transcription factor binding to an activator protein-2/Sp1 element of the urokinase-type plasminogen activator receptor promoter in a first large series of resected gastrointestinal cancers. *Clin Cancer Res,* 9**,** 2267-76.

SCHMAIER, A. H., ROJKJAER, R. & SHARIAT-MADAR, Z. 1999. Activation of the plasma kallikrein/kinin system on cells: a revised hypothesis. *Thromb Haemost,* 82**,** 226-33.

SCHNEIDER, A., SCHWARZBACH, J., FADERL, B., WELKER, L., KARSCH-VOLK, M. & JORRES, R. A. 2012. FENO measurement and sputum analysis for diagnosing asthma in clinical practice. *Respir Med*.

SCHOLS, A. M., SOETERS, P. B., DINGEMANS, A. M., MOSTERT, R., FRANTZEN, P. J. & WOUTERS, E. F. 1993. Prevalence and characteristics of nutritional depletion in patients with stable COPD eligible for pulmonary rehabilitation. *Am Rev Respir Dis,* 147**,** 1151-6.

SCHORK, N. J., MURRAY, S. S., FRAZER, K. A. & TOPOL, E. J. 2009. Common vs. rare allele hypotheses for complex diseases. *Curr Opin Genet Dev,* 19**,** 212-9.

SCHUG, J. 2008. Using TESS to predict transcription factor binding sites in DNA sequence. *Curr Protoc Bioinformatics,* Chapter 2**,** Unit 2 6.

SELLERI, C., MONTUORI, N., RICCI, P., VISCONTE, V., CARRIERO, M. V., SIDENIUS, N., SERIO, B., BLASI, F., ROTOLI, B., ROSSI, G. & RAGNO, P. 2005. Involvement of the urokinase-type plasminogen activator receptor in hematopoietic stem cell mobilization. *Blood,* 105**,** 2198-205.

SHANKLAND, S. J. & POLLAK, M. R. 2011. A suPAR circulating factor causes kidney disease. *Nat Med,* 17**,** 926-7.

SHENDURE, J. & JI, H. 2008. Next-generation DNA sequencing. *Nat Biotechnol,* 26**,** 1135-45.

SHETTY, S. 2005. Regulation of urokinase receptor mRNA stability by hnRNP C in lung epithelial cells. *Mol Cell Biochem,* 272**,** 107-18.

SHETTY, S., GANACHARI, M., LIU, M. C., AZGHANI, A., MUNIYAPPA, H. & IDELL, S. 2005. Regulation of urokinase receptor expression by phosphoglycerate kinase is independent of its catalytic activity. *Am J Physiol Lung Cell Mol Physiol,* 289**,** L591-8.

SHETTY, S. & IDELL, S. 1999. Posttranscriptional regulation of urokinase receptor gene expression in human lung carcinoma and mesothelioma cells in vitro. *Mol Cell Biochem,* 199**,** 189-200.

SHETTY, S., KUMAR, A. & IDELL, S. 1997. Posttranscriptional regulation of urokinase receptor mRNA: identification of a novel urokinase receptor mRNA binding protein in human mesothelioma cells. *Mol Cell Biol,* 17**,** 1075-83.

SHETTY, S., MUNIYAPPA, H., HALADY, P. K. & IDELL, S. 2004. Regulation of urokinase receptor expression by phosphoglycerate kinase. *Am J Respir Cell Mol Biol,* 31**,** 100-6.

SHETTY, S., VELUSAMY, T., IDELL, S., SHETTY, P., MAZAR, A. P., BHANDARY, Y. P. & SHETTY, R. S. 2007a. Regulation of urokinase receptor expression by p53: novel role in stabilization of uPAR mRNA. *Mol Cell Biol,* 27**,** 5607-18.

SHETTY, S., VELUSAMY, T., IDELL, S., TANG, H. & SHETTY, P. K. 2007b. Regulation of urokinase receptor expression by protein tyrosine phosphatases. *Am J Physiol Lung Cell Mol Physiol,* 292**,** L414-21.

SHIH, C. M., KUO, W. H., LIN, C. W., CHEN, W., CHENG, W. E., CHEN, S. C. & LEE, Y. L. 2011. Association of polymorphisms in the genes of the urokinase plasminogen

activation system with susceptibility to and severity of non-small cell lung cancer. *Clin Chim Acta,* 412**,** 194-8.

SHINAGAWA, K., MARTIN, J. A., PLOPLIS, V. A. & CASTELLINO, F. J. 2007. Coagulation factor Xa modulates airway remodeling in a murine model of asthma. *Am J Respir Crit Care Med,* 175**,** 136-43.

SHINAGAWA, K., PLOPLIS, V. A. & CASTELLINO, F. J. 2009. A severe deficiency of coagulation factor VIIa results in attenuation of the asthmatic response in mice. *Am J Physiol Lung Cell Mol Physiol,* 296**,** L763-70.

SIBBALD, B. & TURNER-WARWICK, M. 1979. Factors influencing the prevalence of asthma among first degree relatives of extrinsic and intrinsic asthmatics. *Thorax,* 34**,** 332-7.

SIDENIUS, N. & BLASI, F. 2000. Domain 1 of the urokinase receptor (uPAR) is required for uPAR-mediated cell binding to vitronectin. *FEBS Lett,* 470**,** 40-6.

SIDENIUS, N., SIER, C. F., ULLUM, H., PEDERSEN, B. K., LEPRI, A. C., BLASI, F. & EUGEN-OLSEN, J. 2000. Serum level of soluble urokinase-type plasminogen activator receptor is a strong and independent predictor of survival in human immunodeficiency virus infection. *Blood,* 96**,** 4091-5.

SIDNEY, S., SOREL, M., QUESENBERRY, C. P., JR., DELUISE, C., LANES, S. & EISNER, M. D. 2005. COPD and incident cardiovascular disease hospitalizations and mortality: Kaiser Permanente Medical Care Program. *Chest,* 128**,** 2068-75.

SIEDLINSKI, M., TINGLEY, D., LIPMAN, P. J., CHO, M. H., LITONJUA, A. A., SPARROW, D., BAKKE, P., GULSVIK, A., LOMAS, D. A., ANDERSON, W., KONG, X., RENNARD, S. I., BEATY, T. H., HOKANSON, J. E., CRAPO, J. D., LANGE, C. & SILVERMAN, E. K. 2013. Dissecting direct and indirect genetic effects on chronic obstructive pulmonary disease (COPD) susceptibility. *Hum Genet,* 132**,** 431-41.

SILLABER, C., BAGHESTANIAN, M., BEVEC, D., WILLHEIM, M., AGIS, H., KAPIOTIS, S., FUREDER, W., BANKL, H. C., KIENER, H. P., SPEISER, W., BINDER, B. R., LECHNER, K. & VALENT, P. 1999. The mast cell as site of tissue-type plasminogen activator expression and fibrinolysis. *J Immunol,* 162**,** 1032-41.

SILVERMAN, E. K., CHAPMAN, H. A., DRAZEN, J. M., WEISS, S. T., ROSNER, B., CAMPBELL, E. J., O'DONNELL, W. J., REILLY, J. J., GINNS, L., MENTZER, S., WAIN, J. & SPEIZER, F. E. 1998. Genetic epidemiology of severe, early-onset chronic obstructive pulmonary disease. Risk to relatives for airflow obstruction and chronic bronchitis. *Am J Respir Crit Care Med,* 157**,** 1770-8.

SILVERMAN, E. K., MOSLEY, J. D., PALMER, L. J., BARTH, M., SENTER, J. M., BROWN, A., DRAZEN, J. M., KWIATKOWSKI, D. J., CHAPMAN, H. A., CAMPBELL, E. J., PROVINCE, M. A., RAO, D. C., REILLY, J. J., GINNS, L. C., SPEIZER, F. E. & WEISS, S. T. 2002. Genome-wide linkage analysis of severe, early-onset chronic obstructive pulmonary disease: airflow obstruction and chronic bronchitis phenotypes. *Hum Mol Genet,* 11**,** 623-32.

SIMPSON, A. J., BOOTH, N. A., MOORE, N. R. & BENNETT, B. 1991. Distribution of plasminogen activator inhibitor (PAI-1) in tissues. *J Clin Pathol,* 44**,** 139-43.

SINGH, J., COHEN, S., MEHENDIRATTA, V., MENDOZA, F., JIMENEZ, S. A., DIMARINO, A. J. & RATTAN, S. 2012. Effects of Scleroderma Antibodies and Pooled Human Immunoglobulin on Anal Sphincter and Colonic Smooth Muscle Function. *Gastroenterology*.

SIVAMANI, R. K., PULLAR, C. E., MANABAT-HIDALGO, C. G., ROCKE, D. M., CARLSEN, R. C., GREENHALGH, D. G. & ISSEROFF, R. R. 2009. Stress-mediated increases in systemic and local epinephrine impair skin wound healing: potential new indication for beta blockers. *PLoS Med,* 6**,** e12.

SMITH, H. W., MARRA, P. & MARSHALL, C. J. 2008. uPAR promotes formation of the p130Cas-Crk complex to activate Rac through DOCK180. *J Cell Biol,* 182**,** 777-90.

SMITH, H. W. & MARSHALL, C. J. 2010. Regulation of cell signalling by uPAR. *Nat Rev Mol Cell Biol,* 11**,** 23-36.

SOLBERG, H., PLOUG, M., HOYER-HANSEN, G., NIELSEN, B. S. & LUND, L. R. 2001. The murine receptor for urokinase-type plasminogen activator is primarily expressed in tissues actively undergoing remodeling. *J Histochem Cytochem,* 49**,** 237-46.

SOLER ARTIGAS, M., WAIN, L. V., REPAPI, E., OBEIDAT, M., SAYERS, I., BURTON, P. R., JOHNSON, T., ZHAO, J. H., ALBRECHT, E., DOMINICZAK, A. F., KERR, S. M., SMITH, B. H., CADBY, G., HUI, J., PALMER, L. J., HINGORANI, A. D., WANNAMETHEE, S. G., WHINCUP, P. H., EBRAHIM, S., SMITH, G. D., BARROSO, I., LOOS, R. J., WAREHAM, N. J., COOPER, C., DENNISON, E., SHAHEEN, S. O., LIU, J. Z., MARCHINI, J., DAHGAM, S., NALUAI, A. T., OLIN, A. C., KARRASCH, S., HEINRICH, J., SCHULZ, H., MCKEEVER, T. M., PAVORD, I. D., HELIOVAARA, M., RIPATTI, S., SURAKKA, I., BLAKEY, J. D., KAHONEN, M., BRITTON, J. R., NYBERG, F., HOLLOWAY, J. W., LAWLOR, D. A., MORRIS, R. W., JAMES, A. L., JACKSON, C. M., HALL, I. P. & TOBIN, M. D. 2011. Effect of five genetic variants associated with lung function on the risk of chronic obstructive lung disease, and their joint effects on lung function. *Am J Respir Crit Care Med,* 184**,** 786-95.

SORAVIA, E., GREBE, A., DE LUCA, P., HELIN, K., SUH, T. T., DEGEN, J. L. & BLASI, F. 1995. A conserved TATA-less proximal promoter drives basal transcription from the urokinase-type plasminogen activator receptor gene. *Blood,* 86**,** 624-35.

SORIO, C., MAFFICINI, A., FURLAN, F., BARBI, S., BONORA, A., BROCCO, G., BLASI, F., TALAMINI, G., BASSI, C. & SCARPA, A. 2011. Elevated urinary levels of urokinase-type plasminogen activator receptor (uPAR) in pancreatic ductal adenocarcinoma identify a clinically high-risk group. *BMC Cancer,* 11**,** 448.

SPORER, B., KOEDEL, U., POPP, B., PAUL, R. & PFISTER, H. W. 2005. Evaluation of cerebrospinal fluid uPA, PAI-1, and soluble uPAR levels in HIV-infected patients. *J Neuroimmunol,* 163**,** 190-4.

STEFANSSON, S. & LAWRENCE, D. A. 1996. The serpin PAI-1 inhibits cell migration by blocking integrin alpha V beta 3 binding to vitronectin. *Nature,* 383**,** 441-3.

STEWART, C. E., HALL, I. P., PARKER, S. G., MOFFAT, M. F., WARDLAW, A. J., CONNOLLY, M. J., RUSE, C. & SAYERS, I. 2009. PLAUR polymorphisms and lung function in UK smokers. *BMC Med Genet,* 10**,** 112.

STEWART, C. E., NIJMEH, H. S., BRIGHTLING, C. E. & SAYERS, I. 2012. uPAR regulates bronchial epithelial repair in vitro and is elevated in asthmatic epithelium. *Thorax,* 67**,** 477-87.

STEWART, C. E. & SAYERS, I. 2009. Characterisation of urokinase plasminogen activator receptor variants in human airway and peripheral cells. *BMC Mol Biol,* 10**,** 75.

STEWART, C. E. & SAYERS, I. 2013. Urokinase receptor orchestrates the plasminogen system in airway epithelial cell function. *Lung,* 191**,** 215-25.

STEWART, L. & KATIAL, R. K. 2012. Exhaled nitric oxide. *Immunol Allergy Clin North Am,* 32**,** 347-62.

SUZUKI, N., YOSHIDA, A. & NAKANO, Y. 2005. Quantitative analysis of multi-species oral biofilms by TaqMan Real-Time PCR. *Clin Med Res,* 3**,** 176-85.

SYROVETS, T., JENDRACH, M., ROHWEDDER, A., SCHULE, A. & SIMMET, T. 2001. Plasmin-induced expression of cytokines and tissue factor in human monocytes involves AP-1 and IKKbeta-mediated NF-kappaB activation. *Blood,* 97**,** 3941-50.

TAKEUCHI, Y., MIYAMOTO, E. & FUKUNAGA, K. 2002. Activation of the rat dopamine D2 receptor promoter by mitogen-activated protein kinase and Ca2+/calmodulin-dependent protein kinase II pathways. *J Neurochem,* 83**,** 784-96.

TEE, Y. T., WANG, P. H., TSAI, H. T., LIN, L. Y., LIN, H. T., YANG, S. F., HSIEH, Y. H. & YING, T. H. 2012. Genetic polymorphism of urokinase-type plasminogen activator is

interacting with plasminogen activator inhibitor-1 to raise risk of cervical neoplasia. *J Surg Oncol,* 106**,** 204-8.

TERRACCIANO, D., BRUZZESE, D., FERRO, M., AUTORINO, R., DI LORENZO, G., BUONERBA, C., MARIANO, A., MACCHIA, V., ALTIERI, V. & DI CARLO, A. 2011. Soluble interleukin-6 receptor to interleukin-6 (sIL6R/IL-6) ratio in serum as a predictor of high Gleason sum at radical prostatectomy. *Oncol Lett,* 2**,** 861-864.

THE_INTERNATIONAL_HAPMAP_CONSORTIUM 2003. The International HapMap Project. *Nature,* 426**,** 789-96.

THUNO, M., MACHO, B. & EUGEN-OLSEN, J. 2009. suPAR: the molecular crystal ball. *Dis Markers,* 27**,** 157-72.

TOELLE, B. G., PEAT, J. K., SALOME, C. M., MELLIS, C. M. & WOOLCOCK, A. J. 1992. Toward a definition of asthma for epidemiology. *Am Rev Respir Dis,* 146**,** 633-7.

TORGERSON, D. G., CAPURSO, D., MATHIAS, R. A., GRAVES, P. E., HERNANDEZ, R. D., BEATY, T. H., BLEECKER, E. R., RABY, B. A., MEYERS, D. A., BARNES, K. C., WEISS, S. T., MARTINEZ, F. D., NICOLAE, D. L. & OBER, C. 2012. Resequencing candidate genes implicates rare variants in asthma susceptibility. *Am J Hum Genet,* 90**,** 273-81.

TOWBIN, H., STAEHELIN, T. & GORDON, J. 1979. Electrophoretic transfer of proteins from polyacrylamide gels to nitrocellulose sheets: procedure and some applications. *Proc Natl Acad Sci U S A,* 76**,** 4350-4.

TUCKER, T. A., DEAN, C., KOMISSAROV, A. A., KOENIG, K., MAZAR, A. P., PENDURTHI, U., ALLEN, T. & IDELL, S. 2010. The urokinase receptor supports tumorigenesis of human malignant pleural mesothelioma cells. *Am J Respir Cell Mol Biol,* 42**,** 685-96.

TURATO, G., ZUIN, R., MINIATI, M., BARALDO, S., REA, F., BEGHE, B., MONTI, S., FORMICHI, B., BOSCHETTO, P., HARARI, S., PAPI, A., MAESTRELLI, P., FABBRI, L. M. & SAETTA, M. 2002. Airway inflammation in severe chronic obstructive pulmonary disease: relationship with lung function and radiologic emphysema. *Am J Respir Crit Care Med,* 166**,** 105-10.

TURKMEN, B., SCHMITT, M., SCHMALFELDT, B., TROMMLER, P., HELL, W., CREUTZBURG, S., GRAEFF, H. & MAGDOLEN, V. 1997. Mutational analysis of the genes encoding urokinase-type plasminogen activator (uPA) and its inhibitor PAI-1 in advanced ovarian cancer. *Electrophoresis,* 18**,** 686-9.

UYTTERSPROT, N., COSTAGLIOLA, S. & MIOT, F. 1998. A new tool for efficient transfection of dog and human thyrocytes in primary culture. *Mol Cell Endocrinol,* 142**,** 35-9.

VALLABHANENI, K. C., TKACHUK, S., KIYAN, Y., SHUSHAKOVA, N., HALLER, H., DUMLER, I. & EDEN, G. 2011. Urokinase receptor mediates mobilization, migration, and differentiation of mesenchymal stem cells. *Cardiovasc Res,* 90**,** 113-21.

VAN DER DEEN, M., DE VRIES, E. G., VISSERMAN, H., ZANDBERGEN, W., POSTMA, D. S., TIMENS, W. & TIMMER-BOSSCHA, H. 2007. Cigarette smoke extract affects functional activity of MRP1 in bronchial epithelial cells. *J Biochem Mol Toxicol,* 21**,** 243-51.

VAN DER POUW KRAAN, T. C., KUCUKAYCAN, M., BAKKER, A. M., BAGGEN, J. M., VAN DER ZEE, J. S., DENTENER, M. A., WOUTERS, E. F. & VERWEIJ, C. L. 2002. Chronic obstructive pulmonary disease is associated with the -1055 IL-13 promoter polymorphism. *Genes Immun,* 3**,** 436-9.

VANGUILDER, H. D., VRANA, K. E. & FREEMAN, W. M. 2008. Twenty-five years of quantitative PCR for gene expression analysis. *Biotechniques,* 44**,** 619-26.

VASSALLI, J. D., BACCINO, D. & BELIN, D. 1985. A cellular binding site for the Mr 55,000 form of the human plasminogen activator, urokinase. *J Cell Biol,* 100**,** 86-92.

VASSALLI, J. D., SAPPINO, A. P. & BELIN, D. 1991. The plasminogen activator/plasmin system. *J Clin Invest,* 88**,** 1067-72.

VELUSAMY, T., SHETTY, P., BHANDARY, Y. P., LIU, M. C. & SHETTY, S. 2008. Posttranscriptional regulation of urokinase receptor expression by heterogeneous nuclear ribonuclear protein C. *Biochemistry,* 47**,** 6508-17.

VESTBO, J., HURD, S. S. & RODRIGUEZ-ROISIN, R. 2012. The 2011 revision of the Global Strategy for the Diagnosis, Management, and Prevention of COPD (GOLD) -why and what? *Clin Respir J.*

VOLLMER, W. M., MARKSON, L. E., O'CONNOR, E., SANOCKI, L. L., FITTERMAN, L., BERGER, M. & BUIST, A. S. 1999. Association of asthma control with health care utilization and quality of life. *Am J Respir Crit Care Med,* 160**,** 1647-52.

WADSWORTH, S. J., NIJMEH, H. S. & HALL, I. P. 2006. Glucocorticoids increase repair potential in a novel in vitro human airway epithelial wounding model. *J Clin Immunol,* 26**,** 376-87.

WAGERS, S. S., NORTON, R. J., RINALDI, L. M., BATES, J. H., SOBEL, B. E. & IRVIN, C. G. 2004. Extravascular fibrin, plasminogen activator, plasminogen activator inhibitors, and airway hyperresponsiveness. *J Clin Invest,* 114**,** 104-11.

WAHLBERG, K., HOYER-HANSEN, G. & CASSLEN, B. 1998. Soluble receptor for urokinase plasminogen activator in both full-length and a cleaved form is present in high concentration in cystic fluid from ovarian cancer. *Cancer Res,* 58**,** 3294-8.

WAN, Y. I., SHRINE, N. R., SOLER ARTIGAS, M., WAIN, L. V., BLAKEY, J. D., MOFFATT, M. F., BUSH, A., CHUNG, K. F., COOKSON, W. O., STRACHAN, D. P., HEANEY, L., AL-MOMANI, B. A., MANSUR, A. H., MANNEY, S., THOMSON, N. C., CHAUDHURI, R., BRIGHTLING, C. E., BAFADHEL, M., SINGAPURI, A., NIVEN, R., SIMPSON, A., HOLLOWAY, J. W., HOWARTH, P. H., HUI, J., MUSK, A. W., JAMES, A. L., BROWN, M. A., BALTIC, S., FERREIRA, M. A., THOMPSON, P. J., TOBIN, M. D., SAYERS, I. & HALL, I. P. 2012. Genome-wide association study to identify genetic determinants of severe asthma. *Thorax,* 67**,** 762-8.

WAN, Y. I., STRACHAN, D. P., EVANS, D. M., HENDERSON, J., MCKEEVER, T., HOLLOWAY, J. W., HALL, I. P. & SAYERS, I. 2011. A genome-wide association study to identify genetic determinants of atopy in subjects from the United Kingdom. *J Allergy Clin Immunol,* 127**,** 223-31, 231 e1-3.

WANG, G. J., COLLINGE, M., BLASI, F., PARDI, R. & BENDER, J. R. 1998. Posttranscriptional regulation of urokinase plasminogen activator receptor messenger RNA levels by leukocyte integrin engagement. *Proc Natl Acad Sci U S A,* 95**,** 6296-301.

WANG, H., HICKS, J., KHANBOLOOKI, P., KIM, S. J., YAN, C., WANG, Y. & BOYD, D. 2003. Transgenic mice demonstrate novel promoter regions for tissue-specific expression of the urokinase receptor gene. *Am J Pathol,* 163**,** 453-64.

WANG, H., YANG, L., JAMALUDDIN, M. S. & BOYD, D. D. 2004. The Kruppel-like KLF4 transcription factor, a novel regulator of urokinase receptor expression, drives synthesis of this binding site in colonic crypt luminal surface epithelial cells. *J Biol Chem,* 279**,** 22674-83.

WANG, I. M., STEPANIANTS, S., BOIE, Y., MORTIMER, J. R., KENNEDY, B., ELLIOTT, M., HAYASHI, S., LOY, L., COULTER, S., CERVINO, S., HARRIS, J., THORNTON, M., RAUBERTAS, R., ROBERTS, C., HOGG, J. C., CRACKOWER, M., O'NEILL, G. & PARE, P. D. 2008. Gene expression profiling in patients with chronic obstructive pulmonary disease and lung cancer. *Am J Respir Crit Care Med,* 177**,** 402-11.

WANG, R. D., WRIGHT, J. L. & CHURG, A. 2005. Transforming growth factor-beta1 drives airway remodeling in cigarette smoke-exposed tracheal explants. *Am J Respir Cell Mol Biol,* 33**,** 387-93.

WANG, Y., DANG, J., JOHNSON, L. K., SELHAMER, J. J. & DOE, W. F. 1995. Structure of the human urokinase receptor gene and its similarity to CD59 and the Ly-6 family. *Eur J Biochem,* 227**,** 116-22.

WANG, Y., DANG, J., WANG, H., ALLGAYER, H., MURRELL, G. A. & BOYD, D. 2000. Identification of a novel nuclear factor-kappaB sequence involved in expression of urokinase-type plasminogen activator receptor. *Eur J Biochem,* 267**,** 3248-54.

WANG, Y., JONES, C. J., DANG, J., LIANG, X., OLSEN, J. E. & DOE, W. F. 1994. Human urokinase receptor expression is inhibited by amiloride and induced by tumor necrosis factor and phorbol ester in colon cancer cells. *FEBS Lett,* 353**,** 138-42.

WARE, L. B., FANG, X. & MATTHAY, M. A. 2003. Protein C and thrombomodulin in human acute lung injury. *Am J Physiol Lung Cell Mol Physiol,* 285**,** L514-21.

WEBER, M., MOLLER, K., WELZECK, M. & SCHORR, J. 1995. Short technical reports. Effects of lipopolysaccharide on transfection efficiency in eukaryotic cells. *Biotechniques,* 19**,** 930-40.

WEI, C., EL HINDI, S., LI, J., FORNONI, A., GOES, N., SAGESHIMA, J., MAIGUEL, D., KARUMANCHI, S., YAP, H.-K., SALEEM, M., ZHANG, Q., NIKOLIC, B., CHAUDHURI, A., DAFTARIAN, P., SALIDO, E., TORRES, A., SALIFU, M., SARWAL, M., SCHAEFER, F., MORATH, C., SCHWENGER, V., ZEIER, M., GUPTA, V., ROTH, D., RASTALDI, M., BURKE, G., RUIZ, P. & REISER, J. 2011. Circulating urokinase receptor as a cause of focal segmental glomerulosclerosis. *Nature medicine,* 17**,** 952-1012.

WEI, C., MOLLER, C. C., ALTINTAS, M. M., LI, J., SCHWARZ, K., ZACCHIGNA, S., XIE, L., HENGER, A., SCHMID, H., RASTALDI, M. P., COWAN, P., KRETZLER, M., PARRILLA, R., BENDAYAN, M., GUPTA, V., NIKOLIC, B., KALLURI, R., CARMELIET, P., MUNDEL, P. & REISER, J. 2008. Modification of kidney barrier function by the urokinase receptor. *Nat Med,* 14**,** 55-63.

WEI, Y., LUKASHEV, M., SIMON, D. I., BODARY, S. C., ROSENBERG, S., DOYLE, M. V. & CHAPMAN, H. A. 1996. Regulation of integrin function by the urokinase receptor. *Science,* 273**,** 1551-5.

WEI, Y., TANG, C. H., KIM, Y., ROBILLARD, L., ZHANG, F., KUGLER, M. C. & CHAPMAN, H. A. 2007. Urokinase receptors are required for alpha 5 beta 1 integrin-mediated signaling in tumor cells. *J Biol Chem,* 282**,** 3929-39.

WEI, Y., WALTZ, D. A., RAO, N., DRUMMOND, R. J., ROSENBERG, S. & CHAPMAN, H. A. 1994. Identification of the urokinase receptor as an adhesion receptor for vitronectin. *J Biol Chem,* 269**,** 32380-8.

WEIDE, I., ROMISCH, J. & SIMMET, T. 1994. Contact activation triggers stimulation of the monocyte 5-lipoxygenase pathway via plasmin. *Blood,* 83**,** 1941-51.

WENZEL, S. E. 2006. Asthma: defining of the persistent adult phenotypes. *Lancet,* 368**,** 804-13.

WENZEL, S. E., SZEFLER, S. J., LEUNG, D. Y., SLOAN, S. I., REX, M. D. & MARTIN, R. J. 1997. Bronchoscopic evaluation of severe asthma. Persistent inflammation associated with high dose glucocorticoids. *Am J Respir Crit Care Med,* 156**,** 737-43.

WETZELS, R. H., SCHAAFSMA, H. E., LEIGH, I. M., LANE, E. B., TROYANOVSKY, S. M., WAGENAAR, S. S., VOOIJS, G. P. & RAMAEKERS, F. C. 1992. Laminin and type VII collagen distribution in different types of human lung carcinoma: correlation with expression of keratins 14, 16, 17 and 18. *Histopathology,* 20**,** 295-303.

WHYTE, C., THIES, F., PEYROL, L. & BALCERZAK, D. 2012. N-3 long-chain polyunsaturated fatty acids inhibit smooth muscle cell migration by modulating urokinase plasminogen activator receptor through MEK/ERK-dependent and -independent mechanisms. *J Nutr Biochem*.

WILCOX-ADELMAN, S. A., WILKINS-PORT, C. E. & MCKEOWN-LONGO, P. J. 2000. Localization of urokinase type plasminogen activator to focal adhesions requires ligation of vitronectin integrin receptors. *Cell Adhes Commun,* 7**,** 477-90.

WILHELM, O. G., WILHELM, S., ESCOTT, G. M., LUTZ, V., MAGDOLEN, V., SCHMITT, M., RIFKIN, D. B., WILSON, E. L., GRAEFF, H. & BRUNNER, G. 1999. Cellular

glycosylphosphatidylinositol-specific phospholipase D regulates urokinase receptor shedding and cell surface expression. *J Cell Physiol,* 180**,** 225-35.

WILLART, M. A., DESWARTE, K., POULIOT, P., BRAUN, H., BEYAERT, R., LAMBRECHT, B. N. & HAMMAD, H. 2012. Interleukin-1alpha controls allergic sensitization to inhaled house dust mite via the epithelial release of GM-CSF and IL-33. *J Exp Med,* 209**,** 1505-17.

WILLIAMS, A. E., LARNER-SVENSSON, H., PERRY, M. M., CAMPBELL, G. A., HERRICK, S. E., ADCOCK, I. M., ERJEFALT, J. S., CHUNG, K. F. & LINDSAY, M. A. 2009. MicroRNA expression profiling in mild asthmatic human airways and effect of corticosteroid therapy. *PLoS One,* 4**,** e5889.

WILSON, J. W. 1998. What causes airway remodelling in asthma? *Clin Exp Allergy,* 28**,** 534-6.

XIAO, W., HSU, Y. P., ISHIZAKA, A., KIRIKAE, T. & MOSS, R. B. 2005. Sputum cathelicidin, urokinase plasminogen activation system components, and cytokines discriminate cystic fibrosis, COPD, and asthma inflammation. *Chest,* 128**,** 2316-26.

XU, X., GARDSVOLL, H., YUAN, C., LIN, L., PLOUG, M. & HUANG, M. 2012. Crystal structure of the urokinase receptor in a ligand-free form. *J Mol Biol,* 416**,** 629-41.

XUE, A., XUE, M., JACKSON, C. & SMITH, R. C. 2009. Suppression of urokinase plasminogen activator receptor inhibits proliferation and migration of pancreatic adenocarcinoma cells via regulation of ERK/p38 signaling. *Int J Biochem Cell Biol,* 41**,** 1731-8.

XUE, W., KINDZELSKII, A. L., TODD, R. F., 3RD & PETTY, H. R. 1994. Physical association of complement receptor type 3 and urokinase-type plasminogen activator receptor in neutrophil membranes. *J Immunol,* 152**,** 4630-40.

XUE, W., MIZUKAMI, I., TODD, R. F., 3RD & PETTY, H. R. 1997. Urokinase-type plasminogen activator receptors associate with beta1 and beta3 integrins of fibrosarcoma cells: dependence on extracellular matrix components. *Cancer Res,* 57**,** 1682-9.

YE, J., COULOURIS, G., ZARETSKAYA, I., CUTCUTACHE, I., ROZEN, S. & MADDEN, T. 2012. Primer-BLAST: A tool to design target-specific primers for polymerase chain reaction. *BMC Bioinformatics,* 13**,** 134.

YOUSEF, G. M. & DIAMANDIS, E. P. 2001. The new human tissue kallikrein gene family: structure, function, and association to disease. *Endocr Rev,* 22**,** 184-204.

YU, H., MAURER, F. & MEDCALF, R. L. 2002. Plasminogen activator inhibitor type 2: a regulator of monocyte proliferation and differentiation. *Blood,* 99**,** 2810-8.

ZHANG, Y., MA, T., YANG, S., XIA, M., XU, J., AN, H., YANG, Y. & LI, S. 2011. High-mobility group A1 proteins enhance the expression of the oncogenic miR-222 in lung cancer cells. *Mol Cell Biochem,* 357**,** 363-71.

ZHANG, Y., XIAO, W., JIANG, Y., WANG, H., XU, X., MA, D., CHEN, H. & WANG, X. 2012. Levels of Components of the Urokinase-type Plasminogen Activator System are Related to Chronic Obstructive Pulmonary Disease Parenchymal Destruction and Airway Remodelling. *J Int Med Res,* 40**,** 976-85.

ZIMMERMANN, H. W., KOCH, A., SEIDLER, S., TRAUTWEIN, C. & TACKE, F. 2012. Circulating soluble urokinase plasminogen activator is elevated in patients with chronic liver disease, discriminates stage and aetiology of cirrhosis and predicts prognosis. *Liver Int,* 32**,** 500-9.